UNIVERSITY OF CALIFORNIA SAN DIEGO

SAN DIEGO STATE UNIVERSITY

# Practical and selective functionalizations of aromatics and heteroarenes via radical processes

A dissertation submitted in partial satisfaction of the
requirements for the degree Doctor of Philosophy

in

Chemistry

by

Ashley Dang-Nguyen

Committee in charge:

University of California San Diego

Professor Joseph M. O'Connor
Professor Jerry Yang

San Diego State University

Professor Jeffrey L. Gustafson, Chair
Professor Douglas B. Grotjahn
Professor Eunha Hoh

2023

The dissertation of Ashley Dang-Nguyen is approved, and it is acceptable in quality and for publication on microfilm and electronically:

_____

_____

_____

_____

_____

Chair

University of California San Diego

San Diego State University

2023

# DEDICATION

To everyone who I call family,

You know who you are whether you like it or not.

TABLE OF CONTENTS

LIST OF FIGURES

LIST OF SCHEMES

LIST OF TABLES

# ACKNOWLEDGEMENTS

This dissertation is the culmination of years of support, pain, excitement, and inspiration from teachers, peers, and friends I have crossed paths with during my time in graduate school.

First and foremost, I would like to express my sincere gratitude to Dr. Jeffrey Gustafson for his unwavering support and guidance during my graduate school career. You have given me every opportunity to succeed and without your enthusiasm and encouragement, I would not be the scientist I am today.

To the previous Gustafson lab that recruited me in 2018, Andrew, Della, Sean, Sagar, and Mariel: Thank you for making me feel welcomed and subsequently abandoning me when it was your time to leave the nest.

To the current Gustafson lab members who will remain, Mariam, Zach, Bahar, Beeta, Jim, Ryan, and Zhao: to put it simply, I wish you luck in your future endeavors.

To the undergraduates I've trained and had the pleasure of working with, Ernesto Millan, Samuel Albright, Connor McCarty, Nicholas Tabares, Chase Totherow, and Rachel Khoury: Thank you for all your efforts both in the hood and out of it, making my time in the Gustafson lab memorable.

To my '1451' family who's supported me from the very beginning, thank you for sending me care packages and ice chests full of food every time I came home to visit. I've been away for so long that I can't wait for you to be annoyed with me now that I am coming back home.

To Nathan Vega, I love you. Oli and I are so lucky to have you in our lives. Graduate school was hard for the both of us, and I'm thankful we now get to close this chapter of our lives.

Lastly, shoutout to the people who made sure I saw this through: JT, SMY, MP, CJB, JC, MB, AMA, KJW, MHG, DJS, KCL, RM, JSM, YS, AV, GE, LE, DO, DS.

Chapter 1, in part is a reprint of 'Photocatalytic Oxidative C-H Thiolation: Synthesis of Benzothiazoles and Sulfenylated Indoles' *Synlett*. 2019, *30*, 1648-1655. Dinh, A.D. ‡; Nguyen, A.D. ‡; Millan-Aceves, E.; Albright, S. T.; Cedano, M.; Smith, D. K.; Gustafson, J. L. The dissertation author was co-primary investigator and co-author of this paper.

Chapter 2, in full is a reprint of material as it appears in 'A light-mediated trifluoromethylation of pyridones and related N-heteroarenes" *Org. Lett*. 2023, *25,* 26, 4898-4902. Nguyen, A. D.; Legaspi, K. L.; McCarty, C. T.; Smith, D. K.; Gustafson, J. L. The dissertation author was the primary investigator and primary author of this paper.

Chapter 3 contains unpublished materials describing a regioselective perfluoroalkylation and is reproduced in part as it appears in 'Selective Functionalizations of Arenes and Heteroarenes via $S_EAr$ and Related Transformations' *Wiley*. 2022. Handbook of C-H Functionalization. ISBN: 9783527834242. Nguyen, A. D.; Zanolini, R. J.; Gustafson, J. L. The dissertation author is the primary investigator and author of this paper.

## VITA

| | |
|---|---|
| 2013-2017 | Bachelor of Science, Chemistry concentration in Biochemistry, San Jose State University |
| 2019-2020 | Teaching Assistant, San Diego State University |
| 2019-2023 | Graduate Research Assistant, San Diego State University |
| 2018-2023 | Doctor of Philosophy, Chemistry, University of California San Diego and San Diego State University |

## PUBLICATIONS

1. Nguyen, A. D; Legaspi, K. C; McCarty, C. T.; Smith, D. K; Gustafson, J. L. A practical photocatalyst-free, light promoted trifluoromethylation of pyridones and related N-heteroarenes. *Org. Lett*. **2023**, *25,* 26*,* 4898-4902.

2. Nguyen, A. D; Zanolini, R. J.; Gustafson, J. Selective functionalizations of arenes and heteroarenes via $S_EAr$ and related transformations. *Wiley*. Handbook of C-H Functionalization. **2022**. ISBN: 9783527834242

3. Cardenas, M.; Nguyen, A. D.; Brown, Z.; Heydari, B.; Heydari, B.; Vaidya, S.; Gustafson, J. L. Atropisomerism as an inspiration for new chemistry. *Arkivoc*. **2021**, *i*, 20-47.

4. Dinh, A. N. ‡; Nguyen, A. D. ‡; Millan, E. A.; Albright, S. T.; Cedano, M.; Smith, D. K.; Gustafson, J. L. Photocatalytic Oxidative C-H Thiolation: Synthesis of Benzothiazoles and Sulfenylated Indoles. *Synlett.* **2019**, *30*, 1648-1655

PRESENTATIONS

1. “Light and catalyst-promoted inherent and regioselective perfluoroalkylation of arenes and heteroarenes.” **Nguyen, A.D**.; McCarty, C.T.; Legaspi, K.C.; Gustafson, J.L., poster presentation at the 2022 Gordon Research Conference (GRC): Stereochemistry, Newport, RI, July 2022

2. **“**Inherent and Lewis base catalyzed promoted regioselective perfluoroalkylation of arenes and heteroarenes.” **Nguyen, A.D**.; McCarty, C.T.; Legaspi, K.C.; Gustafson, J.L., poster presentation at the 2022 ACS Division of Organic Chemistry (DOC) Graduate Research Symposium (GRS), Santa Barbara, CA, July 2022

3. “Lewis base catalyzed regioselective trifluoromethylation of heteroarenes and arenes.” **Nguyen, A.D**.; McCarty, C.T.; Gustafson, J.L., poster presentation at the 2022 National Organic Chemistry Symposium (NOS) by American Chemical Society Division of Organic Chemistry, University of California San Diego, CA, June 2022

4. “Lewis base catalyzed regioselective trifluoromethylation and Lewis acid catalyzed alkylation of heteroarenes and arenes.” **Nguyen, A.D**.; Zanolini, R.J.; McCarty, C.T.; Gustafson, J.L., poster presentation at the 2022 ACS National Meeting, San Diego, CA, March 2022

5. “Lewis base catalyzed regioselective trifluoromethylation of heteroarenes and arenes.” **Nguyen, A.D**.; McCarty, C.T.; Gustafson, J.L., poster presentation at the FloHet 2022 Florida Heterocyclic and Synthetic Chemistry Conference, Gainsville, FL, March 2022

6. “Oxidative C-H Thiolation: Synthesis of Benzothiazoles and Sulfenylated Indoles.” Dinh, A.N.; **Nguyen, A.D**.; Millan, E.; Albright, S.T.; Cedano, M.; Smith, D.; Gustafson, J.L. 32nd CSU Biotechnology Symposium, Santa Clara, CA, January 2020

7. “Oxidative C-H Thiolation: Synthesis of Benzothiazoles and Sulfenylated Indoles.” Dinh, A.N.; **Nguyen, A.D**.; Millan, E.; Albright, S.T.; Cedano, M.; Smith, D.; Gustafson, J.L., poster presentation at the 258th ACS National Meeting, San Diego, CA, August 2019

8. “*Photocatalytic Oxidative C-H Thiolation: Synthesis of Benzothiazoles and Sulfenylated Indoles.”* Dinh, A.N.; **Nguyen, A.D**.; Millan, E.; Albright, S.T.; Cedano, M.; Smith, D.; Gustafson, J.L., poster presentation at the 2019 National Organic Chemistry Symposium (NOS) by American Chemical Society Division of Organic Chemistry, Indiana University, Bloomington, IN, June 2019

9. “*Oxidative Sulfenylation of Substituted Benzothiazoles and Indoles”*, **Nguyen, A.D**.; Millan, E.; Gustafson, J.L., poster presentation at the 2019 SDSU Student Research Symposium, San Diego, CA, March 2019

## HONORS AND AWARDS

Susan and Stephen Weber Endowed Scholarship (2022-2023)

Michael and Donna Malley Endowed Fellowship (2022-2023)

SDSU Graduate Student Travel Grant (2020-2023)

Mentoring Pathways Scholarship (NSF #1929758) (2022-2023)

Achievement Rewards for College Scientists Fellowship (ARCS) (2021-2023)

University Graduate Fellowship (UGF) (2020-2022)

Harry E. Hamber Memorial Scholarship (2020-2022)

Tom Ragan Memorial Endowed Fellowship (2020-2021)

## MAJOR FIELD OF STUDY

Major Field: Chemistry (Organic)

Innate and Regioselective C-H Functionalization Utilizing Radical and Organocatalytic Chemical Methodologies

Professor Jeffrey L. Gustafson

ABSTRACT OF THE DISSERTATION

Practical and selective functionalizations of aromatics and heteroarenes via radical processes

by

Ashley Dang-Nguyen

Doctor of Philosophy in Chemistry

University of California San Diego, 2023

San Diego State University, 2023

Professor Jeffrey L. Gustafson, Chair

Aromatic compounds are ubiquitous in everyday life as they are commonly found in the composition of materials, technologies, energy, and medicines. The functionalization of these

compounds via C-H Functionalization strategies are particularly useful in order to access a variety of new compounds, and in regards to medicinal chemistry increasing the capacity to synthesize lead aromatic compounds without the need for *de novo* syntheses. Radical C-H functionalization in particular has become increasing popular due to the resurgence of photochemistry allowing for the generation of more reactive-radical or charged open-shell intermediates. C-H Functionalization as a whole enables Late-stage functionalization of more complex molecules, allowing for the facile transformation of specific C-H bonds and increased diversification of compounds. However, a current limitation in the field is the lack of regio-control on aromatic substrates, known to produce mixtures of constitutional isomers in many reaction methodologies. Our lab has developed radical strategies for the functionalization of aromatic compounds, which is discussed in two manuscripts in Chapter 1 and 2. We also are developing a regioselective-catalyst controlled Lewis base perfluoroalkylation of anilides which is discussed in Chapter 3. We believe these works can be utilized in the functionalization of aromatic compounds and relevant for use towards drug discovery efforts.

# CHAPTER 1: Photocatalytic Oxidative C-H Thiolation: Synthesis of Benzothiazoles and Sulfenylated Indoles

## 1.0 Thieme Copyright



## 1.1 C-H Functionalization in Organic Chemistry

The direct functionalization of carbon-hydrogen (C-H) bonds is a long-standing desire in organic chemistry as most organic compounds consist of hydrocarbons, sometimes intertwined with heteroatoms such as but not limited to nitrogen (N), oxygen (O), sulfur (S), and other halogens (X=F, Cl, Br, I). The direct activation and subsequent functionalization of C-H bonds can circumvent the need of harsh, toxic reagents and or development of de novo syntheses for more complex molecules necessitated by the inability to induce a transformation at any given step.[1-4] Due to the ubiquity of C-H bonds in organic molecules, a drawback to C-H functionalization is the lack of selectivity regarding functionalization between electronically similar C-H bonds;[5] however, we will discuss this issue more in depth in Chapter 3. Due to the broad definition of C-H functionalization, Jin Quan Yu and coworkers categorized it into two subfields known as 'first functionalization' and 'further functionalization'.[6] The first functionalization approach involves reactions using unfunctionalized C-H bonds amongst aromatic and aliphatic compounds where non-polar and or hydrophobic compounds interact weakly with a polar metal species.[7] Further functionalization is defined for molecules that contain one or more functional groups that can be

used to interact non-covalently with catalysts (organic or metal based), which may in turn also increase the preferential selectivity towards some C-H bonds over others.[8] Using intrinsic functional groups in a target molecule can prevent the need for prefunctionalization or the installation of unnecessary directing groups that may be difficult to remove at a late stage. The work discussed in this thesis would be classified in this category.

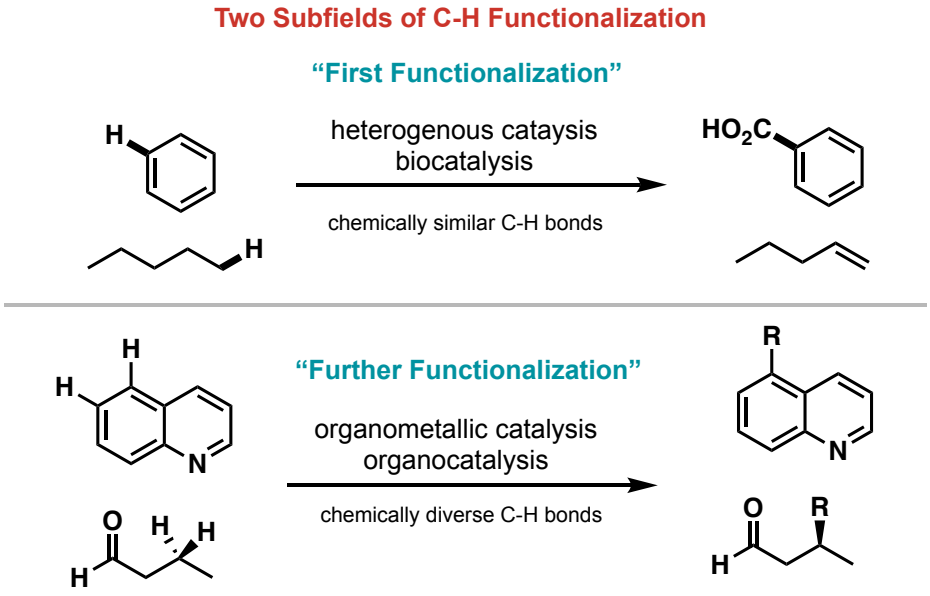


**Scheme 1.1.1 Subfields of C-H Functionalization**

Over the past vicennial, we have seen a growing interest towards developing new C-H functionalization methodologies using transition metal catalysis,[2, 9-12] organocatalysis,[3, 13, 14] and radical chemistry in the context of photocatalysis.[15-19] These advancements have also contributed to the global goal to efficiently synthesize relevant compounds from a low cost, 'green', sustainability perspective.[20-23] This thesis will focus on advancements in radical chemistries initiated by light, otherwise known as photochemistry, which fulfills several principals of green chemistry.[24-26]

## 1.2 Radical Chemistry via Photocatalysis in Organic Chemistry

We often teach radical-based transformations in our sophomore-organic chemistry courses as reactions that utilize highly reactive intermediates with unpaired electrons, or partially filled orbitals, that tend to dimerize or polymerize. In fact, industry use of radical transformations were dominated by polymer and material chemistries to synthesize metric tons of plastics, Plexiglas, Teflon, and acrylonitrile-butadiene-styrene copolymer (ABS) rubbers.[27-29] Beyond these fields, the use of radical reactions towards syntheses of small molecules were sporadically utilized until the 1970s aided by the development of Wohl-Ziegler reaction, which is an allylic radical bromination strategy.[30-32] However, it wasn't until a few years later in 1975 with the development of Barton-McCombie deoxygenation using a tin initiator and asobisisobutyronitrile (AIBN) where synthetic chemists begun to realize the full potential of radical chemistry.[33, 34] These reactions along with the Giese Reaction, formation of C-C bonds through the addition of radicals to alkenes, are some of the most classical radical reactions (Scheme 1.2.1).[35-37] (34-36)

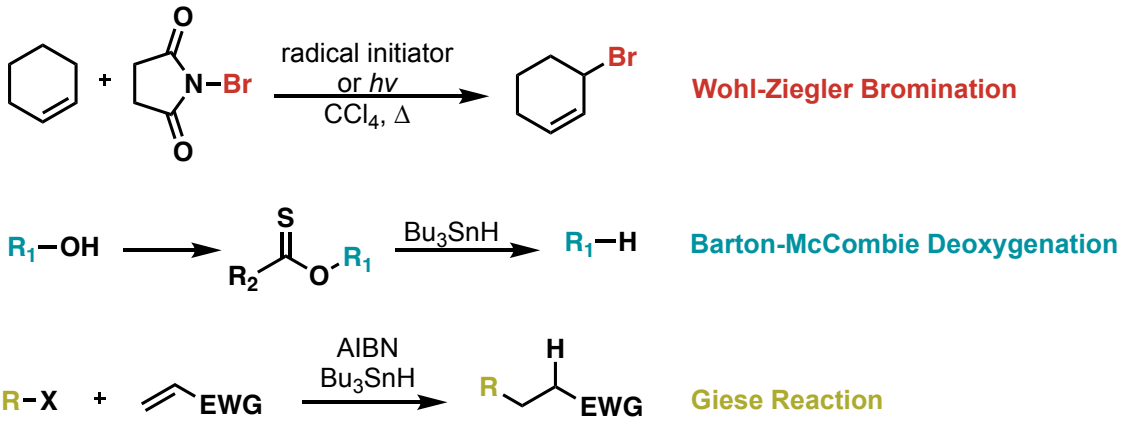


**Scheme 1.2.1 Classical Radical Reactions**

Nearly four decades later, radical chemistry has been popularized by photocatalysis. This strategy is used to form a variety of traditional and non-traditional bond formations due to the facile activation of metal-based and organic photosensitizers.[15] Previous developments in

photochemistry have encompassed the fields of water splitting,[38] carbon dioxide reduction,[39] and solar cell materials,[40] however recent developments have been focused on applications in organic syntheses with an emphasis for use in industry.[41] There are several different modes of photocatalysis which include: photoredox catalysis, involving a reductive and oxidative quenching cycle, proton-coupled electron transfer (PCET),[42-44] which can be transferred sequentially or concerted, hydrogen atom transfer (HAT),[42, 45] and or energy transfer (ET).[23, 46] Depending on the irradiation source, the specific wavelengths of light can be used to tune the chemoselectivity of the reaction if the starting material does not absorb in the wavelength necessary for a given reaction to occur.[47, 48] This allows for selective excitation of a photosensitizer, where in the context of an iridium-based catalyst $Ir(ppy)_3$, via a metal to ligand charge transfer (MLCT), the resulting excitation photosensitizer can act as both a strong oxidant or reductant (Figure 1.2.1, adapted from review by MacMillan).[15, 34] This reactive intermediate can allow for transformations otherwise known to be difficult using traditional methods and circumvents the need for toxic radical initiators.

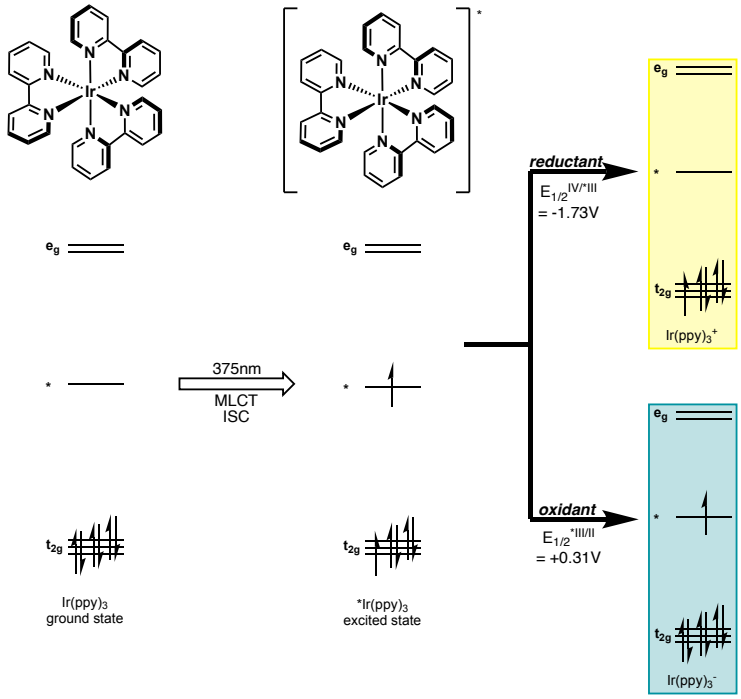


**Figure 1.2.1 General Molecular Orbital Diagram of an $Ir(ppy)_3$ Photocatalyst**

## 1.3 Late-Stage C-H Functionalization via Photocatalysis

The transformative nature of C-H Functionalization has led to other developments such as late-stage functionalization (LSF), which enables the ability to rapidly diversify pharmaceutical cores and potential lead therapeutic compounds in order to develop vast compound libraries. The potential of these libraries can bring advancement in the efficient identification of structure-activity relationships (SAR) and further optimization of absorption, distribution, metabolic, and excretion (ADME) properties of a potential pharmaceutical.[49, 50] Since photoredox chemistries are often mild in reaction conditions and are a direct method to achieve chemoselective functionalization based on a compound's innate reactivity profile, there have been more recent examples of LSF using photocatalysis.[42, 51, 52] For example, MacMillan and coworkers published a seminal, simplified photocatalyzed trifluoromethylation across a variety of arenes and heteroarenes, which was

exemplified by LSF of blockbuster drug Lipitor, which is one of the highest-selling drugs of all time (Scheme 1.3.1).

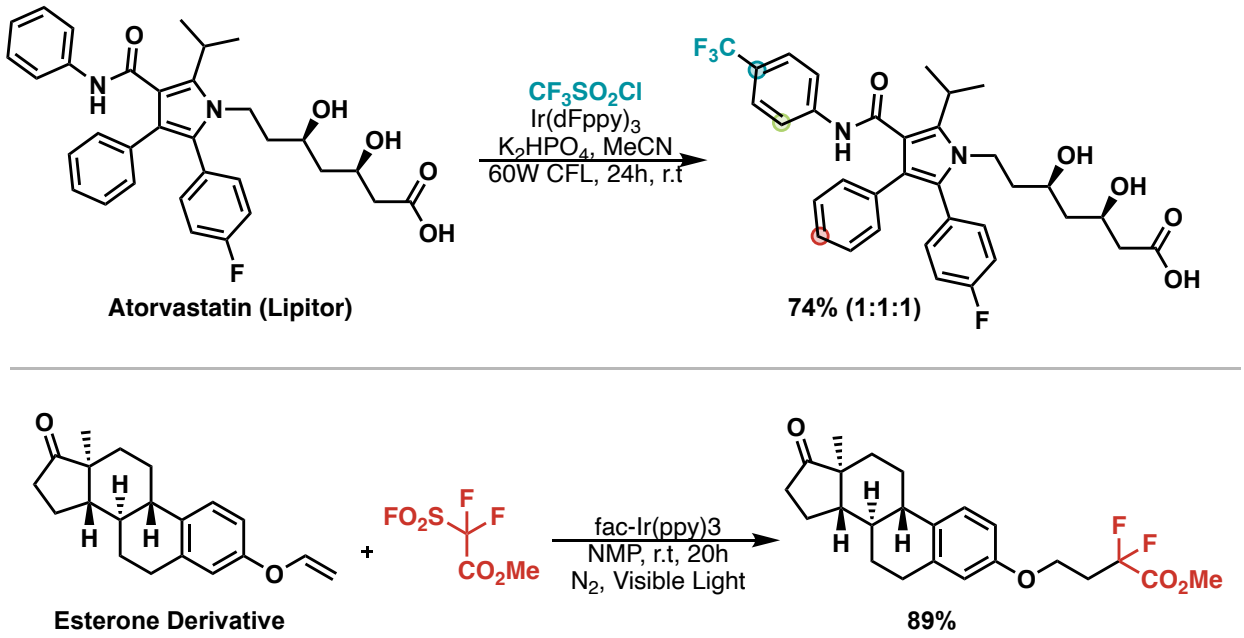


**Scheme 1.3.1 Examples of LSF via Photochemistry**

## 1.4 Sulfenylated Compounds in Drug Discovery

From a medicinal chemistry perspective, sulfur containing compounds are ubiquitous in drug discovery. In general, heterocyclic compounds are one of the most abundant scaffolds in medicinal chemistry, and there is considerable interest in incorporating sulfur into pharmaceutical scaffolds.[53, 54] Sulfur is unique as there are multiple methods for post translational functionalization of sulfur (II) to different oxidative forms of sulfur such as sulfur (IV) and sulfur (VI).[55] These processes are typically reversible, allowing for facile diversification of sulfur containing compounds.[56, 57] Sulfur (II), in the form of a thiol, also can reversibly bind to itself or another sulfur (II) species forming disulfide bonds which is also commonly found in some proteins.[58] These favorable properties have led to the incorporation of sulfur in pharmaceuticals such as but not limited to Omeprazole, a suppressant for gastric acid, Azitinib, a chemotherapeutic for renal cell

carcinoma (RCC), Albendazole, a treatment for parasites, and Riluzole, a benzothiazole containing pharmaceutical that is a glutamate blocker for amyotrophic lateral sclerosis (ALS) (Figure 1.4.1).[59, 60]

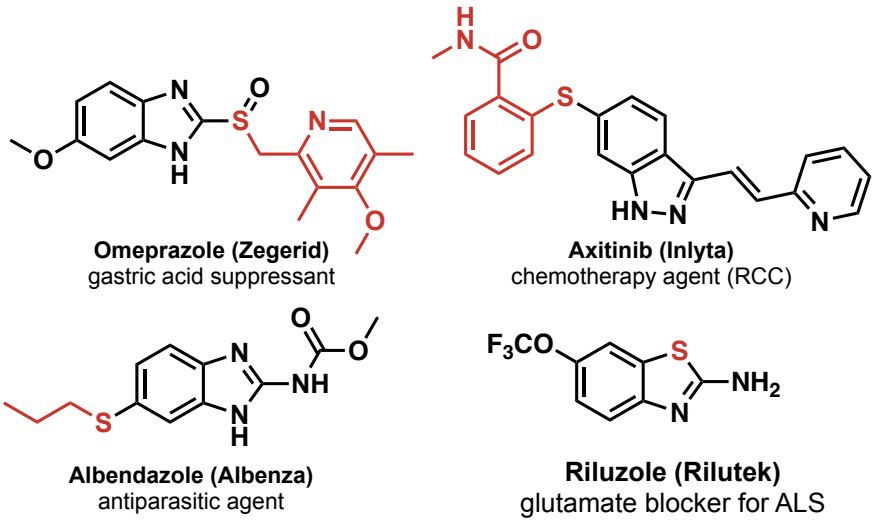


**Figure 1.4.1 Sulfur Containing Pharmaceuticals**

The incorporation of sulfur in aromatic and heteroaromatic compounds is commonly achieved through cross-couplings via metal catalysis[61-63] and more recently through electrophilic aromatic substitution ($S_EAr$)[64, 65] reactions via the in situ formation of sulfenyl halide intermediates, however these methods often result in mixtures of halogenated or sulfenylated compounds.[66, 67] From a biological standpoint, sulfur species are great redox partners as one can achieve reversible sulfur redox[57, 68] which is a positive quality for photocatalytic processes.[69-73] Thus, there is still need for development of new methodologies for facile transformations of C-H bonds to C-S bonds.

## 1.5 Previous Strategies for C-S Bond Formation Using Photocatalysis

In the past decade, there have been multiple accounts of C-S bond formation through the use of photocatalysis (Scheme 1.5.1). In 2015, Lei and coworkers demonstrated the synthesis of benzothiazoles using a dual catalytic system featuring cobalt and a ruthenium photosensitizer

($Ru(bpy)_3(PF_6)_2$).[74] In 2017, Xu and coworkers also published a similar transformation using a TEMPO-catalyzed electrochemical C-H strategy of benzothioamides.[75] Alternatively Fan and coworkers reported a photocatalytic sulfenylation of indoles using an organic dye, Rose Bengal, and thiols.[76, 77] More recently, Konig and Rehbein demonstrated a C-H thiolation of electron rich arenes via diaryl and dialkyl sulfudes and an iridium photosensitizer ($Ir[dF(CF_3)ppy]_2(dtbpy)]PF_6$ assisted by a persulfate salt to produce aryl- and alkyl-thioethers.[78]

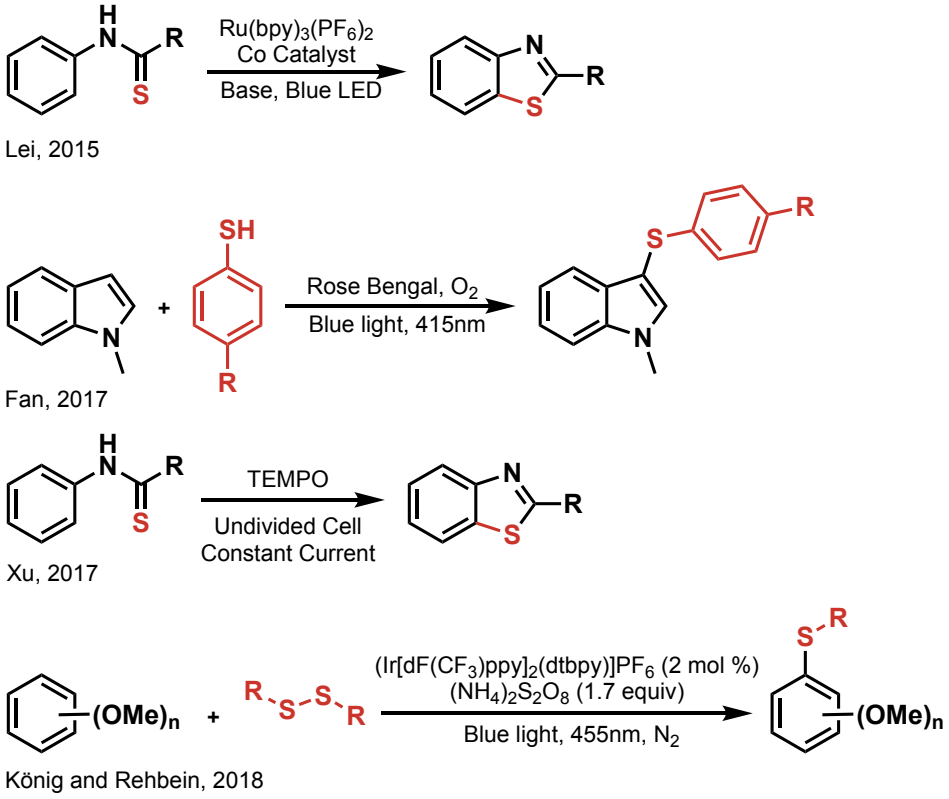


**Scheme 1.5.1 Previous Strategies for Photocatalytic C-S Bond Formation**

These are examples of radical chemistry via electrochemical and photoredox methods in the context of C-H to C-S functionalization, however, we also hypothesized at this time that different sulfur sources could be activated via photocatalytic oxidation or reduction to give an electrophilic or a nucleophilic sulfur species. Thus, herein we report a C-H thiolation that has dual functionalization. In the presence of a benzothioamide, we observed intramolecular C-H thiolation

to form a benzothiazole, while alternatively in the presence of indole and a thiol, we observed sulfenylated indoles in an intermolecular fashion (Scheme 1.5.2).[79]

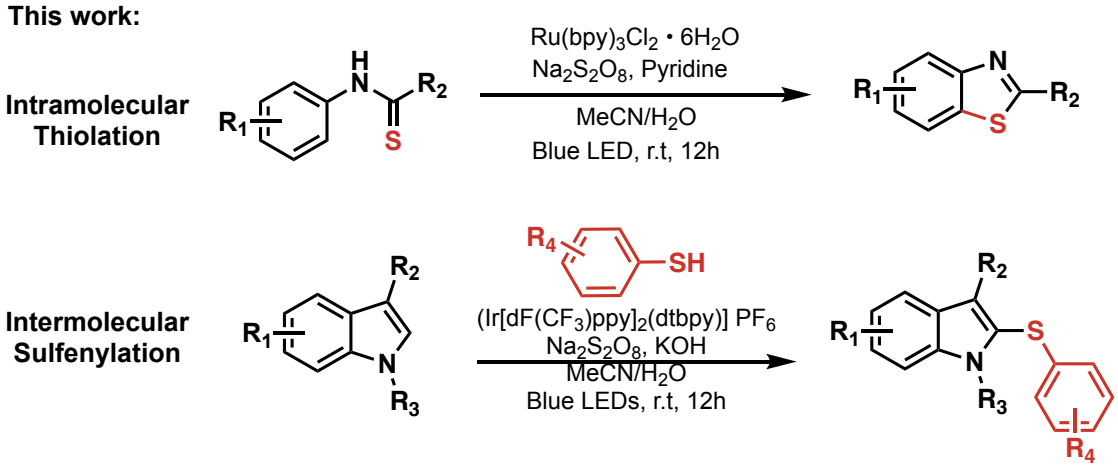


**Scheme 1.5.2 Intramolecular and Intermolecular Syntheses of Benzothiazoles and Sulfenylated Indoles**

## 1.6 Discussion

The discovery of this reaction was serendipitous as compound **1.1a** was synthesized for another project involving a photocatalytic chlorination using a protocol developed by Hu and coworkers (Table 1.6.1, entry 1).[80] Interestingly, chlorination was not observed however formation of compound **1.1b** was observed. The removal of sodium chloride resulted in similar conversion of **1.1b**, suggesting that this chemistry proceeds via an oxidative mechanism rather than through a sulfenylhalide intermediate (Table 1.6.1, entry 2). When removing sodium persulfate and the photosensitizer (Table 1.6.1, entry 3 and 4) we observed a significant decrease in conversion, however in the presence of persulfate alone 5% of benzothiazole formation was still observed. We then wanted to evaluate other photosensitizers as $Ru(bpy)_3Cl_2$ ($I_{max}$ = 452nm) to see if we can increase the conversion of **1.1b**. This reaction utilizes a 390nm Kessil LED, thus we tried several photosensitizers such as $Ru(phen)_3Cl_2$, which has an $I_{max}$ = 422nm, as we hypothesized that this

catalyst would be in a higher absorbance range relative to $Ru(bpy)_3Cl_2$, however no increase in conversion was observed, in fact we noticed a large decrease to 15% conversion (Table 1.6.1, entry 5). 4CzIPN is an organic photosensitizer that was found to improve conversion in comparison to $Ru(phen)_3Cl_2$ (Table 1.6.1, entry 6), but there is no improvement in conversion. An iridium based photosensitizer proved similar to the aforementioned entries (Table 1.6.1, entry 7), which is surprising as $Ir[dF(CF_3)ppy]_2(dtbpy)]PF_6$ has a higher oxidation potential in its excited state [Ir(III)*/Ir(II) = 1.21V vs. SCE (saturated calomel electrode)] compared to the ruthenium photosensitizer [Ru(II)*/Ru(I) = 0.77V vs. SCE] and would be expected to oxidize **1.1a** more efficiently, but this was not observed. This suggests that $Ru(bpy)_3Cl_2$ has a significant effect on the conversion of benzothiazole formation, not by oxidizing **1.1a**, but rather the persulfate radical anion ($SO4^{\cdot-}$) in the reaction. Solvent conditions were next explored and we noticed a decrease in conversion when the reaction medium was changed from a 1:1 ratio of acetonitrile and water ($MeCN:H_2O$) to a 9:1 ratio (Table 1.6.1, entry 9) product **1.1b** was not observed but **1.1c** was observed. Product **1.1c** is a common degradation product of **1.1a**, as noted by the synthesis of **1.1a** from **1.1c**. If we were to increase the equivalences of persulfate in the reaction from 5 to 10 (Table 1.6.1, entry 10), we observe similar outcomes as mentioned previously. Finally, we achieved improved conversions to **1.1b** by adding an organic base, pyridine, to the reaction to achieve up to 79% of **1.1b** (Table 1.6.1, entry 11).

**Table 1.6.1 Optimization of Intramolecular Benzothiazole Formation**

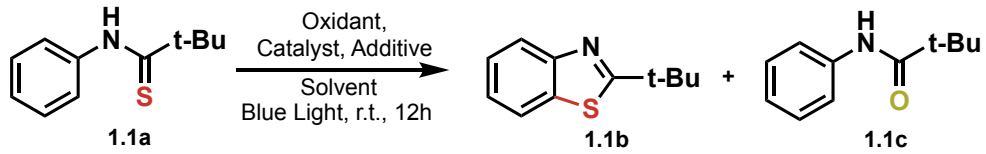


1.1a 1.1b 1.1c

| Entry | Catalyst | Oxidant (Equiv) | Additive (Equiv) | Solvent | Conversion (%) |
|---|---|---|---|---|---|
| 1 | $Ru(bpy)_3Cl_2$ | $Na_2S_2O_8$ (2) | NaCl (3) | $CH_3CN/H_2O$ (1:1) | 52% |
| 2 | $Ru(bpy)_3Cl_2$ | $Na_2S_2O_8$ (2) | None | $CH_3CN/H_2O$ (1:1) | 57% |
| 3 | $Ru(bpy)_3Cl_2$ | None | None | $CH_3CN/H_2O$ (1:1) | 0% |
| 4 | None | $Na_2S_2O_8$ (2) | None | $CH_3CN/H_2O$ (1:1) | 5% |
| 5 | $Ru(phen)_3Cl_2$ | $Na_2S_2O_8$ (2) | None | $CH_3CN/H_2O$ (1:1) | 15% |
| 6 | 4CzIPN | $Na_2S_2O_8$ (2) | None | $CH_3CN/H_2O$ (1:1) | 30% |
| 7 | Ir{df($CF_3$)... | $Na_2S_2O_8$ (2) | None | $CH_3CN/H_2O$ (1:1) | 20% |
| 8 | $Ru(bpy)_3Cl_2$ | $Na_2S_2O_8$ (2) | None | $CH_3CN/H_2O$ (9:1) | 34% |
| 9 | $Ru(bpy)_3Cl_2$ | $Na_2S_2O_8$ (5) | None | $CH_3CN/H_2O$ (1:1) | 0% (1.1c obtained) |
| 10 | $Ru(bpy)_3Cl_2$ | $Na_2S_2O_8$ (10) | None | $CH_3CN/H_2O$ (1:1) | 0% (1.1c obtained) |
| 11 | $Ru(bpy)_3Cl_2$ | $Na_2S_2O_8$ (2) | Pyridine (2) | $CH_3CN/H_2O$ (1:1) | 79% |

We then evaluated the optimal conditions from Table 1.6.1 across a variety of benzothioamide derivatives (Scheme 1.6.1) both without and with pyridine to monitor to test our initial hypothesis. When varying the electronics of the aryl ring at $R^1$ (**1.1**-**1.7**), we observed minor decreases in yields of **1.1b** – **1.7b** from 28-55% without pyridine and 34-79% yield with pyridine. Notably, there is no improvement in yield for the formation of **1.6b**, which is a napthyl based substrate (55% without and 54% with base). This lack of increased yield remained true for other substrates that possess these aryl groups such as **1.9b** (43% without and 38% with base). When replacing the *tert*-butyl substituent with a phenyl ring at $R^2$ as seen in **1.8b**, we observed a decrease in yield (17% without and 32% with base). Finally, when evaluating substrates with aliphatic groups other than tert-butyl, while varying the electronics of $R^1$, for **1.11** – **1.15** we observed benzothiazole formation in good yields 31-55% without and 55-73% with base for **1.11b** – **1.15b**. Interestingly, when $R^2$ is changed to a methyl **1.16a** or trifluoromethyl **1.17a**, no benzothiazole

**1.16b** and **1.17b** formation was observed possibly due to the thioamide being too electron-poor, a lower innate nucleophilicity at sulfur, or a higher redox potential.

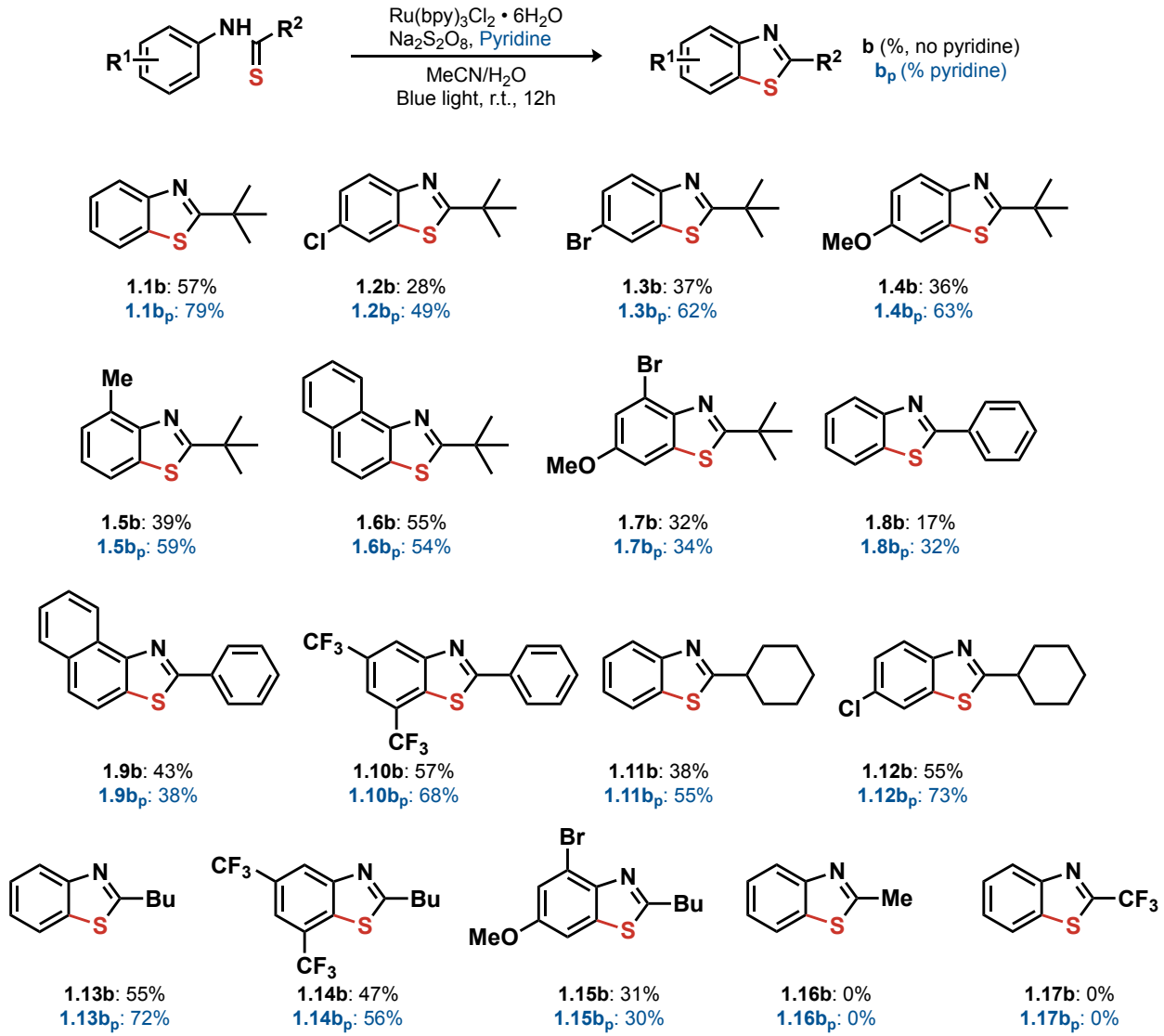


**Scheme 1.6.1 Benzothiazole Substrate Scope**

In order to explain the following transformation of benzothioamides to benzothiazoles, we first wanted to study the effect of pyridine, which was found to increase yields possibly due to a Lewis base effect where the pyridine can coordinate or deprotonate the N-H of the corresponding benzothioamide.[81] We used cyclic voltammetry (CV) experiments to study the redox potential of compound **1.1a** as well as to see the effect of pyridine (Scheme 1.6.2).[82] In pure MeCN, compound

**1.1a** was found to have two half wave oxidation potentials at 1.5V and 1.9V vs. SCE, which is out of range of $Ru(bpy)_3Cl_2$ reduction potential. Upon titration of pyridine up to 4 equivalences to **1.1a**, a distinct shift was observed in the two oxidation potentials to 1.2V and 1.5V vs. SCE.

Interestingly, the first oxidation potential of **1.1a** in the presence of pyridine was found to be within the ground state range of $Ru(bpy)_3Cl_2$ [Ru(III)/Ru(II) = 1.29V vs. SCE], which suggests that the photosensitizer in its excited state is reducing persulfate initially.

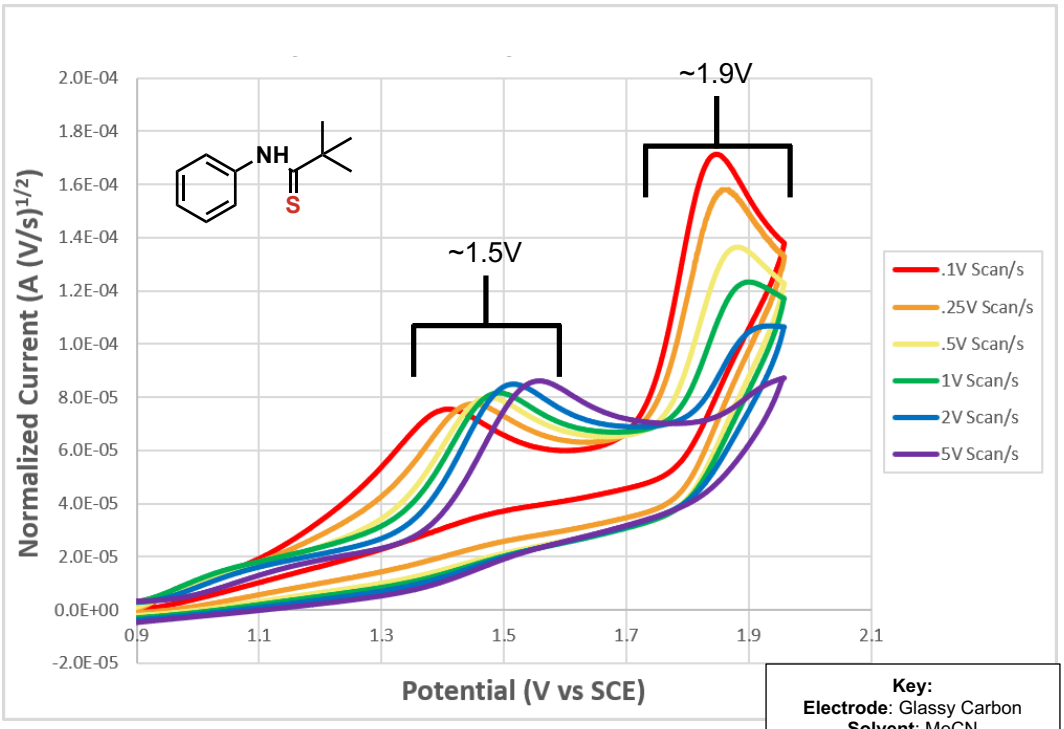


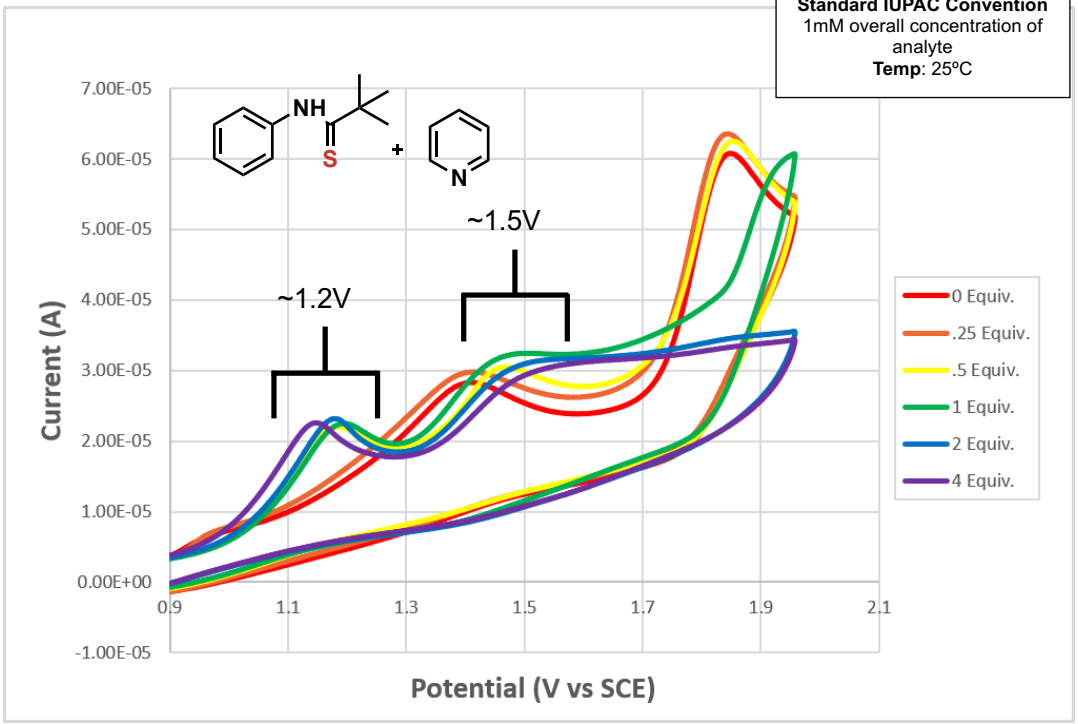


**Scheme 1.6.2 CV Measurements for 1.1a in the Absence and Presence of Pyridine**

Based on the CV findings, we propose the following mechanism for this transformation (Scheme 1.6.3). When the photosensitizer is in its excited state, the persulfate is reduced to $SO_4^{2-}$

anion and the corresponding $SO_4^{\cdot-}$ anion radical. The corresponding benzothiazole in the presence of pyridine is in the same range as the ground-state photosensitizer, resulting in an oxidation of sulfur to a radical cation. This is followed by a rapid radical cyclization to give the corresponding cyclized radical intermediate which is then oxidized again potentially by the persulfate anion radical giving a Wheland-type intermediate that undergoes rearomatization to generate the desired benzothiazole. This proposed mechanism is also further validated by computational evidence (Scheme 1.6.4).

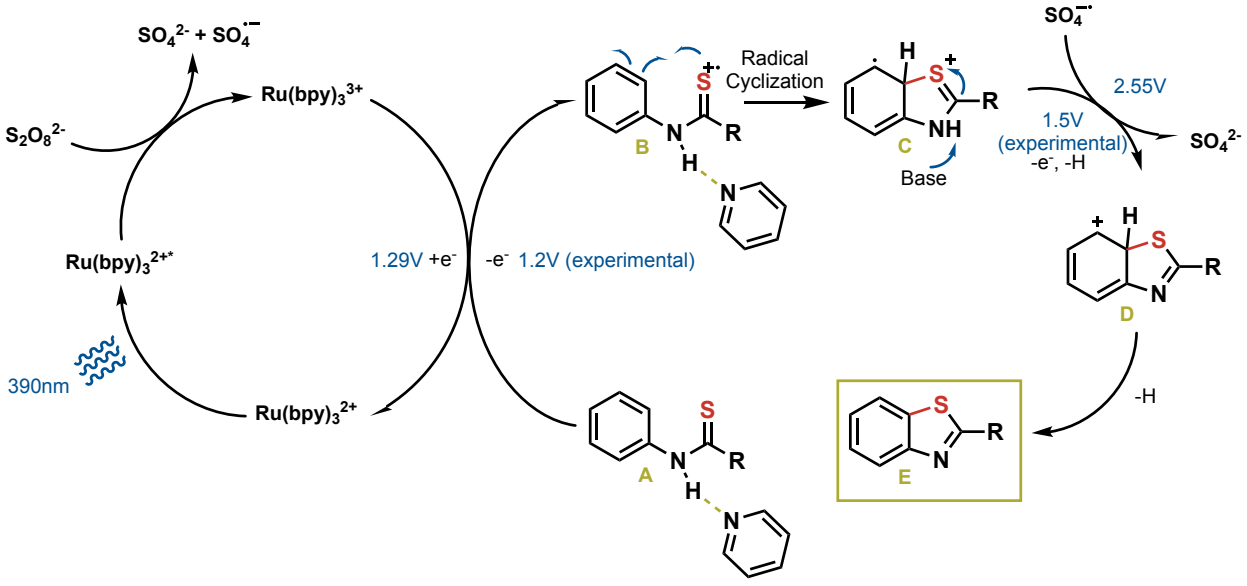


**Scheme 1.6.3 Proposed Mechanism for Intramolecular Thiolation**

Density Functional Theory (DFT) calculations were implemented to predict the electron density maps for several benzothioamide intermediates to predict favorable sites of oxidation (Scheme 1.6.4). In map **A**, there is a larger concentration of electron density at the sulfur compared to the rest of the compound, which implies that the initial oxidation will occur there. This finding is also supported by work by Nicewicz and coworkers regarding allylic thioamides.[83, 84] Once formed, intermediate **B** will rapidly undergo cyclization to **C** which is supported by the CV

findings where the second oxidation potential of the benzothioamide diminishes at higher scan rates. A possible explanation for this is that there is possibly a new intermediate that is formed between the first and second oxidation potential (*i.e* radical thioamide cyclization step), thus the increased scan rate applied to the system can outcompete reaction which will hinder a subsequent oxidation (Scheme 1.6.2). Additionally, the electron density has shifted from sulfur to the aryl ring, which may suggest the likelihood of the aryl ring acting as the nucleophile attacking the more electron deficient sulfur during the cyclization step. The persulfate can then promote the formation of a thiyl radical cation as seen in map **D** which then undergoes rearomatization to form the corresponding benzothiazole.

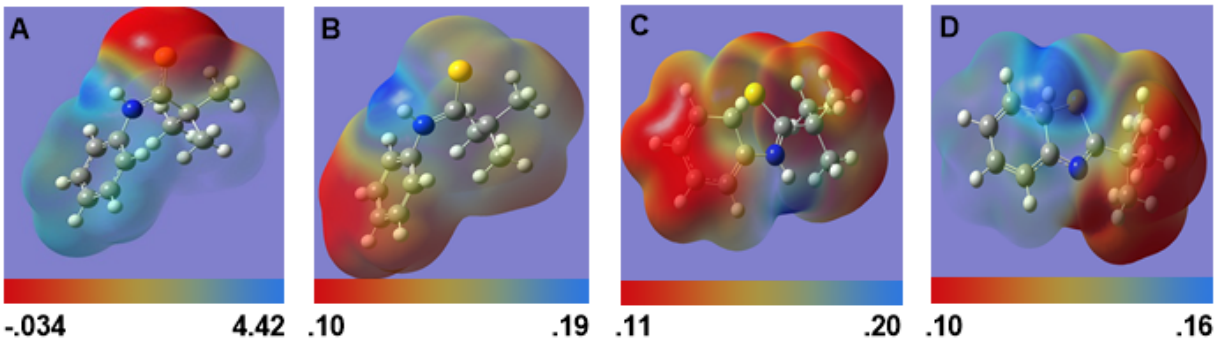


**Scheme 1.6.4 Electron Density Maps of Predicted Intermediates**

While concurrently working on the benzothiazole formation, we also wanted to explore if this methodology can be amenable for an intermolecular C-H thiolation applied to other arenes specifically, more electron-rich heteroarenes such as indoles. Our initial experiment was performed on melatonin (**1.18a**) using the optimal conditions for the benzothiazole formation, without the addition of pyridine, and 4-methyllthiophenol as the sulfenylation source yielded 29% of **1.18b** (Table 1.6.2, entry 1). Upon the addition of pyridine (Table 1.6.2, entry 2 and 3), we observed similar trends in increased yields to 31% and 40% for one and two equivalents of pyridine respectively. As a control, when removing the photosensitizer we observed a significant decrease

in conversion to 8% (Table 1.6.2, entry 4), however as mentioned previously there is still a background reaction due to the presence of persulfate. When reducing the equivalents of persulfate in the presence of the photosensitizer, we observed a similar decrease in conversion (Table 1.6.2, entry 5) to 5%. As expected, when removing the persulfate altogether we do not observe the formation of **1.18b** (Table 1.6.2, entry 6). Similar trends to the benzothiazole formation were observed when increasing the amount of MeCN used (Table 1.6.2, entry 7 and 8), we noticed a decrease in conversion to 30% in 9:1 MeCN: $H_2O$ and 15% in only MeCN. When evaluating other photosensitizers (Table 1.6.2, entry 9-11) we observed that $Ir[dF(CF_3)ppy]_2(dtbpy)]PF_6$ was more amenable for this transformation yielding 52% compared to the ruthenium photosensitizer. Interestingly, trace amounts of disulfenylated side product **1.18c** were observed suggesting that at some point over prolonged periods of reaction time, the thiol reagent (or product sulfide) is reacting with a second equivalent of thiol. Finally, we explored several exogenous bases as the addition of pyridine was found to increase the conversion of the reaction. The addition of potassium phosphate dibasic (Table 1.6.2, entry 12) yielded 61%, however potassium phosphate tribasic (Table 1.6.2, entry 13) yielded 28% of **1.18b**. It was observed that the addition of potassium hydroxide (Table 1.6.2, entry 14) gave the best results yielding 68% of sulfenylated melatonin.

**Table 1.6.2 Optimization of Intermolecular Sulfenylation of Melatonin**

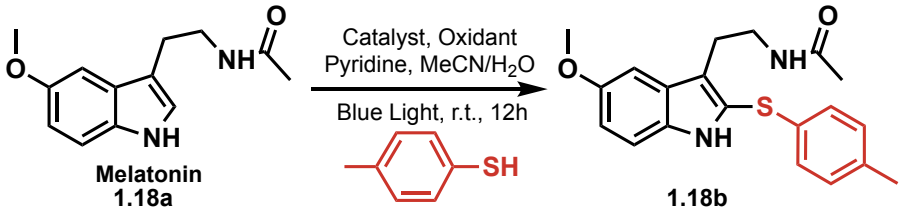


| Entry | Catalyst | Oxidant (equiv) | Solvent | Base (equiv) | Yield (%) |
|---|---|---|---|---|---|
| 1 | $Ru(bpy)_3Cl_2$ | $Na_2S_2O_8$ (2) | $CH_3CN/H_2O$ (1:1) | Pyridine (0) | 29 |
| 2 | $Ru(bpy)_3Cl_2$ | $Na_2S_2O_8$ (2) | $CH_3CN/H_2O$ (1:1) | Pyridine (1) | 31 |
| 3 | $Ru(bpy)_3Cl_2$ | $Na_2S_2O_8$ (2) | $CH_3CN/H_2O$ (1:1) | Pyridine (2) | 40 |
| 4 | None | $Na_2S_2O_8$ (2) | $CH_3CN/H_2O$ (1:1) | Pyridine (2) | 8 |
| 5 | $Ru(bpy)_3Cl_2$ | $Na_2S_2O_8$ (1) | $CH_3CN/H_2O$ (1:1) | Pyridine (2) | 5 |
| 6 | $Ru(bpy)_3Cl_2$ | None | $CH_3CN/H_2O$ (1:1) | Pyridine (2) | 0 |
| 7 | $Ru(bpy)_3Cl_2$ | $Na_2S_2O_8$ (2) | $CH_3CN/H_2O$ (9:1) | Pyridine (2) | 30 |
| 8 | $Ru(bpy)_3Cl_2$ | $Na_2S_2O_8$ (2) | $CH_3CN$ | Pyridine (2) | 15 |
| 9 | CzIPN | $Na_2S_2O_8$ (2) | $CH_3CN/H_2O$ (1:1) | Pyridine (2) | 25 |
| 10 | 9-Mesi-Acri | $Na_2S_2O_8$ (2) | $CH_3CN/H_2O$ (1:1) | Pyridine (2) | 8 |
| 11 | Ir{df($CF_3$)... | $Na_2S_2O_8$ (2) | $CH_3CN/H_2O$ (1:1) | Pyridine (2) | 52 |
| 12 | Ir{df($CF_3$)... | $K_2S_2O_8$ (2) | $CH_3CN/H_2O$ (1:1) | $K_2HPO_4$ (2) | 61 |
| 13 | Ir{df($CF_3$)... | $(NH_4)_2S_2O_8$ (2) | $CH_3CN/H_2O$ (1:1) | $K_3PO_4$ (2) | 28 |
| 14 | Ir{df($CF_3$)... | $(NH_4)_2S_2O_8$ (2) | $CH_3CN/H_2O$ (1:1) | KOH (2) | 68 |

With optimized conditions in hand, we next evaluated several substituted, electron-neutral and rich indoles where we reported isolated yields of sulfenylated product as well as disulfenylated product when applicable. A majority of the substrates (Scheme 1.6.5, **1.19**-**1.27**, excluding **1.20**) provided exclusively the monosulfenylated product between 9 – 36% yield. However, similar to melatonin, *N*-methyl-3-methyl indole **1.20** gave a mixture of mono sulfenylated **1.20b** and disulfenylated **1.20c** product in 28% and 14% respectively. Additionally, we also tested different arylthiols, varying the electronics, to observe its effect. We observed attenuated yields of **1.25b**-

**1.17b** of 16-31% yields. While this methodology on electron-neutral and rich indoles is not as robust as other conditions, including traditional $S_EAr$, it is important to note the ability to sulfenylate biologically relevant indoles such as melatonin and tryptophan, which is considered LSF viable on more simplified molecules. While these conditions are similar to the previously mentioned benzothiazole formation, interestingly we offer evidence of a divergent mechanism.

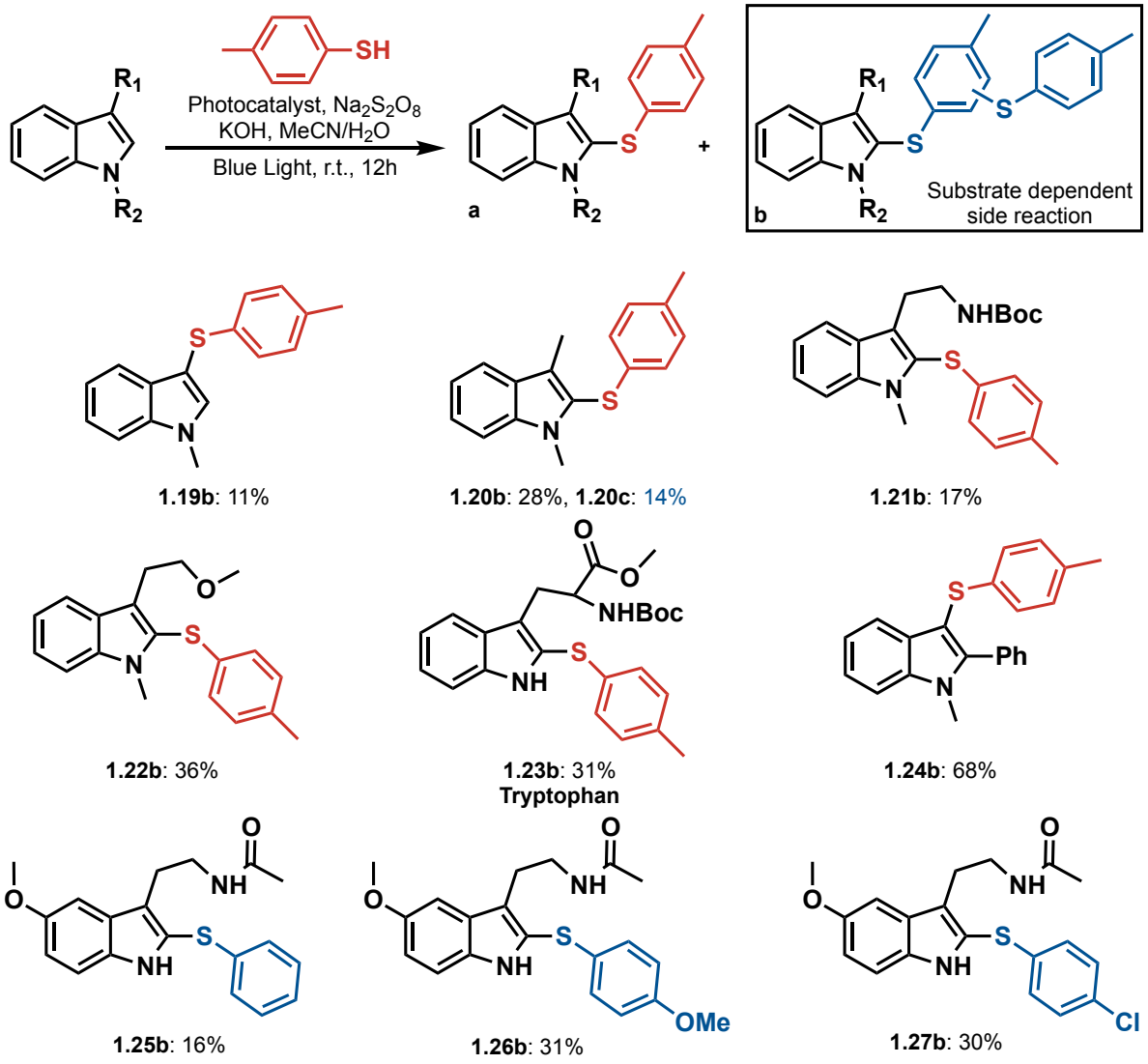


**Scheme 1.6.5 Indole Sulfenylation Substrate Scope**

In order to elucidate the mechanism, we first wanted to determine the redox potentials of melatonin and 4-methylbenzenethiol (see following experimental section, Figures 1.6.71 and

1.6.72). It was found that melatonin has two half wave oxidation potentials at 1.1V vs. SCE and 1.2V vs. SCE, while 4-methylbenzenethiol has two half wave oxidation potentials at 1.5V vs. SCE and 1.8V vs. SCE. Based on the excited state of the iridium photosensitizer, as previously mentioned earlier, only melatonin falls within that range suggesting that the initial oxidation most likely occurs at melatonin. Stern-Vollmer quenching studies of the iridium photosensitizer with melatonin and 4-methylbenzenethiol also supports this hypothesis as melatonin was found to be quenched ($K_{sv}$ = 4.2 $M^{-1}L$) at a higher rate than the thiol ($K_{sv}$ = 0.1$M^{-1}L$) (Scheme 1.6.6). Additionally, we ran the photocatalytic reaction without the presence of indole and observed a significant amount of disulfide byproduct, which is known to undergo a homolytic cleavage under photo-conditions to form thiyl radicals (see following experimental section, Scheme 1.7.1).[85] Thus, we next set to evaluate if formation of the disulfide was indeed an intermediate in this methodology by using 4-methyldiphenyldisulfude as the sulfur source. We observed comparable yields to that of the thiophenol in the reaction with melatonin, and additional Stern Vollmer quenching studies of the photocatalyst revealed that the disulfide was quenched ($K_{sv}$ = 0.6 $M^{-1}L$) at a slightly higher rate than the corresponding 4-methylbenzenethiol ($K_{sv}$ = 0.1 $M^{-1}L$), but still significantly less than melatonin. To confirm this finding we ran additional cross experiments using both 4-methylbenzene thiol and phenyldisulfide, and we observed dominant formation of the thiolated indole with 4-methybenzenthiol via mass spectrometry (Scheme 1.7.1).

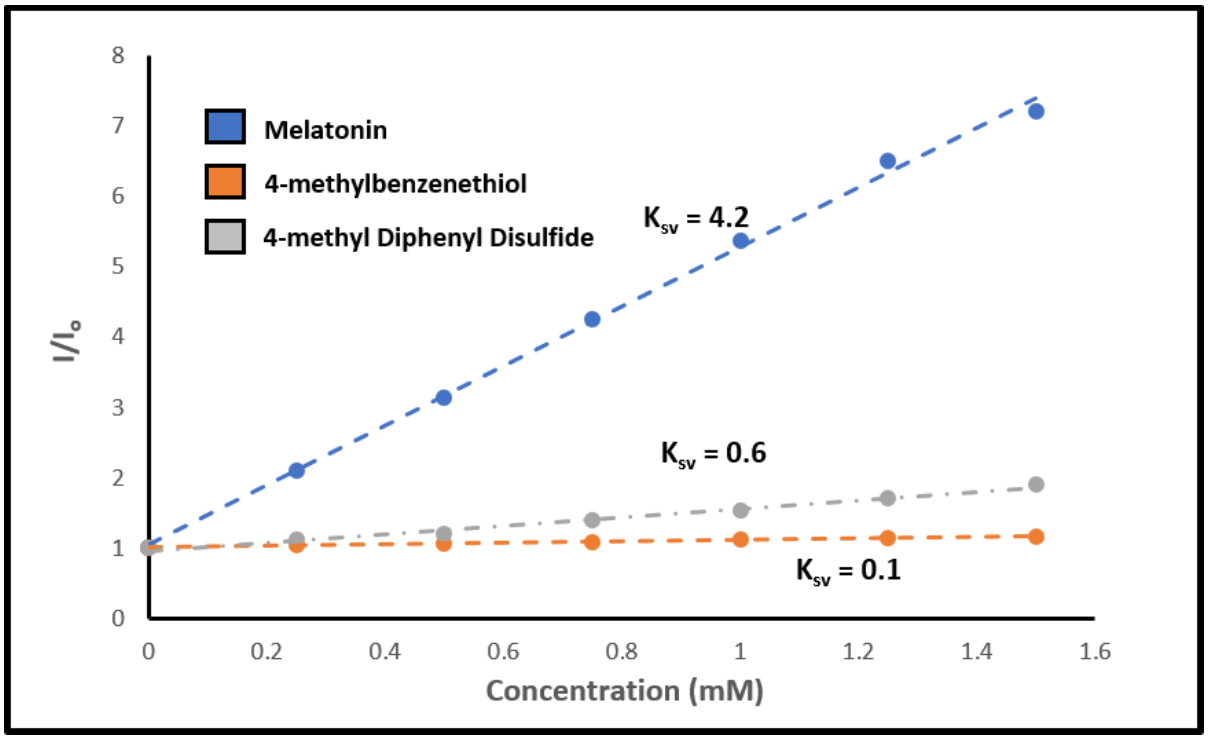


**Scheme 1.6.6 Stern-Vollmer Quenching Studies of [Ir[df(CF3)ppy]2(dtbpy)]PF6 with Melatonin, 4-Methylbenzenethiol, and 4-Methyldiphenyldisulfide**

Based on our mechanistic findings, we are proposing two plausible, simultaneous mechanisms that can occur. Upon excitation of the iridium photosensitizer, melatonin A will initially be oxidized to the radical cation where, in pathway 1, 4-methylbenzenethiol can be deprotonated by potassium hydroxide which then can nucleophilically add onto the oxidized melatonin to form B'. From here, a subsequent oxidation from persulfate followed by a rearomatization event will form the sulfenylated product C. Alternatively we also propose, in pathway 2, that under photocatalytic conditions 4-methylbenzenethiol can form the corresponding disulfide which can be homolytically dissociated to generate a thiyl radical that can couple with A to form a Wheland intermediate B". This is followed by a subsequent deprotonation and rearomatization to form the desired sulfenylated product. While both mechanisms may be plausible

for this transformation, we believe that the nucleophilic addition, pathway 1, is predominant based on our Stern-Vollmer studies and crossover experiments.

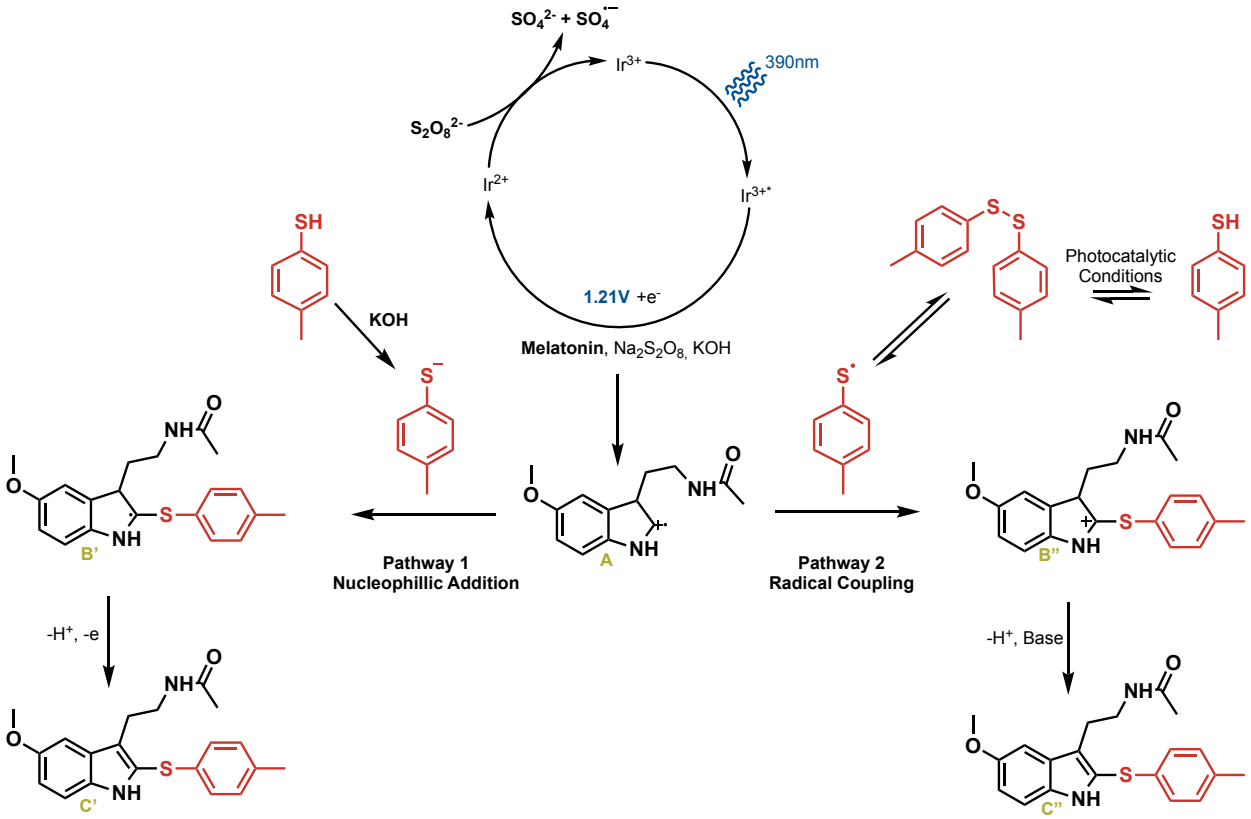


**Scheme 1.6.7 Proposed Mechanism for Intermolecular Indole Sulfenylation**

In conclusion, we have developed a simplified procedure to synthesize benzothiazoles intramolecularly from its corresponding benzothioamide as well sulfenylating electron-neutral and rich indoles using arylthiols. While this methodology encompasses both reactions, based on our mechanistic investigation we offer evidence to support divergent activity that produces a nucleophilic or electrophilic thiyl radical species in the two reactions.

## 1.7 Experimental Section

### 1.7.1 General Information

All $^{1}H$ and $^{13}C$ NMR Spectra were recorded on Varian VNMRS 400MHz, Bruker Avance $AV_1$ 400MHz and a Varian Inova 500MHz. All chemical shifts were reported in parts per million (δ) and internally referenced to residual solvent proton signals unless otherwise noted. All spectral data were reported as follows: (multiplicity [singlet (s), doublet (d), doublet of doublets (dd), doublet of doublet of doublets (ddd), doublet of triplets (dt), triplet (t), triplet of triplets (tt), quartet (q), quintet (qn), and multiplet (m), heptet (h)], coupling constants [Hz], integration). Carbon spectra were recorded with complete decoupling. Conventional mass spectra were obtained using Advion Expression$^{s}$ CMS APCI/ASAP. All chemicals and catalysts were purchased from Acros Organics, Cambridge Isotope Laboratories, Fisher Scientific, Frontier Scientific, Oakwood Chemicals, Sigma Aldrich, or TCI America. All normal phase flash column chromatography (FCC) was performed using Grade 60 Silica Gel (230-400 mesh) purchased from Fisher Scientific. Preparative Thin Layer Chromatography (TLC) plates contained grade 60 silica gel coated with fluorescent indicator $F_{254}$ and were purchased from Fisher Scientific. Reflux conditions were done using an Anton Paar Monowave 400, G10, and G30 vials.

### 1.7.2 Abbreviations

**Conc.**: Concentration (M)

**DCM**: Methylene Chloride

**Eq.**: Equivalent

**$Et_3N$**: Triethylamine

**EtOAc**: Ethyl Acetate

**FCC**: Flash Column Chromatography

**Hex**: Hexanes

**$H_2O$**: Deionized Water

**HCl**: Hydrochloric Acid

**HSPh**: Thiophenol

**$Ir[dF(CF_3)ppy]_2(dtbpy)]PF_6$:**[4,4′-*Bis*(1,1-dimethylethyl)-2,2′-bipyridine-*N*1,*N*1′]*bis*[3,5-difluoro-2-[5-(trifluoromethyl)-2-pyridinyl-*N*]phenyl-C]Iridium(III) hexafluorophosphate

**MeCN**: Acetonitrile

**$Na_2SO_4$**: Sodium Sulfate

**r.t**: Room Temperature

**$Ru(bpy)_3Cl_2•6H_2O$**:Tris(2,2'-bipyridyl)dichlororuthenium(II) hexahydrate

**SM** - Starting Material

### 1.7.3 Experimental Procedures

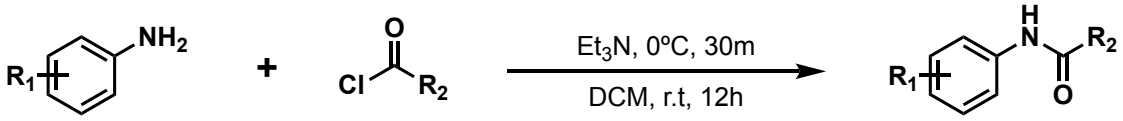


**Scheme 1.7.1 Preparation of substituted benzamides**

A solution of substituted aniline (1.0 eq.) and $Et_3N$ (1.5 eq.) in DCM (0.1M) was prepared and stirred at 0 ºC for 30 minutes. Acyl chloride (1.0 eq.) was then added drop wise. The mixture was warmed to room temperature and stirred additionally for 12 hours. The resulting solution was then quenched with 2 M HCl and extracted with two equal volumes of DCM before being dried over $Na_2SO_4$. Evaporation of solvent gave crude product that was purified by FCC using a 4:1 Hex: EtOAc gradient.

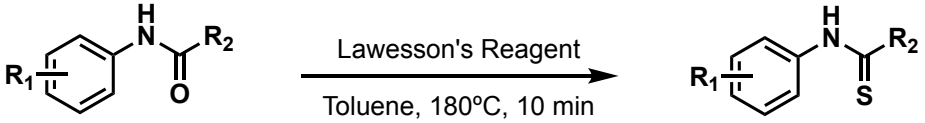


**Scheme 1.7.2 Preparation of substituted thiobenzamides**

A solution of benzamide (1.0 eq.), Lawesson's reagent (0.6 eq.), and toluene (0.1M) were added to either a G10 or G30 microwave vial and was heated to 180ºC for 10 minutes in the

microwave. The resulting solution was then concentrated down and purified by FCC using a 4:1 Hex: EtOAc gradient.

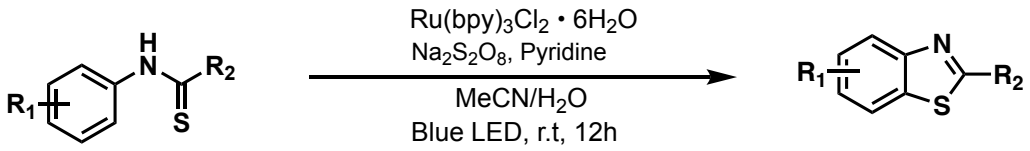


**Scheme 1.7.3 Preparation of substituted benzothiazoles**

In a 2 dram vial, substituted thiobenzamide (1.0 eq.), $Ru(bpy)_3Cl_2$ (2.0 mg, 0.05 eq.), sodium persulfate (2.0 eq.), and pyridine (B only, 2.0 eq.) were added to a solution of 1:1 MeCN:$H_2O$ (25 mg/1mL). The reaction was left to stir under blue LEDs for 12 hours at room temperature. The resulting solution was then quenched with $H_2O$, extracted with EtOAc and dried over $Na_2SO_4$. Evaporation of solvent gave crude product that was purified by prep TLC with a gradient from hexanes to 8:2 hexanes:EtOAc.

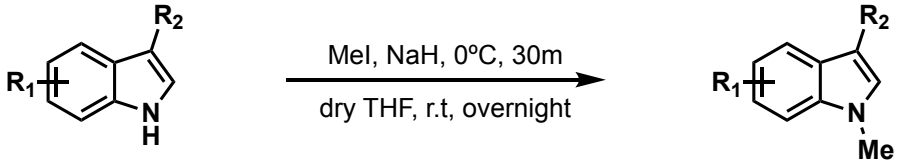


**Scheme 1.7.4 Preparation of N-methylated indoles**

NaH (2.0 eq.) was added in a round bottom flask with anhydrous THF (1M) under inert atmosphere at 0ºC. A solution of substituted indole (1.0 eq.) and anhydrous THF was then added to the mixture, and the reaction was warmed to room temperature and stirred overnight. The resulting solution was then quenched with 2M HCl, washed with EtOAc, and dried over $Na_2SO_4$. Evaporation of solvent gave crude N-methylated indole that was purified by FCC.

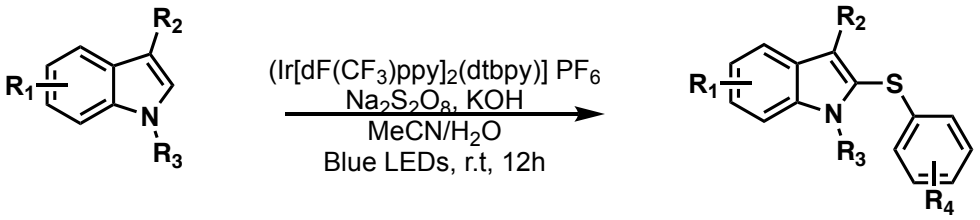


**Scheme 1.7.5 Preparation of sulfenylated indoles**

In a 10mL vial, substituted indole (1.0 eq.), (Ir[dF($CF_3$)ppy]$_2$(dtbpy)]$PF_6$ (0.01 eq.), sodium persulfate (2.0 eq.), KOH (2.0 eq.), and 4-methylthiophenol (1.0 eq.) were added to a solution of 1:1 MeCN: $H_2O$ (25mg/1mL). The reaction was left to stir under blue LEDs for 12 hours at room temperature. The resulting solution was then quenched with $H_2O$ and extracted with DCM before being dried over $Na_2SO_4$. Evaporation of solvent gave crude product that was purified by prep TLC (9:1 Hex: EtOAc (**1.19b-1.23b**), 9:1 Hex: DCM (**1.20b**), or 10:0 Hex (**1.24b**)). Melatonin substrates were purified via FCC (8:2 EtOAc: Hex)

### 1.7.4 Characterization of Substituted Benzothiazoles

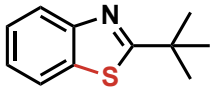


**Figure 1.7.1 Product 1.1b**

**2-(*tert*-butyl)benzo[*d*]thiazole:** Compound was synthesized using the general procedures for synthesizing the substituted benzamide, substituted thiobenzamide, and substituted benzothiazole. **Yields** (0.129 mmol scale): No Pyridine- 14.2mg, 57% & Pyridine- 19.8mg, 79%, off white solid. **$^1$H NMR (500MHz, $CDCl_3$)** δ= 8.00 (dt, J= 8.2, 0.9Hz, 1H), 7.85 (dd, J= 8.0, 0.45Hz, 1H), 7.44 (ddd, J= 8.3, 7.2, 1.3Hz, 1H), 7.34 (ddd, J= 8.2, 7.2, 1.2Hz, 1H), 1.53 (s, 9H). The spectral data is in agreement with the reported literature: Zhang, G.; Liu, C.; Yi, H.; Meng, Q.; Bian, C.; Chen, H.; Jian, J. X.; Wu, L. Z.; Lei, A. *J. Am. Chem. Soc.* **2015**, *137*, 9273-9280. **MS-APCI Calculated:** $C_{11}H_{13}NS$ $[M+H]^+$ 192.3, Found: 192.1 m/z

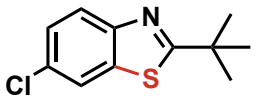


**Figure 1.7.2 Product 1.2b**

**2-(*tert*-butyl)-6-chlorobenzo[*d*]thiazole:** Compound was synthesized using the general procedures for synthesizing the substituted benzamide, substituted thiobenzamide, and substituted benzothiazole. **Yields** (0.110 mmol scale): No Pyridine- 7.0mg, 28% & Pyridine- 12.2mg, 49%, off white solid. **$^1$HNMR (500MHz, $CDCl_3$)** δ= 7.88 (dd, J= 8.7, 0.5Hz, 1H), 7.82 (dd, J= 2.1, 0.5, 1H), 7.44 (dd, J= 8.7, 2.1Hz, 1H), 1.51 (s, 9H). The spectral data is in agreement with the reported literature: Zhang, G.; Liu, C.; Yi, H.; Meng, Q.; Bian, C.; Chen, H.; Jian, J. X.; Wu, L. Z.; Lei, A. *J. Am. Chem. Soc.* **2015**, *137*, 9273-9280. **MS-APCI Calculated:** $C_{11}H_{12}ClNS$ $[M+H]^+$ 226.7, Found: 226.2, 226.4 m/z

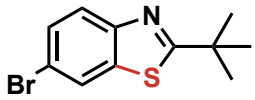


**Figure 1.7.3 Product 1.3b**

**6-bromo-2-(*tert*-butyl)benzo[*d*]thiazole**: Compound was synthesized using the general procedures for synthesizing the substituted benzamide, substituted thiobenzamide, and substituted benzothiazole. **Yields** (0.092 mmol scale): No pyridine- 9.2mg, 37% & Pyridine- 15.5mg, 62%, off white solid. **$^1$HNMR** (500MHz, $CDCl_3$) δ= 7.98 (dd, J= 2.0, 0.5Hz, 1H), 7.83 (dd, J= 8.7, 0.5Hz, 1H), 7.54 (dd, J= 8.7, 2.0Hz, 1H), 1.51 (s, 9H). The spectral data is in agreement with the reported literature: Zhang, G.; Liu, C.; Yi, H.; Meng, Q.; Bian, C.; Chen, H.; Jian, J. X.; Wu, L. Z.; Lei, A. *J. Am. Chem. Soc.* **2015**, *137*, 9273-9280. **MS-APCI Calculated:** $C_{11}H_{12}BrNS$ $[M+H]^+$ 271.2, Found: 271.0, 271.2, 271.3 m/z

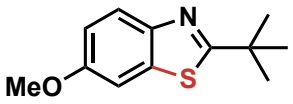


**Figure 1.7.4 Product 1.4b**

**2-(*tert*-butyl)-6-methoxybenzo[*d*]thiazole**: Compound was synthesized using the general procedures for synthesizing the substituted benzamide, substituted thiobenzamide, and substituted benzothiazole. **Yields** (0.112 mmol scale): No pyridine- 9.0mg, 36% & Pyridine- 15.8mg, 63%, off white solid. **$^1$HNMR (500MHz, $CDCl_3$)** δ= 7.86 (dd, J= 8.9, 0.5Hz, 1H), 7.31 (d, J= 2.6Hz, 1H), 7.04 (dd, J= 8.9, 2.6Hz, 1H), 3.87 (s, 3H), 1.50 (s, 9H). The spectral data is in agreement with the reported literature: Zhang, G.; Liu, C.; Yi, H.; Meng, Q.; Bian, C.; Chen, H.; Jian, J. X.; Wu, L. Z.; Lei, A. *J. Am. Chem. Soc.* **2015**, *137*, 9273-9280. **MS-APCI Calculated:** $C_{12}H_{15}NOS$ $[M+H]^+$ 222.3, Found: 222.0 m/z

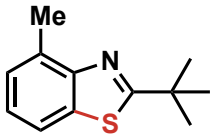


**Figure 1.7.5 Product 1.5b**

**2-(*tert*-butyl)-4-methylbenzo[*d*]thiazole**: Compound was synthesized using the general procedures for synthesizing the substituted benzamide, substituted thiobenzamide, and substituted benzothiazole. **Yields** (0.121 mmol scale): No pyridine- 9.8mg, 39% & Pyridine- 14.8mg, 59%, slight pink solid. **$^1$HNMR (500MHz, $CDCl_3$)** δ= 7.69-7.66 (m, 1H), 7.25-7.20 (m, 2H), 2.75 (s, 3H), 1.52 (s, 9H). The spectral data is in agreement with the reported literature: Zhang, G.; Liu, C.; Yi, H.; Meng, Q.; Bian, C.; Chen, H.; Jian, J. X.; Wu, L. Z.; Lei, A. *J. Am. Chem. Soc.* **2015**, *137*, 9273-9280. **MS-APCI Calculated:** $C_{12}H_{15}NS$ $[M+H]^+$ 206.3, Found: 206.2

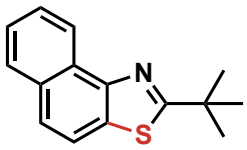


**Figure 1.7.6 Product 1.6b**

**2-(*tert*-butyl)napthol[1,2-*d*]thiazole**: Compound was synthesized using the general procedures for synthesizing the substituted benzamide, substituted thiobenzamide, and substituted benzothiazole. **Yields** (0.103 mmol scale): No pyridine- 13.8mg, 55% & Pyridine- 13.5mg, 54%, yellow-green solid. **$^{1}$HNMR (500 MHz, $CDCl_3$)** δ= 8.82 (dt, J= 8.0, 0.8Hz, 1H), 7.93 (d, J= 8.1Hz, 1H), 7.87 (d, J= 8.7Hz, 1H), 7.75 (d, J= 8.7Hz, 1H), 7.65 (ddd, J= 8.2, 6.9, 1.3Hz, 1H), 7.55 (ddd, J=8.2, 6.9, 1.3Hz, 1H), 1.59 (s, 9H). **$^{13}$CNMR (101Hz, $CDCl_3$)** δ= 180.7, 149.2, 131.8, 131.2, 128.6, 127.9, 126.6, 125.7, 125.0, 124.0, 119.0, 38.4, 31.0. **MS-APCI Calculated:** $C_{15}H_{15}NS$ $[M+H]^+$: 242.4 Found: 242.1 m/z

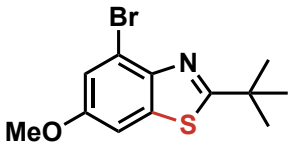


**Figure 1.7.7 Product 1.7b**

**4-bromo-2-(*tert*-butyl)-6-methoxybenzo[*d*]thiazole**: Compound was synthesized using the general procedures for synthesizing the substituted benzamide, substituted thiobenzamide, and substituted benzothiazole. **Yields** (0.083 mmol scale): No pyridine- 8.0mg, 32% & Pyridine- 8.5mg, 34%, slight pink solid. **$^{1}$HNMR (500 MHz, $CDCl_3$)** δ= 7.87 (d, J= 8.8Hz, 1H), 7.07 (d, J= 8.9Hz, 1H), 3.97 (s, 3H), 1.51 (s, 9H). **$^{13}$CNMR (101Hz, $CDCl_3$)** δ= 170.59, 157.34, 146.03, 136.69, 118.13, 115.79, 103.88, 56.02, 36.22, 29.68, 23.34, 13.74. **MS-APCI Calculated:** $C_{12}H_{14}BrNOS$ $[M+H]^+$: 301.2, Found: 301.0, 301.2, 300.5 m/z

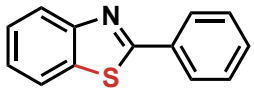


**Figure 1.7.8 Product 1.8b**

**2-phenylbenzo[*d*]thiazole**: Compound was synthesized using the general procedures for synthesizing the substituted benzamide, substituted thiobenzamide, and substituted benzothiazole. **Yields** (0.117 mmol scale): No pyridine- 4.3mg, 17% & Pyridine- 8.0mg, 32%, yellow-green solid. **$^1$HNMR** (500 MHz, $CDCl_3$) δ= 8.13-8.07 (m, 3H), 7.92 (d, J= 8.0Hz. 1H), 7.53-7.46 (m, 4H), 7.39 (ddd, J= 8.3, 7.1, 1.2Hz, 1H). The spectral data is in agreement with the reported literature: Zhang, G.; Liu, C.; Yi, H.; Meng, Q.; Bian, C.; Chen, H.; Jian, J. X.; Wu, L. Z.; Lei, A. *J. Am. Chem. Soc.* **2015**, *137*, 9273-9280. **MS-APCI Calculated:** $C_{13}H_9NS$ $[M+H]^+$: 212.3, Found: 212.1 m/z

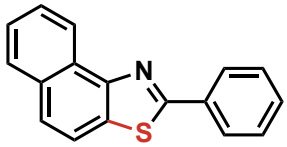


**Figure 1.7.9 Product 1.9b**

**2-phenylnaptho[1,2-*d*]thiazole**: Compound was synthesized using the general procedures for synthesizing the substituted benzamide, substituted thiobenzamide, and substituted benzothiazole. **Yields** (0.095 mmol scale): No pyridine- 13.8mg, 55% & Pyridine- 13.5mg, 54%, dark green solid. **$^1$HNMR (400 MHz, $CDCl_3$)** δ= 8.93 (ddt, J=8.3, 1.4, 0.7Hz, 1H), 8.24-8.18 (m, 2H), 7.99-7.90 (m, 2H), 7.82 (dt, J= 8.7, 0.6Hz, 1H), 7.70 (ddd, J= 8.2, 6.9, 1.3Hz, 1H), 7.60 (ddd, J= 8.2, 6.9, 1.3Hz, 1H), 7.57-7.46 (m, 3H). The spectral data is in agreement with the reported literature: Zhang, G.; Liu, C.; Yi, H.; Meng, Q.; Bian, C.; Chen, H.; Jian, J. X.; Wu, L. Z.; Lei, A. *J. Am. Chem. Soc.* **2015**, *137*, 9273-9280. **MS-APCI Calculated:** $C_{17}H_{11}NS$ $[M+H]^+$: 262.3, Found: 262.2 m/z

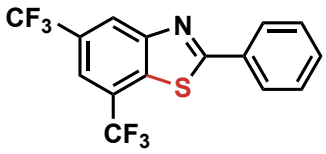


**Figure 1.7.10 Product 1.10b**

**2-phenyl-5,7-bis(trifluoromethyl)benzo[*d*]thiazole**: Compound was synthesized using the general procedures for synthesizing the substituted benzamide, substituted thiobenzamide, and substituted benzothiazole. **Yields** (0.072 mmol scale): No pyridine- 14.3mg, 57% & Pyridine- 17.0mg, 68%, yellow solid. **$^1$HNMR** (400 MHz, $CDCl_3$) δ= 8.5 (s, 1H), 8.16-8.12 (m, 2H), 7.91 (s, 1H), 7.59-7.52 (m, 3H). The spectral data is in agreement with the reported literature: Folgueiras-Amador, A. A.; Qian, X. Y.; Xu, H. C.; Wirth, T. *Chem. Eur. J.* **2018**, *24*, 487-491. **MS-APCI Calculated:** $C_{15}H_7F_6NS$ $[M+H]^+$: 348.3, Found: 348.1 m/z

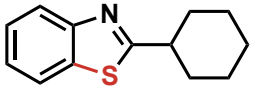


**Figure 1.7.11 Product 1.11b**

**2-cylcohexylbenzo[*d*]thiazole**: Compound was synthesized using the general procedures for synthesizing the substituted benzamide, substituted thiobenzamide, and substituted benzothiazole. **Yields** (0.114 mmol scale): No pyridine- 9.5mg, 38% & Pyridine- 13.8mg, 55%, off white solid. **$^1$HNMR (500 MHz, $CDCl_3$)** δ= 7.99-7.96 (m, 1H), 7.85 (ddd, J= 8.0, 1.3, 0.6Hz, 1H), 7.44 (ddd, J= 8.2, 7.2, 1.2Hz, 1H), 7.34 (ddd, J= 8.3, 7.2, 1.2Hz, 1H), 3.11 (tt, J= 11.7, 3.6Hz, 1H), 2.25-2.17 (m, 2H), 1.89 (dt, J= 12.8, 3.5Hz, 2H), 1.77 (dd, J= 12.7, 3.2, 1.6Hz, 1H), 1.70-1.58 (m, 2H), 1.45 (qt, J= 12.4, 3.3Hz, 2H), 1.34 (tt, J= 12.4, 3.2Hz, 1H). The spectral data is in agreement with the reported literature: Zhang, G.; Liu, C.; Yi, H.; Meng, Q.; Bian, C.; Chen, H.; Jian, J. X.; Wu, L. Z.; Lei, A. *J. Am. Chem. Soc.* **2015**, *137*, 9273-9280. **MS-APCI Calculated:** $C_{13}H_{15}NS$ $[M+H]^+$: 218.3, Found: 218.3 m/z

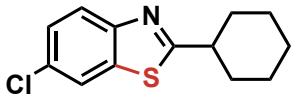


**Figure 1.7.12 Product 1.12b**

**6-chloro-2-cyclohexylbenzo[*d*]thiazole**: Compound was synthesized using the general procedures for synthesizing the substituted benzamide, substituted thiobenzamide, and substituted benzothiazole. **Yields** (0.099 mmol scale): No pyridine- 13.8mg, 55% & Pyridine 18.3mg, 73%, off white solid. **$^{1}$HNMR (500 MHz, $CDCl_3$)** δ= 7.87 (d, J= 8.7Hz, 1H), 7.82 (d, J= 1.9Hz, 1H), 7.40 (d, J= 13.3, 3.5Hz, 2H), 3.09 (tt, J= 11.6, 3.6Hz, 1H), 2.23-2.16 (m, 2H), 1.89 (dt, J= 13.3, 3.5Hz, 2H), 1.77 (dtt, J= 12.8, 3.2, 1.5Hz, 1H), 1.68-1.57 (m, 2H), 1.44 (qt, J= 12.7, 3.4Hz, 2H), 1.33 (tt, J=12.4, 3.4Hz, 1H). **$^{13}$CNMR (101Hz, $CDCl_3$)** δ= 178.11, 151.65, 135.75, 130.34, 126.53, 123.25, 121.13, 43.36, 33.30, 25.97, 25.70. **MS-APCI Calculated:** $C_{13}H_{14}ClNS$ $[M+H]^+$: 252.8, Found: 252.3, 252.5 m/z

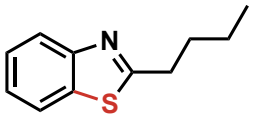


**Figure 1.7.13 Product 1.13b**

**2-propylbenzo[*d*]thiazole**: Compound was synthesized using the general procedures for synthesizing the substituted benzamide, substituted thiobenzamide, and substituted benzothiazole. **Yields** (0.129 mmol scale): No pyridine- 13.8mg, 55% & Pyridine- 18.0mg, 72%, orange oil. **$^{1}$HNMR (500 MHz, $CDCl_3$)** δ= 7.99-7.95 (m, 1H), 7.86-7.82 (m, 1H), 7.45 (ddd, J= 8.2, 7.3, 1.3Hz, 1H), 7.37-7.32 (m, 1H), 3.13-3.06 (m, 2H), 1.92 (m, 2H), 1.06 (t, J= 7.4, 3H). The spectral data is in agreement with the reported literature: Vechorkin, O.; Proust, V.; Hu, X. *Angew. Chem. Int. Ed.* **2010**, *49*. 3061-3064. **MS-APCI Calculated:** $C_{11}H_{13}NS$ $[M+H]^+$: 192.3, Found: 192.2 m/z

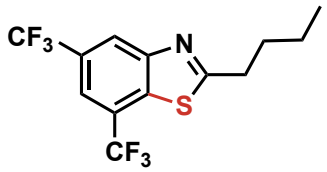


**Figure 1.7.14 Product 1.14b**

**2-propyl-5,7-bis(trifluoromethyl)benzo[*d*]thiazole**: Compound was synthesized using the general procedures for synthesizing the substituted benzamide, substituted thiobenzamide, and substituted benzothiazole. **Yields** (0.076 mmol scale): No pyridine- 11.8mg, 47% & Pyridine- 14.0mg, 56%, orange solid. **$^{1}$HNMR (500 MHz, $CDCl_3$)** δ= 8.40 (s, 1H), 7.88 (s, 1H), 3.19-3.13 (m, 2H), 1.96 (m, 2H, 1.09 (t, J= 7.4Hz, 3H). **$^{13}$CNMR (126 MHz, $CDCl_3$)** δ= 176.06, 154.58, 135.41, 128.85 (q, J= 33.9), 125.36 (q, J= 35.1), 124.34 (d, J= 60.7), 123.03 (m), 122.18 (d, J= 61.1), 118.75 (h), 36.08, 22.81, 13.65. **$^{19}$FNMR (470 MHz, $CDCl_3$)** δ= -61.11, -62.78. **MS-APCI Calculated:** $C_{13}H_{11}F_6NS$ $[M+H]^+$: 328.3, Found: 328.3 m/z

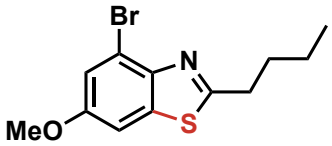


**Figure 1.7.15 Product 1.15b**

**4-bromo-6-methoxy-2-propylbenzo[*d*]thiazole**: Compound was synthesized using the general procedures for synthesizing the substituted benzamide, substituted thiobenzamide, and substituted benzothiazole. **Yields** (0.083 mmol scale): No pyridine- 7.8mg, 31% & Pyridine- 7.5mg, 30%, off white oil. **$^{1}$HNMR (500 MHz, $CDCl_3$)** δ= 7.27 (d, J= 2.4Hz, 1H), 7.24 (d, J= 2.4Hz, 1H), 3.85 (s, 3H), 3.13-3.00 (m, 3H), 1.88 (m, 3H), 1.06 (t, J= 7.4Hz, 4H). **$^{13}$CNMR (126Hz, $CDCl_3$)** δ= 179.65, 157.23, 146.03, 136. 68, 118.03, 116.21, 103.85, 56.03 (d, J= 5.0) 38.51, 30.71. **MS-APCI Calculated:** $C_{12}H_{14}BrNOS$ $[M+H]^+$: 301.2, Found: 301.2, 301.3 m/z

### 1.7.5 Characterization of Substituted Indoles

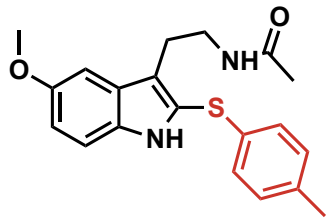


**Figure 1.7.16 Product 1.18b**

**N-(2-(5-methoxy-2-(p-tolylthio)-1H-indol-3-yl)ethyl)acetamide:** Compound was synthesized using the general procedures for the synthesis of substituted indoles. **Yields** (0.107 mmol scale): 52%, pale tan solid. **$^{1}$HNMR (400 MHz, CDCl3)** $\delta$ = 8.12 (s, 1H), 7.22 (d, $J$ = 8.8 Hz, 1H), 7.02-7.06 (m, 3H), 6.98 (d, $J$ = 8.3 Hz, 2H), 6.91 (dd, $J$ = 8.8, 2.4 Hz, 1H), 5.50 (s, 1H), 3.86 (s, 3H), 3.52 (q, $J$ = 6.4 Hz, 2H), 3.05 (t, $J$ = 6.5 Hz, 2H), 2.27 (s, 3H), 1.78 (s, 3H). **$^{13}$CNMR (126 MHz, CDCl3)** $\delta$ = 170.28, 154.36, 136.17, 133.22, 132.07, 130.04, 128.13, 127.00, 123.50, 119.64, 114.32, 111.93, 100.32, 55.87, 40.01, 24.75, 23.13, 20.89. **MS-APCI Calculated:** $C_{20}H_{22}N_2O_2S$ [M+H]+: 355.5, Found: 355.5 m/z

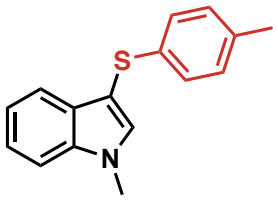


**Figure 1.7.17 Product 1.19b**

**1-methyl-3-(p-tolylthio)-1H-indole:** Compound was synthesized using the general procedures for the synthesis of substituted indoles. **Yields** (0.098 mmol scale): 10.67 mg, 11%, white solid. **$^{1}$HNMR (400 MHz, CDCl3)** $\delta$ = 7.62 (td, $J$ = 7.8, 1.0 Hz, 1H), 7.38 (td, $J$ = 7.9, 1.0 Hz, 1H), 7.33 (s, 1H), 7.29 (ddd, $J$ = 7.1, 6.9, 1.0 Hz, 1H), 7.17 (ddd, $J$ = 7.0, 6.9, 1.0 Hz, 1H), 7.03 (d, $J$ = 8.6 Hz, 2H), 6.97 (d, $J$ = 8.6 Hz, 2H), 3.84 (s, 3H), 2.25 (s, 3H). **$^{13}$CNMR (126 MHz, CDCl3)** $\delta$ = 137.48, 135.92, 134.83, 134.49, 129.82, 129.42, 126.08, 122.46, 120.39, 119.75,

109.64, 101.16, 33.10, 20.86. **MS-APCI Calculated:** $C_{16}H_{15}NS$ [M+H]+: 254.4, Found: 254.4 m/z

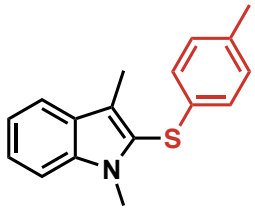


**Figure 1.7.18 Product 1.20b**

**1,3-dimethyl-2-(p-tolylthio)-1H-indole**: Compound was synthesized using the general procedures for the synthesis of substituted indoles. **Yields** (.172mmol scale): 26.2 mg, 28%, white solid. **$^1$HNMR (400 MHz, CDCl3)** $\delta$ = 7.63 (ddd, $J$ = 7.9, 1.0, 0.9 Hz, 1H) 7.28-7.33 (m, 2H), 7.15 (ddd, $J$ = 8.0, 1.0, 0.9 Hz, 1H), 7.01 (d, $J$ = 8.3 Hz, 2H), 6.88 (d, $J$ = 8.2 Hz, 2H), 3.70 (s, 3H), 2.45 (s, 3H), 2.27 (s, 3H). **$^{13}$CNMR (126 MHz, CDCl3)** $\delta$ = 137.98, 135.30, 133.70, 132.61, 129.82, 127.41, 126.14, 124.62, 123.05, 119.44, 119.07, 109.58, 29.98, 20.96, 9.97. **MS- APCI Calculated:** $C_{23}H_{21}NS_2$ [M+H]+: 268.4, Found: 268.4 m/z

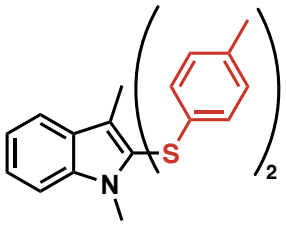


**Figure 1.7.19 Product 1.20c**

**1,3-dimethyl-2-((4-methyl-2-(p-tolylthio)phenyl)thio)-1H-indole**: Compound was synthesized using the general procedures for the synthesis of substituted indoles. There is the presence of rotamers in both 1H and 13C NMR. The peaks for the major rotamer is reported. **Yields** (.172mmol scale): 13.1 mg, 14%, white solid. **$^1$HNMR (400 MHz, CDCl3)** $\delta$ = 7.63 (d, $J$ = 7.9 Hz, 1H), 7.26-7.32 (m, 2H), 7.24 (broad singlet, 1H), 7.12-7.18 (m, 4H), 7.04 (dd, $J$ = 8.2,

2.2 Hz, 1H), 6.82 (dd, $J$ = 8.2, 2.0 Hz) 6.32 (d, $J$ = 8.2 Hz, 1H), 3.62 (s, 3H), 2.39 (s, 3H), 2.35 (s, 3H), 2.20 (s, 3H). **$^{13}$CNMR (126 MHz, CDCl3)** $\delta$ = 138.17, 137.90, 136.71, 136.75, 134.49, 131.98, 130.74, 130.02, 129.95, 129.90, 129.67, 129.64, 128.50, 125.92, 123.08, 119.44, 119.09, 109.63, 29.85, 21.10, 20.64, 9.88. **MS-APCI Calculated**: $C_{24}H_{23}NS_2$ [M+H]+: 390.6, Found: 390.6 m/z

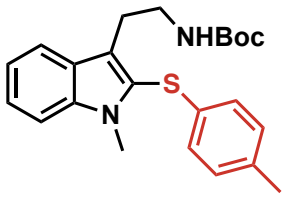


**Figure 1.7.20 Product 1.21b**

**tert-butyl (2-(1-methyl-2-(p-tolylthio)-1H-indol-3-yl)ethyl)carbamate:** Compound was synthesized using the general procedures for the synthesis of substituted indoles. **Yields** (.091 mmol scale): 11.7 mg, 17%, white solid. **$^{1}$HNMR (400 MHz, CDCl3)** $\delta$ = 7.71 (d, $J$ = 7.0 Hz, 1H), 7.29-7.36 (m, 2H), 7.17 (ddd, $J$ = 8.3, 6.0, 1.8 Hz, 1H), 7.02 (d, $J$ = 8.3 Hz, 2H), 6.86 (d, $J$ = 8.3 Hz, 2H), 4.57 (s, 1H), 3.70 (s, 3H), 3.39 (broad q, 2H), 3.14 (t, $J$ = 6.8Hz, 2H), 2.28 (s, 3H), 1.43 (s, 9H). **$^{13}$CNMR (126 MHz, CDCl3)** $\delta$ = 155.90, 138.11, 135.44, 133.60, 132.72, 132.61, 131.61, 129.96, 128.61, 128.48, 126.97, 125.96, 125.37, 123.24, 119.60, 109.76, 30.06, 28.41, 20.89. **MS-APCI Calculated:** $C_{24}H_{23}NS_2$ [M+H]+: 397.6, Found: 397.6 m/z

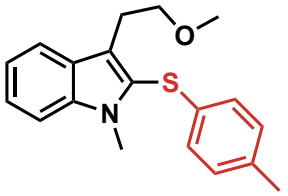


**Figure 1.7.21 Product 1.22b**

**3-(2-methoxyethyl)-1-methyl-2-(p-tolylthio)-1H-indole:** Compound was synthesized using the general procedures for the synthesis of substituted indoles. **Yields** (.132 mmol scale): 13.7 mg, 36%, brown oil. **$^{1}$HNMR (400 MHz, CDCl3)** $\delta$ = 7.70 (td, $J$ = 7.8, 1.0 Hz, 1H), 7.27-7.34 (m, 2H), 7.16 (ddd, $J$ = 7.8, 6.4, 1.1 Hz, 1H), 7.01 (d, $J$ = 8.2 Hz, 2H), 6.88 (d, $J$ = 8.2 Hz, 2H), 3.69 (s, 3H), 3.58 (t, $J$ = 7.6 Hz, 2H), 3.33 (s, 3H), 3.22 (t, $J$ = 7.6Hz, 2H), 2.27 (s, 3H). **$^{13}$CNMR (126 MHz, CDCl3)** $\delta$ = 138.07, 135.39, 133.71, 129.83, 126.99, 126.19, 125.43, 123.08, 120.06, 119.54, 119.35, 109.73, 73.01, 58.52, 30.03, 25.96, 20.88. **MS-APCI Calculated**: $C_{19}H_{21}NOS$ [M+H]+: 312.4, Found: 312.4 m/z

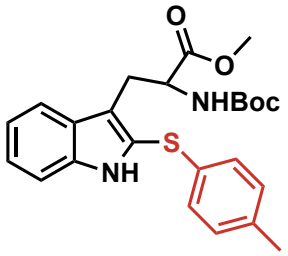


**Figure 1.7.22 Product 1.23b**

**Methyl-2-((tert-butoxycarbonyl)amino)-3-(2-(p-tolylthio)-1H-indol-3-yl)propanoate:** Compound was synthesized using the general procedures for the synthesis of substituted indoles. **Yields** (.078 mmol scale): 12.1 mg, 31%, white solid. **$^{1}$HNMR (400 MHz, CDCl3)** $\delta$ = 8.33 (d, $J$ = 15.4 Hz, 1H) 7.60 (d, $J$ = 7.9 Hz, 1H) 7.25 (d, $J$ = 7.9 Hz, 1H), 7.21 (td, $J$ = 6.9, 1.1 Hz, 1H), 7.13 (td, $J$ = 7.0, 1.1 Hz, 1H), 7.02 (q, $J$ = 5.9 Hz, 4H), 4.65 (q, $J$ = 6.7 Hz, 1H), 3.67 (s, 3H), 3.39 (q, $J$ = 5.7 Hz, 2H), 2.28 (s, 3H), 1.40 (s, 9H). **$^{13}$CNMR (126 MHz, CDCl3)** $\delta$ = 172.66, 155.12, 136.92, 136.23, 132.46, 129.98, 127.96, 127.63, 124.55, 123.38, 119.99, 119.21, 116.78, 110.97, 79.71, 54.15, 52.36, 28.30, 27.76, 20.94. **MS-APCI Calculated:** $C_{24}H_{28}N_2O_4S$ [M+H]+: 441.6, Found: 441.6 m/z

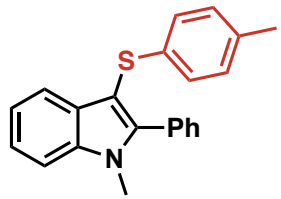


**Figure 1.7.23 Product 1.24b**

**1-methyl-2-phenyl-3-(*p*-tolythio)-1H-indole:** Compound was synthesized using the general procedures for the synthesis of substituted indoles. **Yields** (.241 mmol scale): 6.9 mg, 9.0%, white solid. **$^{1}$HNMR (500 MHz, CDCl3)** $\delta$ = 7.65 (dt, $J$ = 7.9, 0.9 Hz, 1H), 7.48-7.40 (m, 6H), 7.33 (ddd, $J$ = 8.2, 7.1, 1.2 Hz, 1H), 7.20 (ddd, $J$ = 7.9, 7.1, 0.9 Hz, 1H), 6.96 (s, 4H), 3.74 (s, 3H), 2.25 (s, 3H). The spectral data is in agreement with the reported literature: Chen, Y.; Cho, C.; Shi, F.; Larock, R. *J. Org. Chem*. **2009**, *74*. 6802-6811 **MS-APCI Calculated:** $C_{22}H_{19}NS$ [M+H]+: 329.5, Found: 330.3 m/z

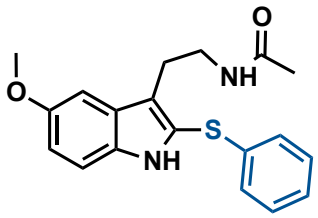


**Figure 1.7.24 Product 1.25b**

**(*N*-(2-(5-methoxy-2-(phenylthio)-1H-indol-3-yl)ethyl)acetamide**: Compound was synthesized using the general procedures for the synthesis of substituted indoles. **Yields** (.107 mmol scale): 6.2 mg, 16%, clear oil. **$^{1}$HNMR (400 MHz, CDCl3)** $\delta$ = 8.12 (s, 1H), 7.20-7.25 (m, 3H), 7.13 (ddd, $J$ = 7.4, 2.0, 1.9 Hz, 1H) 7.04-7.08 (m, 3H), 6.93 (dd, $J$ = 8.8, 2.4 Hz, 1H), 5.47 (s, 1H), 3.87 (s, 1H), 3.50 (q, $J$ = 6.3 Hz, 2H) 3.05 (t, $J$ = 6.4 Hz, 2H), 1.76 (s, 3H). **$^{13}$CNMR (126 MHz, CDCl3)** $\delta$ = 170.14, 154.41, 137.18, 132.16, 129.28, 128.10, 126.35, 125.99, 122.59, 120.30, 114.56, 112.00, 100.37, 55.86, 39.97, 24.83, 23.17. **MS-APCI Calculated:** $C_{19}H_{20}N_2O_2S$ [M+H]+: 341.4, Found: 341.5 m/z

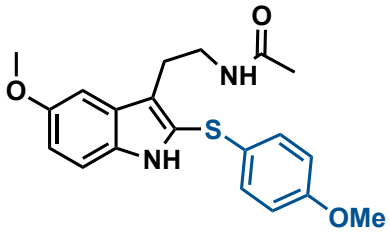


**Figure 1.7.25 Product 1.26b**

***N*-(2-(5-methoxy-2-((4-methoxyphenyl)thio)-1H-indol-3-yl)ethyl)acetamide:**

Compound was synthesized using the general procedures for the synthesis of substituted indoles. **Yields** (.107 mmol scale): 12.2 mg, 31%, brown solid. **$^{1}$HNMR (400 MHz, CDCl3)** $\delta$ = 8.09 (s, 1H), 7.20 (d, $J$ = 8.9 Hz, 1H), 7.11 (dd, $J$ = 6.8, 2.3Hz, 2H), 7.03 (d, $J$ = 2.5 Hz, 1H), 6.89 (dd, $J$ = 8.8, 2.4 Hz, 1H), 6.78 (dd, $J$ = 6.7, 2.3 Hz, 2H), 5.52 (s, 1H), 3.86 (s, 3H), 3.75 (s, 3H), 3.51 (q, $J$ = 6.5 Hz, 2H), 3.06 (t, $J$ = 6.6 Hz, 2H), 1.82 (s, 3H). **$^{13}$CNMR (126 MHz, CDCl3)** $\delta$ = 170.16, 158.73, 154.33, 131.95, 129.76, 128.20, 126.72, 124.80, 118.75, 114.98, 114.06, 111.84, 100.30, 55.85, 55.38, 40.02, 24.76, 23.26. **MS-APCI Calculated**: $C_{20}H_{22}N_2O_3S$ [M+H]+: 370.5, Found: 370.5 m/z

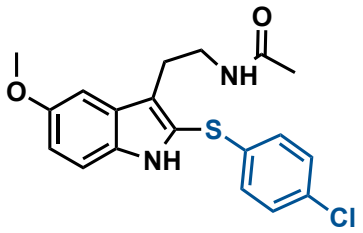


**Figure 1.7.26 Product 1.27b**

***N*-(2-(2-((4-chlorophenyl)thio)-5-methoxy-1H-indol-3-yl)ethyl)acetamide**: Compound was synthesized using the general procedures for the synthesis of substituted indoles. **Yields** (.107 mmol scale): 11.4 mg, 30%, brown solid. **$^{1}$HNMR (400 MHz, CDCl3)** $\delta$ = 8.03 (s, 1H), 7.24 (d, $J$ = 8.1 Hz, 1H), 7.19 (d, $J$ = 6.4 Hz, 2H), 7.08 (d, $J$ = 2.4 Hz, 1H), 6.93-6.98 (m, 3H), 5.47 (s, 1H), 3.88 (s, 3H), 3.52 (q, $J$ = 6.3 Hz, 2H), 3.04 (t, $J$ = 6.4 Hz, 2H), 1.84 (s, 3H). **$^{13}$CNMR (126 MHz,**

**CDCl3)** $\delta$ = 155.90, 138.11, 135.44, 133.60, 132.72, 132.61, 129.96, 128.61, 128.48, 126.97, 125.96, 123.24, 119.55, 109.76, 30.06, 28.41, 20.89. **MS-APCI Calculated:** $C_{19}H_{19}ClN_2O_2S$ [M+H]+: 375.9, Found: 376.0 m/z

### 1.7.6 Spectral Data for Characterized Molecules ($^{1}H$, $^{13}C$, $^{19}F$ NMR)

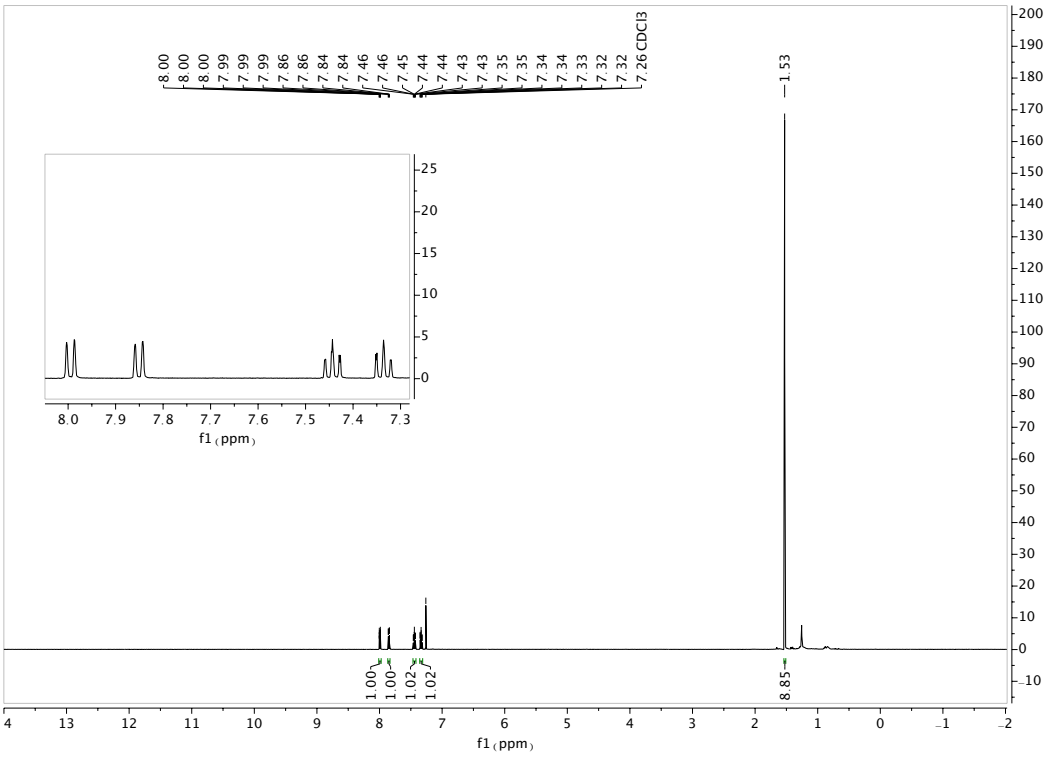


**Figure 1.7.27 500MHz $^{1}$HNMR of 1.1b**

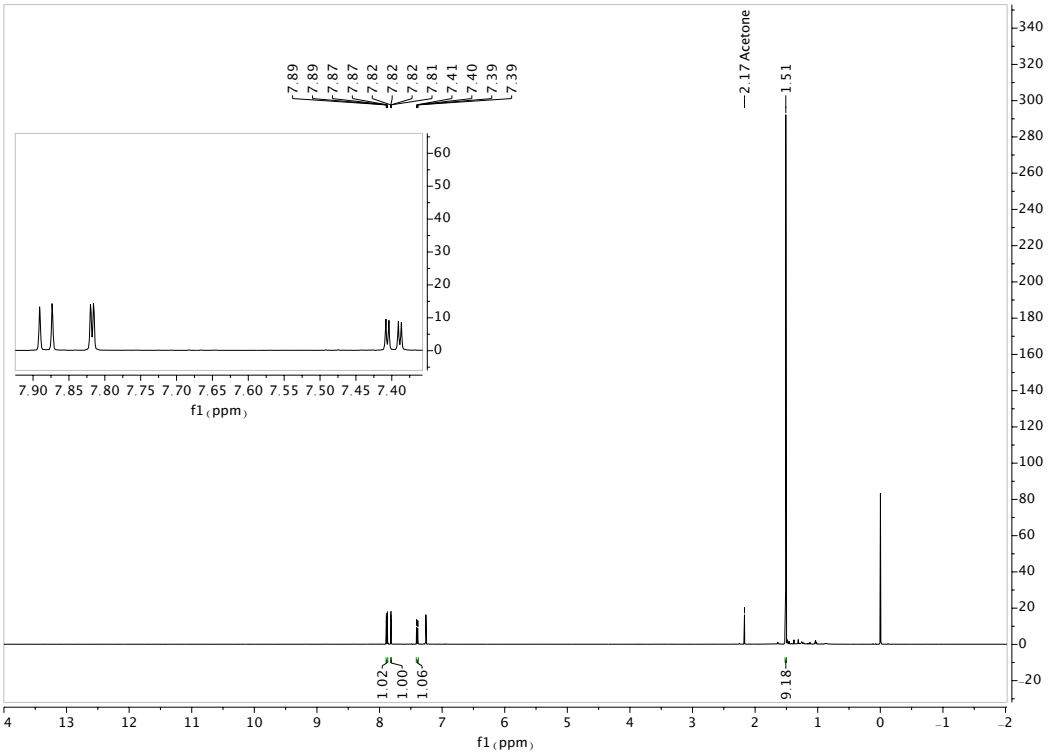


**Figure 1.7.28 500MHz [1]HNMR of 1.2b**

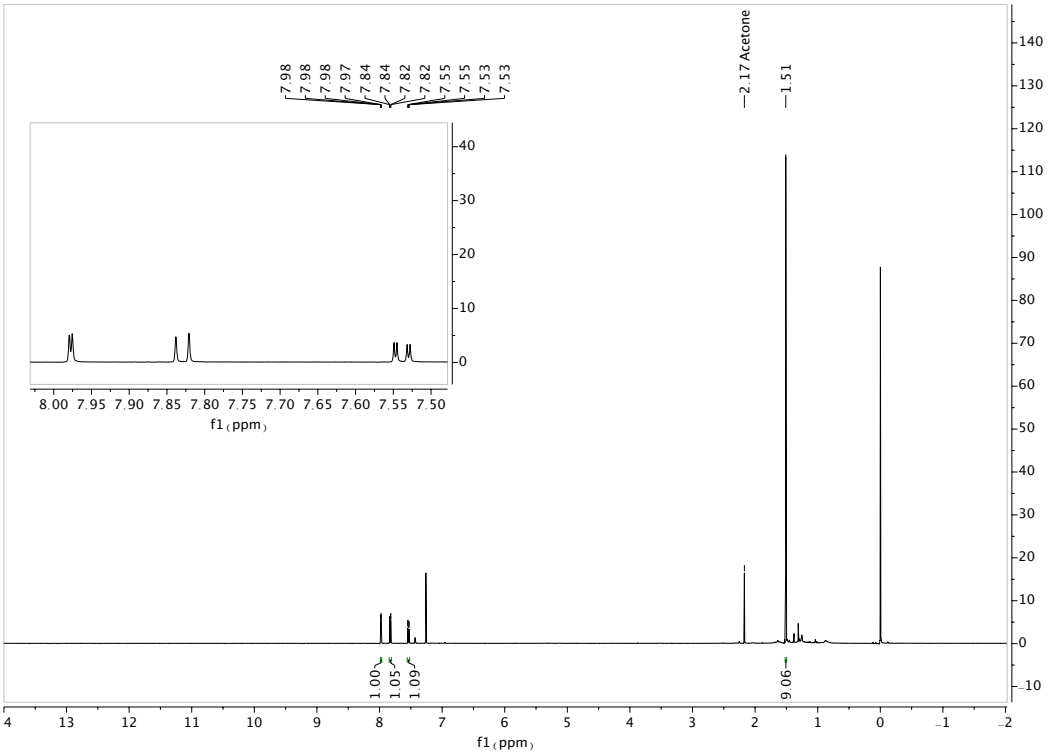


**Figure 1.7.29 500MHz [1]HNMR of 1.3b**

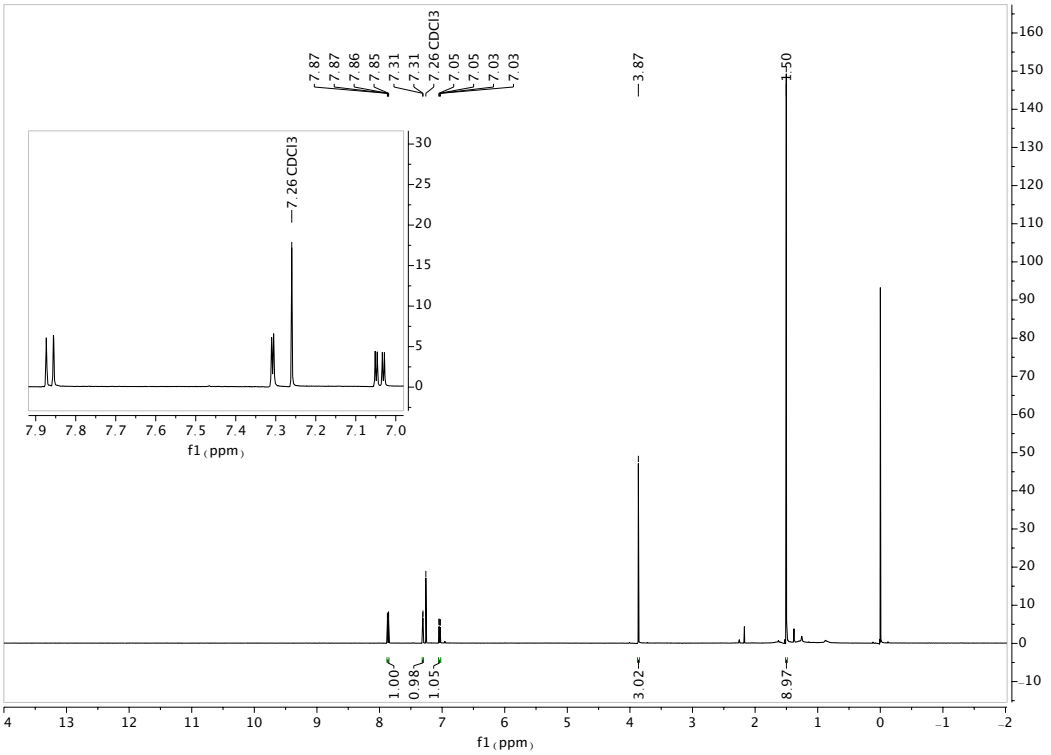


**Figure 1.7.30 500MHz [1]HNMR of 1.4b**

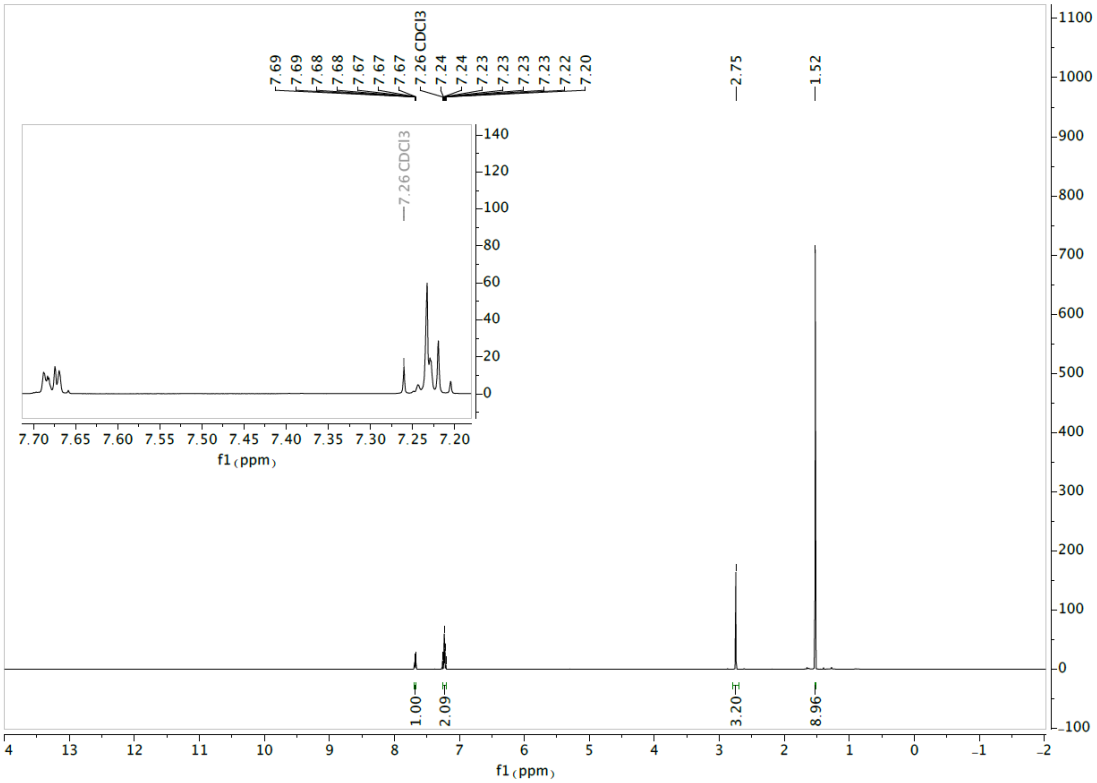


**Figure 1.7.31 500MHz [1]HNMR of 1.5b**

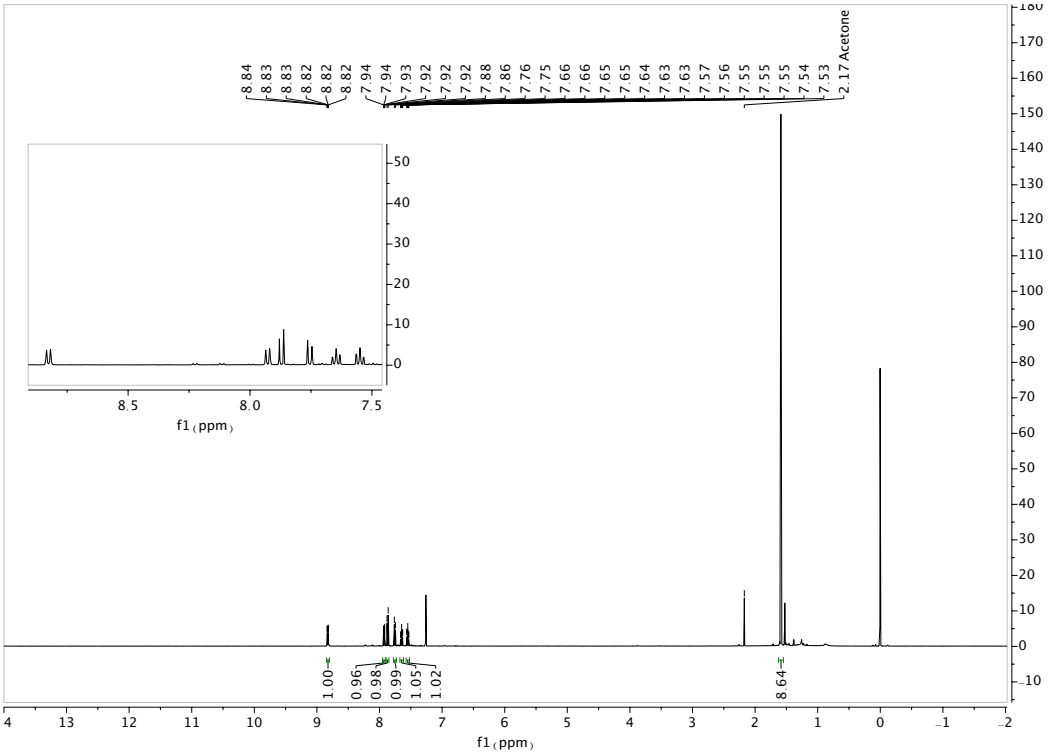


**Figure 1.7.32 500MHz $^{1}$HNMR of 1.6b**

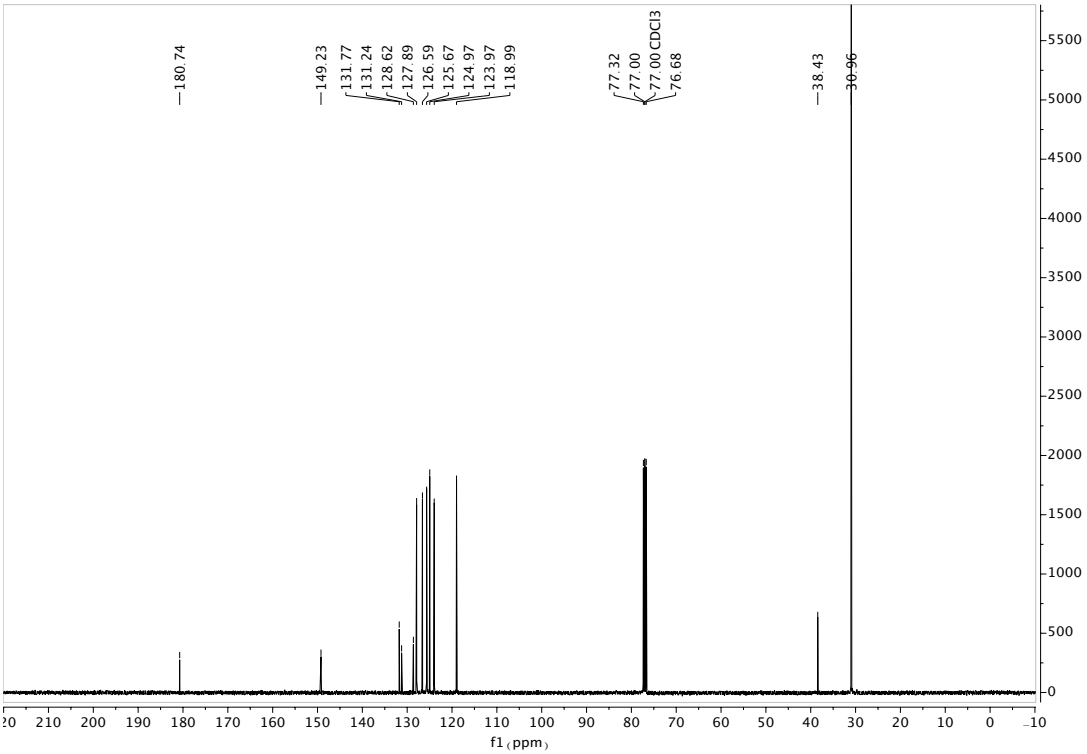


**Figure 1.7.33 126MHz $^{13}$CNMR of 1.6b**

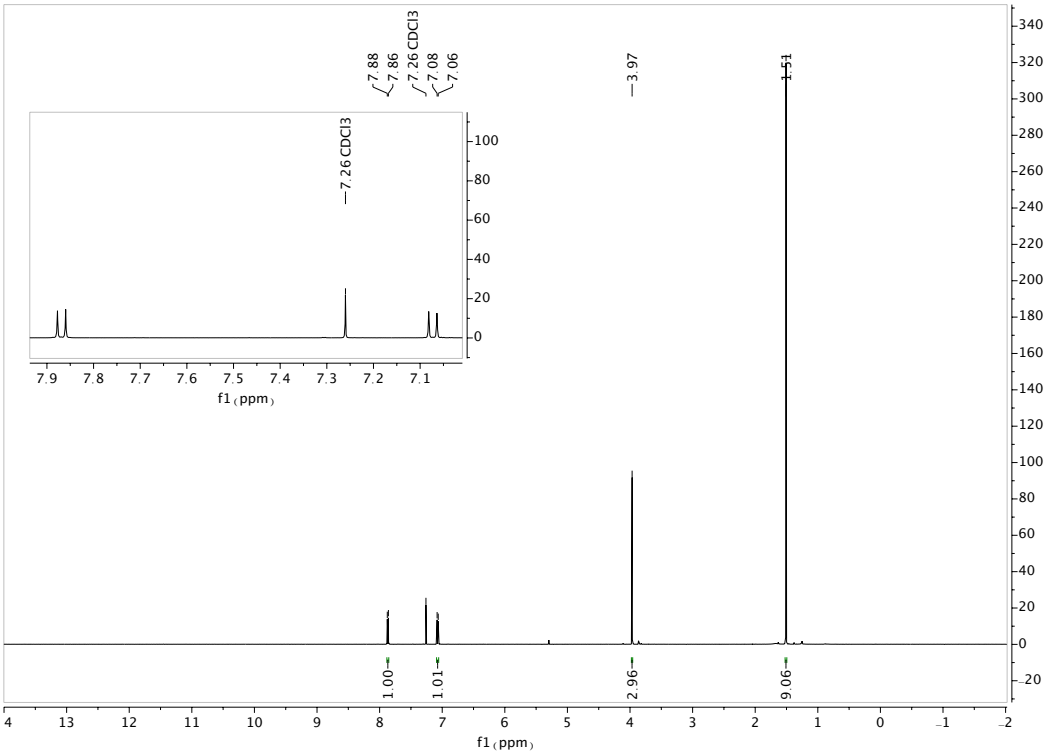


**Figure 1.7.34 500MHz $^{1}$HNMR of 1.7b**

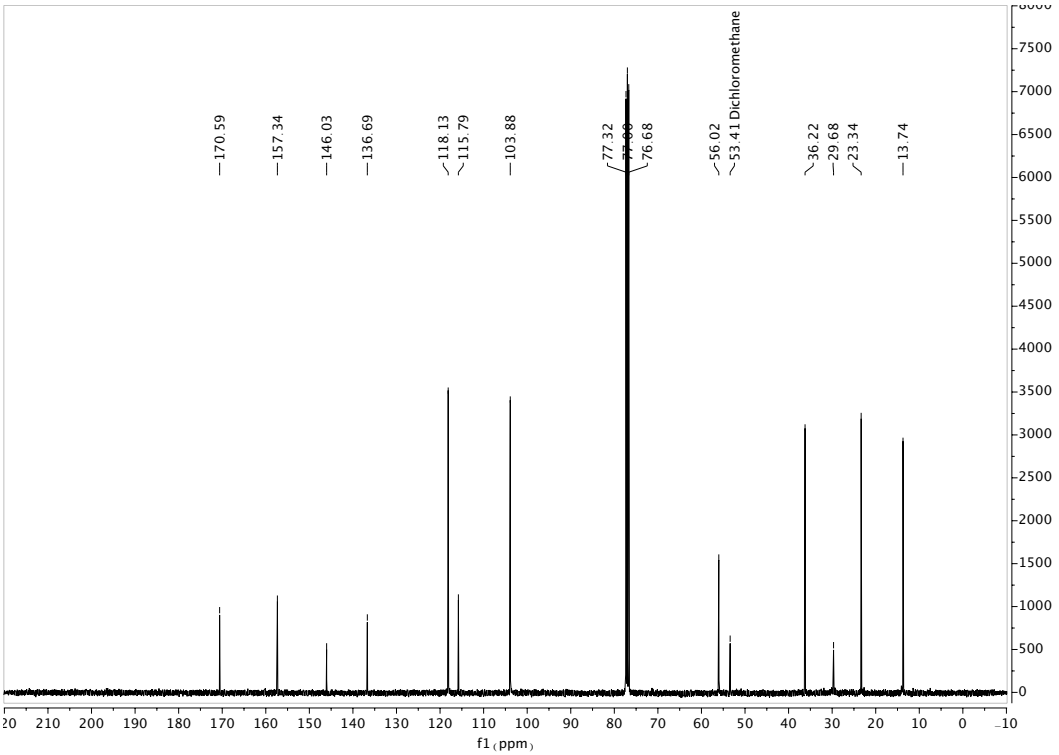


**Figure 1.7.35 126MHz $^{13}$CNMR of 1.7b**

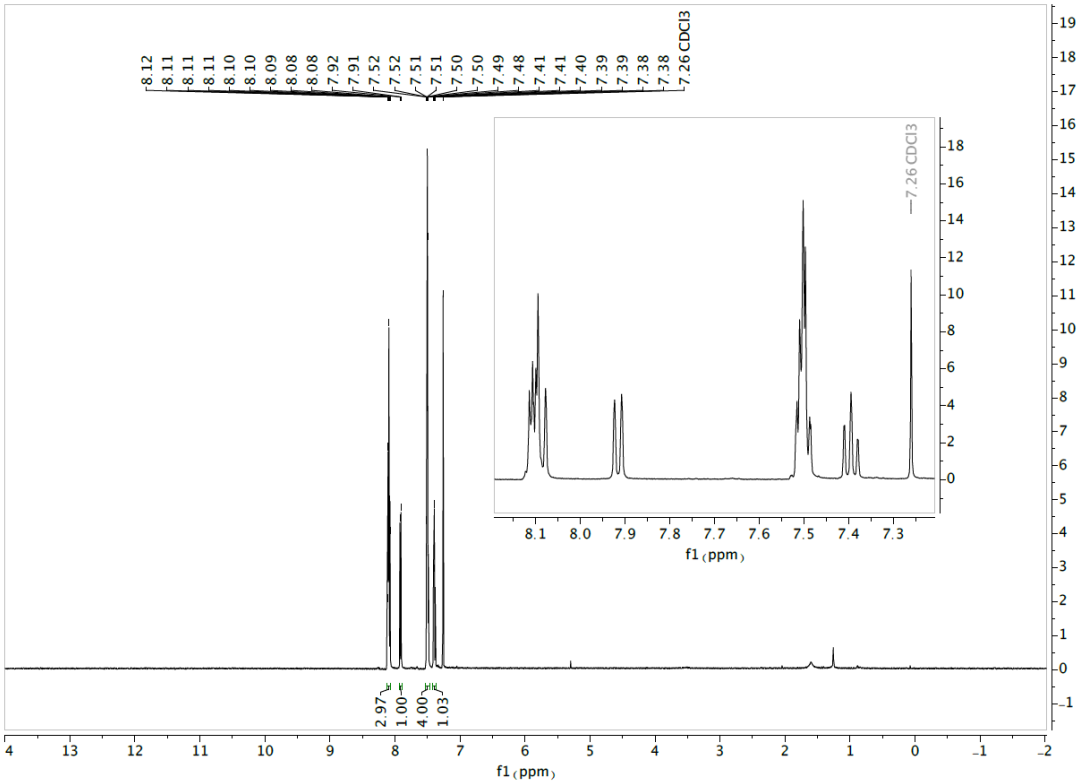


**Figure 1.7.36 500MHz [1]HNMR of 1.8b**

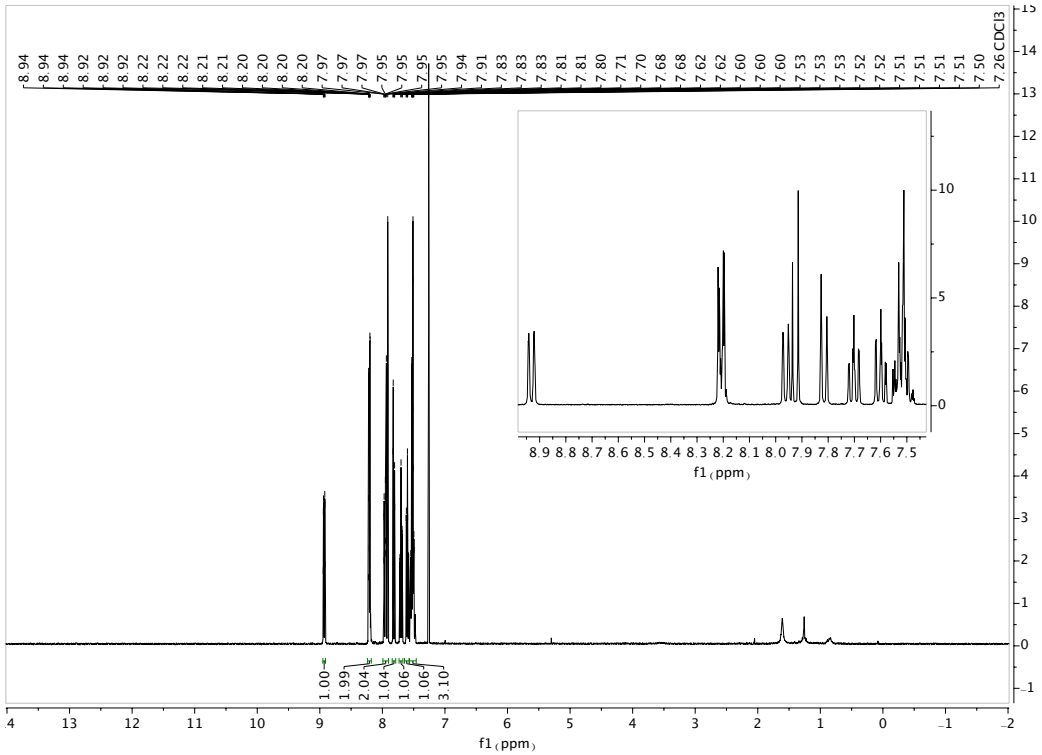


**Figure 1.7.37 500MHz [1]HNMR of 1.9b**

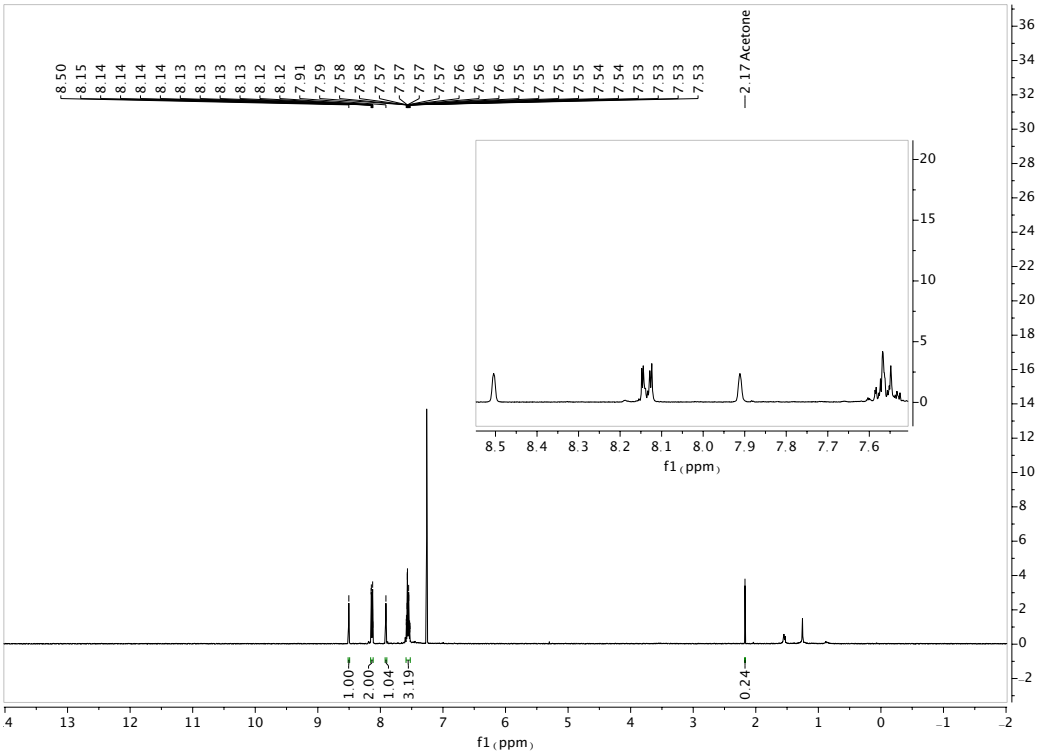

**Figure 1.7.38 500MHz $^{1}$HNMR of 1.10b**

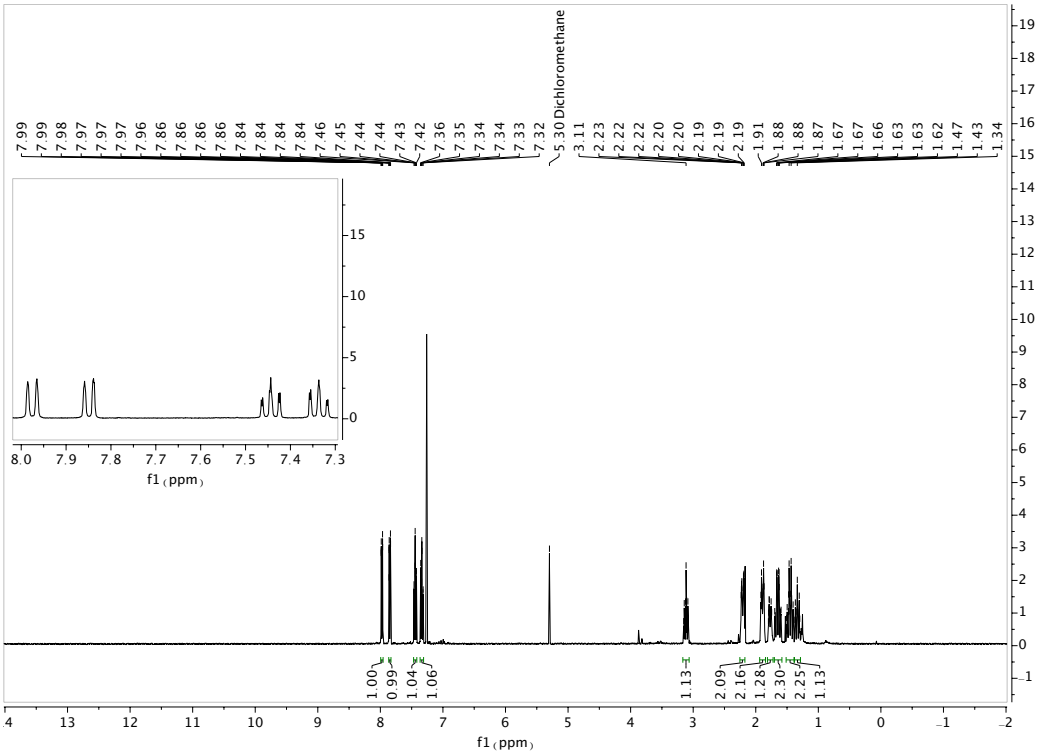

**Figure 1.7.39 500MHz $^{1}$HNMR of 1.11b**

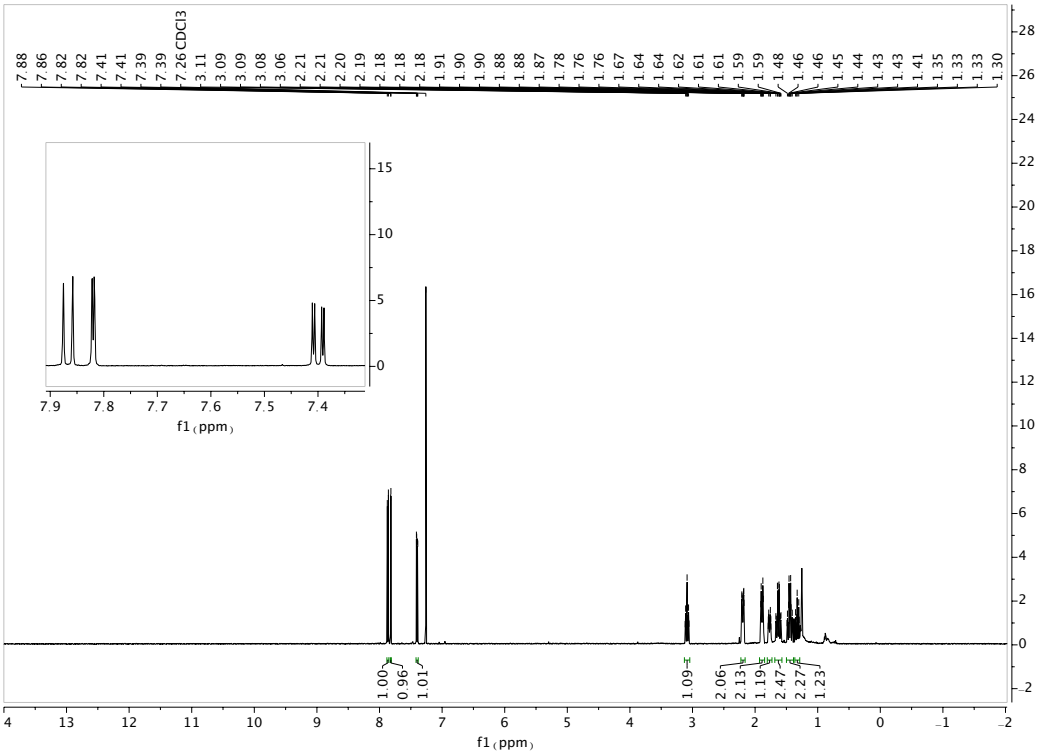

**Figure 1.7.40 500MHz $^{1}$HNMR of 1.12b**

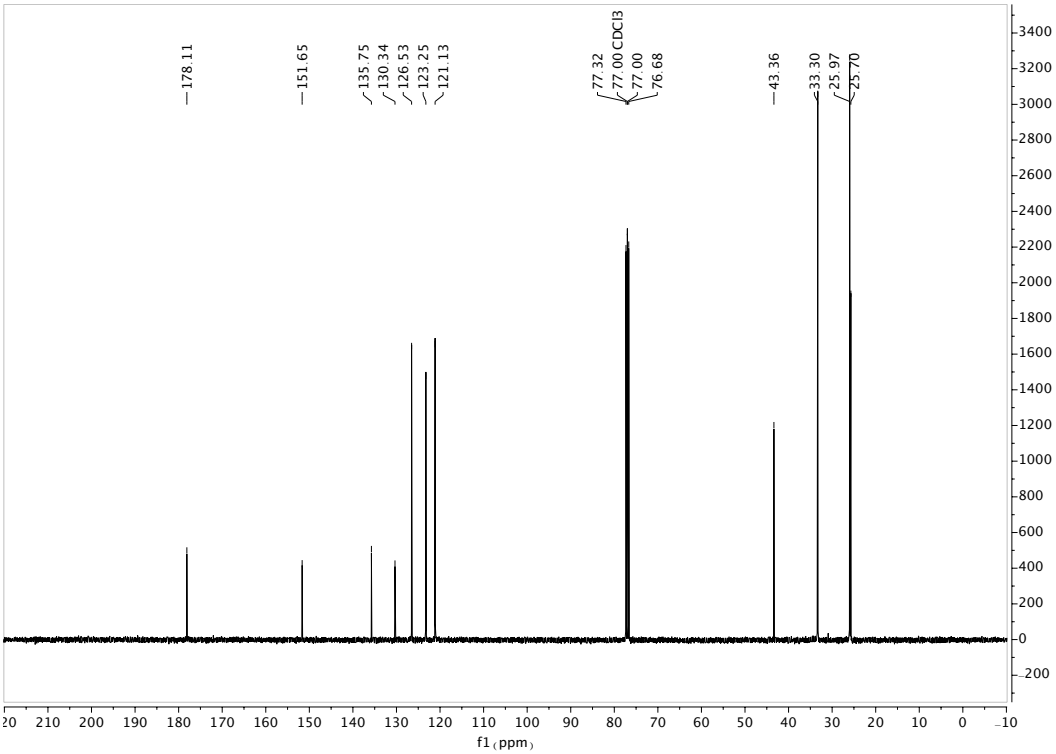

**Figure 1.7.41 126MHz $^{13}$CNMR of 1.12b**

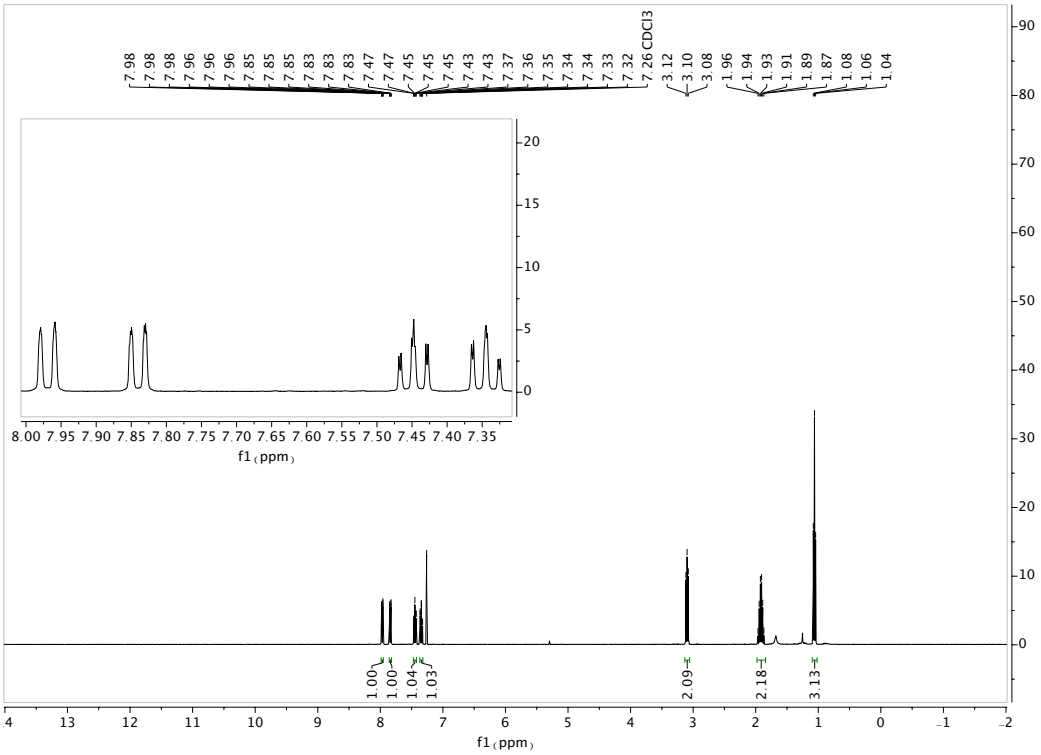


**Figure 1.7.42 500MHz $^{1}$HNMR of 1.13b**

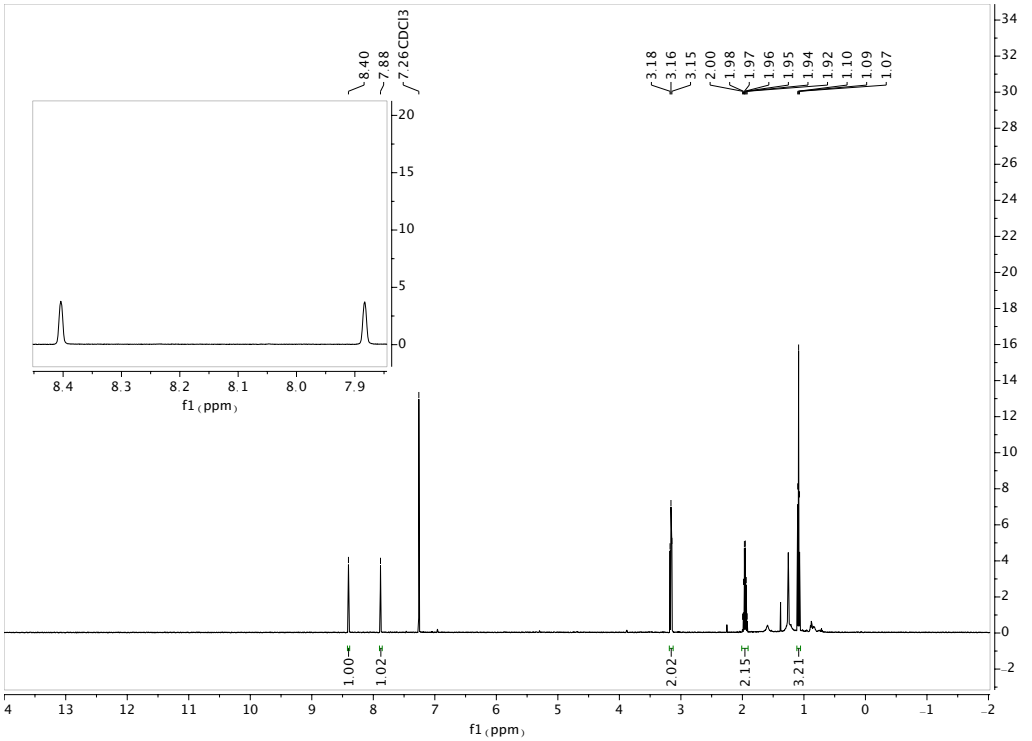


**Figure 1.7.43 500MHz $^{1}$HNMR of 1.14b**

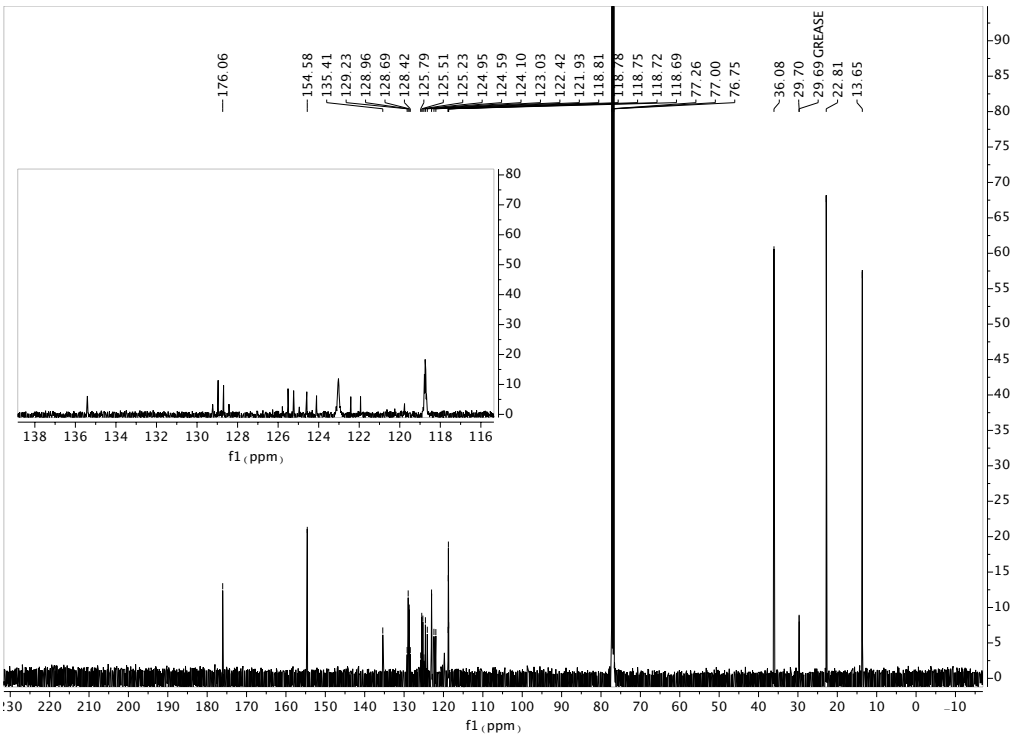


**Figure 1.7.44 126MHz $^{13}$CNMR of 1.14b**

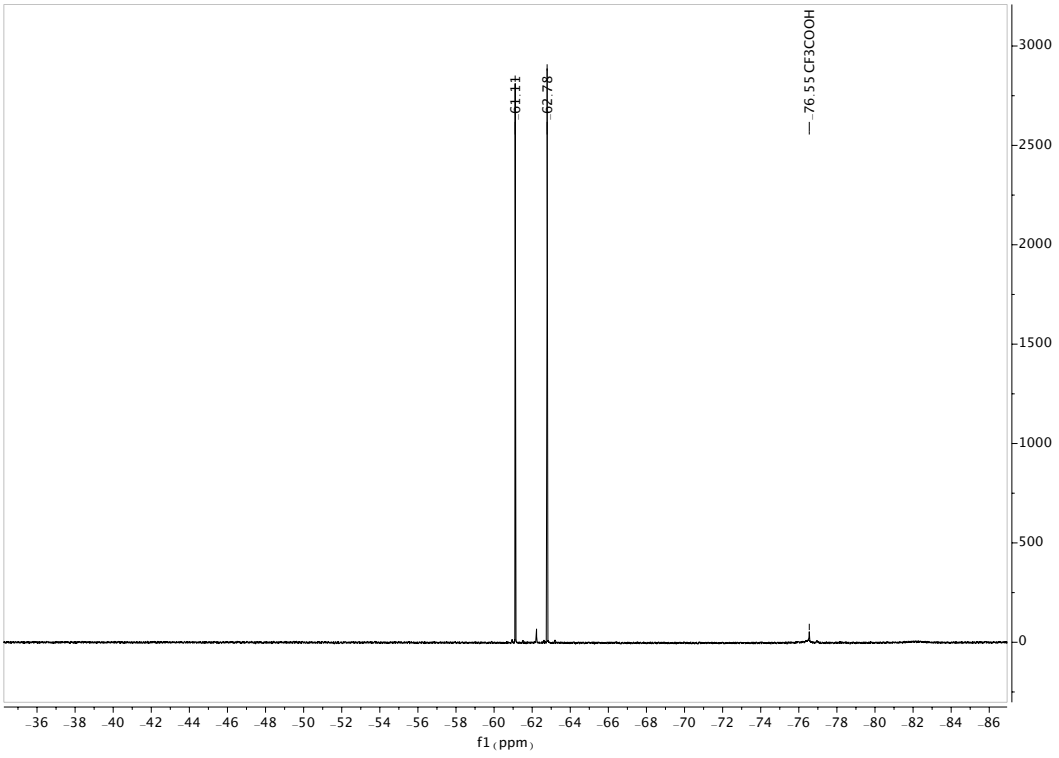


**Figure 1.7.45 376MHz $^{19}$FNMR of 1.14b**

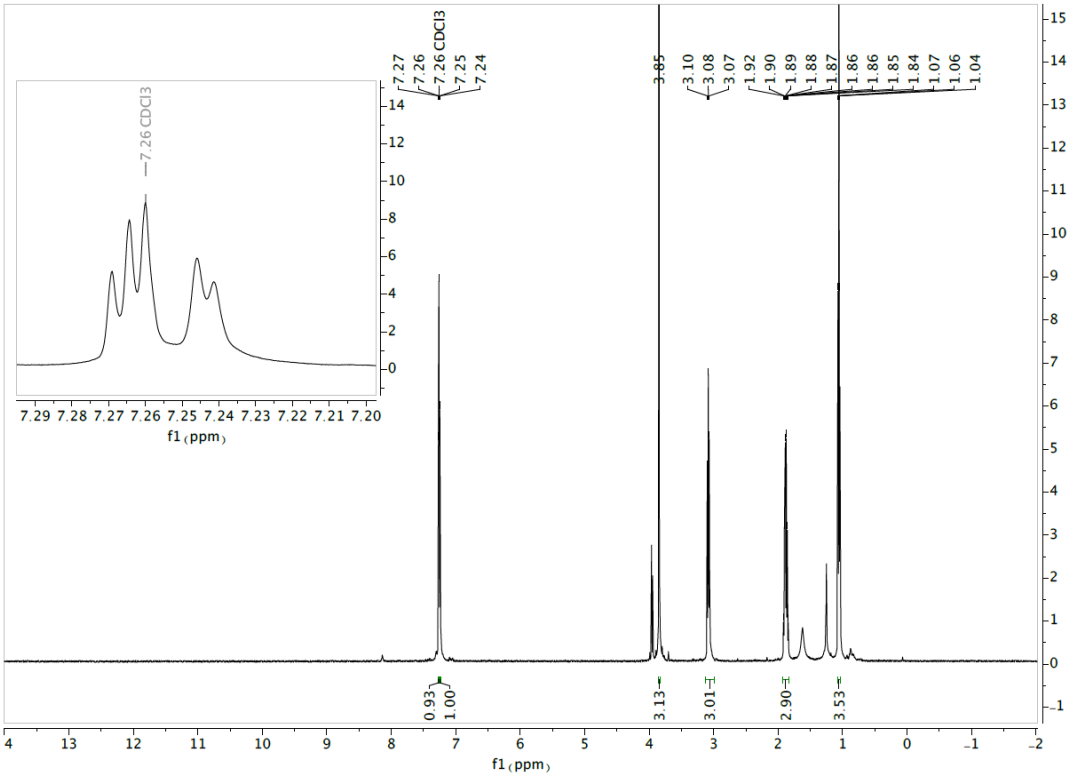


**Figure 1.7.46 500MHz $^{1}$HNMR of 1.15b**

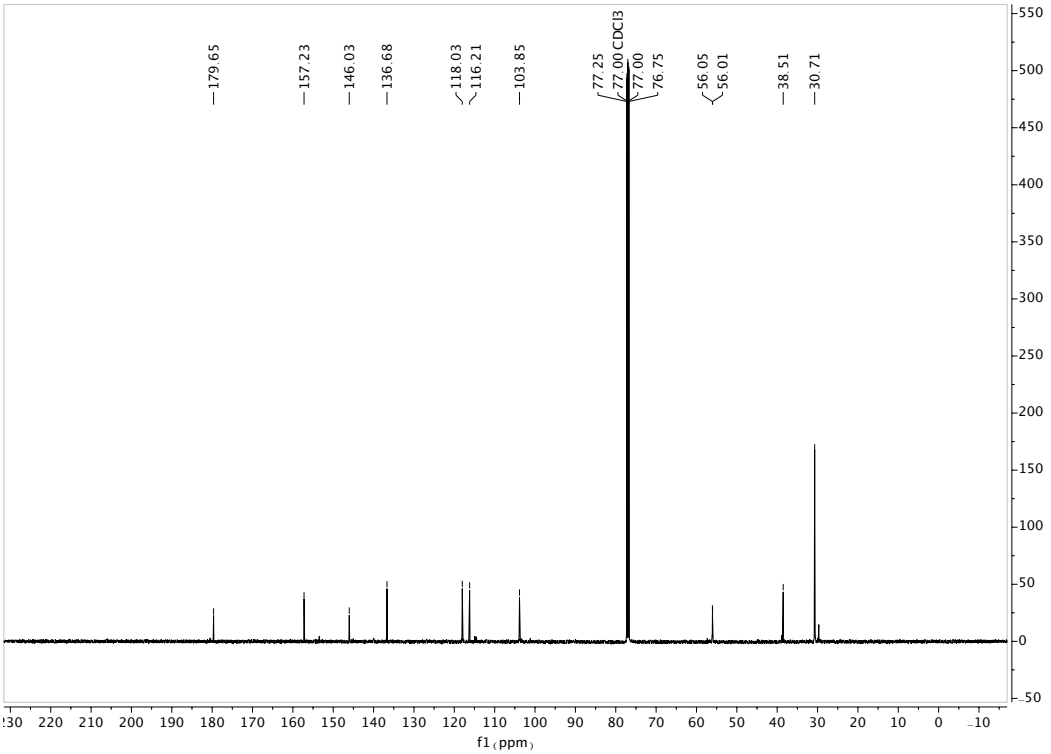


**Figure 1.7.47 126MHz $^{13}$CNMR of 1.15b**

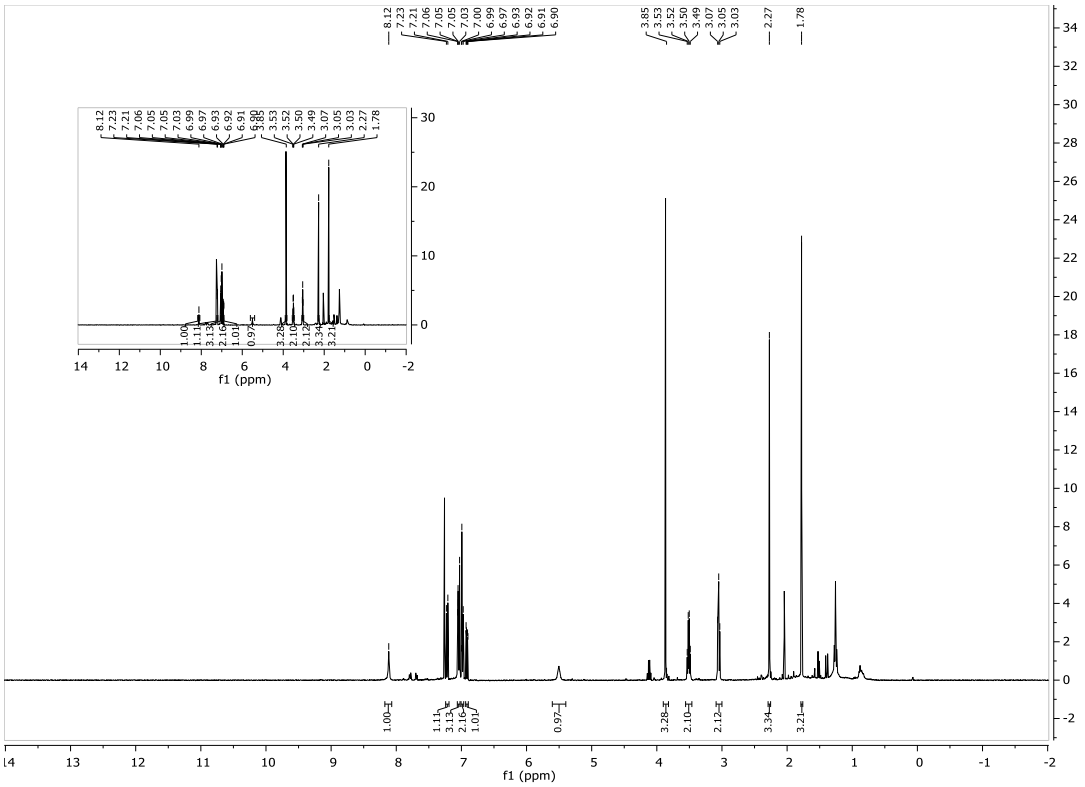


**Figure 1.7.48 500MHz $^{1}$HNMR of 1.18b**

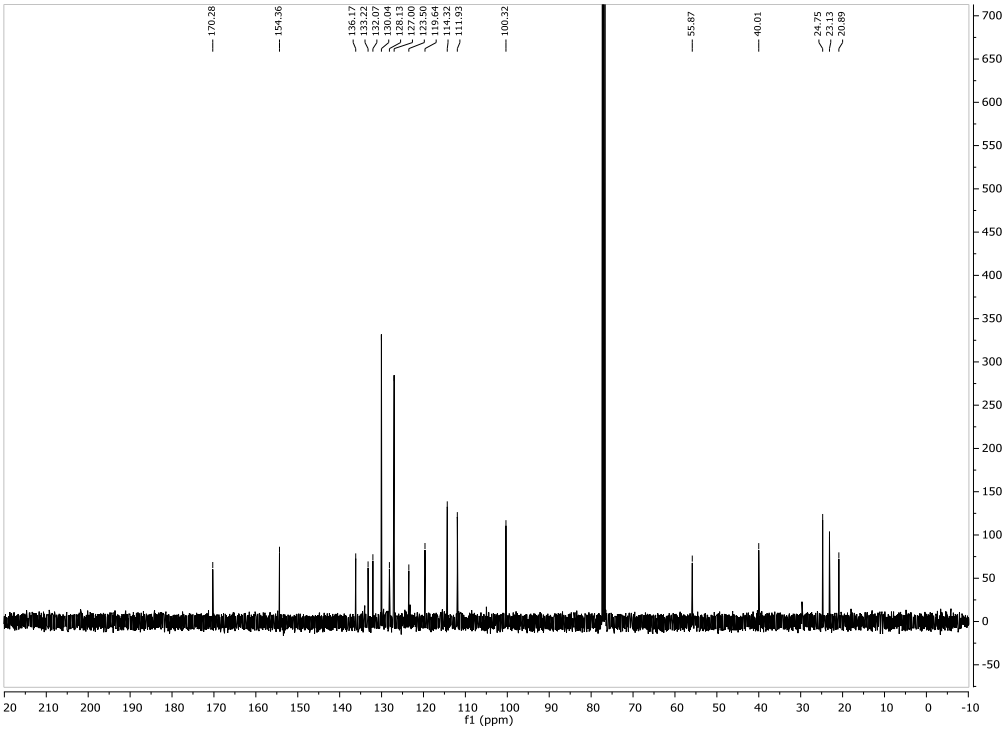


**Figure 1.7.49 126MHz $^{13}$CNMR of 1.18b**

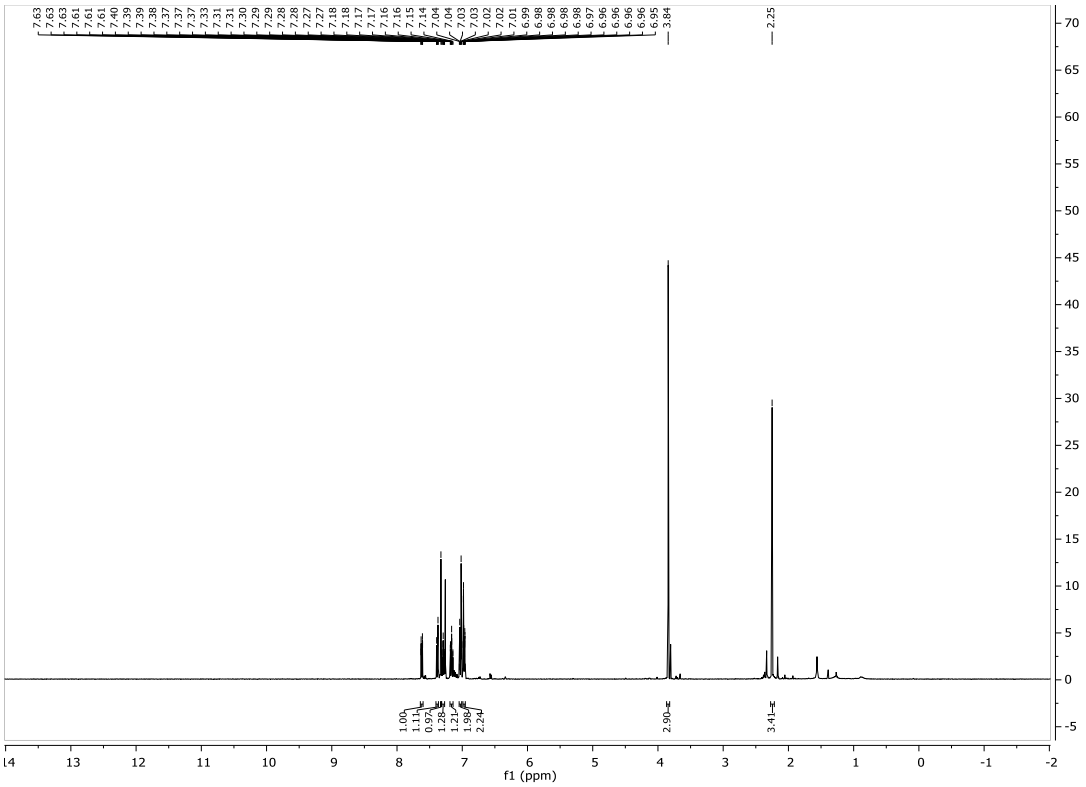


**Figure 1.7.50 500MHz $^{1}$HNMR of 1.19b**

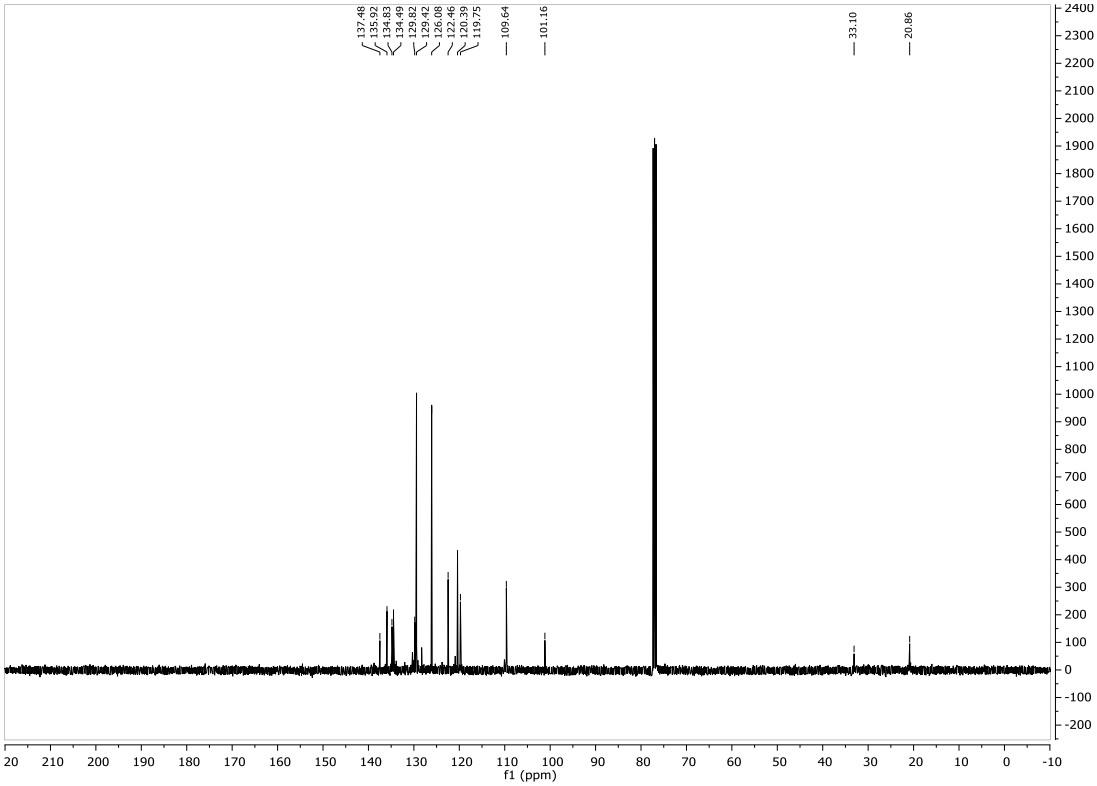


**Figure 1.7.51 126MHz $^{13}$CNMR of 1.19b**

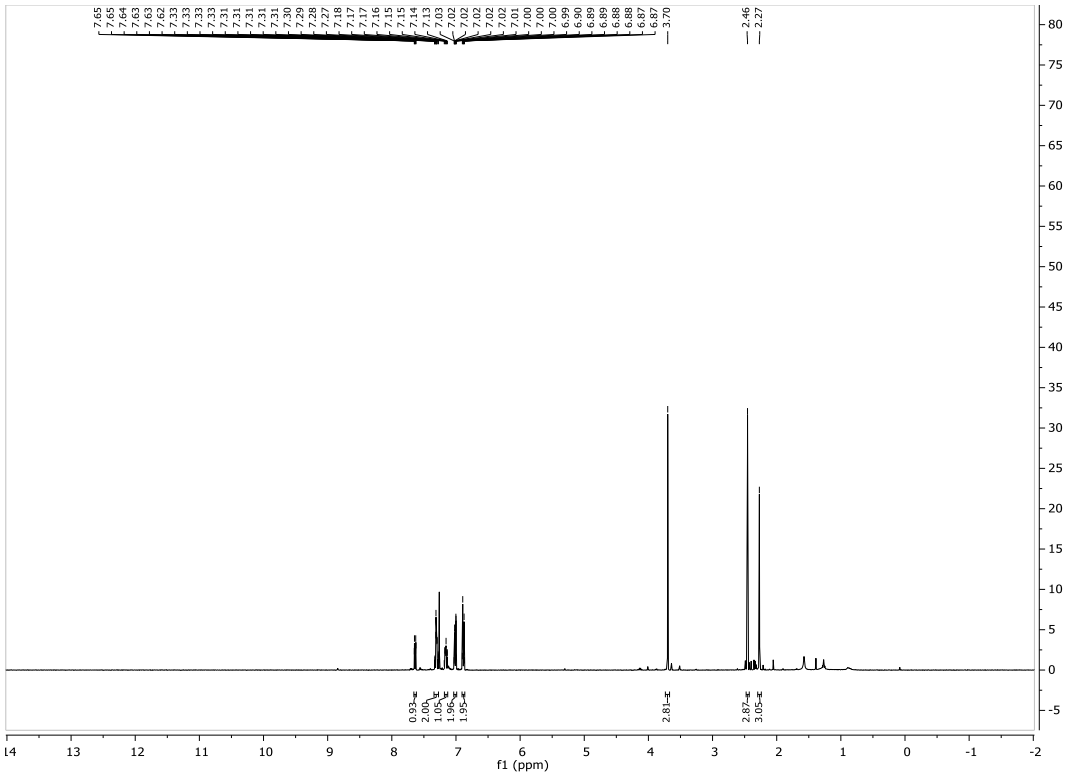


**Figure 1.7.52 500MHz $^{1}$HNMR of 1.20b**

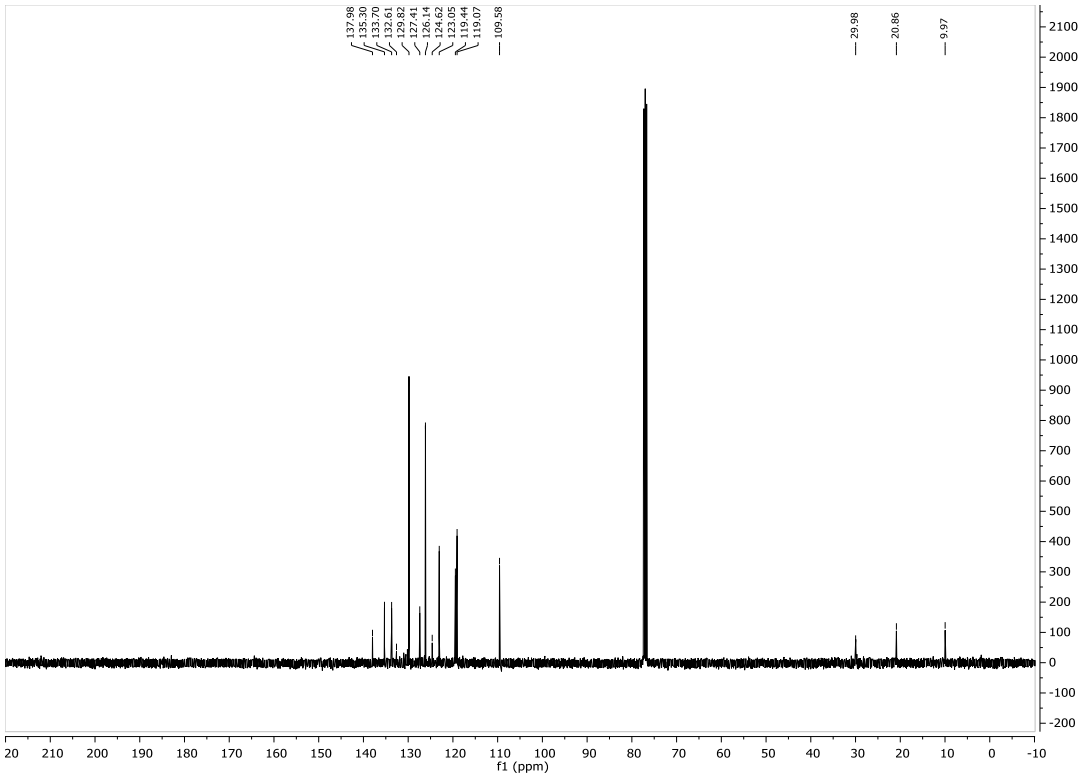


**Figure 1.7.53 126MHz $^{13}$CNMR of 1.20b**

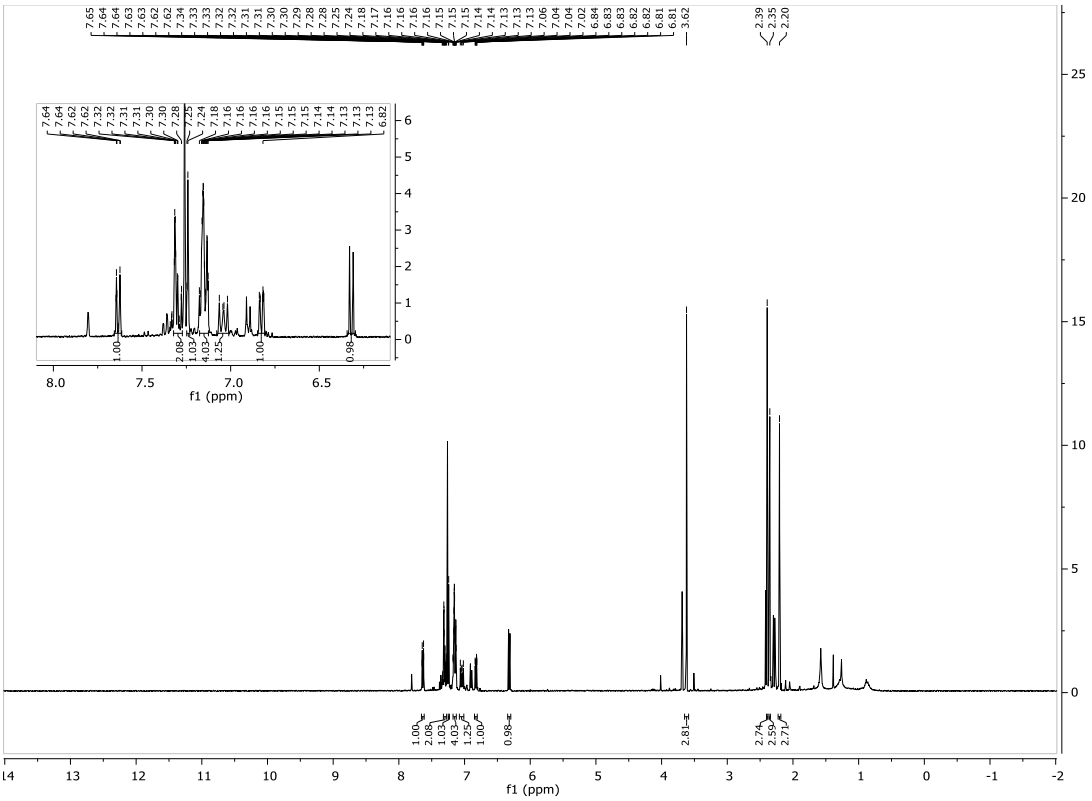


**Figure 1.7.54 500MHz $^{1}$HNMR of 1.21b**

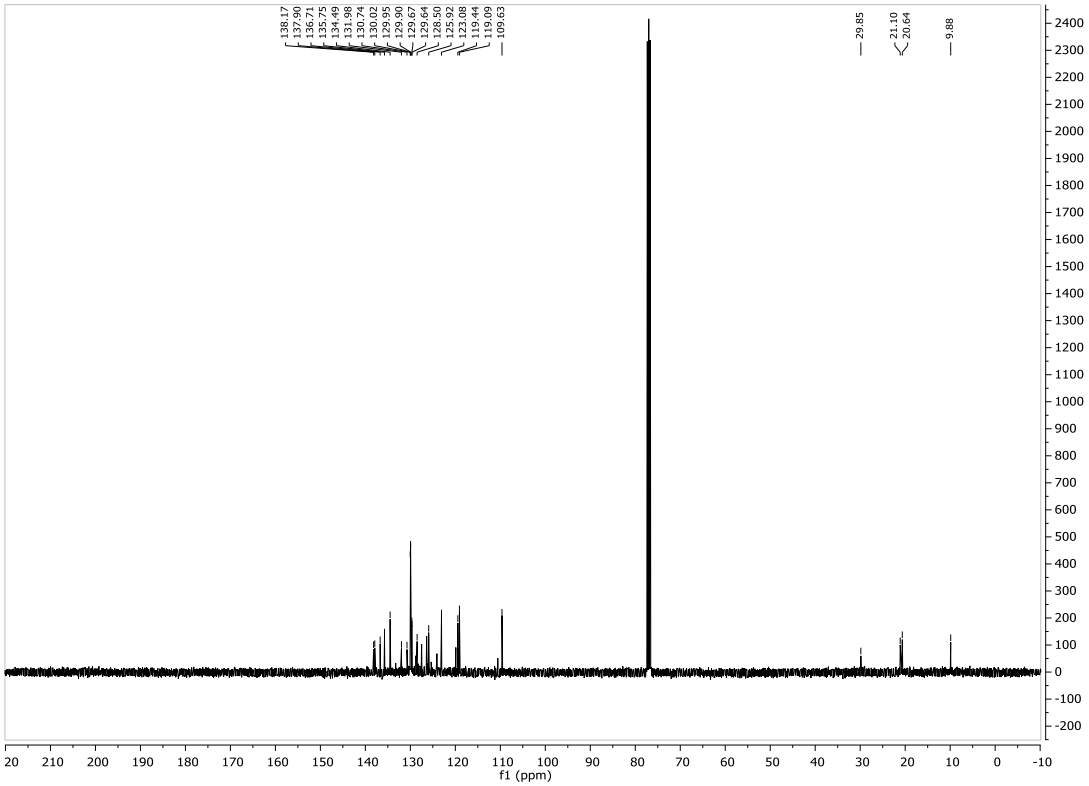


**Figure 1.7.55 126MHz $^{13}$CNMR of 1.21b**

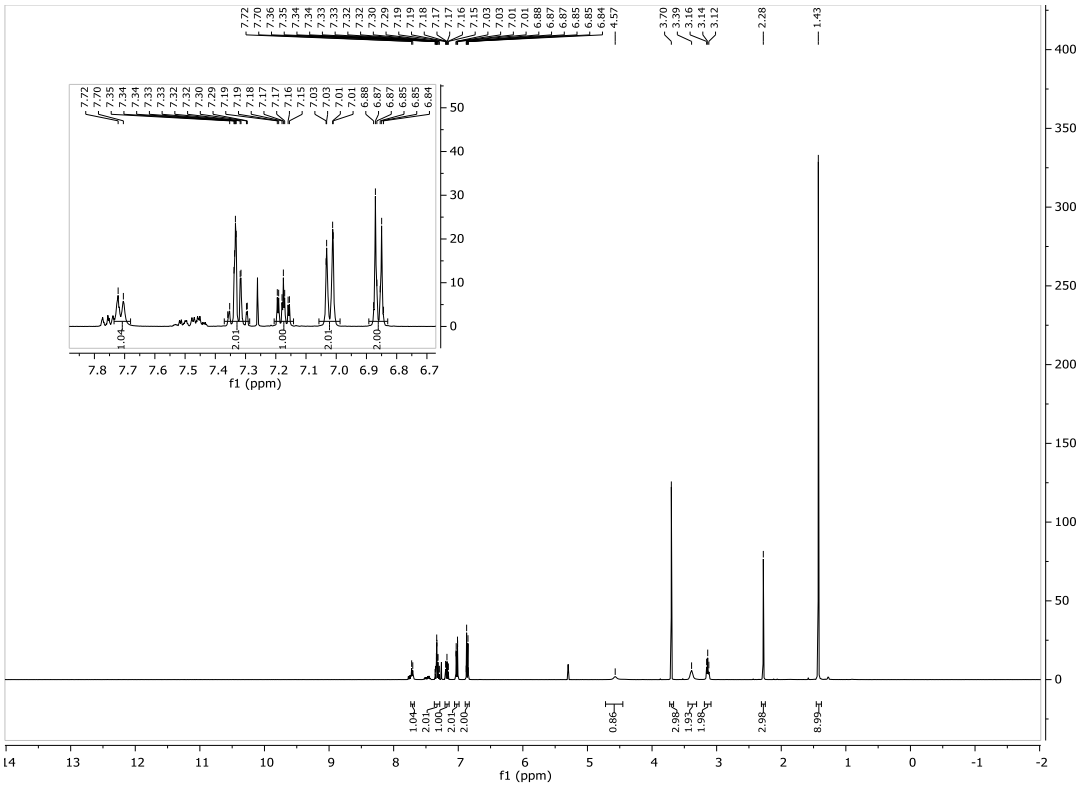


**Figure 1.7.56 500MHz $^{1}$HNMR of 1.22b**

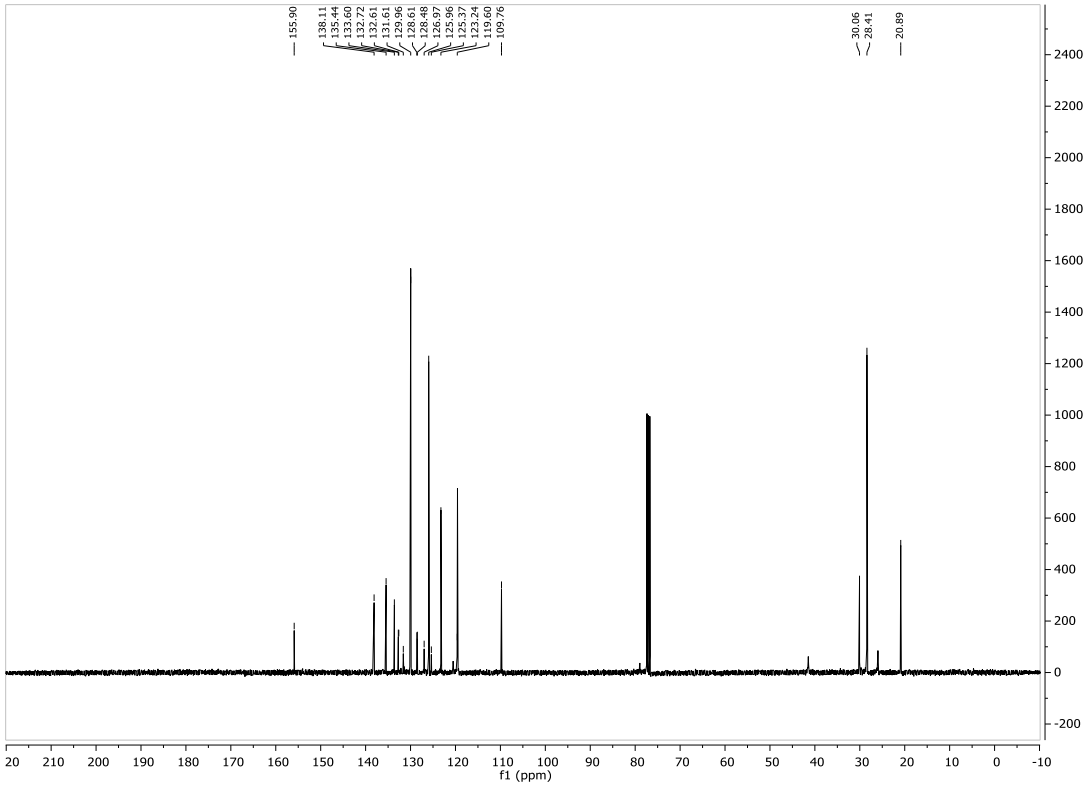


**Figure 1.7.57 126MHz $^{13}$CNMR of 1.22b**

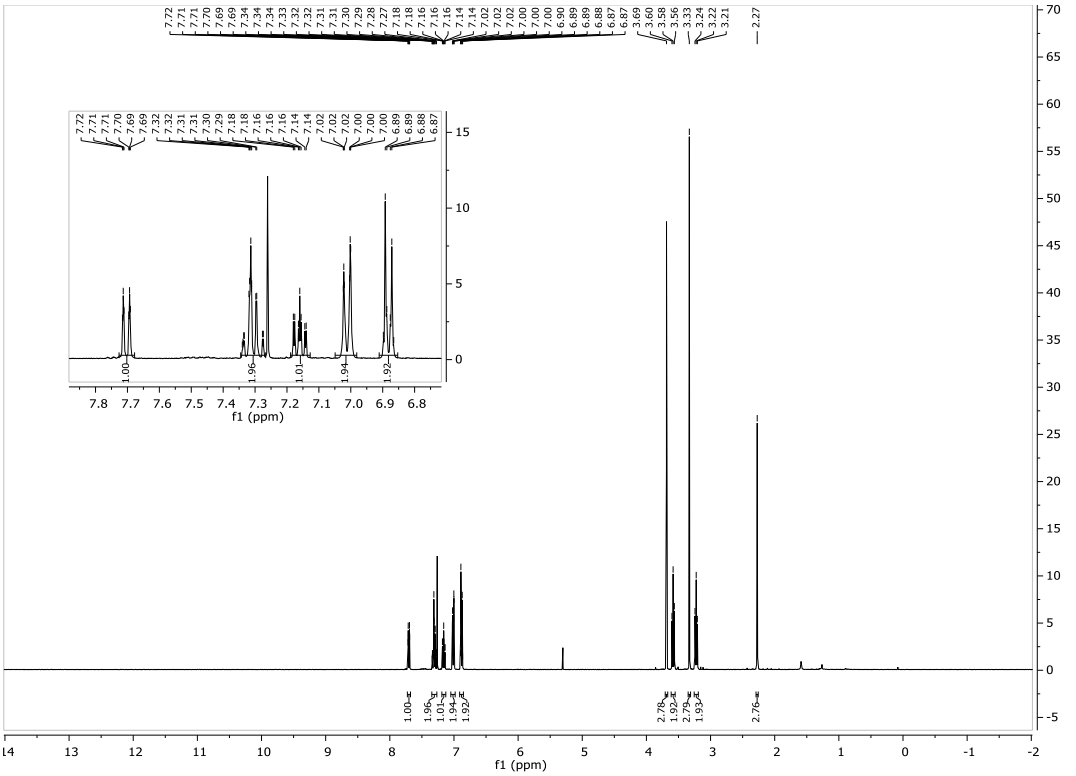


**Figure 1.7.58 500MHz $^{1}$HNMR of 1.23b**

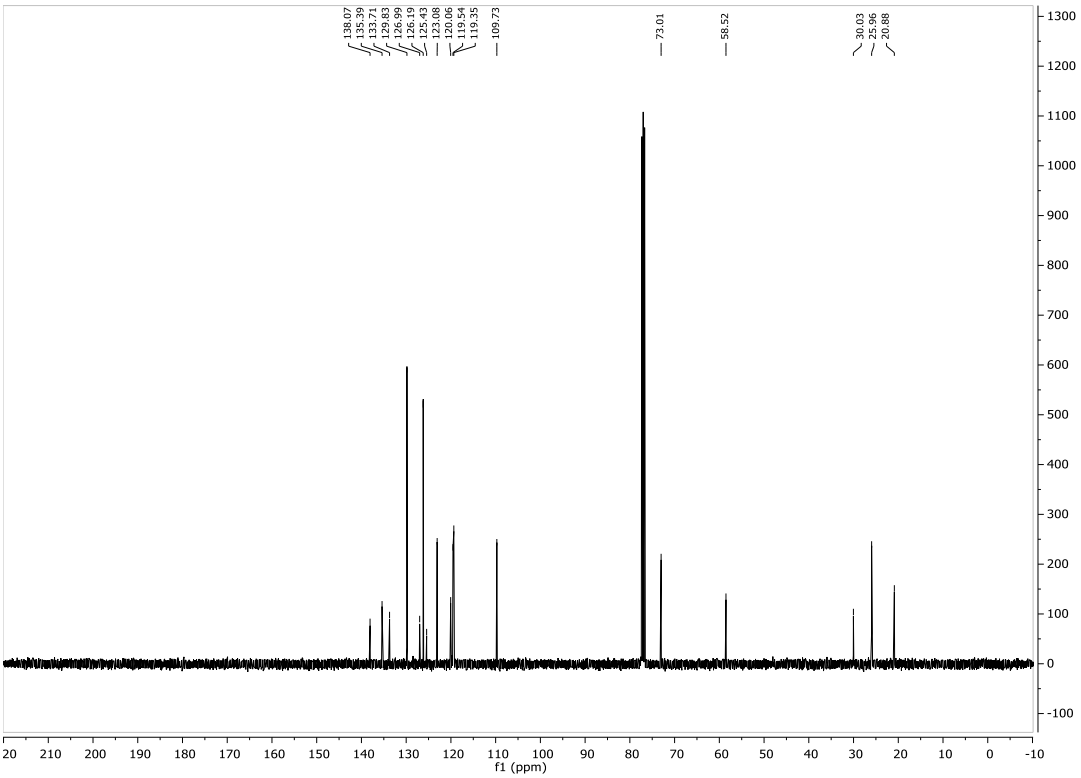


**Figure 1.7.59 126MHz $^{13}$CNMR of 1.23b**

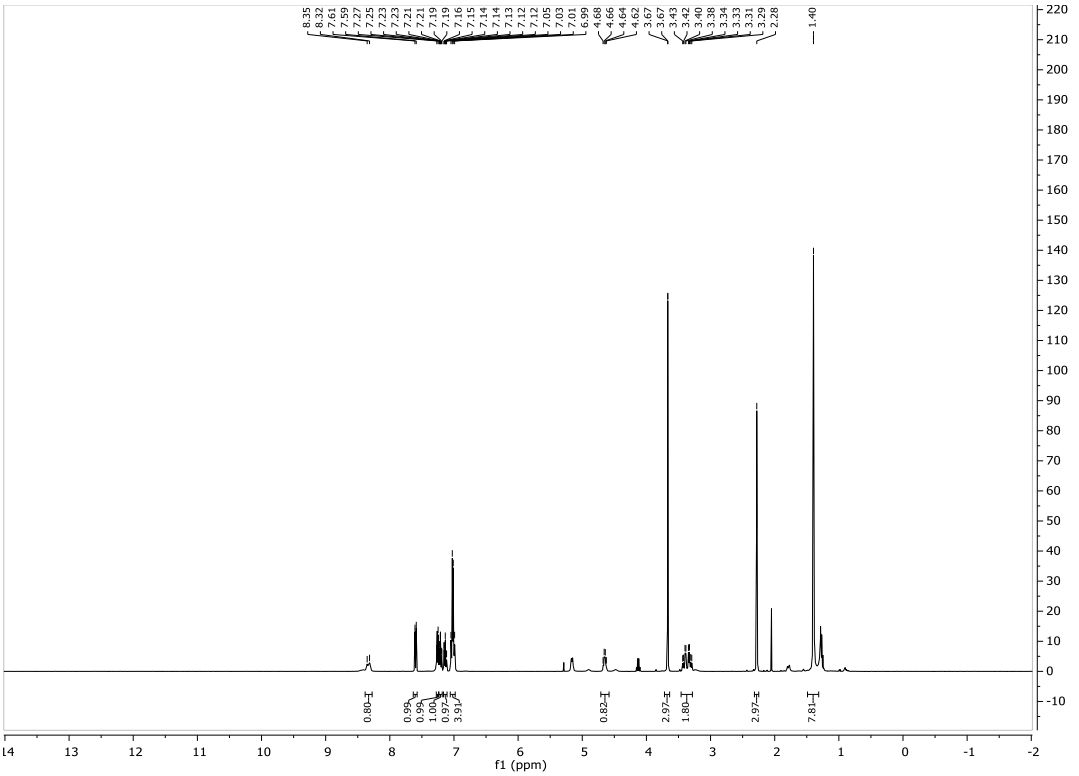


**Figure 1.7.60 500MHz $^{1}$HNMR of 1.24b**

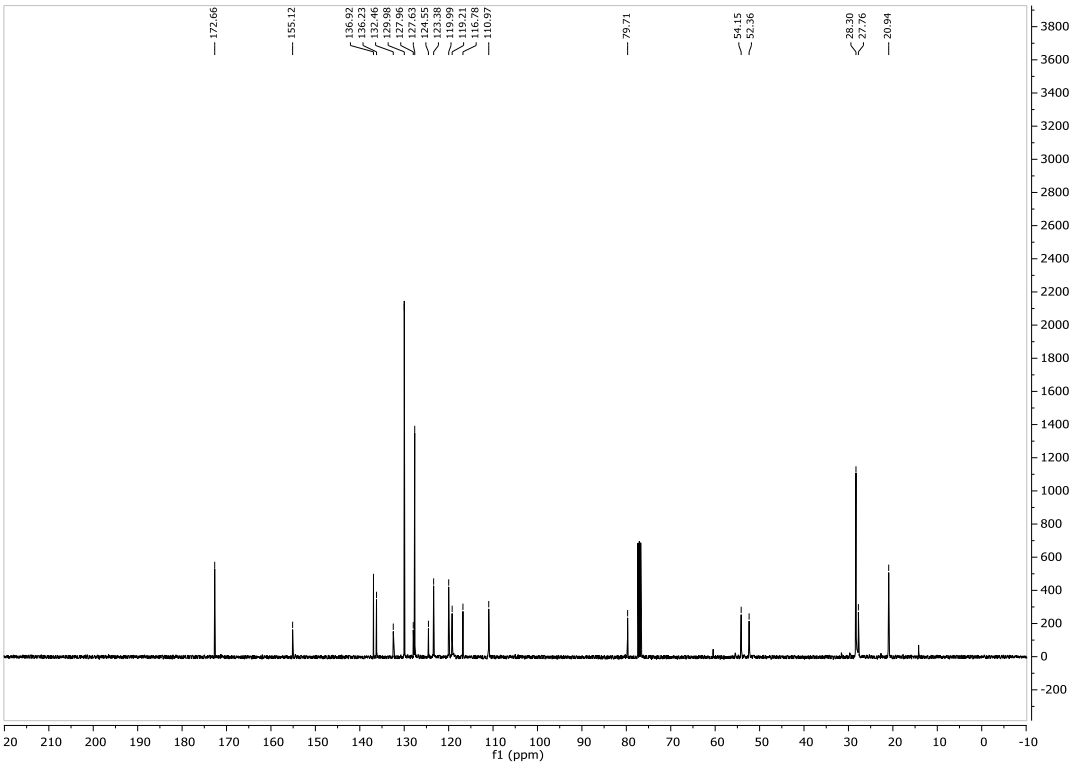


**Figure 1.7.61 126MHz $^{13}$CNMR of 1.24b**

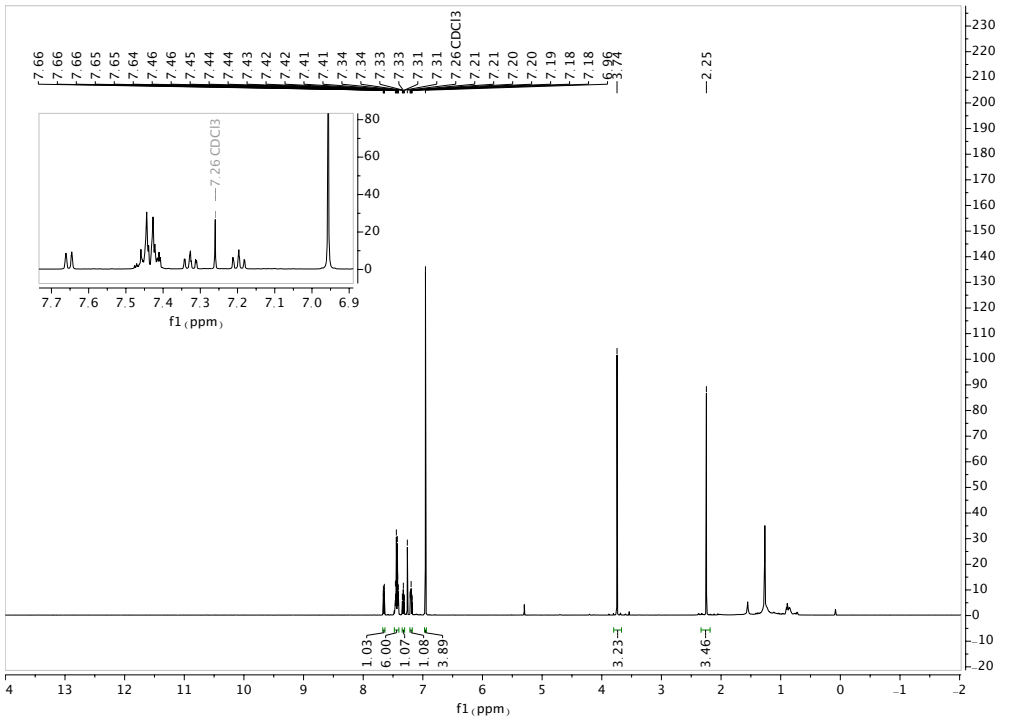

**Figure 1.7.62 500MHz $^{1}$HNMR of 1.25b**

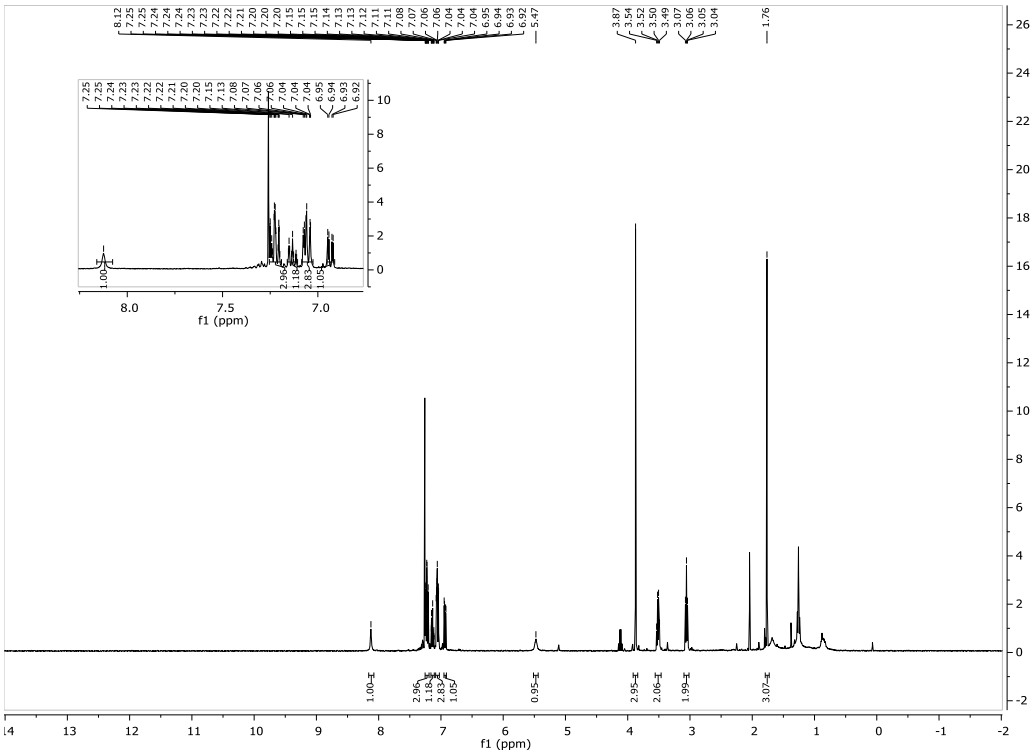

**Figure 1.7.63 500MHz $^{1}$HNMR of 1.26b**

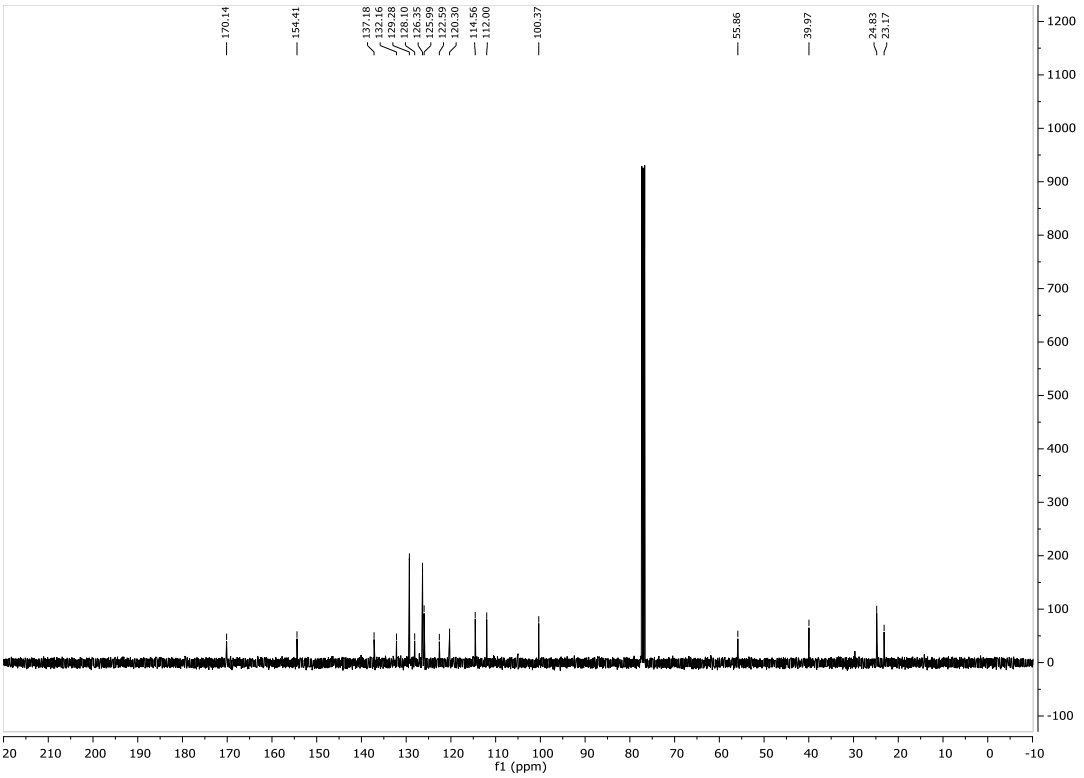


**Figure 1.7.64 126MHz $^{13}$CNMR of 1.26b**

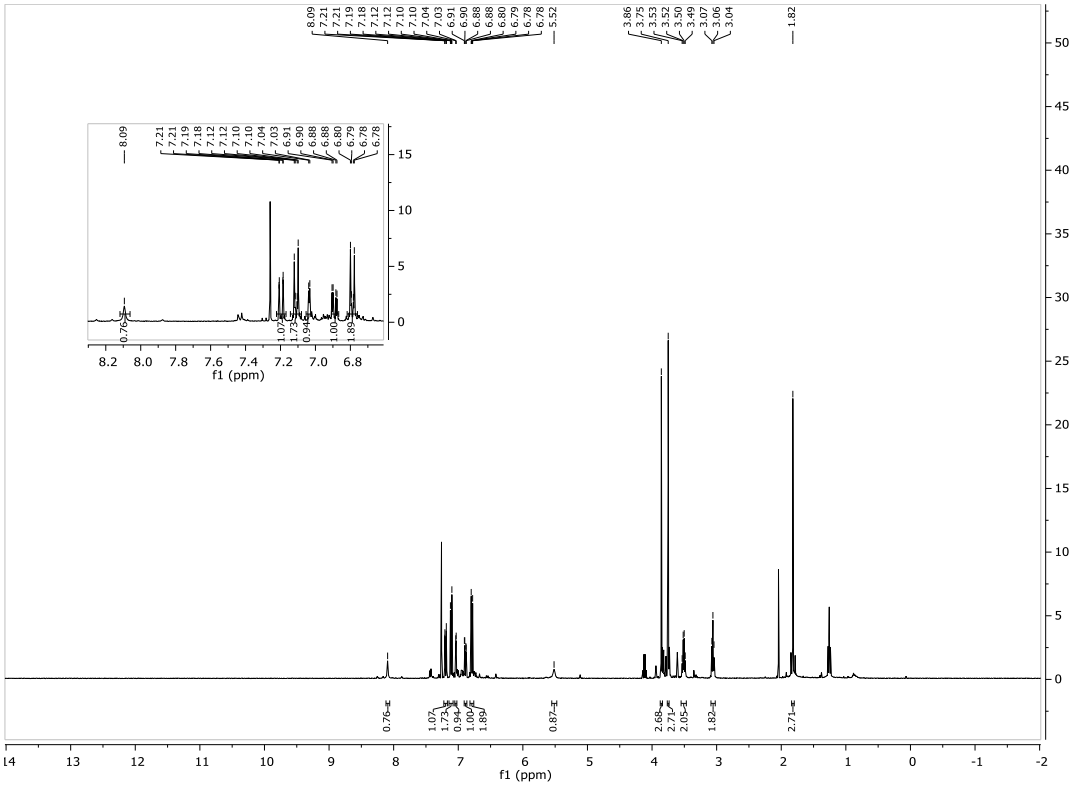


**Figure 1.7.65 500MHz $^{1}$HNMR of 1.27b**

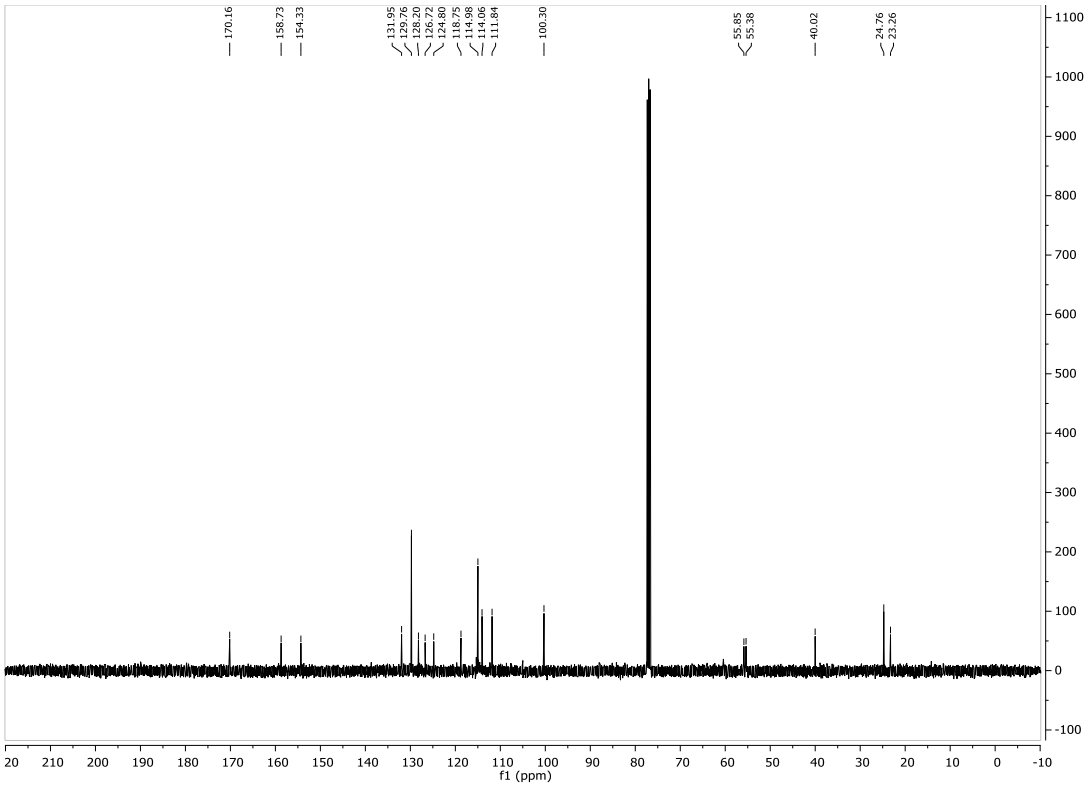


**Figure 1.7.66 126MHz $^{13}$CNMR of 1.27b**

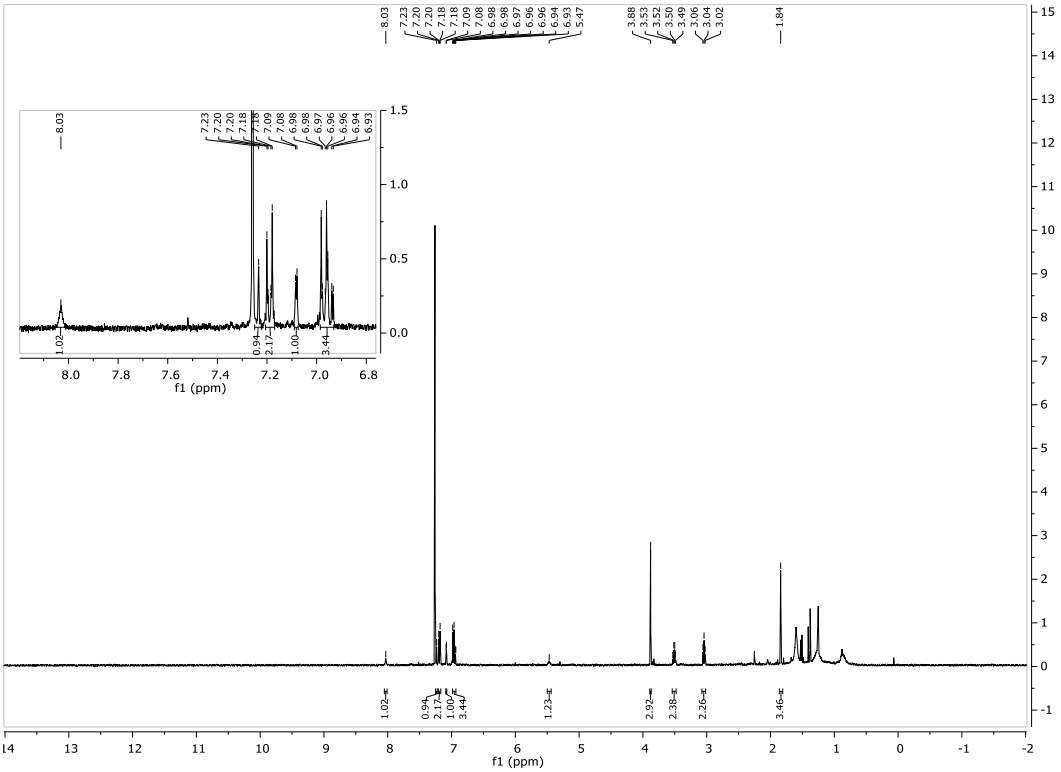


**Figure 1.7.67 126MHz $^{13}$CNMR of 1.28b**

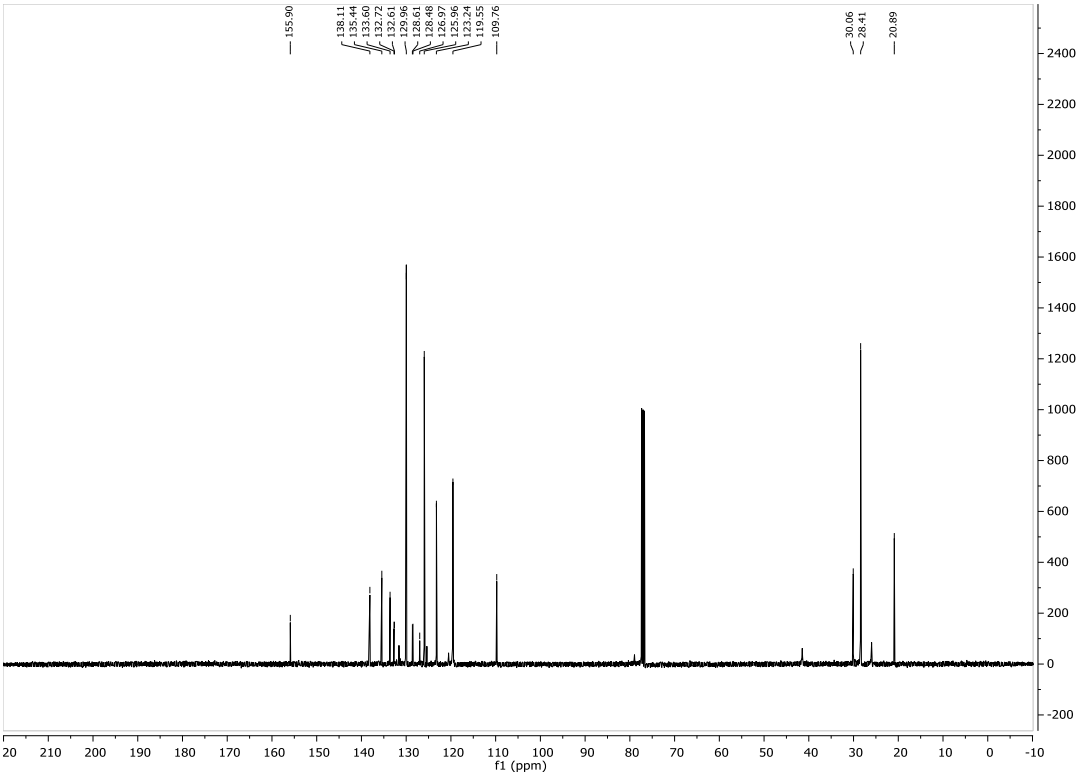


**Figure 1.7.68 126MHz $^{13}$CNMR of 1.28b**

### 1.7.7 Computational Geometries/Electron Density Maps

All geometry optimizations and frequency calculations were performed in Gaussian 09 using density functional theory, B3LYP/6-31(d) in gas phase. Gaussian 09, Revision D.01. M. J. Frisch, G. W. Trucks, H. B. Schlegel, G. E. Scuseria,M. A. Robb, J. R. Cheeseman, G. Scalmani, V. Barone, B. Mennucci, G. A. Petersson,H. Nakatsuji, M. Caricato, X. Li, H. P. Hratchian, A. F. Izmaylov, J. Bloino, G. Zheng, J.L. Sonnenberg, M. Hada, M. Ehara, K. Toyota, R. Fukuda, J. Hasegawa, M. Ishida, T.Nakajima, Y. Honda, O. Kitao, H. Nakai, T. Vreven, J. A. Montgomery, Jr., J. E.Peralta, F. Ogliaro, M. Bearpark, J. J. Heyd, E. Brothers, K. N. Kudin, V. N. Staroverov,T. Keith, R. Kobayashi, J. Normand, K. Raghavachari, A. Rendell, J. C. Burant, S. S.Iyengar, J. Tomasi, M. Cossi, N. Rega, J. M. Millam, M. Klene, J. E. Knox, J. B. Cross,V. Bakken, C. Adamo, J. Jaramillo, R. Gomperts, R. E. Stratmann, O. Yazyev, A. J.Austin, R. Cammi, C. Pomelli, J. W.

Ochterski, R. L. Martin, K. Morokuma, V. G.Zakrzewski, G. A. Voth, P. Salvador, J. J. Dannenberg, S. Dapprich, A. D. Daniels, O.Farkas, J. B. Foresman, J. V. Ortiz, J. Cioslowski, and D. J. Fox, Gaussian, Inc.,Wallingford CT, 2013.

**(A) Thioamide Starting material**

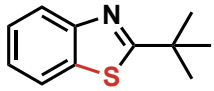


| Center Number | Atomic Number | Atomic Type | Coordinates (Angstroms) X | Y | Z |
|---|---|---|---|---|---|
| 1 | 6 | 0 | -3.875848 | 0.246685 | 0.001251 |
| 2 | 6 | 0 | -3.211295 | 0.030509 | -1.207307 |
| 3 | 6 | 0 | -1.881057 | -0.391506 | -1.210413 |
| 4 | 6 | 0 | -1.204721 | -0.584301 | -0.000782 |
| 5 | 6 | 0 | -1.879113 | -0.391184 | 1.209887 |
| 6 | 6 | 0 | -3.209342 | 0.030875 | 1.208800 |
| 7 | 1 | 0 | -4.911900 | 0.573471 | 0.002038 |
| 8 | 1 | 0 | -3.728637 | 0.183823 | -2.150230 |
| 9 | 1 | 0 | -1.360106 | -0.575513 | -2.145067 |
| 10 | 1 | 0 | -1.356743 | -0.575102 | 2.143763 |
| 11 | 1 | 0 | -3.725174 | 0.184425 | 2.152511 |
| 12 | 7 | 0 | 0.129077 | -1.126932 | -0.001910 |
| 13 | 1 | 0 | 0.167375 | -2.142991 | -0.002203 |
| 14 | 6 | 0 | 1.384189 | -0.591396 | -0.000395 |
| 15 | 16 | 0 | 2.662266 | -1.676430 | 0.000870 |
| 16 | 6 | 0 | 1.583460 | 0.943920 | -0.000272 |
| 17 | 6 | 0 | 3.082302 | 1.305763 | -0.001051 |
| 18 | 1 | 0 | 3.593786 | 0.910919 | 0.880111 |
| 19 | 1 | 0 | 3.592843 | 0.910939 | -0.882779 |
| 20 | 1 | 0 | 3.179311 | 2.398277 | -0.001096 |
| 21 | 6 | 0 | 0.954010 | 1.568053 | -1.270457 |
| 22 | 1 | 0 | 1.358022 | 1.099897 | -2.175160 |
| 23 | 1 | 0 | -0.133753 | 1.482547 | -1.290561 |
| 24 | 1 | 0 | 1.203555 | 2.634618 | -1.306249 |
| 25 | 6 | 0 | 0.955466 | 1.567666 | 1.270842 |
| 26 | 1 | 0 | -0.132300 | 1.482433 | 1.292002 |
| 27 | 1 | 0 | 1.360300 | 1.099019 | 2.174921 |
| 28 | 1 | 0 | 1.205329 | 2.634153 | 1.306821 |

Zero-point correction= 0.238571 (Hartree/Particle)
Thermal correction to Energy= 0.251857
Thermal correction to Enthalpy= 0.252801
Thermal correction to Gibbs Free Energy= 0.197414
Sum of electronic and zero-point Energies= -880.903848
Sum of electronic and thermal Energies= -880.890562
Sum of electronic and thermal Enthalpies= -880.889617
Sum of electronic and thermal Free Energies= -880.945005

**(B) Radical Cation Intermediate**

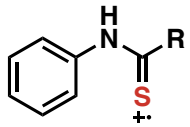


| Center Number | Atomic Number | Atomic Type | Coordinates (Angstroms) X | Y | Z |
|---|---|---|---|---|---|
| 1 | 6 | 0 | 3.867669 | 0.264444 | 0.000237 |
| 2 | 6 | 0 | 3.209002 | 0.040502 | 1.211204 |
| 3 | 6 | 0 | 1.884787 | -0.400381 | 1.219324 |
| 4 | 6 | 0 | 1.232884 | -0.592211 | -0.000027 |
| 5 | 6 | 0 | 1.884892 | -0.399954 | -1.219255 |
| 6 | 6 | 0 | 3.209106 | 0.040927 | -1.210866 |
| 7 | 1 | 0 | 4.898756 | 0.603816 | 0.000340 |
| 8 | 1 | 0 | 3.724422 | 0.200923 | 2.152838 |
| 9 | 1 | 0 | 1.370272 | -0.593802 | 2.155534 |
| 10 | 1 | 0 | 1.370458 | -0.593047 | -2.155576 |
| 11 | 1 | 0 | 3.724608 | 0.201677 | -2.152399 |
| 12 | 7 | 0 | -0.113084 | -1.158594 | -0.000184 |
| 13 | 1 | 0 | -0.113400 | -2.178513 | -0.000344 |
| 14 | 6 | 0 | -1.299722 | -0.580512 | -0.000161 |
| 15 | 16 | 0 | -2.683681 | -1.609290 | -0.000410 |
| 16 | 6 | 0 | -1.575023 | 0.933619 | 0.000073 |
| 17 | 6 | 0 | -3.100750 | 1.197995 | 0.000029 |
| 18 | 1 | 0 | -3.597209 | 0.809641 | -0.897005 |
| 19 | 1 | 0 | -3.597315 | 0.809324 | 0.896866 |
| 20 | 1 | 0 | -3.263530 | 2.281063 | 0.000210 |
| 21 | 6 | 0 | -0.970707 | 1.567543 | 1.278887 |
| 22 | 1 | 0 | -1.364232 | 1.097141 | 2.186055 |
| 23 | 1 | 0 | 0.118380 | 1.518483 | 1.294751 |
| 24 | 1 | 0 | -1.262450 | 2.622632 | 1.298100 |
| 25 | 6 | 0 | -0.970560 | 1.567966 | -1.278462 |
| 26 | 1 | 0 | 0.118528 | 1.518908 | -1.294219 |
| 27 | 1 | 0 | -1.363983 | 1.097866 | -2.185832 |
| 28 | 1 | 0 | -1.262298 | 2.623062 | -1.297358 |

```
Zero-point correction=                           0.238132 (Hartree/Particle)
 Thermal correction to Energy=                    0.250715
 Thermal correction to Enthalpy=                  0.251659
 Thermal correction to Gibbs Free Energy=         0.198722
 Sum of electronic and zero-point Energies=          -880.629402
 Sum of electronic and thermal Energies=             -880.616819
 Sum of electronic and thermal Enthalpies=           -880.615874
 Sum of electronic and thermal Free Energies=        -880.668812
```

**(C) Cyclized Radical Cation**

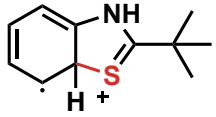


| Center Number | Atomic Number | Atomic Type | Coordinates (Angstroms) X | Y | Z |
|---|---|---|---|---|---|

| | | | | | |
|---|---|---|---|---|---|
| 1 | 6 | 0 | 3.747847 | -0.330874 | -0.304238 |
| 2 | 6 | 0 | 2.765790 | -1.222761 | 0.019072 |
| 3 | 6 | 0 | 1.246395 | 0.731463 | 0.316887 |
| 4 | 6 | 0 | 2.263231 | 1.604990 | 0.007413 |
| 5 | 6 | 0 | 3.538589 | 1.079171 | -0.257508 |
| 6 | 1 | 0 | 4.722276 | -0.702291 | -0.606462 |
| 7 | 1 | 0 | 2.949967 | -2.292029 | 0.013776 |
| 8 | 1 | 0 | 2.073003 | 2.669878 | -0.096344 |
| 9 | 1 | 0 | 4.352061 | 1.751885 | -0.504995 |
| 10 | 16 | 0 | -0.156508 | -1.514152 | -0.096802 |
| 11 | 6 | 0 | -0.959090 | 0.014121 | 0.055166 |
| 12 | 6 | 0 | -2.456219 | 0.194044 | -0.078330 |
| 13 | 6 | 0 | -2.817359 | 1.680753 | -0.278744 |
| 14 | 6 | 0 | -2.962234 | -0.634852 | -1.283633 |
| 15 | 6 | 0 | -3.113971 | -0.329488 | 1.230399 |
| 16 | 1 | 0 | -2.561443 | 2.295280 | 0.593887 |
| 17 | 1 | 0 | -2.347239 | 2.103417 | -1.174290 |
| 18 | 1 | 0 | -3.899289 | 1.768185 | -0.409512 |
| 19 | 1 | 0 | -2.754564 | -1.703397 | -1.163516 |
| 20 | 1 | 0 | -4.047159 | -0.519074 | -1.362233 |
| 21 | 1 | 0 | -2.513444 | -0.296938 | -2.223003 |
| 22 | 1 | 0 | -4.198081 | -0.199489 | 1.154167 |
| 23 | 1 | 0 | -2.907841 | -1.392147 | 1.387224 |
| 24 | 1 | 0 | -2.765574 | 0.226676 | 2.106933 |
| 25 | 7 | 0 | -0.119780 | 1.019835 | 0.294470 |
| 26 | 1 | 0 | -0.461665 | 1.977388 | 0.301564 |
| 27 | 6 | 0 | 1.464923 | -0.726368 | 0.547737 |
| 28 | 1 | 0 | 1.394175 | -0.960958 | 1.625019 |

Zero-point correction= 0.237715 (Hartree/Particle)
Thermal correction to Energy= 0.250583
Thermal correction to Enthalpy= 0.251527
Thermal correction to Gibbs Free Energy= 0.197930
Sum of electronic and zero-point Energies= -880.637693
Sum of electronic and thermal Energies= -880.624825
Sum of electronic and thermal Enthalpies= -880.623881
Sum of electronic and thermal Free Energies= -880.677477

**(D) Cyclized Cation**

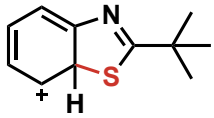


| Center Number | Atomic Number | Atomic Type | Coordinates (Angstroms) X | Y | Z |
|---|---|---|---|---|---|
| 1 | 6 | 0 | 3.737835 | 0.320718 | 0.283393 |
| 2 | 6 | 0 | 2.746903 | 1.225990 | 0.090377 |
| 3 | 6 | 0 | 1.155423 | -0.731717 | -0.218261 |
| 4 | 6 | 0 | 2.244795 | -1.620706 | -0.106218 |
| 5 | 6 | 0 | 3.491545 | -1.093273 | 0.153301 |
| 6 | 1 | 0 | 4.737035 | 0.653774 | 0.544581 |
| 7 | 1 | 0 | 2.926346 | 2.295013 | 0.146565 |
| 8 | 1 | 0 | 2.062413 | -2.689754 | -0.107952 |

```
     9          1           0        4.324527   -1.772585    0.312574
    10         16           0       -0.178836    1.540375   -0.009532
    11          6           0       -0.941201   -0.037975   -0.033076
    12          6           0       -2.434295   -0.198602    0.068296
    13          6           0       -2.720755   -1.145985    1.266404
    14          6           0       -3.151497    1.146566    0.271603
    15          6           0       -2.913556   -0.869615   -1.250336
    16          1           0       -2.221386   -2.109391    1.140575
    17          1           0       -2.397205   -0.700528    2.212875
    18          1           0       -3.800547   -1.315684    1.321843
    19          1           0       -2.999474    1.827426   -0.573523
    20          1           0       -4.227920    0.972172    0.357063
    21          1           0       -2.831211    1.646871    1.193414
    22          1           0       -3.992859   -1.037577   -1.180896
    23          1           0       -2.725518   -0.227755   -2.117492
    24          1           0       -2.420600   -1.832261   -1.408088
    25          7           0       -0.129387   -1.086128   -0.149117
    26          6           0        1.424581    0.734091   -0.385029
    27          1           0        1.494810    0.870221   -1.487933
---------------------------------------------------------------------

Zero-point correction=                           0.226086 (Hartree/Particle)
Thermal correction to Energy=                    0.238592
Thermal correction to Enthalpy=                  0.239536
Thermal correction to Gibbs Free Energy=         0.187408
Sum of electronic and zero-point Energies=           -880.049093
Sum of electronic and thermal Energies=              -880.036587
Sum of electronic and thermal Enthalpies=            -880.035643
Sum of electronic and thermal Free Energies=         -880.087771
```

### 1.7.8 Cyclic Voltammetry

**General Procedure**: A CH Instruments Model 630c Electrochemical Workstation potentiostat was utilized. Experiments were run in a jacketed single compartment cell with a glassy carbon disk working electrode, a platinum wire counter electrode, and a Ag wire pseudo reference electrode. Immediately before use, the working electrode was polished with 0.25 μm diamond polishing paste, rinsed thoroughly with DI water, then polished with 0.25 μm alumina suspension, followed by a thorough rinse with DI water and acetone. The Ag wire pseudo reference electrode was housed in a separate compartment containing 3 M KCl(aq) and was allowed to soak for at least 30 minutes before experiments. The potential of the pseudo-reference was later measured relative to a standard Ag/AgCl(4 M KCl)reference electrode to allow conversion of the data to V vs. SCE. Temperature was controlled during experiments by running 25 °C through the cell jacket using a circulating

water bath. The electrolyte solution was 0.10 M $NBu_4PF_6$ in MeCN, unless noted otherwise. The solution was purged for several minutes with Ar gas prior to running CVs. An analyte concentration of 0.1 mM in 5 mL of electrolyte was used for voltage experiments and 0.2 mM in mL of electrolyte was used for pyridine titration. Background scans without analyte were taken at each scan rate and subtracted from the analyte scan. All scan experiments were normalized by dividing the measured current by the square root of scan rate. The potentials were converted from AgCl/Ag reference values to SCE by subtraction of 0.045 V.

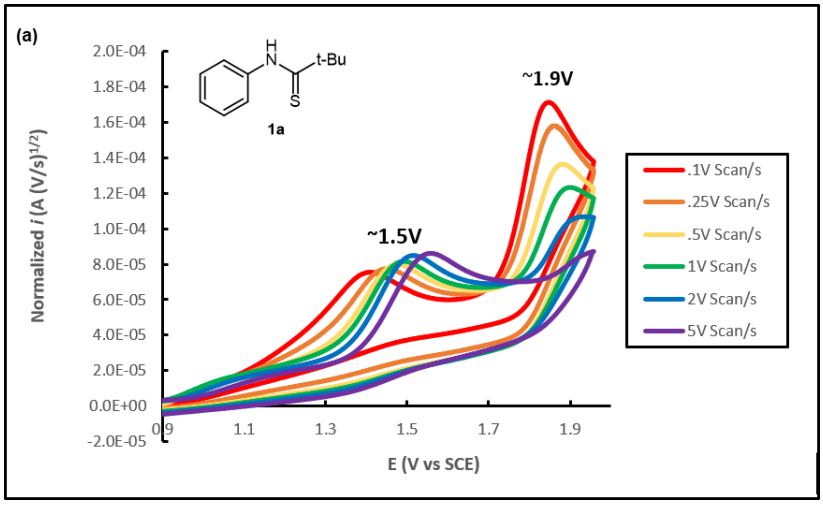


**Figure 1.7.69 CV Scan of 1.1a**

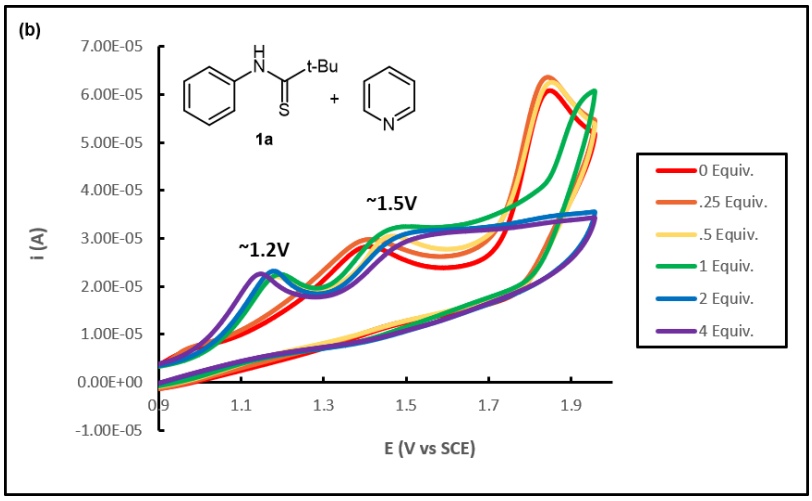


**Figure 1.7.70 CV Scan of Pyridine Titration of 1.1a**

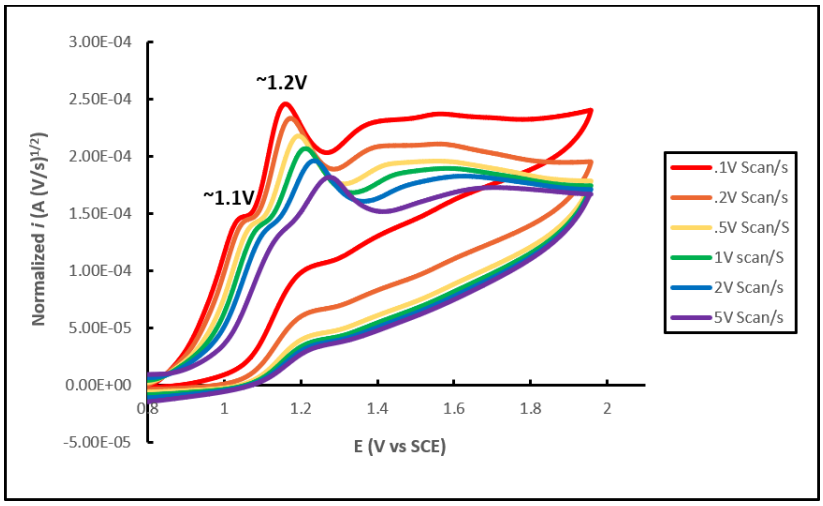


**Figure 1.7.71 CV Scan of Melatonin 1.18a**

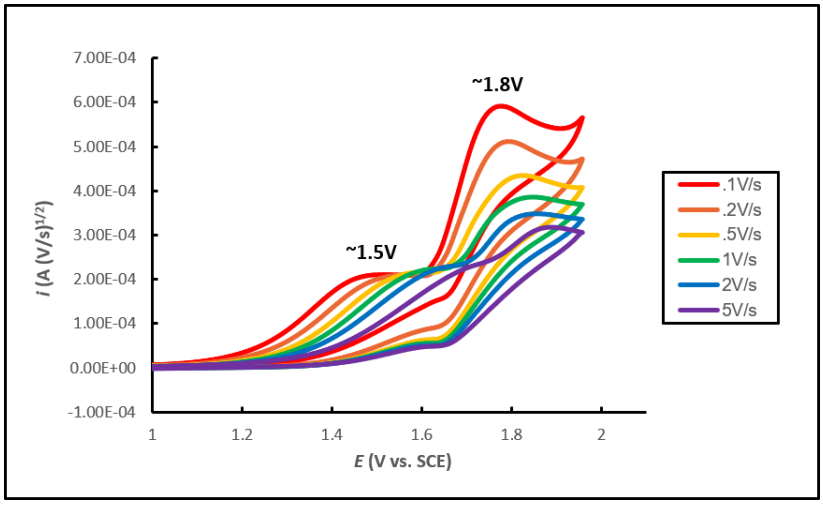


**Figure 1.7.72 CV Scan of 4-methylbenzenethiol**

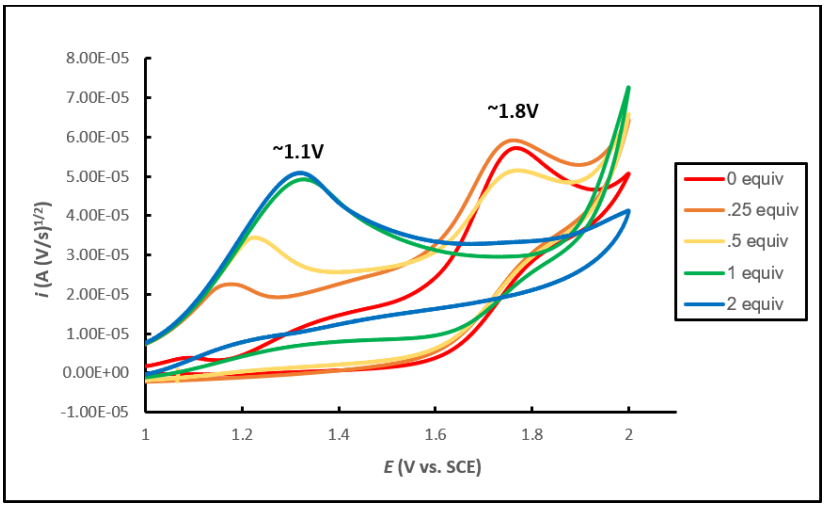


**Figure 1.7.73 CV Scan of 1.10a**

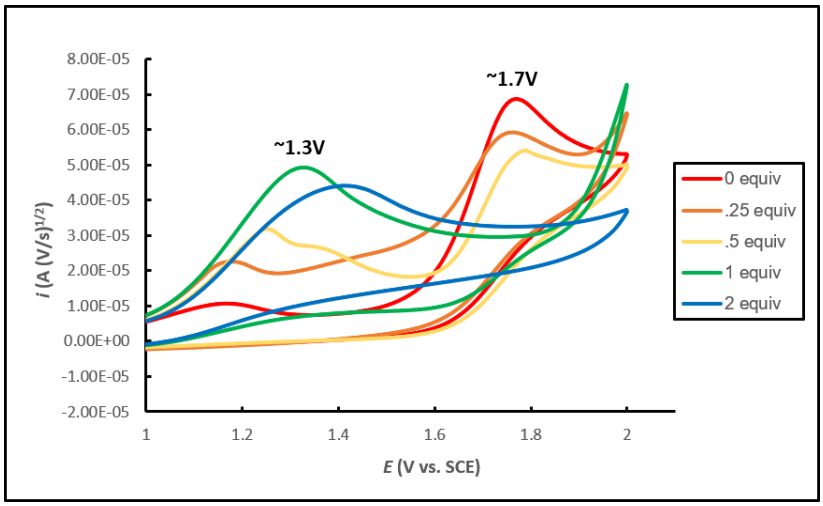


**Figure 1.7.74 CV Scan of 1.14a**

### 1.7.9 Stern-Vollmer Analysis

Stern-Volmer experiments were done at 410nm detection on a Horiba Fluoromax-4 spectrofluorometer. A solution of $(Ir[dF(CF_3)ppy]_2(dtbpy)]PF_6$ photocatalyst in acetonitrile ($2.0 \times 10^{-5}$M) and a quencher in acetonitrile (.1M) stock solution was prepared. Stern-Volmer analysis was conducted according to the following relationship:

$$\tau_o/\tau = 1 + K_{SV}[Q] = 1 + k_q\tau_o[Q]$$

where $\tau_o$ and $\tau$ are the fluorescence lifetime in the absence and presence of Q, $K_{sv}$ is the Stern-Volmer constant, $k_q$ is the bimolecular quenching constant, and [Q] is the concentration of quencher.

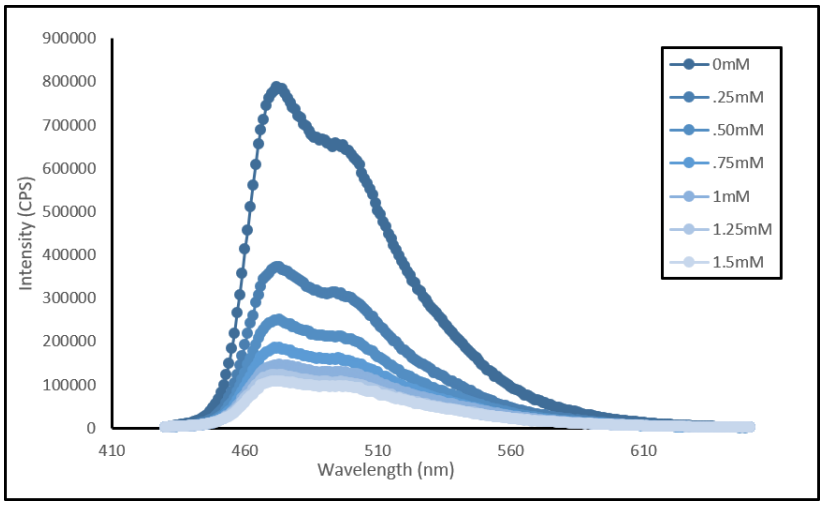


**Figure 1.7.75 Stern Vollmer Quenching with Melatonin**

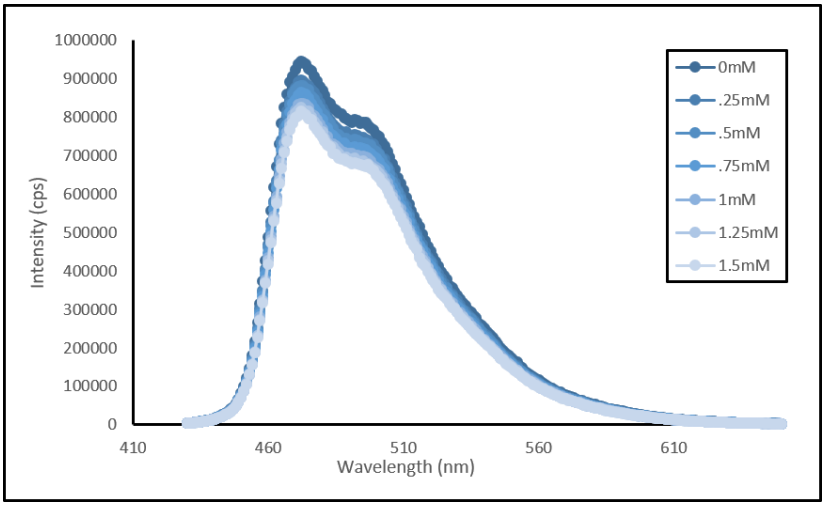


**Figure 1.7.76 Stern Vollmer Quenching with 4-methylbenzenethiol**

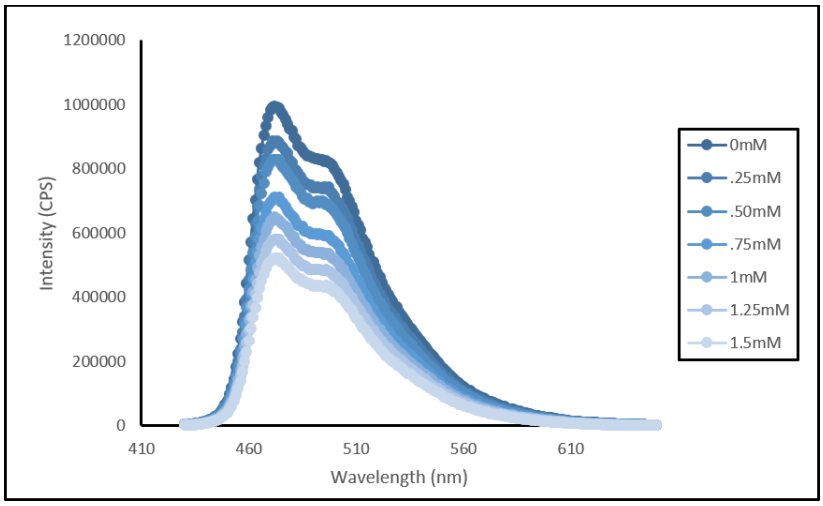


**Figure 1.7.77 Stern Vollmer Quenching with 4-methyl diphenyldisulfide**

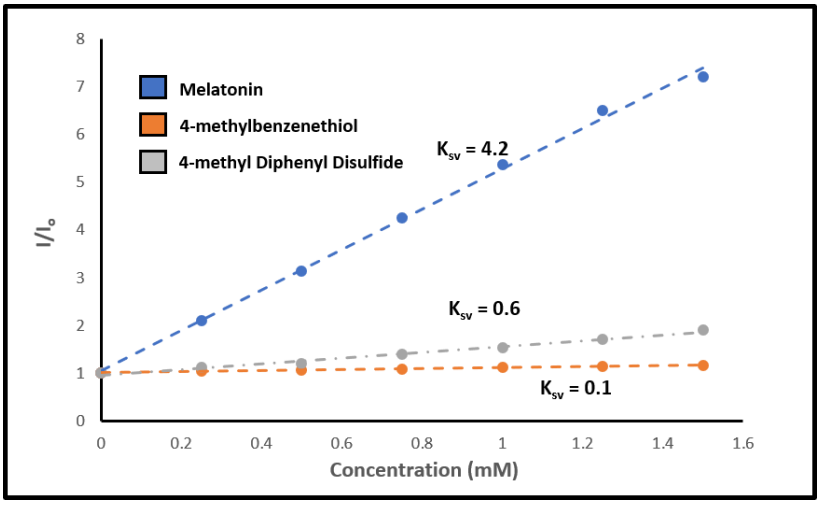


**Figure 1.7.78 $K_{SV}$ Constant Measurement of Stern Vollmer Plots**

## 1.7.10 Mechanistic Experiments

**Equation 1:**

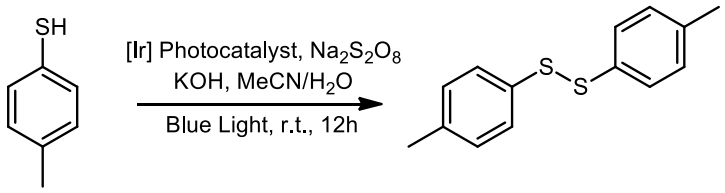


**Equation 2:**

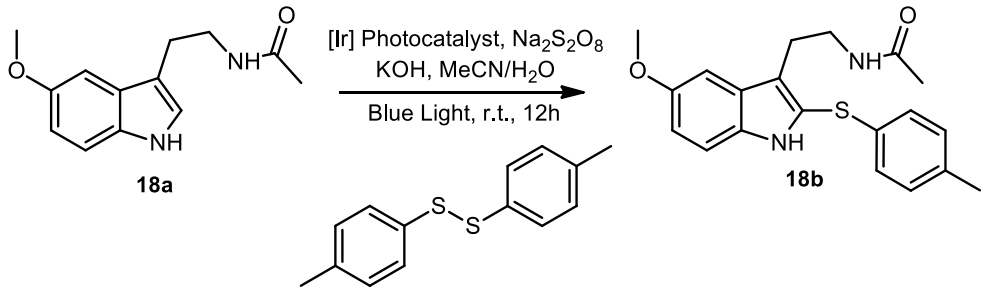


**Equation 3:**

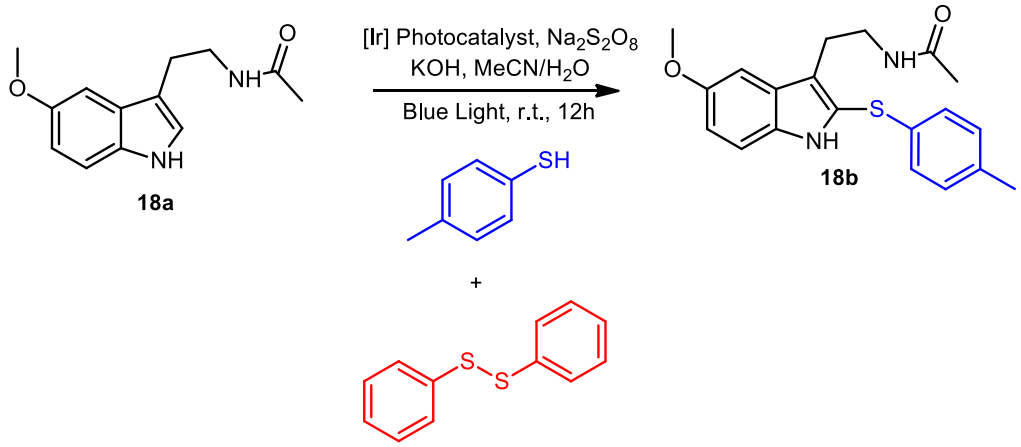


**Scheme 1.7.79 Control Experiments to Probe Sulfenylation Mechanism**

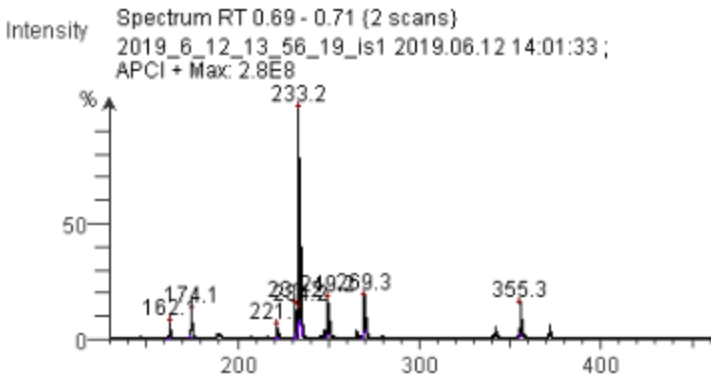


**Figure 1.7.80 Mass Spectrum of Cross Experiment Showing Disulfide Byproduct**

### 1.7.11 Photo-Chamber Set Up (2019-2021)

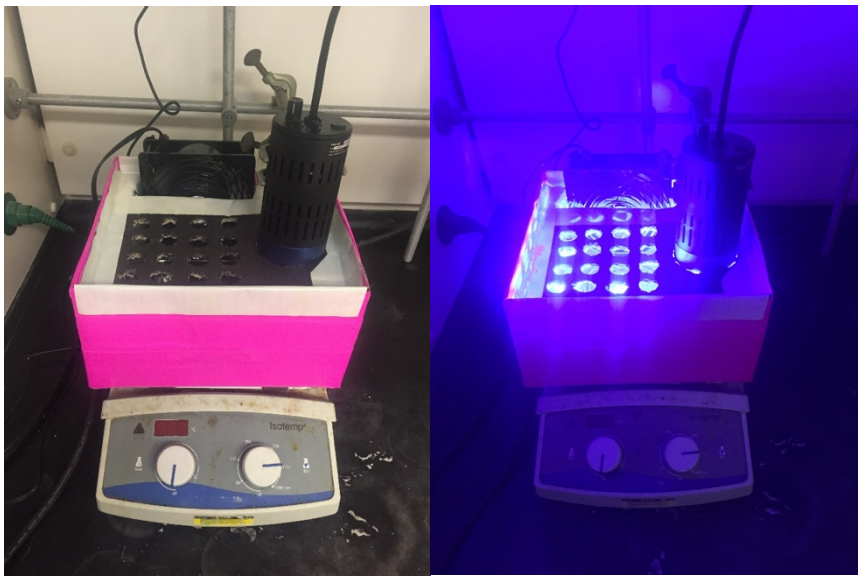

A PR160 LED photoredox Kessil lamp (370nm) was inserted into a cutout cardboard box with angled mirrors inside for even distribution of light. A computer fan was used to minimize heat output from the lamp. Stir rate is >600 rpm

## 1.8 Acknowledgements

The contents in Chapter 1 are in part a reformatted reprint of the following manuscript with permission from the Thieme Connect: Dinh, A; Nguyen, A; Millan Aceves E.; Albright, S.; Cedano, M.; Smith D.; Gustafson, J. "Photocatalytic Oxidative C-H Thiolation: Synthesis of Benzothiazoles and Sulfenylated Indoles." *Synlett* **2019** *30* 1648-1655. I was co-first author of the following manuscript, providing work for the optimization, substrate scope evaluation, and assisted during the mechanistic work for the manuscript. Andrew Dinh is the co-first author who primarily wrote the manuscript and provided data for optimization, substrate scope evaluation, and led the mechanistic studies. Ernesto Milan Aceves and Samuel Albright contributed equally to substrate scope evaluation. Mario Cedano is graduate student with experience in electrochemistry and trained Andrew and I regarding the cyclic voltammetry. Dr. Diane Smith gave insightful discussions regarding the electrochemistry and mechanisms, while providing the facilities to run cyclic voltammetry. The dissertation author was co-primary researcher for the data presented and this work was supported by the National Science Foundation (CHE – 1664565).

# CHAPTER 2: A Light-Promoted Innate Trifluoromethylation of Pyridones and Related *N*-Heteroarenes

## 2.0 *Organic Letters* Copyright



## 2.1 Incorporation of Perfluoroalkyl Groups on Bioactive Molecules

Perfluoroalkyl groups impart unique electronic effects to small molecules which has led to their widespread incorporation in such.[86, 87] In drug discovery these groups have been shown to increase metabolic stability, lipophilicity, and overall activity.[88] Perfluoroalkylated functionalities are often added to arenes and *N*-heteroarenes necessitating the development of strategies to further incorporate these groups. Recent developments in perfluoroalkylation methods have been employed by reagents such as, but not limited to: Prakash's Reagent,[89] Langlois' Reagent,[90] Togni's reagent,[91] Umemoto's Reagent,[92] Baran's Reagent,[93] Ritter's Reagent,[94] $CF_3I$,[95] triflyl chloride,[51] triflic anhydride,[96] and trifluoroacetic acid (TFA).[97] These reagents can be either oxidized or reduced to generate a perfluoroalkyl radical with electrophilic or nucleophilic behavior.[93, 98, 99] While many of the methods developed alongside these reagents have been shown to functionalize a range of *N*-heteroarenes, they often require harsh conditions, precious metal catalysts, or pre-functionalization of substrates which can limit their practicality on large-scale and limit the utility for late-stage functionalization (LSF) of more complex *N*-heteroarenes.

## 2.2 Previous Radical Perfluoroalkylation Strategies on a Pyridone Scaffold

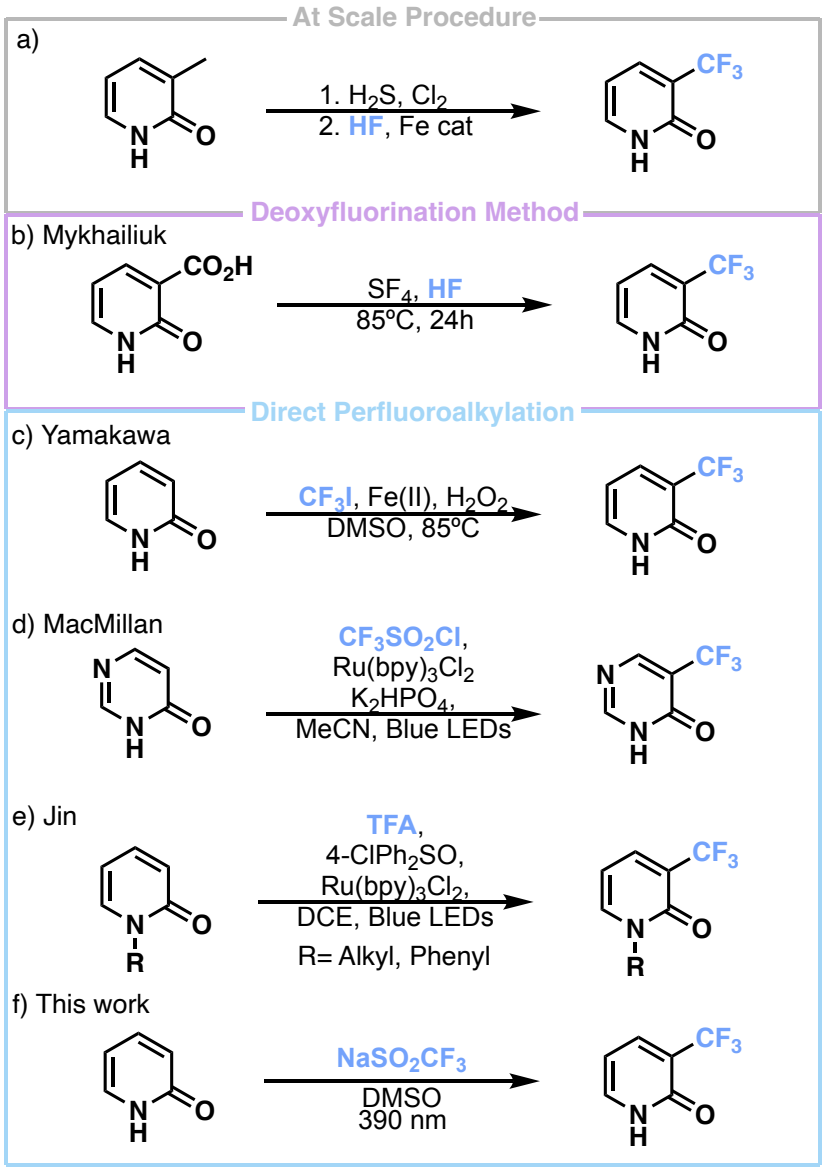


**Scheme 2.2.1 Previous Strategies to Achieve Perfluoroalkylated Pyridones**

There are fewer methodologies that afford pyridone perfluoroalkylation compared to other arenes and heteroarenes. Pyridones are a privileged scaffold and are common bioisosteres for a variety of functional groups such as amides, pyranones, pyrimidines, pyrazines, and phenols.[100-102] There are several biologically relevant perfluoroalkylated pyridones including: FDA-approved drug Pifeltro, an HIV-1 medication for use in combination with other antiretroviral medicines, and

Fusilade DX, an EPA approved herbicide used to treat weeds for cotton and soybeans. Despite their ubiquity, there are few direct, mild synthetic methods towards trifluoromethylated pyridones. They are often synthesized on scale from the corresponding methylated pyridine, which then undergoes a chlorination and subsequent fluorination before transforming it to a pyridone (Scheme 2.2.1a).[103-105] In the context of Pifeltro, the perfluoroalkyl group was pre-installed onto a halogenated pyridine, which was subsequently reacted in a $S_NAr$ fashion followed by oxidation to produce the trifluoromethylated pyridone moiety.[106] Another common route to achieve fluorinated pyridones involves a deoxyfluorination from the corresponding hydroxypicolinic acids from the Mykhailiuk[107] group (Scheme 1b). Direct strategies to incorporate perfluoroalkyl groups onto pyridones are highly desirable.[108] Current strategies to directly obtain trifluoromethylated pyridones and similar scaffolds include: an iron (II) mediated trifluoromethylation using $CF_3I$ and hydrogen peroxide from the Yamakawa[95] group (Scheme 1c), photoredox trifluoromethylations using triflyl chloride from the MacMillan[51] group (Scheme 1d) and TFA from the Jin[97] group (Scheme 1e). Herein, we report a simple light-mediated radical trifluoromethylation strategy that circumvents the need for harsh, expensive conditions that does not use any photocatalyst or oxidative additive on pyridones (Scheme 1f). This methodology has also been extended to include *N*-heteroarenes as well as some examples of Late-stage functionalization (LSF)

## 2.3 Optimization of Light-Mediated Perfluoroalkylation of 2-Pyridone

**Table 2.3.1 Optimization of Perfluoroalkylation of 2-Pyridone**

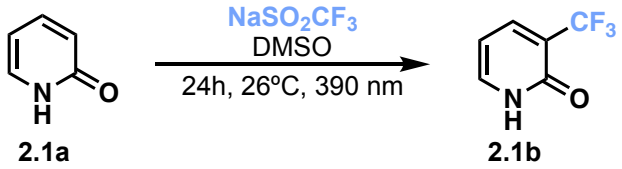


**2.1a** **2.1b**

| entry | variations from standard conditions | conversion[b] (%) |
|---|---|---|
| 1 | standard conditions | 96 |
| 2 | no light | ND |
| 3 | $K_2S_2O_8$ additive (3 equiv.), no light | 95 |
| 4 | MeCN:$H_2O$ (1:1) instead of DMSO | 60 |
| 5 | DMF instead of DMSO | 90 |
| 6 | 440nm instead of 390nm | 65 |
| 7 | 467nm instead of 390nm | 60 |
| 8 | Sparge with Ar, FPT | 54 |
| 9 | Sparge with $O_2$ | 98 |
| 10 | $Zn(SO_2CF_3)_2$ (1.4 equiv.) | 80 |
| 11 | $NaSO_2CH_3$ | ND |
| 12 | $NaSO_2CF_2H$ | 17 |

While studying the perfluoroalkylation of aromatics, we noticed a unique reactivity where pyridones such as **2.1a** could undergo a trifluoromethylation at the 3-position using Langlois' reagent ($NaSO_2CF_3$), DMSO, and 390nm LEDs (Table 1, entry 1) without the need for any photocatalyst or additive under ambient atmosphere. The functionalization is occurring at the most nucleophilic site on **2.1a**, and we postulated that this proceeds through an electrophilic perfluoroalkylation mechanism.[109] This observation is noteworthy as there was no need for any photocatalyst or terminal oxidant as is typically needed for such transformations. In the absence of light, we observed no conversion (Table 2.3.1, entry 2), however reactivity can be regained in the absence of light by using $K_2S_2O_8$ as a terminal oxidant (Table 2.3.1, entry 3) which would be

expected based on work by Baran and coworkers. Next, we observed moderate solvent effects, for example a 1:1 mixture of MeCN and $H_2O$ (Table 2.3.1, entry 4) resulted in a decrease in conversion; however, DMF (Table 2.3.1, entry 5) gave near indistinguishable conversions from DMSO. When changing the wavelength of light from 390nm to 440nm (Table 2.3.1, entry 6) or 467nm (Table 2.3.1, entry 7), we observed a continual decrease in conversion. When the reaction contents are sparged with Argon (Table 2.3.1, entry 8), we noticed a decrease in conversion, however upon sparging with $O_2$ (Table 2.3.1, entry 9), we noticed a large effect compared to the Argon results suggesting the importance of oxygen in this reaction. Regarding the sulfinate used, the metal counter ion had a small effect on reactivity as $Zn(SO_2CF_3)_2$ can be used, albeit resulting in lower yields despite a larger equivalence used (Table 2.3.1, entry 10). The corresponding methyl sulfinate ($NaSO_2CH_3$) resulted in no conversion, suggesting the need for electron poor sulfinates (Table 2.3.1, entry 11). Upon using sodium difluorosulfinate ($NaSO_2CF_2H$) (Table 2.3.1, entry 12). we noticed a significant decrease in conversion compared to Langlois' reagent, possibly due to the decrease in electrophilicity of $CF_2H$ radical in comparison.[110]

## 2.4 Discussion

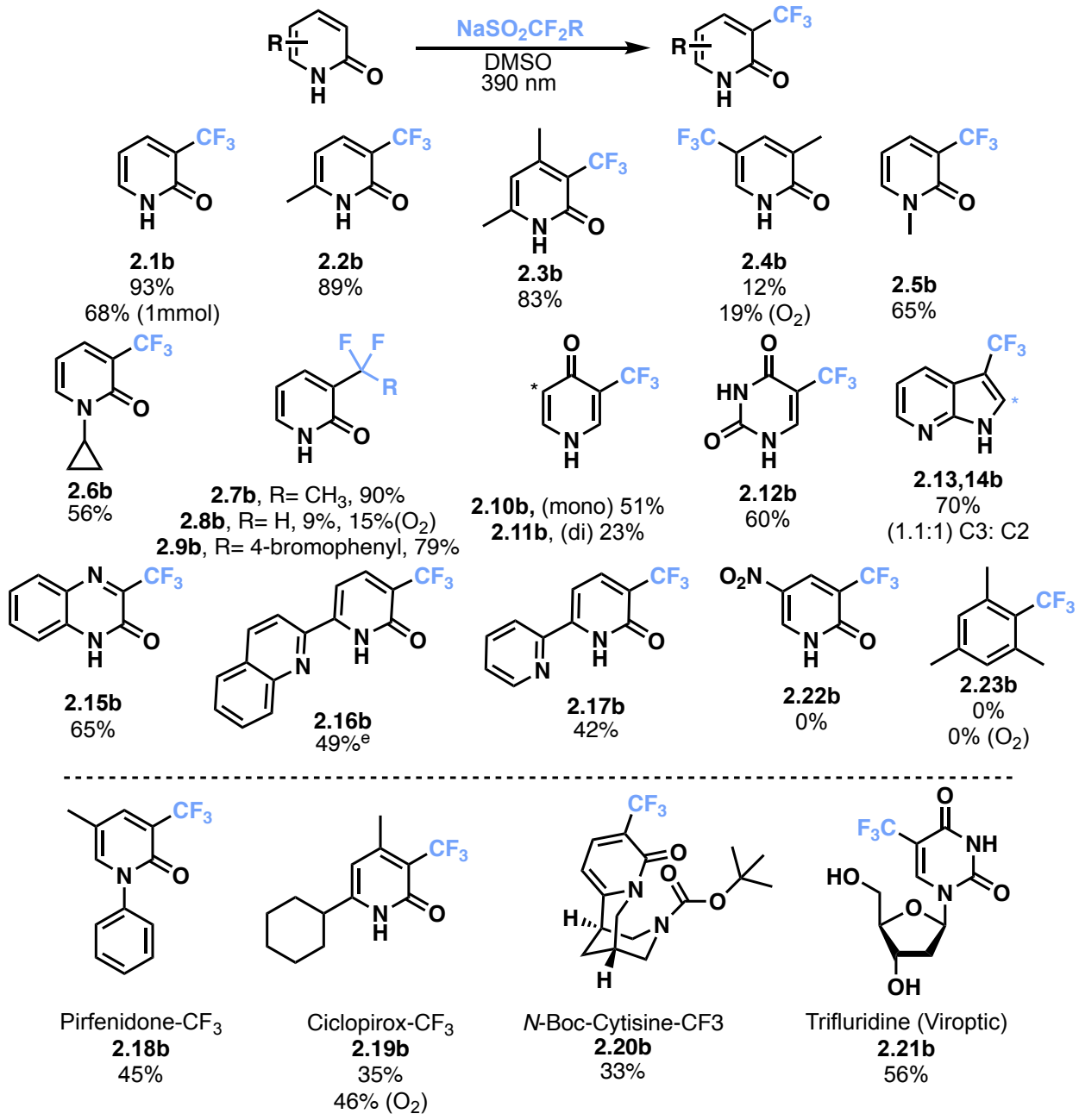


**Scheme 2.4.1 Substrate Scope of Perfluoroalkylated *N*-heteroarenes**

We next evaluated the optimal conditions across a variety of pyridones to demonstrate the versatility of this approach. As shown in Scheme 2, the reaction is tolerable amongst different pyridones including aryl alkylated (**2.2b**, **2.3b**) and N-alkylated pyridones (**2.5b**, **2.6b**) in good

yields ranging from 56-93%. Interestingly, when the 3-position is methylated, there is considerably lower yield, 12%, of the 5-trifluoromethylated product (**2.4b**), 19% when the reaction is sparged with $O_2$, which suggests that electronics of the substrate are important in determining whether the reaction can occur. Swapping Langlois's reagent for other difluorosulfinate salts such as $NaSO_2CF_2CH_3$ resulted in 90% of **2.7b** , $NaSO_2CF_2H$ resulted in 9% of **2.8b,** 15% when the reaction is sparged with $O_2$, and $NaSO_2CF_2C_8H_6Br$ resulted in 79% of **2.9b**. 4-pyridone, another bioactive pyridone scaffold, was also subjected to this methodology and produced a mixture of mono- and di-trifluoromethylated products (**2.10b, 2.11b**) in 51% and 23% yields. While we initially thought that pyridones were unique to this methodology, we were pleasantly surprised that other *N*-heteroarenes were also perfluoroalkylated. We were able to obtain trifluoromethylated uracil (**2.12b**) and azaindole (**2.13b, 2.14b**) in 60% and 70% yields respectively. 2-quinazoline was also perfluoroalkylated using these conditions generating product up to 65% yield (**2.15b)**. We evaluated different pyridone containing ligands as seen in the literature for use in catalysis[111-113] and we obtained **2.16b** and **2.17b** in moderate yields of 49% and 42% respectively. We did observe some substrate limitations as we were unable to perfluoroalkylate 5-nitro-2-pyridone **2.22b** and mesitylene **2.23b**. We believe that in the case of **2.22a**, the pyridone ring is too electron poor due to the nitro- substituent. However, in the context of **2.23a** it appears the photocatalyst and oxidant-free chemistry necessitates a heteroatom bearing lone pairs which is believed to interact with the sulfinate (*vide infra*) despite sparging the reaction with $O_2$, which we note has an improving effect on yields.

Inspired by the ability to perfluoroalkylate pyridone containing ligands, we postulated that this methodology would also be suitable for late-stage functionalization of bioactive molecules. To evaluate this strategy, we selected bioactive pyridones including: Pirfenidone (**2.18b**), used in

the treatment of idiopathic pulmonary fibrosis, Cicloprox (**2.19b**) used as a treatment for fungal infections, Cytisine (**2.20b**), a former therapy for smoking cessation in Europe and Asia, and Trifluridine (**2.21b)**, an ophthalmic treatment for viral infections. We were able to perfluoroalkylate these bioactive molecules in isolated yields of 45%, 35%, 33%, and 56% of **2.18b – 2.21b** respectively. We were able to increase the yield of **2.19b** when the reaction was sparged with oxygen to 46%. In the case of **2.20a**, the secondary amine was identified to be an issue, however upon Boc-protection compound **1.20a** was able to produce 33% of **2.20b**.

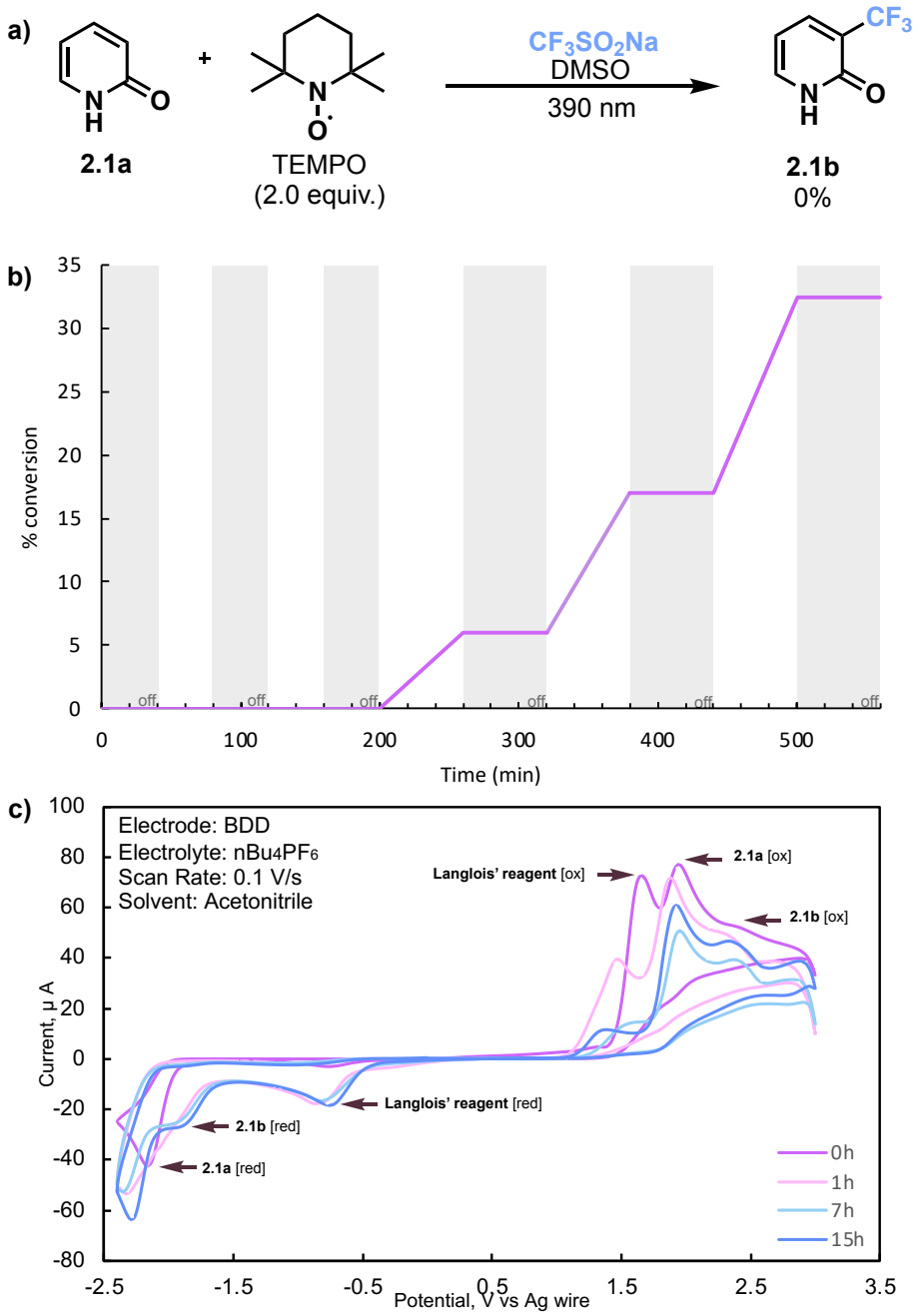


**Scheme 2.4.2 Mechanistic Studies of Perfluoroalkylation**

To gain more insight into the reaction mechanism we performed the following experiments to elucidate the order of transformation. Firstly, when adding TEMPO to the reaction, no product **2.1b** was formed, suggesting that the trifluoromethylation occurred via a radical pathway (Scheme 2.4.2a).[114] Next, we investigated the role of the light by performing a light on/off experiment to

see whether the reaction occurs through a chain propagation mechanism and whether it could be initiated in the absence of light.[115] The reaction was sluggish to occur using 20 minute intervals, thus was increased to hourly intervals. When light is removed, the reaction ceased and would only occur in the presence of light (Scheme 2.4.2b). To probe the formation of a charge-transfer complex, all reagents were then analyzed using UV-Vis spectroscopy and were found to absorb in the UV-A and UV-B region (see Experimental Section). The reaction mixture was measured and no significant bathochromic shift was observed suggesting another mode of radical generation, possibly via n, $\pi^*$ as postulated by Mi, Li and coworkers.[116] To better visualize the reaction, we ran cyclic voltammetry (CV) experiments to observe the presence of all reagents in the reaction and to study their redox potentials. We found that pyridone **2.1a** has an oxidative potential of 1.94V and reductive potential of -2.16V (Figure 2.5.110) and Langlois' reagent has an oxidative potential of 1.65V and -0.76V (Figure 2.5.111) We were unable to introduce DMSO in the CVs to study its effect as DMSO is oxidized at the same potential as Langlois' reagent, which prevented analysis. When both reagents are in solution, we can see distinct peaks depending on the concentration; 100mM was most optimal for irradiation and all CVs were run at a 1mM overall concentration (Scheme 2.4.2c). At 0 h, we observed approximately a 1:1 ratio of reagents, however after irradiation of the solution at 1h, we noticed a significant decrease in relative peaks between **2.1a** and sulfinate, suggesting the consumption of sulfinate initially. This is in line with finding from the Kim group that the sulfinate would be easier to oxidize prior to **2.1a**. When comparing the data at 7h and 15h, we noticed a decrease in both **2.1a** and the sulfinate, and the distinct formation of **2.1b**, which has an oxidative potential of 2.41V and reductive potential of -1.83V (Figure 2.5.112). Based on our experimental probes, I postulated that the sulfinate undergoes a light mediated oxidation to generate a $CF_3$ radical, which then reacts with the *N*-aryl substrate generating a

trifluoromethylated intermediate bearing a radical, which then undergoes oxidation to the cationic product, followed by rearomatization.[88] Based on the results in Table 2.3.1, entry 8 and 9, we note the dependence of oxygen, thus it may be plausible that these conditions are exciting oxygen which can then oxidize Langlois' reagent, and or participate in the oxidation to rearomatize the product.[39,40] Further mechanistic studies to better understand the full breath of the mechanism is currently underway and will be the subject of future work.

In summary we have described a new, light-promoted method for the trifluoromethylation of pyridones and related *N*-heteroarenes that does not need any photocatalyst or oxidant. This methodology is also inclusive of using a variety of sulfinate salts bearing two or more fluorine substituents. This approach is operationally simple and is minimally affected by inert gasses or water in the reaction. While Langlois' reagent can generate a $CF_3$ radical via reduction or oxidation, this project offers evidence suggesting an oxidative mechanism for this electrophilic trifluoromethylation of pyridones and related N-heteroarenes.

## 2.5 Experimental Section

### 2.5.1 General Information

All $^{1}H$, $^{13}C$, and $^{19}F$ NMR Spectra were recorded on Varian VNMRS 400 MHz, Bruker Avance $AV_1$ 400MHz, Varian Inova 500 MHz, and Bruker Avance III HD 600MHz at room temperature. All chemical shifts were reported in parts per million (δ) and internally referenced to residual solvent proton signals unless otherwise noted. All spectral data were reported as follows: (multiplicity [singlet (s), doublet (d), doublet of doublets (dd), doublet of doublet of doublets (ddd), doublet of triplets (dt), triplet (t), triplet of triplets (tt), quartet (q), quintet (qn), and multiplet (m), heptet (h)], coupling constants [Hz], integration). Carbon and Fluorine spectra were recorded with complete decoupling. Conventional mass spectra were obtained using Advion Expression$^{S}$ CMS

APCI/ASAP. HRMS were taken on Agilent 6530 Accurate Mass QTOF ESI. All chemicals and catalysts were purchased or synthesized from materials from Acros Organics, Cambridge Isotope Laboratories, Combi-Blocks, Fisher Scientific, Frontier Scientific, Oakwood Chemicals, Sigma Aldrich, or TCI America. *Note many of these suppliers were purchased by Thermo Scientific and reagents were repurified and or distilled as necessary. All normal phase flash column chromatography (FCC) was performed using Grade 60 Silica Gel (230- 400 mesh) purchased from Fisher Scientific. Preparative Thin Layer Chromatography (TLC) plates contained grade 60 silica gel coated with fluorescent indicator F254 and were purchased from Fisher Scientific. (1) 390nm (PR-160 gen 1, 50W), (3) 390nm (PR-160L gen 1, 50W), (1) 370nm (PR-160L gen 2, 40W) LEDs, and PR-160 Fan Rig Kit were purchased from Kessil (https://kessil.com/products/science_PR160L.php). Kessil PR controller was used for light on/light off experiment. To avoid excess heating from LEDs on older set-up, fan source used: AC Infinity AXIAL 1238, 120V AC 120mm x 38mm High Speed (See Section F). The average distance between reactions and light is 6 cm and no light filters were used.

### 2.5.2 Abbreviations

| | | | |
|---|---|---|---|
| *A* | absorbance | cat | catalytic |
| abs | absolute | cm | centimeter |
| Ac | acetyl | $cm^{-1}$ | wavenumbers(s) |
| AcOH | acetic acid | $^{13}C$ NMR | carbon NMR |
| $Ac_2O$ | acetic anhydride | compd | compound |
| amu | atomic mass units | concn | concentration |
| anhyd | anhydrous | COSY | correlation spectroscopy (2D NMR method) |
| aq | aqueous | | |
| Ar | aryl | cryst | crystalline |
| Boc | *tert*-butoxycarbonyl | CT | charge transfer |
| bp | boiling point | CV | cyclic voltammetry |
| bpy | 2,2'-bipyridine or 2,2'-bipyridyl | $\delta$ | chemical shift (ppm) downfield from TMS |
| Br | bromine | | |
| br | broad (spectral peak) | d | days; doublet (spectral) |
| °C | degrees Celsius | *d* | density |
| calcd | calculated (for MS analysis) | DCM | $CH_2Cl_2$, Dichloromethane |

| | |
|---|---|
| dil | dilute |
| DMF | dimethylformamide |
| DMSO | dimethylsulfoxide |
| e.g. | example (no spaces) |
| EPR | electron paramagnetic resonance |
| eq | equation |
| equiv. | equivalents |
| ESI | electrospray ionization |
| Et | ethyl |
| et al. | and others (co-authors) |
| etc. | and so forth |
| EtOAc | Ethyl Acetate |
| $Et_3N$ | triethylamine (use instead of TEA) |
| $^{19}F$ | fluorine NMR |
| FT | Fourier transform |
| g | gram(s); gas |
| h | hours(s) |
| $^1H$ NMR | proton NMR |
| HRMS | high-resolution mass spectrometry |
| Hz | hertz |
| i.e. | that is |
| insol | insoluble |
| IR | infrared |
| *J* | coupling constant in NMR |
| *k* | rate constant; Boltzmann constant |
| K | Kelvin |
| l | liquid |
| L | liter; ligand |
| lit. | literature value |
| $\lambda_{max}$ | max UV-vis wavelength |
| m | meter; milli; multiplet (spectral) |
| M | molar (moles per liter) |
| $M^+$ | parent molecular ion (in MS) |
| μ | micro |
| max | maximum |
| Me | methyl |
| MeCN | acetonitrile |
| MeOH | Methanol |
| Mes | mesityl (2,4,6-trimethylphenyl) |
| MHz | megahertz |
| min | minute(s); minimum |
| mL | milliliter |
| mm | millimeter |
| mM | millimolar (moles per liter) |
| mmol | millimole(s) |
| mol | mole(s) |
| mol wt | molecular weight |
| mp | melting point |
| MS | mass spectrometry; molecular sieves |
| $M_W$ | weight average molecular weight |
| *m/z* | mass to charge ratio (in MS) |
| N | normal (equiv per liter) |
| NMR | nuclear magnetic resonance |
| Nu | nucleophile |
| obsd | observed |
| PET | photoinduced electron transfer |
| ppm | part per million |
| Pv | pivaloyl |
| py | pyridine |
| q | quartet (spectral) |
| quin | quintet (spectral) |
| R | alkyl group |
| recryst | recrystallized |
| red | reduction |
| redox | reduction-oxidation |
| rt | room temperature |
| sat. | saturated |
| SET | single electron transfer |
| sol | solid |
| soln | solution |
| t | triplet (spectral) |
| *t* | time or temp in °C |
| *T* | temperature in kelvin |
| *t*-Bu | *tert*-butyl |
| temp | temperature |
| THF | tetrahydrofuran |
| TLC | thin-layer chromatography |
| Tol | toluene |
| UV-vis | ultraviolet-visible absorption spectroscopy |
| vis | visible |
| vs. | versus |
| v/v | volume to volume ratio |
| wt | weight |
| w/w | weight to weight ratio |

### 2.5.3 Experimental Procedures

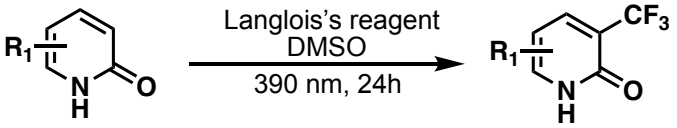


**Scheme 2.5.1 General procedure for trifluoromethylated N-heteroarenes**

To an 8mL vial equipped with a new magnetic stir bar, 2-pyridone (11.8mg, 0.125mmol, 1.0 equiv.) was added followed by sodium trifluoromethanesulfinate (39.0mg, 0.25mmol, 2.0 equiv.) and DMSO (2mL, 0.0625M). For slight increased yields, reactions were purged with $O_2$ gas before sealed. The reaction was then capped and irradiated for 24 hours in 390nm light stirring at a rate >700 per min. The reaction was quenched with DCM first, before extraction with 10% LiCl soln (30mL). Aqueous phase was then extracted 3x more with DCM. All organic layers were combined, back extracted with water, and dried with sodium sulfate before rotary evaporation at 55°C-60°C for several minutes. After solvent evaporation, semi-crude material was then dried further on Schlenk line. Materials were further purified by FCC in 95:5 (DCM: MeOH), and or by prep TLC in 95:5 (DCM:MeOH) to afford trifluoromethylated product unless otherwise stated.

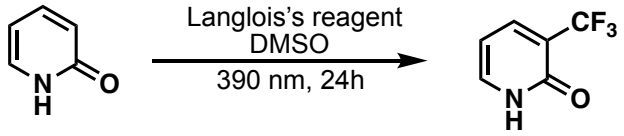


**Scheme 2.5.2 General procedure for trifluoromethylated *2*-pyridone at 1mmol scale**

To an 20mL borosilicate vial equipped with a new magnetic stir bar, 2-pyridone (95.1mg, 1.0 mmol, 1.0 equiv.) was added followed by sodium trifluoromethanesulfinate (312.1 mg, 2.0 mmol, 2.0 equiv.) and DMSO (16mL, 0.0625M). The reaction was purged with $O_2$ and irradiated

for 24 hours in 390nm PR-160L in the Rig Kit stirring at a rate >700. The reaction was quenched with DCM first, before extraction with 10% LiCl soln (160mL). Aqueous phase was then extracted 3x more with DCM. All organic layers were combined, back extracted with water, and dried with sodium sulfate before rotary evaporation at 55ºC - 60ºC for several minutes. After solvent evaporation, semi-crude material was then dried further on Schlenk line. Purified by FCC in 95:5 (DCM: MeOH) to afford trifluoromethylated product.

### 2.5.4 Characterization of Perfluoroalkylated Pyridones and Related N-heteroarenes

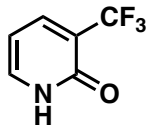


**Figure 2.5.1 Product 2.1b**

**3-(trifluoromethyl)pyridin-2(1*H*)-one:** Compound was synthesized using the general procedure for trifluoromethylated *N*-heteroarenes. **Yields** (0.125 mmol scale): 18.8mg, 92%, white solid. **$^{1}$HNMR (400 MHz, $CDCl_3$)** $\delta$ = 13.37(bs, 1H), 7.88(d, 1H, J= 7.4 Hz), 7.66 (d, 1H, J= 7.1 Hz), 6.41-6.38 (t, 1H, J= 6.6 Hz). **$^{13}$CNMR (126 MHz, $CDCl_3$)** $\delta$ =161.5, 140.7 (q, J= 5 Hz), 139.1, 122.6 (q, J=272 Hz), 118.6, 105.5. **$^{19}$FNMR (376 MHz, $CDCl_3$)** $\delta$ = -65.77. This compound is in spectral agreement as described in *J. Org. Chem*. **2020**, *85*, 3110-3124.

**HRMS (ESI) m/z: $[M+H]^+$** Calcd for $C_6H_5F_3NO$ 164.0323; Found 164.0316

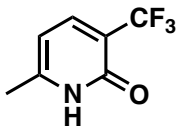


**Figure 2.5.2 Product 2.2b**

**6-methyl-3-(trifluoromethyl)pyridin-2(1*H*)-one:** Compound was synthesized using the general procedure for trifluoromethylated *N*-heteroarenes. **Yields** (0.125 mmol scale): 19.5 mg,

88%, white solid. **$^{1}$HNMR (400 MHz, $CDCl_3$)** $\delta$ = 13.29 (brs, 1H), 7.73 (d, 1H, J= 7.5 Hz), 6.14 (d, 1H, J= 7.5 Hz), 2.42 (s, 3H). **$^{13}$CNMR (126 MHz, $CDCl_3$)** $\delta$ = 161.8, 151.1, 140.7 (q, J= 5 Hz), 122.8 (q, J= 273), 119.9, 104.8, 19.2. **$^{19}$FNMR (376 MHz, $CDCl_3$)** $\delta$ = -65.16. This compound is in spectral agreement as described in *Green. Chem*. **2022**, *24*, 7388-7394. **HRMS (ESI) m/z: $[M+H]^+$** Calcd for $C_7H_7F_3NO$ 178.0473; Found 178.0477

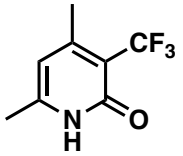


**Figure 2.5.3 Product 2.3b**

**4,6-dimethyl-3-(trifluoromethyl)pyridin-2(1*H*)-one:** Compound was synthesized using the general procedure for trifluoromethylated *N*-heteroarenes using 1.5 equiv. of sulfinate. **Yields** (0.125 mmol scale): 19.8 mg, 83%, white solid. **$^{1}$HNMR (400 MHz, $CDCl_3$)** $\delta$ = 13.10 (bs, 1H), 5.93 (s, 1H), 2.37-2.35 (q, 3H, J= 3.15 Hz), 2.33 (s, 3H). **$^{13}$CNMR (126 MHz, $CDCl_3$)** $\delta$ = 162.4, 154.4, 148.5, 124.5 (q, J= 270 Hz), 114.1 (q, J= 28 Hz), 21.2 (q, J= 4 Hz), 18.7. **$^{19}$FNMR (376 MHz, $CDCl_3$)** $\delta$ = -57.29 (d). **HRMS (ESI) m/z: $[M+H]^+$** Calcd for $C_8H_9F_3NO$ 192.0636; Found 192.0637

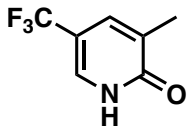


**Figure 2.5.4 Product 2.4b**

**3-methyl-5-(trifluoromethyl)pyridin-2(1*H*)-one:** Compound was synthesized using the general procedure for trifluoromethylated *N*-heteroarenes. **Yields** (0.125 mmol scale): 2.6 mg,

12%, white solid. **$^{1}$HNMR (400 MHz, $CDCl_3$)** $\delta$ = 11.78 (brs, 1H), 7.42 (d, 1H, J= 7.5 Hz), 6.77 (d, 1H, J= 7.5 Hz), 2.24 (s, 3H). **$^{13}$CNMR (126 MHz, $CDCl_3$)** $\delta$ = 163.5, 138.1, 136.1 (q, J= 30 Hz), 131.0, 120.4 (q, J= 271 Hz), 108.2 (q, J= 4 Hz), 16.4. **$^{19}$FNMR (376 MHz, $CDCl_3$)** $\delta$ = -67.17. **HRMS (ESI) m/z: $[M+H]^+$** Calcd for $C_7H_7F_3NO$ 178.0473; Found 178.0470

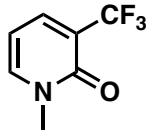


**Figure 2.5.5 Product 2.5b**

**1-methyl-3-(trifluoromethyl)pyridin-2(1*H*)-one:** Compound was synthesized using the general procedure for trifluoromethylated *N*-heteroarenes. **Yields** (0.125 mmol scale): 14.38mg, 65%, beige solid. **$^{1}$HNMR (400 MHz, $CDCl_3$)** $\delta$ = 7.73 (d, 1H, J= 7.15 Hz), 7.52 (d, 1H, J= 6.78 Hz), 6.24-6.20 (t, 1H, J= 6.90 Hz), 3.6 (s, 1H). **$^{13}$CNMR (126 MHz, $CDCl_3$)** $\delta$ = 158.8, 142.2, 138.8 (q, J= 5 Hz), 122.7 (q, J= 272 Hz), 105.9, 103.9, 37.8. **$^{19}$FNMR (376 MHz, $CDCl_3$)** $\delta$ = -66.09. This compound is in spectral agreement as described in *Chem. Commun*. **2018**, *54*, 10574-10577. **HRMS (ESI) m/z: $[M+H]^+$** Calcd for $C_7H_7F_3NO$ 178.0473; Found 178.0472

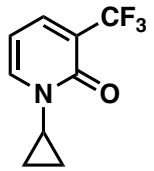


**Figure 2.5.6 Product 2.6b**

**1-cyclopropyl-3-(trifluoromethyl)pyridin-2(1*H*)-one:** Compound was synthesized using the general procedure for trifluoromethylated *N*-heteroarenes. **Yields** (0.125 mmol scale): 14.2mg, 56%, beige solid. **$^{1}$HNMR (400 MHz, $CDCl_3$)** $\delta$ = 7.70 (d, 1H, J=6.3 Hz) 7.49 (d, 1H, J= 6.8 Hz),

6.19 (t, 1H, J= 6.9 Hz), 3.39-3.35 (m, 1H), 1.17 (q, 2H, J= 6.5 Hz), 0.88 (q, 2H, J=6.2 Hz). **$^{13}$CNMR (126 MHz, $CDCl_3$)** $\delta$ = δ 159.7, 140.8, 138.2 (q, J = 5 Hz), 122.8 (q, J= 271 Hz), 119.5, 103.5, 32.6, 6.8. **$^{19}$FNMR (376 MHz, $CDCl_3$)** $\delta$ = -65.88. **HRMS (ESI) m/z: $[M+H]^+$** Calcd for $C_9H_9F_3NO$ 204.0635; Found 204.0646

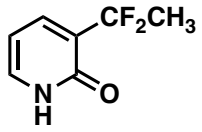


**Figure 2.5.7 Product 2.7b**

**3-(1,1-difluoroethyl)pyridin-2(1*H*)-one:** Compound was synthesized using the general procedure for trifluoromethylated *N*-heteroarenes. **Yields** (0.125 mmol scale): 18.0 mg, 90%, white solid. **$^{1}$HNMR (400 MHz, $CDCl_3$)** $\delta$ = 13.18 (brs, 1H), 7.77 (d, 1H, J= 6.9 Hz), 7.50 (d, 1H, J= 8.3 Hz), 6.35 (t, 1H, J= 6.8 Hz), 2.07 (t, 3H, J= 19.2 Hz). **$^{13}$CNMR (126 MHz, $CDCl_3$)** $\delta$ = 162.5 (t, J= 4 Hz), 138.2 (t, J= 8 Hz), 136.7, 127.2 (t, J= 26 Hz), 120.3 (t, J= 234 Hz), 105.9, 23.2 (t, J= 27 Hz). **$^{19}$FNMR (376 MHz, $CDCl_3$)** $\delta$ = -86.29 (q). **HRMS (ESI) m/z: $[M+H]^+$** Calcd for $C_7H_8F_2NO$ 160.0574; Found 160.0573

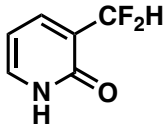


**Figure 2.5.8 Product 2.8b**

**3-(difluoromethyl)pyridin-2(1*H*)-one:** Compound was synthesized using the general procedure for trifluoromethylated *N*-heteroarenes. **Yields** (0.125 mmol scale): 1.6 mg, 9%, off-white solid. **$^{1}$HNMR (400 MHz, $CDCl_3$)** $\delta$ = 13.01 (brs, 1H), 7.82 (d, 1H, J= 6.5 Hz), 7.52 (d, 1H, J= 5.2 Hz), 6.81 (t, 1H, J= 53.8 Hz), 6.41 (t, 1H, J= 6.1 Hz). **$^{13}$CNMR (126 MHz, $CDCl_3$)** $\delta$ =

162.9, 139.3 (t, J= 6 Hz), 137.1, 124.7 (t, J= 22 Hz), 110.9 (t, J= 238 Hz), 106.5. **$^{19}$FNMR (376 MHz, $CDCl_3$)** $\delta$ = -118.88 (d, J= 55.1 Hz). **HRMS (ESI) m/z: $[M+H]^+$** Calcd for $C_6H_6F_2NO$ 146.0417; Found 146.0407

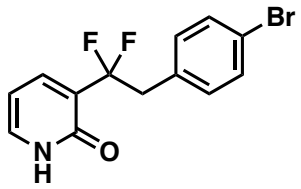


**Figure 2.5.9 Product 2.9b**

**3-(2-(4-bromophenyl)-1,1-difluoroethyl)pyridin-2(1*H*)-one:** Compound was synthesized using the general procedure for trifluoromethylated *N*-heteroarenes. **Yields** (0.125 mmol scale): 31.0 mg, 79 %, off-white solid. **$^1$HNMR (400 MHz, $CDCl_3$)** $\delta$ = 13.03 (brs, 1H), 7.54 (d, 1H, J= 5.9 Hz), 7.49 (d, 1H, J=7.9 Hz), 7.37 (d, 1H, J= 8.4 Hz), 7.10 (d, 1H, J= 7.4), 6.27 (t, 1H, J= 6.7), 3.75 (t, 1H, J= 15.7 Hz). **$^{13}$CNMR (126 MHz, $CDCl_3$)** $\delta$ = 162.3, 139.6 (t, J= 8 Hz), 136.7, 132.1, 131.4, 122.8, 121.4, 120.3, 106.1, 41 (t, J= 26 Hz), 29.7. **$^{19}$FNMR (376 MHz, $CDCl_3$)** $\delta$ = -96.30 (t). **HRMS (ESI) m/z: $[M+H]^+$** Calcd for $C_{13}H_{11}BrF_2NO$ 313.9992; Found: 314.0013, 316.0023 ($^{79}$Br, $^{81}$Br)

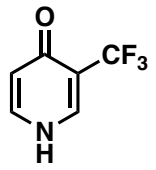


**Figure 2.5.10 Product 2.10b**

**3-(trifluoromethyl)pyridin-4(1*H*)-one:** Compound was synthesized using the general procedure for trifluoromethylated *N*-heteroarenes using 2.2 equiv. of sulfinate. **Yields** (0.125 mmol scale): 10.5mg, 51%, white solid. **$^1$HNMR (400 MHz, $CO(CD_3)_2$)** $\delta$ = 10.87 (brs, 1H), 8.11 (s,

1H), 7.76 (d, 1H, J=7.3 Hz), 6.27 (d, 1H, J= 7.5 Hz). **$^{13}$CNMR (126 MHz, $CD_3OD$)** $\delta$ = 177.9, 141.0, 138.8 (q, J= 5 Hz), 124.9 (q, J= 272 Hz), 120.8, 119.6 (q, J= 28 Hz). **$^{19}$FNMR (376 MHz, $CO(CD_3)_2$)** $\delta$ = -65.62. **HRMS (ESI) m/z: $[M+H]^+$** Calcd for $C_6H_5F_3NO$ 164.0323; Found: 164.0315

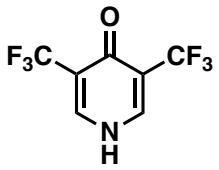


**Figure 2.5.11 Product 2.11b**

**3,5-bis(trifluoromethyl)pyridin-4(1*H*)-one:** Compound was synthesized using the general procedure for trifluoromethylated *N*-heteroarenes using 3.3 equiv. of sulfinate. **Yields** (0.125 mmol scale): 6.5mg, 23%, beige solid. **$^{1}$HNMR (400 MHz, $CD_3OD$)** $\delta$ = 8.24 (s, 2H). **$^{13}$CNMR (126 MHz, $CD_3OD$)** $\delta$ = 210.1, 140.6, 123.1 (q, J= 273), 30.6. **$^{19}$FNMR (376 MHz, $CD_3OD$)** $\delta$ = -66.51. **HRMS (ESI) m/z: $[M+H]^+$** Calcd for $C_7H_4F_6NO$, 232.0197; Found 232.0200

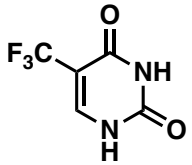


**Figure 2.5.12 Product 2.12b**

**5-(trifluoromethyl)pyrimidine-2,4(1*H*,3*H*)-dione:** Compound was synthesized using the general procedure for trifluoromethylated *N*-heteroarenes. **Yields** (0.125 mmol scale): 13.5mg, 60%, white solid. **$^{1}$HNMR (400 MHz, $CD_3OD$)** $\delta$ = 7.93 (s, 1H). **$^{13}$CNMR (126 MHz, $CD_3OD$)** $\delta$ = 162.0, 152.4, 144.7 (q, J= 6 Hz), 126.0 (q, J= 265 Hz), 101.8. **$^{19}$FNMR (376 MHz, $CD_3OD$)**

$\delta$ = -64.85. This compound is in spectral agreement as described in *Tetrahedron*. **1982**, *23*, 4099-4100 and *Chem. Comm.* **2018**, *54*, 13662-13665. **HRMS (ESI) m/z: [M-H]$^+$** Calcd for $C_5H_2F_3N_2O_2$ 179.0077; Found 179.0081

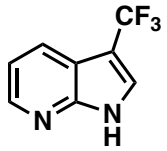


**Figure 2.5.13 Product 2.13b**

**3-(trifluoromethyl)-1*H*-pyrrolo[2,3-*b*]pyridine:** Compound was synthesized using the general procedure for trifluoromethylated *N*-heteroarenes. **Yields** (0.125 mmol scale): 23.4mg, 36%, off-white solid. **$^1$HNMR (400 MHz, $CDCl_3$)** $\delta$ = 13.76 (brs, 1H), 8.50 (d, 1H, J= 4.8 Hz), 8.10 (d, 1H, J= 8.0 Hz), 7.23 (dd, 1H, J= 7.8, 4.7 Hz), 6.91 (d, 1H, J= 1.31). **$^{13}$CNMR (126 MHz, $CDCl_3$)** $\delta$ = 148.5, 144.5, 131.4, 127.4 (q, J= 39 Hz), 121.3 (q, J= 271 Hz), 119.8, 116.9, 101.3 (q, J= 5 Hz). **$^{19}$FNMR (376MHz, $CDCl_3$)** $\delta$ = -61.22 (s). This compound is in spectral agreement as described in *J. Am. Chem. Soc*. **2019**, *141*, 12872-12879. **HRMS (ESI) m/z: [M+H]$^+$** Calcd for $C_8H_5F_3N_2$ 187.0483; Found 187.0468

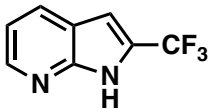


**Figure 2.5.14 Product 2.14b**

**2-(trifluoromethyl)-1*H*-pyrrolo[2,3-*b*]pyridine:** Compound was synthesized using the general procedure for trifluoromethylated *N*-heteroarenes. **Yields** (0.125 mmol scale): 22.1mg, 34%, yellow solid. **$^1$HNMR (400 MHz, $CDCl_3$)** $\delta$ = 11.77 (brs, 1H), 8.45 (dd, 1H, J= 3.16, 1.41 Hz), 8.13 (d, 1H, J= 7.97 Hz), 7.76 (q, 1H, J= 7.97 Hz), 7.25 (q, 1H, J= 4.78 Hz). **$^{13}$CNMR (126**

**MHz, $CDCl_3$)** $\delta$ = 148.3, 143.8, 128.7, 125.3 (q, J= 4 Hz), 123.7 (q, J= 271 Hz), 117.3, 116.8 ,105.9 (q, J = 38 Hz). **$^{19}$FNMR (376 MHz, $CDCl_3$)** $\delta$ = -57.36 (s).

This compound is in spectral agreement as described in *J. Am. Chem. Soc*. **2019**, *141*, 12872-12879. **HRMS (ESI) m/z: $[M+H]^+$** Calcd for $C_8H_5F_3N_2$ 187.0483; Found 187.0468

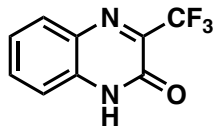


**Figure 2.5.15 Product 2.15b**

**3-(trifluoromethyl)quinoxalin-2(1*H*)-one:** Compound was synthesized using the general procedure for trifluoromethylated *N*-heteroarenes. **Yields** (0.125 mmol scale): 17.3mg, 65%, yellow solid. **$^1$HNMR (400 MHz, $CDCl_3$)** $\delta$ = 10.26 (brs, 1H), 8.42 (d, 1H, J= 8.2), 8.13 (d, 1H, J= 7.6 Hz), 8.07 (s, 1H), 7.60 (t, 1H, J= 7.9 Hz). **$^{13}$CNMR (126 MHz, $CDCl_3$)** $\delta$ = 160.9, 147.5, 146.6, 133.1 (q, J= 6 Hz), 131.6, 127.2, 126.0, 125.5, 123.8. **$^{19}$FNMR (376 MHz, $CDCl_3$)** $\delta$ = -60.59. This compound is in spectral agreement as described in *Org. Chem. Front*. **2019**, *6,* 2392-2397. **HRMS (ESI) m/z: $[M+H]^+$** Calcd for $C_9H_6F_3N_2O$ $[M+H]^+$, 215.0432; Found 215.0448

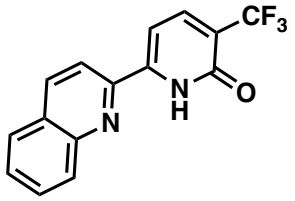


**Figure 2.5.16 Product 2.16b**

**6-(quinolin-2-yl)-3-(trifluoromethyl)pyridin-2(1*H*)-one:** The starting material was synthesized according to a previously published procedure found in *Science*. **2021**, *374*, 1281-1285. Compound was synthesized using the general procedure for trifluoromethylated *N*-

heteroarenes. **Yields** (0.125 mmol scale): 17.6mg, 49%, yellow solid. **$^{1}$HNMR (400 MHz, $CDCl_3$)** $\delta$ = 11.16 (brs, 1H), 8.34 (d, 1H, J=9.2 Hz), 8.16 (d, 1H, J= 8.3 Hz), 7.94-7.88 (m, 3H), 7.83 (t, 1H, J=7.5 Hz), 7.66 (t, 1H, J= 7.5 Hz), 6.99 (d, 1H, J=7.5 Hz). **$^{13}$CNMR (126 MHz, $CDCl_3$)** $\delta$ = 158.4, 147.1, 145.8, 145.3, 139.9 (q, J= 5 Hz), 138.1, 129.8, 128.5, 127.6, 124.0, 121.3, 116.8, 29.7. **$^{19}$FNMR (376 MHz, $CDCl_3$)** $\delta$ = -65.55. **HRMS (ESI) m/z: $[M+H]^+$** Calcd for $C_{15}H_{10}F_3N_2O$ 291.0745; Found 291.0759

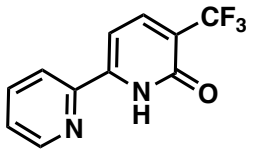


**Figure 2.5.17 Product 2.17b**

**5-(trifluoromethyl)-[2,2'-bipyridin]-6(1*H*)-one:** The starting material was synthesized according to a previously published procedure found in *Science*. **2021***, 374*, 1281-1285. Compound was synthesized using the general procedure for trifluoromethylated *N*-heteroarenes. **Yields** (0.125 mmol scale): 12.5mg, 41.6%, pale yellow solid. **$^{1}$HNMR (400 MHz, $CD_2Cl_2$)** $\delta$ = 10.86 (brs, 1H), 8.70 (d, 1H, J= 4.2 Hz), 7.94-7.87 (m, 3H), 7.45 (t, 1H, J= 5.1 Hz), 6.86 (d, 1H, J= 7.4 Hz). **$^{13}$CNMR (126 MHz, $CD_3OD$)** $\delta$ = 154.1, 145.4, 142.5, 141.7, 136.1 (q, J= 5 Hz), 133.6, 122.3, 121.6, 118.7 (q, J= 270 Hz), 116.5, 96.6. **$^{19}$FNMR (376 MHz, $CD_2Cl_2$)** $\delta$ = -65.82. **HRMS (ESI) m/z: $[M+Na]^+$** Calcd for $C_{11}H_7F_3N_2ONa$ 263.0408; Found 263.0425

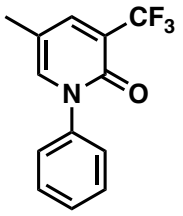


**Figure 2.5.18 Product 2.18b**

**5-methyl-1-phenyl-3-(trifluoromethyl)pyridin-2(1*H*)-one:** Compound was synthesized using the general procedure for trifluoromethylated *N*-heteroarenes. **Yields** (0.125 mmol scale): 14.3mg, 45%, clear oil. **$^{1}$HNMR (400 MHz, $CDCl_3$)** $\delta$ = 7.69 (s, 1H), 7.50-7.47 (m, 2H), 7.44-7.43 (m, 1H), 7.38-7.34 (m, 3H), 2.16 (s, 3H). **$^{13}$CNMR (126 MHz, $CDCl_3$)** $\delta$ = 157.5, 141.7 (q, J= 5 Hz), 139.9, 139.3, 129.3, 128.8, 126.5, 123.7 (q, J = 270 Hz), 121.5 (q, J = 30 Hz), 113.1, 16.9. **$^{19}$FNMR (376 MHz, $CDCl_3$)** $\delta$ = -65.90. This compound is in spectral agreement as described in *Chem. Commun*. **2018**, *54*, 10574-10577. **HRMS (ESI) m/z: $[M+H]^+$** Calcd for $C_{13}H_{11}F_3NO$ 254.0792; Found 254.0794

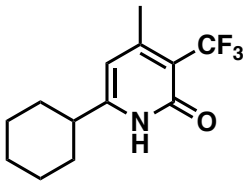


**Figure 2.5.19 Product 2.19b**

**6-cyclohexyl-4-methyl-3-(trifluoromethyl)pyridin-2(1*H*)-one:** Compound was synthesized using the general procedure for trifluoromethylated *N*-heteroarenes. **Yields** (0.125 mmol scale): 11.3mg, 35%, solid/oil. **$^{1}$HNMR (400 MHz, $CDCl_3$)** $\delta$ =12.48 (brs, 1H), 5.90 (s, 1H), 2.51-2.45 (t, 1H, J= 12.0 Hz), 2.38-2.36 (q, 3H, J= 3.3 Hz), 1.91-1.84 (t, 4H, J= 13.78 Hz), 1.74 (d, 1H, J= 10 Hz), 1.53-1.28 (m, 5H). **$^{13}$CNMR (126 MHz, $CDCl_3$)** $\delta$ = 162.2, 156.9, 124.4 (q, J= 274 Hz), 114.3 (q, J= 28 Hz), 107.29, 42.3, 31.3, 26.0, 25.3, 21.2 (q, J= 4 Hz). **$^{19}$FNMR**

**(376 MHz, $CDCl_3$)** $\delta$ = -57.35. **HRMS (ESI) m/z: $[M+H]^+$** Calcd for $C_{13}H_{17}F_3NO$ 260.1262; Found: 260.1260

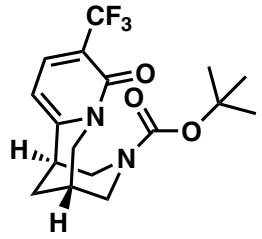

**Figure 2.5.20 Product 2.20b**

***tert*-butyl(1*R*,5*R*)-8-oxo-9-(trifluoromethyl)-1,5,6,8-tetrahydro-2*H*-1,5-methanopyrido[1,2-*a*][1,5]diazocine-3(4*H*)-carboxylate:** Compound was synthesized using the general procedure for trifluoromethylated *N*-heteroarenes. **Yields** (0.125 mmol scale): 14.8mg, 33%, white solid. **$^1$HNMR (400 MHz, $CDCl_3$)** $\delta$ = 7.65 (d, J= 7.9 Hz, 1H), 6.12 (d, J= 5.7 Hz, 1H), 4.36-4.13 (m, 3H), 3.85-3.81 (m, 1H), 3.06-2.97 (m, 3H), 2.44 (brs, 1H), 1.98 (brs, 2H), 1.38-1.21 (m, 9H). **$^{13}$CNMR (126 MHz, $CDCl_3$)** $\delta$ = 159.1, 154.3, 137.6, 123.1 (q, J= 271 Hz), 116.7 (q, J= 29 Hz), 103.9, 80.8, 50.4, 49.1, 35.3, 29.6, 28.0, 27.4, 25.9. **$^{19}$FNMR (376 MHz, $CDCl_3$)** $\delta$ = -65.77. **HRMS (ESI) m/z: $[M+Na]^+$** Calcd for $C_{17}H_{21}F_3N_2O_3Na$, 381.1410; Found: 381.1425

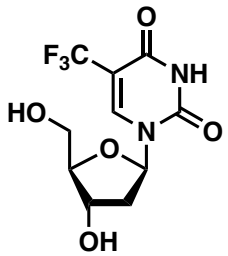

**Figure 2.5.21 Product 2.21b**

**1-((2*R*,4*S*,5*R*)-4-hydroxy-5-(hydroxymethyl)tetrahydrofuran-2-yl)-5-(trifluoromethyl)pyrimidine-2,4(1*H*,3*H*)-dione:** Compound was synthesized using the general procedure for trifluoromethylated *N*-heteroarenes. **Yields** (0.125 mmol scale): 20.8mg, 56%, white solid. **$^{1}$HNMR (400 MHz, $CD_3OD$)** $\delta$ = 8.78 (s, 1H), 6.24 (t, J= 6.15 Hz,1H), 4.43-4.40 (m, 1H), 3.96 (q, J= 3.06 Hz, 1H), 3.79 (dd, J= 2.84, 3.02 Hz, 2H), 2.65 (s, 1H), 2.39-2.34 (m, 1H), 2.30-2.25 (m, 1H), 2.16 (s, 1H). **$^{13}$CNMR (126 MHz, $CD_3OD$)** $\delta$ = 161.18, 151.33, 143.74, 123.94 (q, J=269.15), 105.38 (q, J= 32.77), 89.36, 87.59, 71.74, 62.18, 42.13. **$^{19}$FNMR (376 MHz, $CD_3OD$)** $\delta$ = -64.52. This compound is in spectral agreement as described in Proc. Natl. Acad. Sci. USA. 2011, 35, 14411-14415. **HRMS (ESI) m/z: $[M+Na]^+$** Calcd for $C_{10}H_{11}F_3N_2O_5Na$ 319.0517; Found: 319.0537

### 2.5.5 Spectral Data for Characterized Molecules ($^{1}$H, $^{13}$C, $^{19}$F NMR)

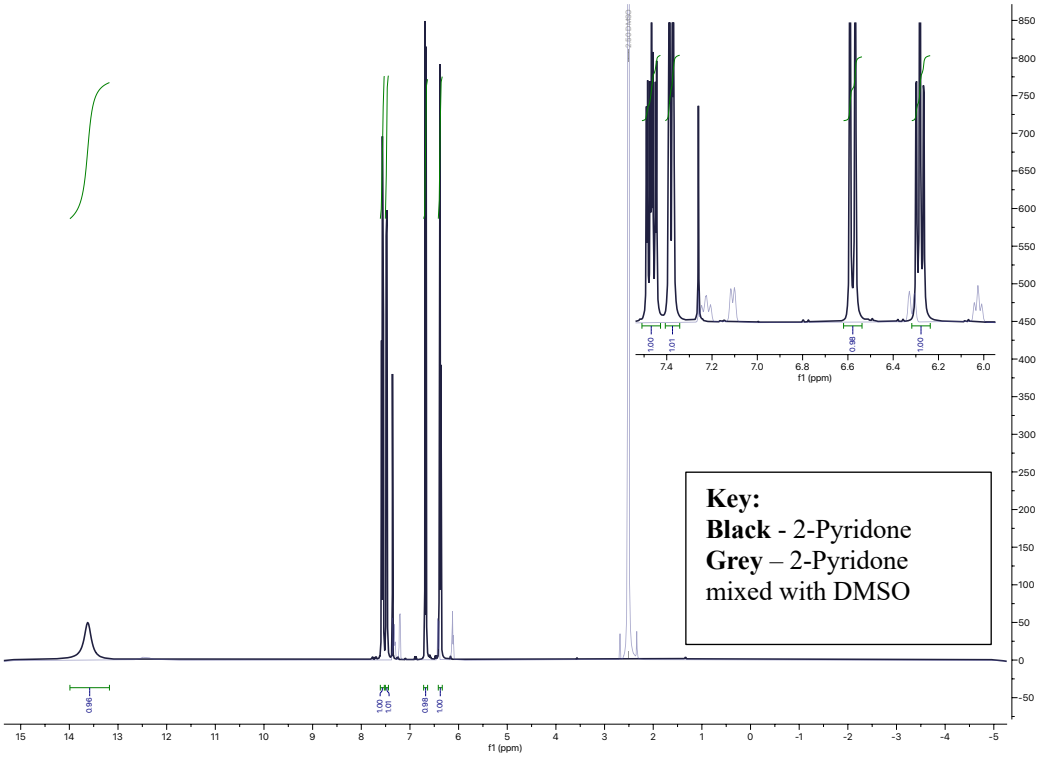


**Figure 2.5.22 400MHz 1HNMR of 2.1b H-Bonding in DMSO in CDCl3**

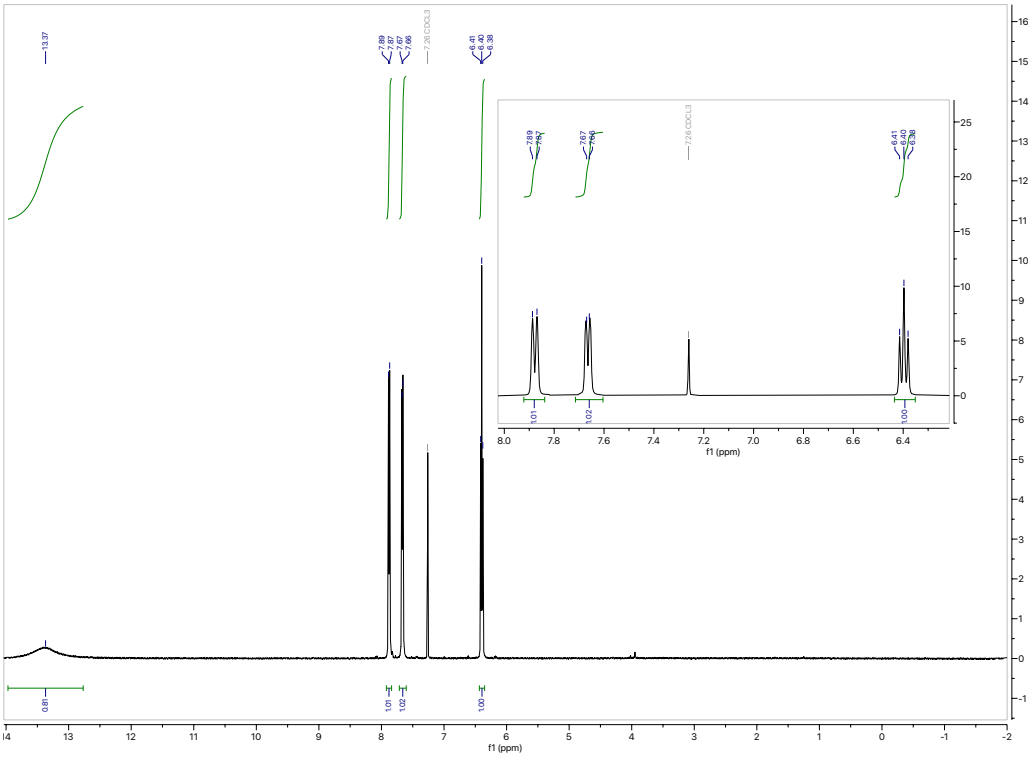


**Figure 2.5.23 400MHz $^{1}$HNMR of 2.1b**

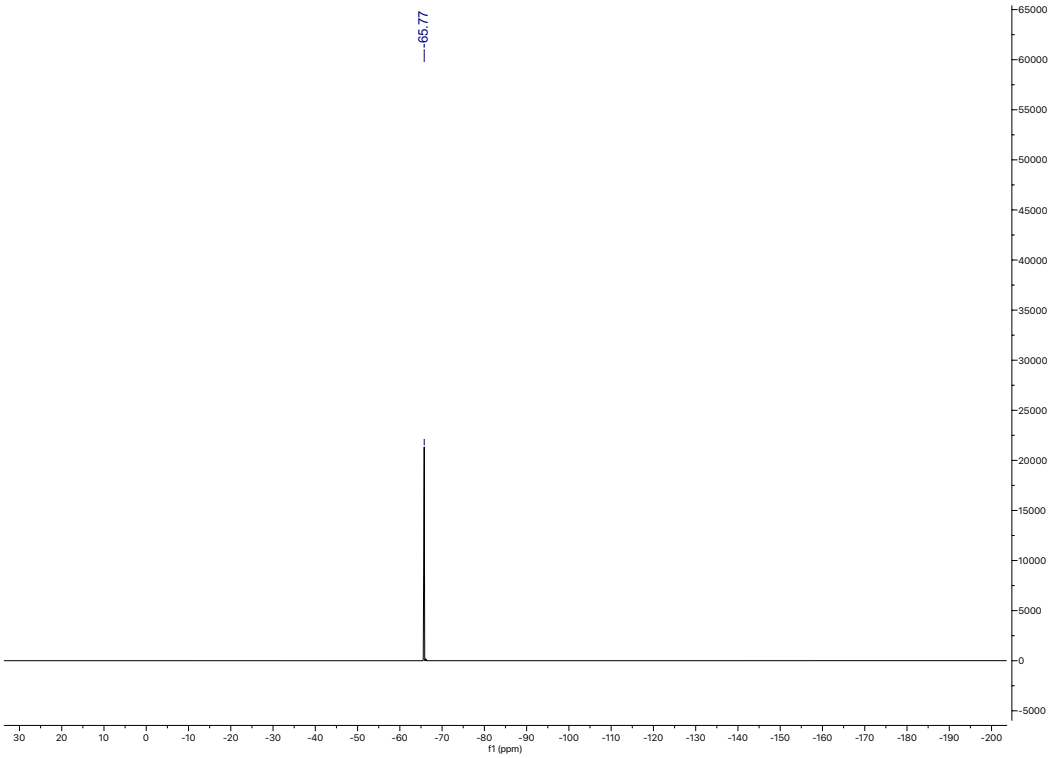


**Figure 2.5.24 376MHz $^{19}$FNMR of 2.1b**

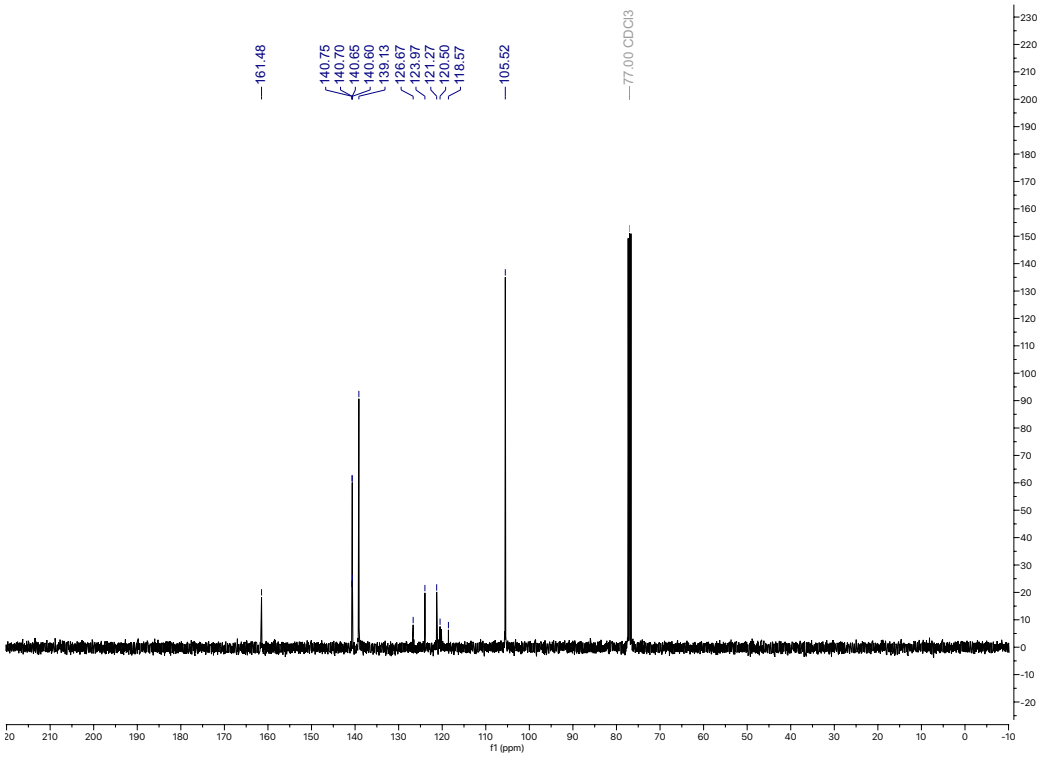


**Figure 2.5.25 126MHz $^{13}$CNMR of 2.1b**

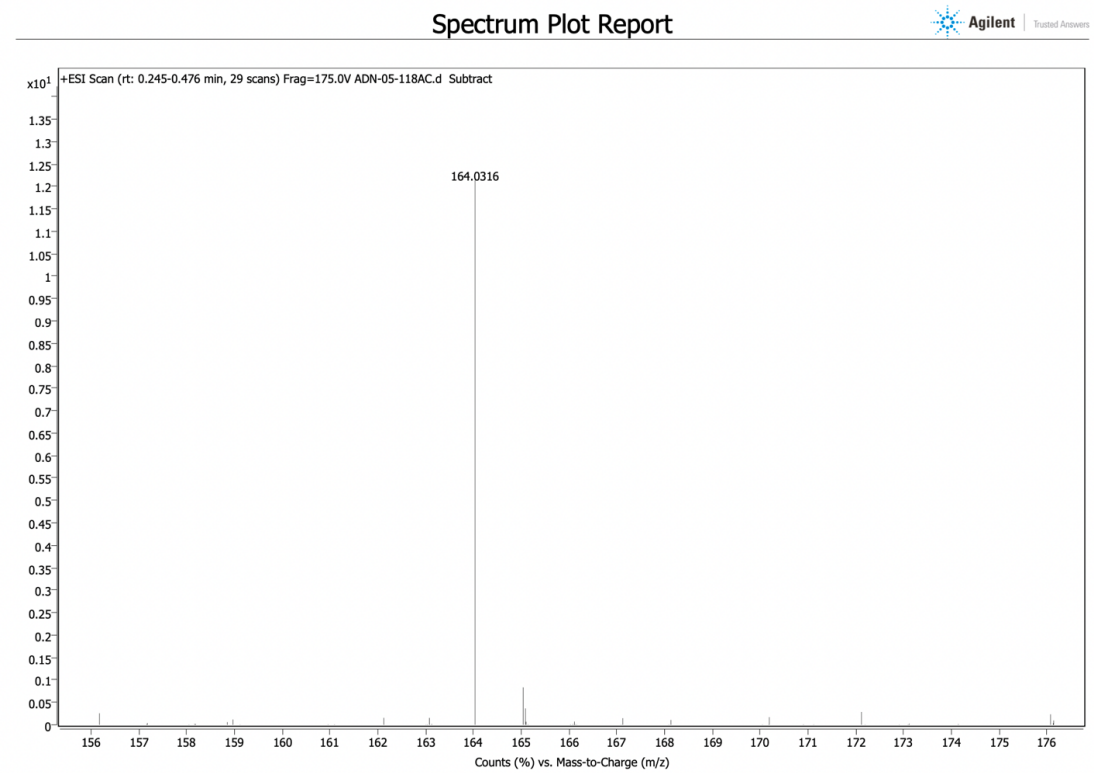


**Figure 2.5.26 HRMS (ESI) of 2.1b**

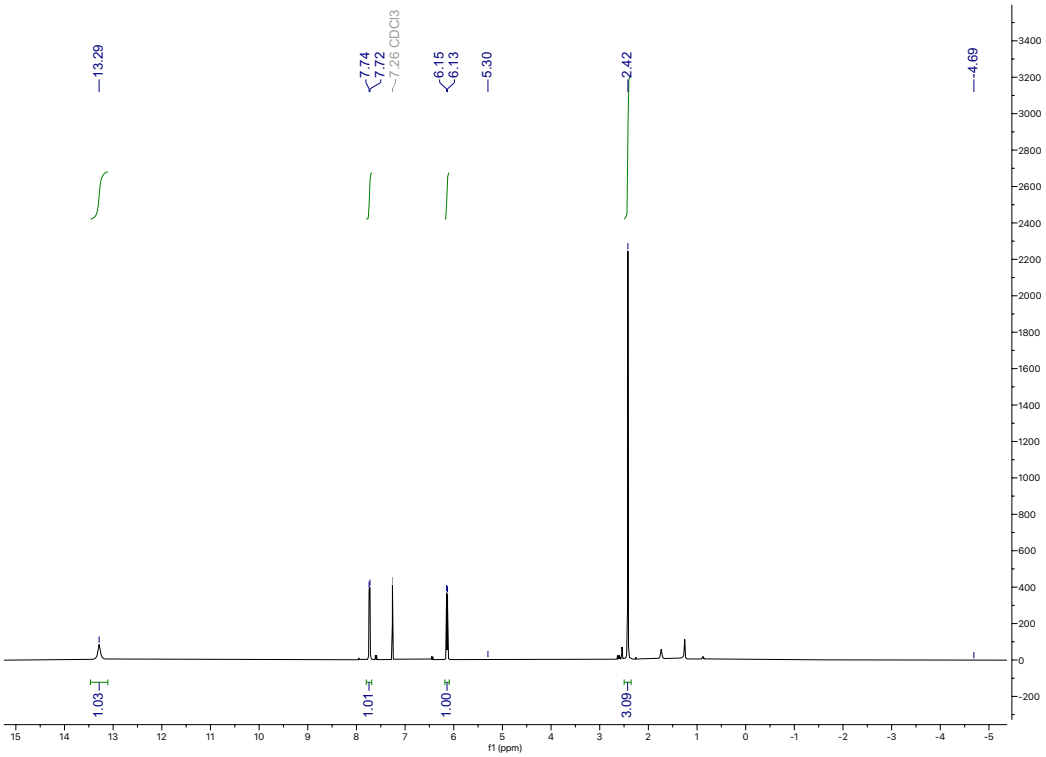


**Figure 2.5.27 400MHz $^{1}$HNMR of 2.2b**

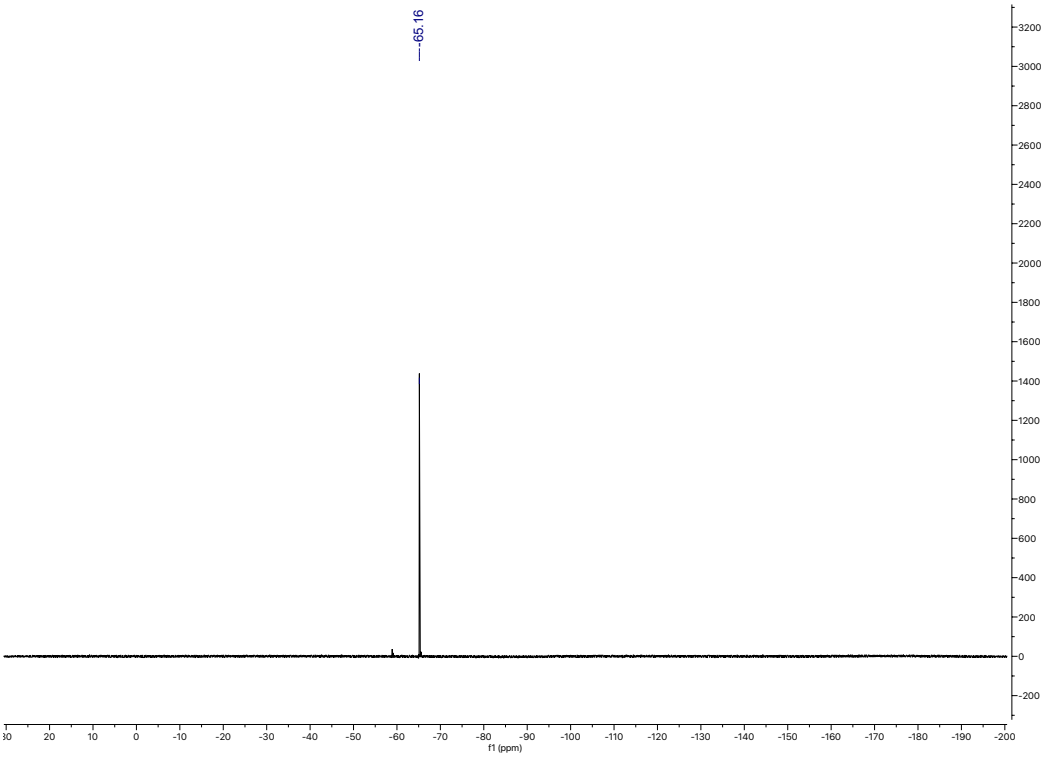


**Figure 2.5.28 376MHz $^{19}$FNMR of 2.2b**

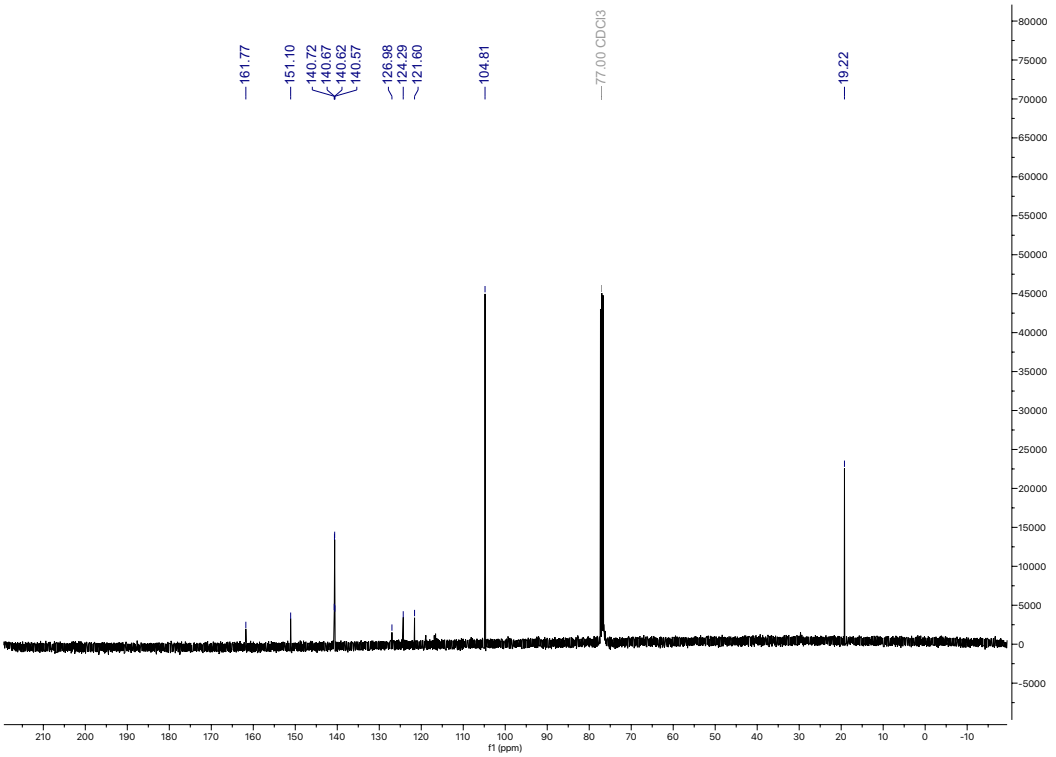


**Figure 2.5.29 126MHz $^{13}$CNMR of 2.2b**

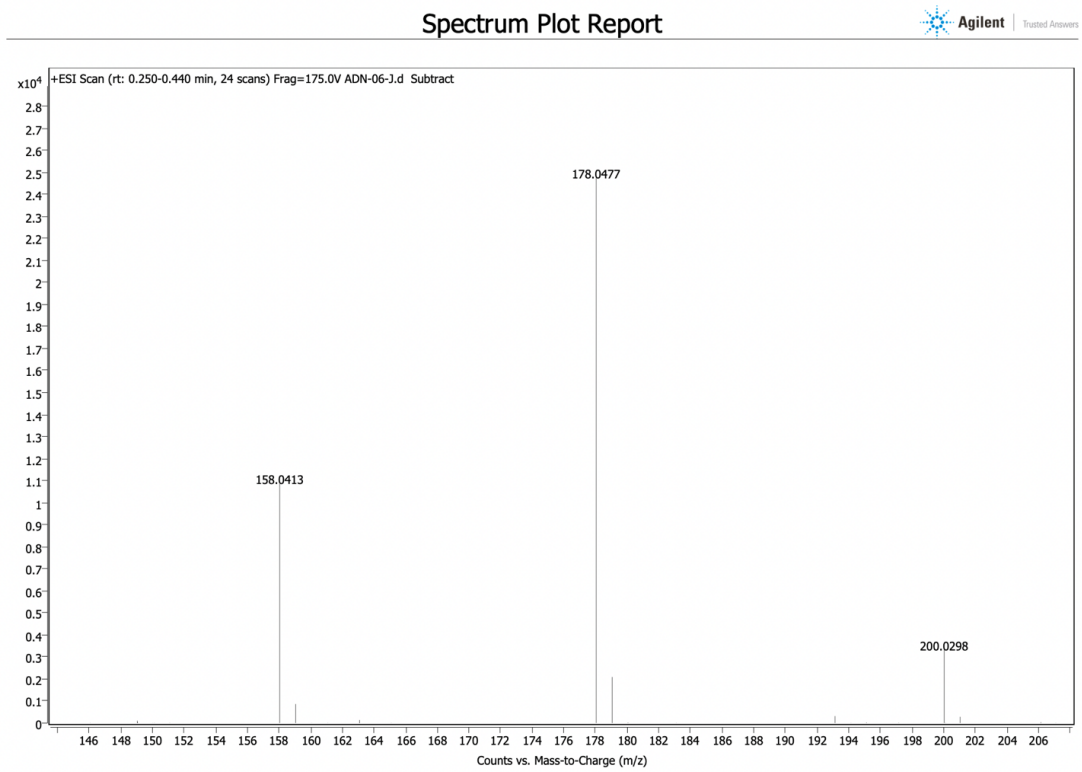


**Figure 2.5.30 HRMS (ESI) of 2.2b**

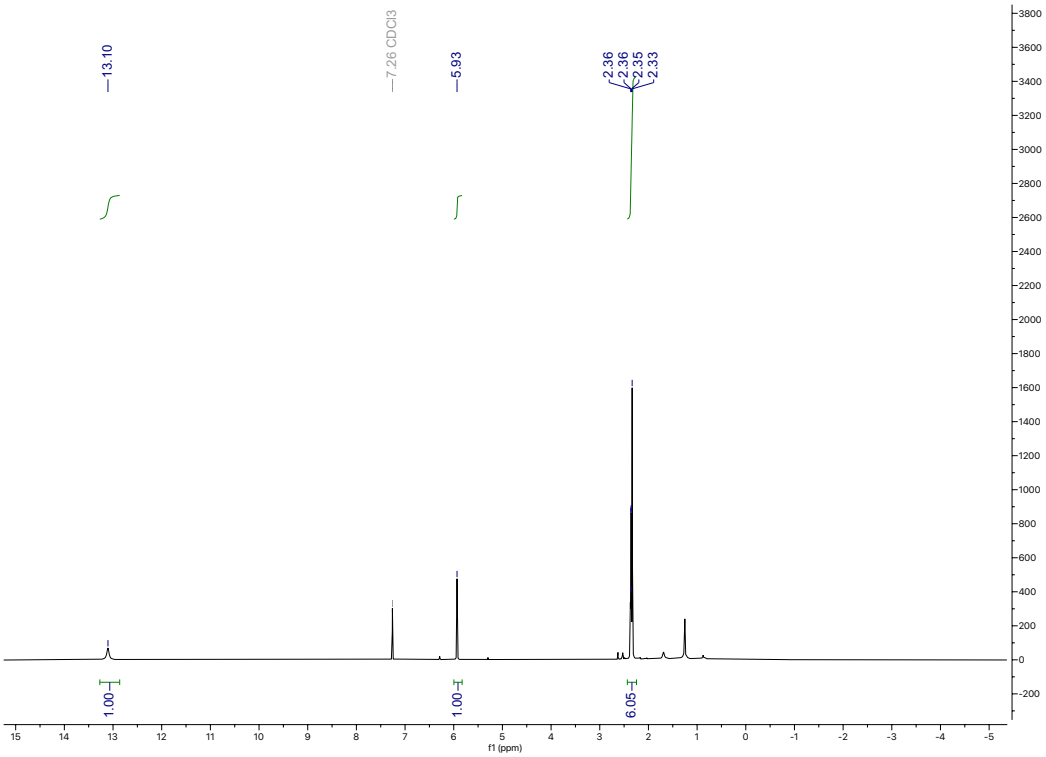


**Figure 2.5.31 400MHz $^{1}$HNMR of 2.3b**

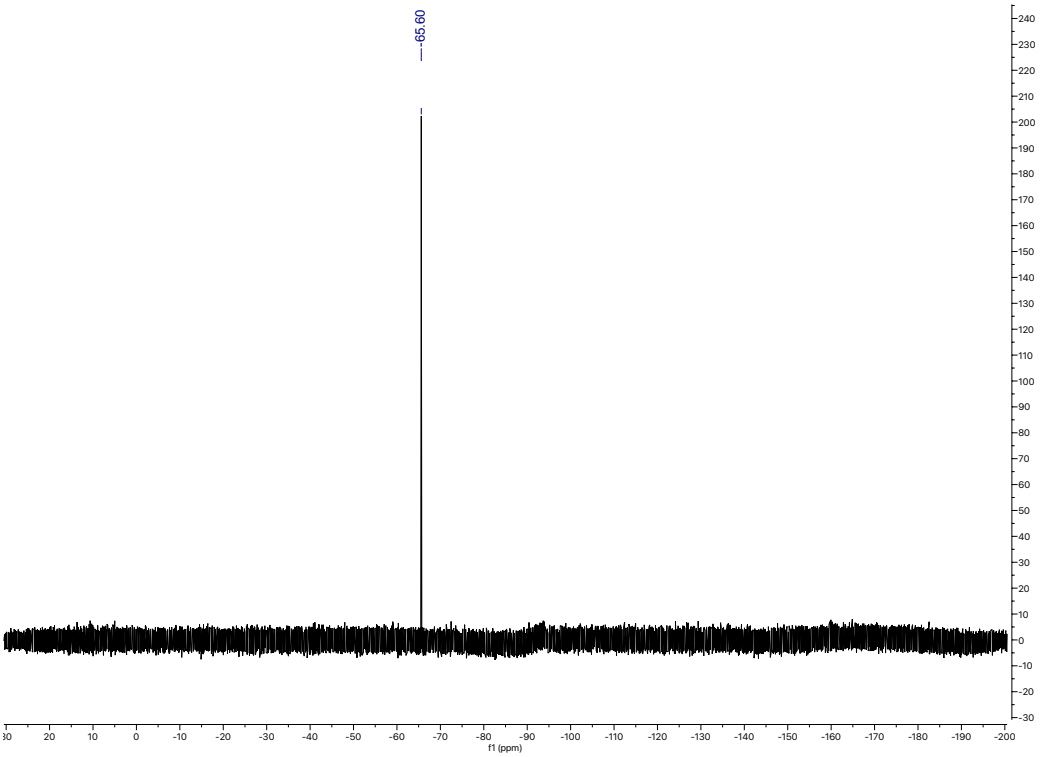


**Figure 2.5.32 376MHz $^{19}$FNMR of 2.3b**

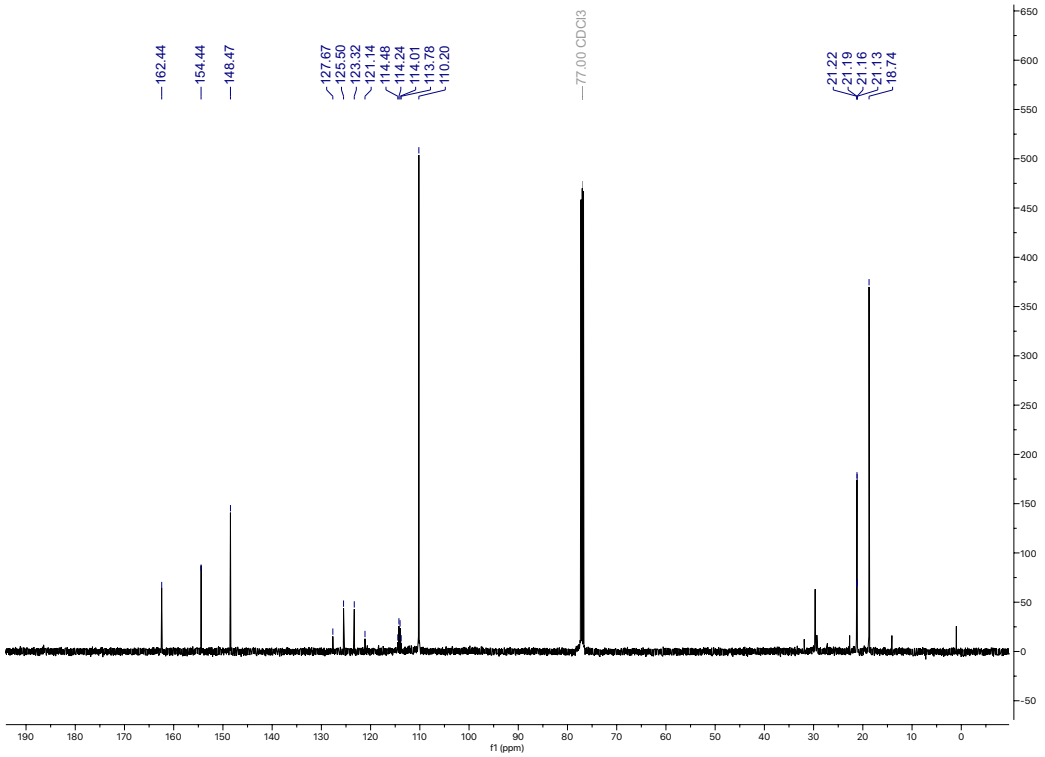


**Figure 2.5.33 126MHz $^{13}$CNMR of 2.3b**

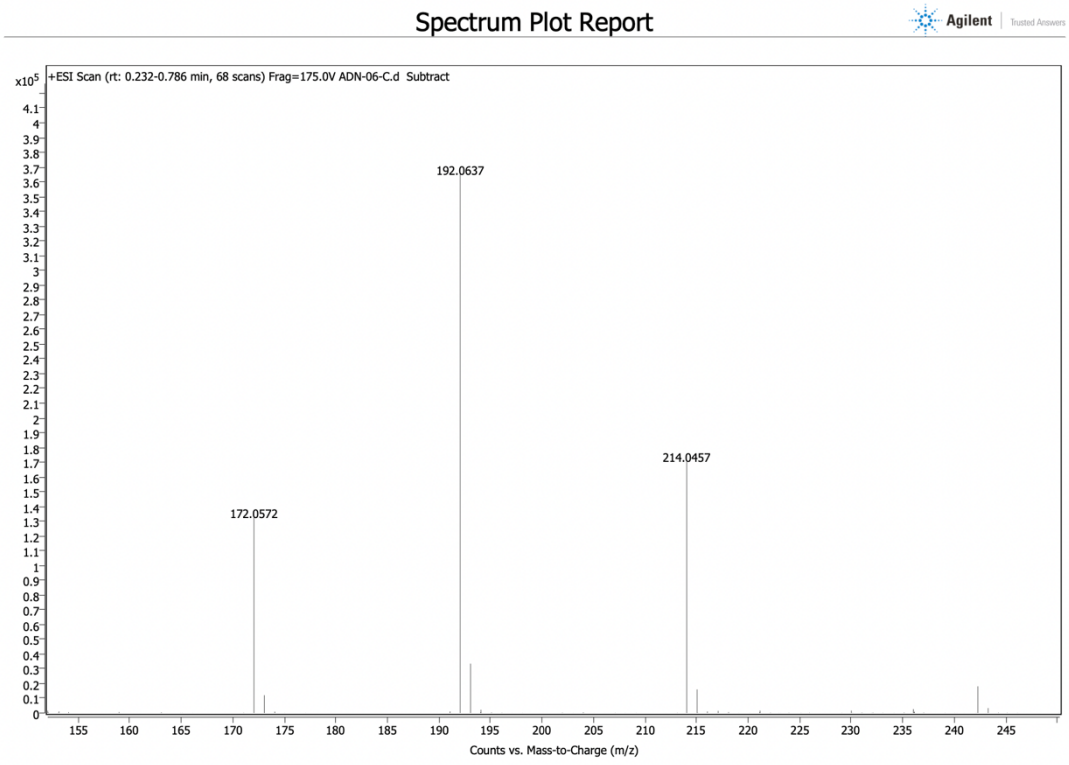


**Figure 2.5.34 HRMS (ESI) of 2.3b**

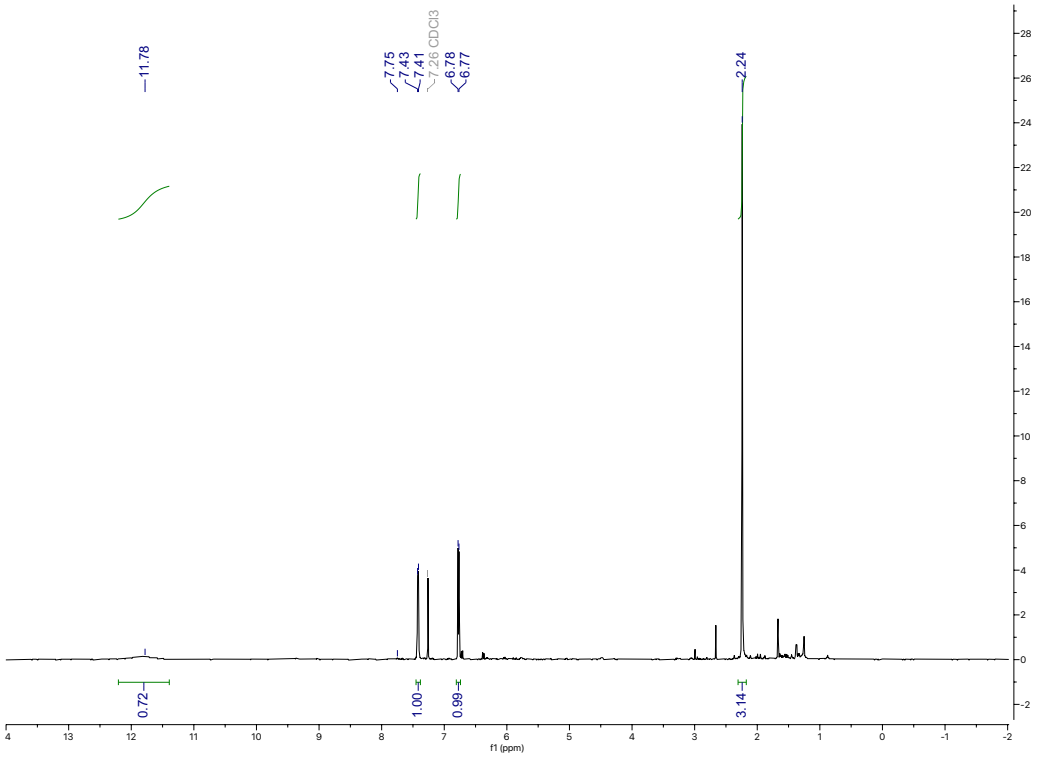


**Figure 2.5.35 400MHz $^{1}$HNMR of 2.4b**

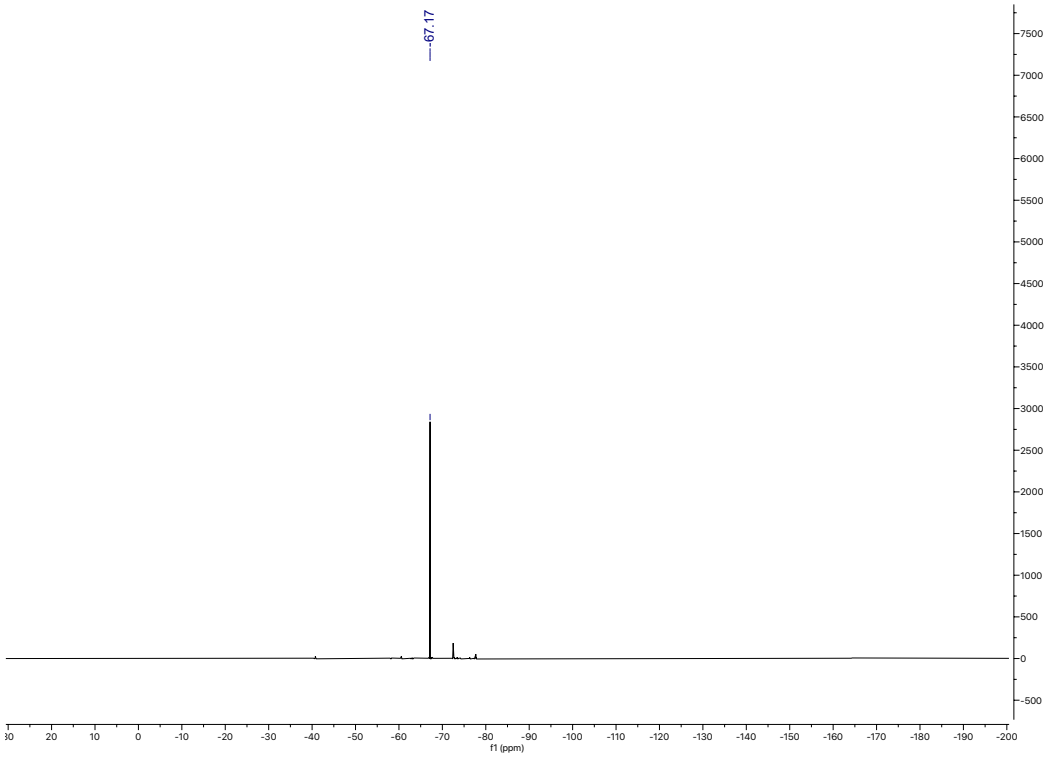


**Figure 2.5.36 376MHz $^{19}$FNMR of 2.4b**

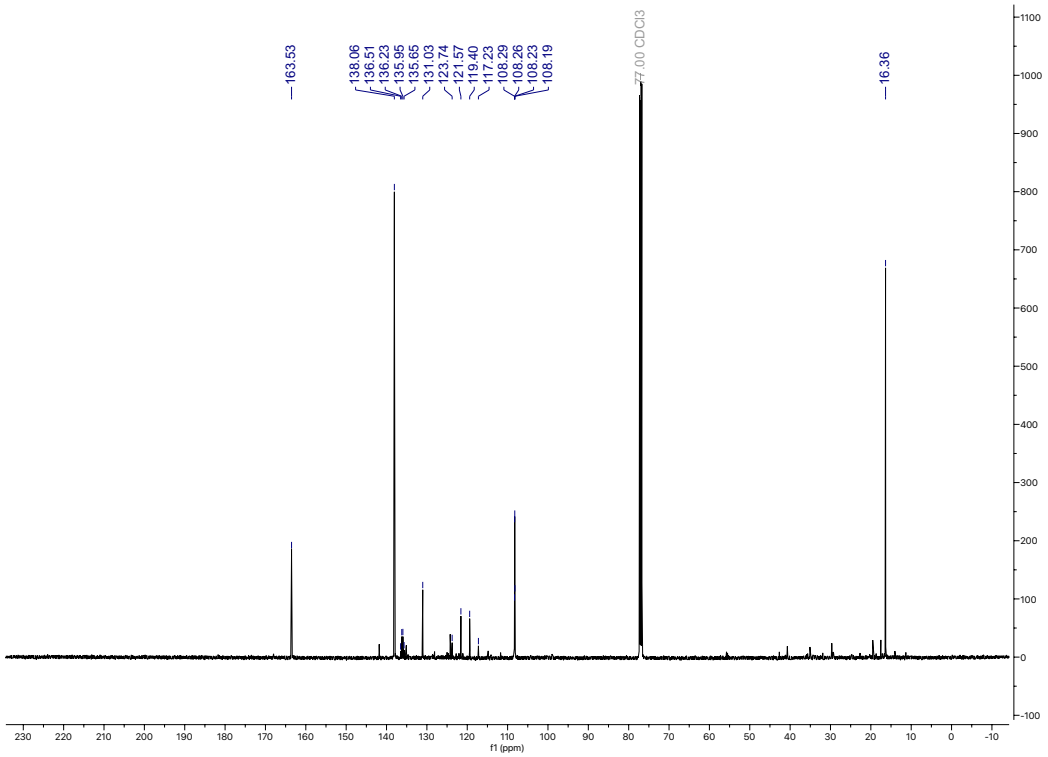


**Figure 2.5.37 126MHz $^{13}$CNMR of 2.4b**

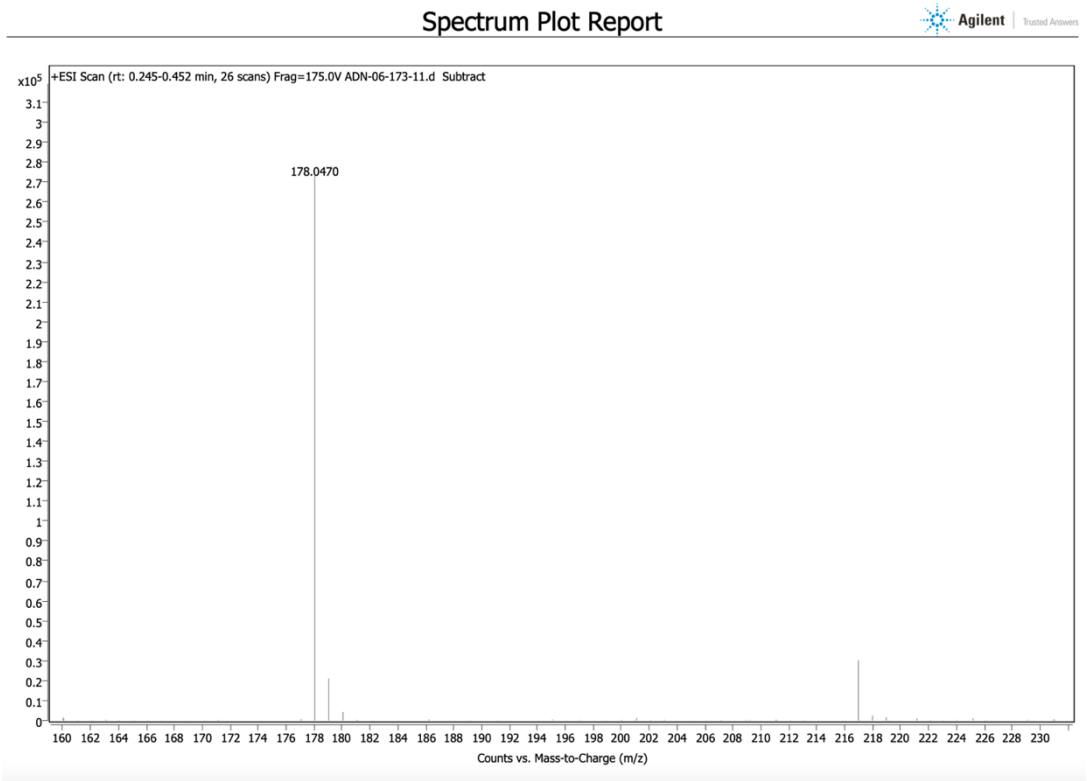


**Figure 2.5.38 HRMS (ESI) of 2.4b**

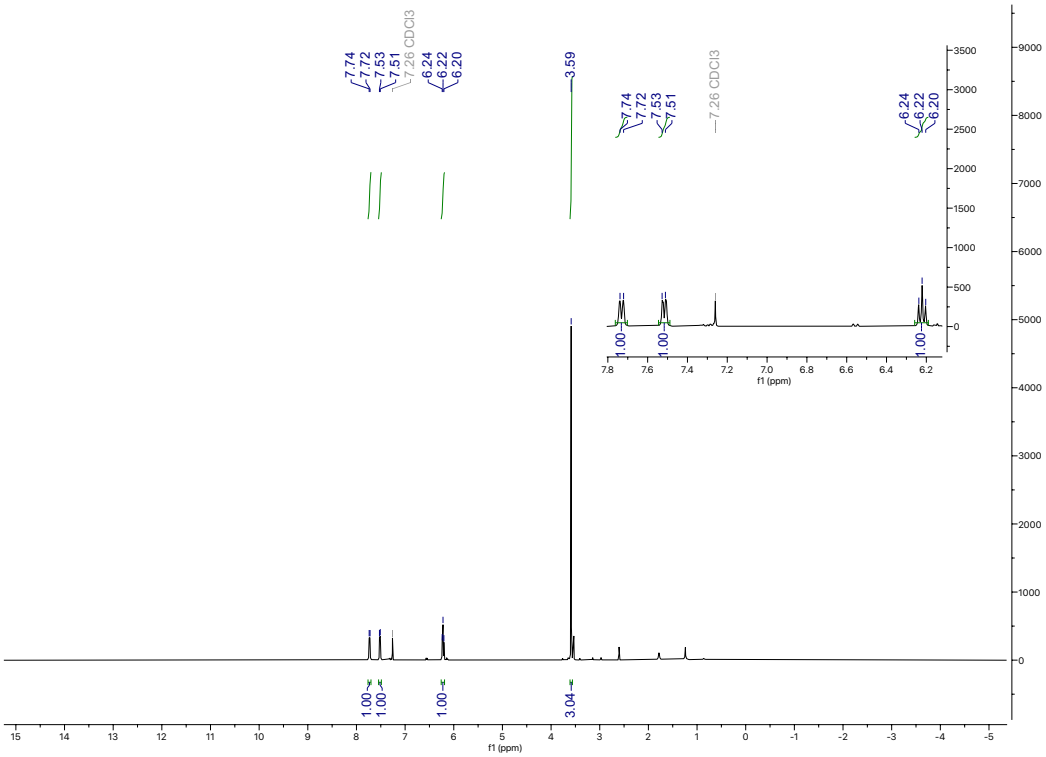


**Figure 2.5.39 400MHz $^{1}$HNMR of 2.5b**

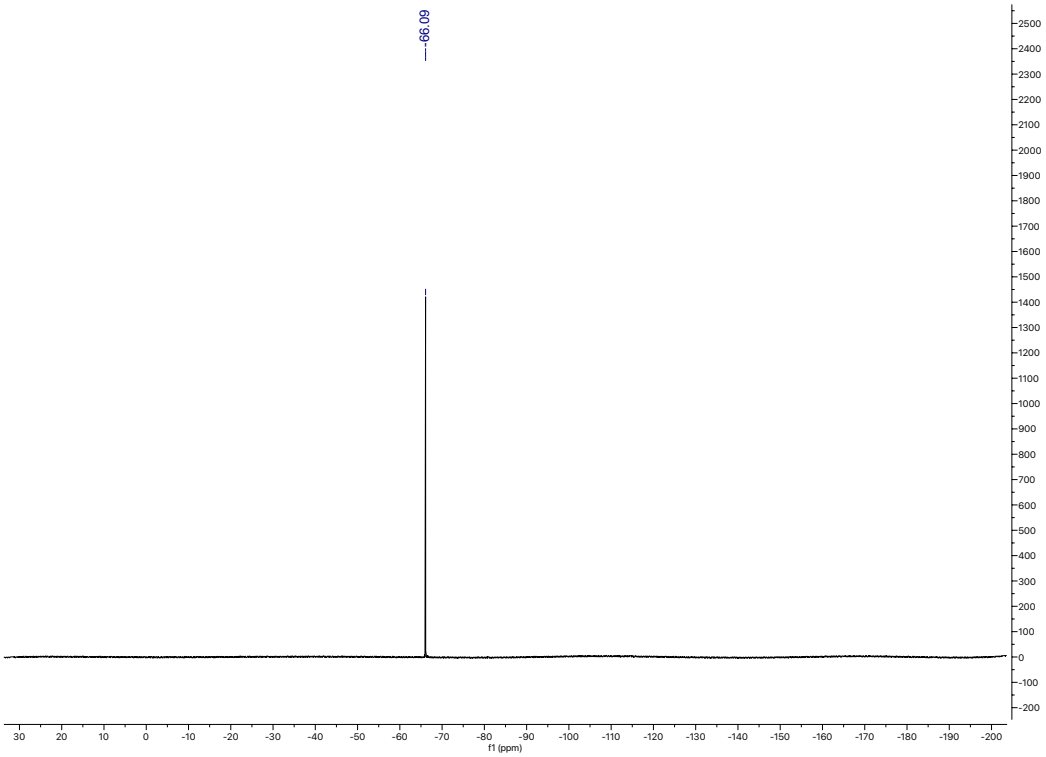


**Figure 2.5.40 376MHz $^{19}$FNMR of 2.5b**

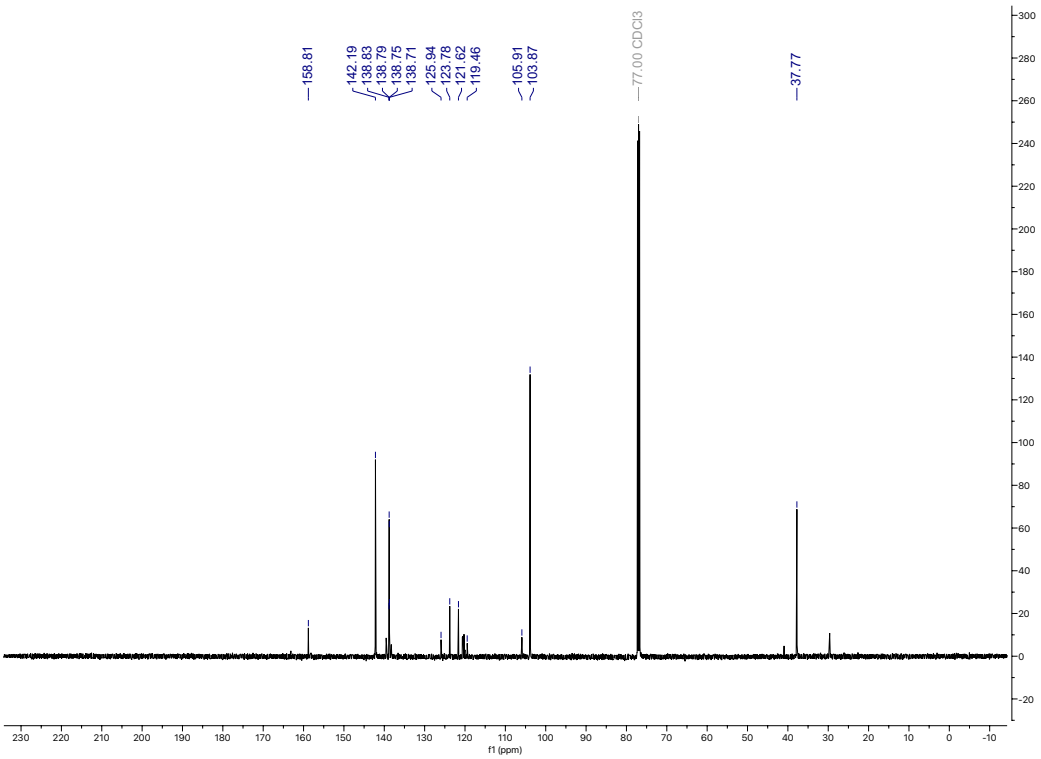


**Figure 2.5.41 126MHz $^{13}$CNMR of 2.5b**

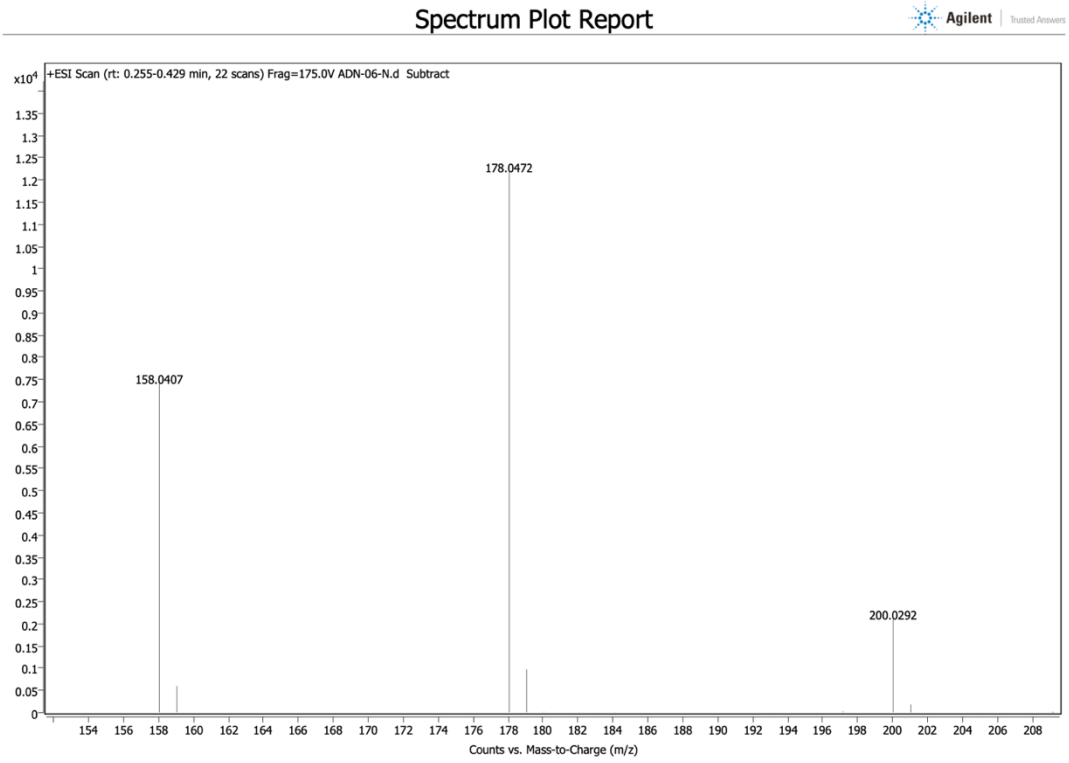


**Figure 2.5.42 HRMS (ESI) of 2.5b**

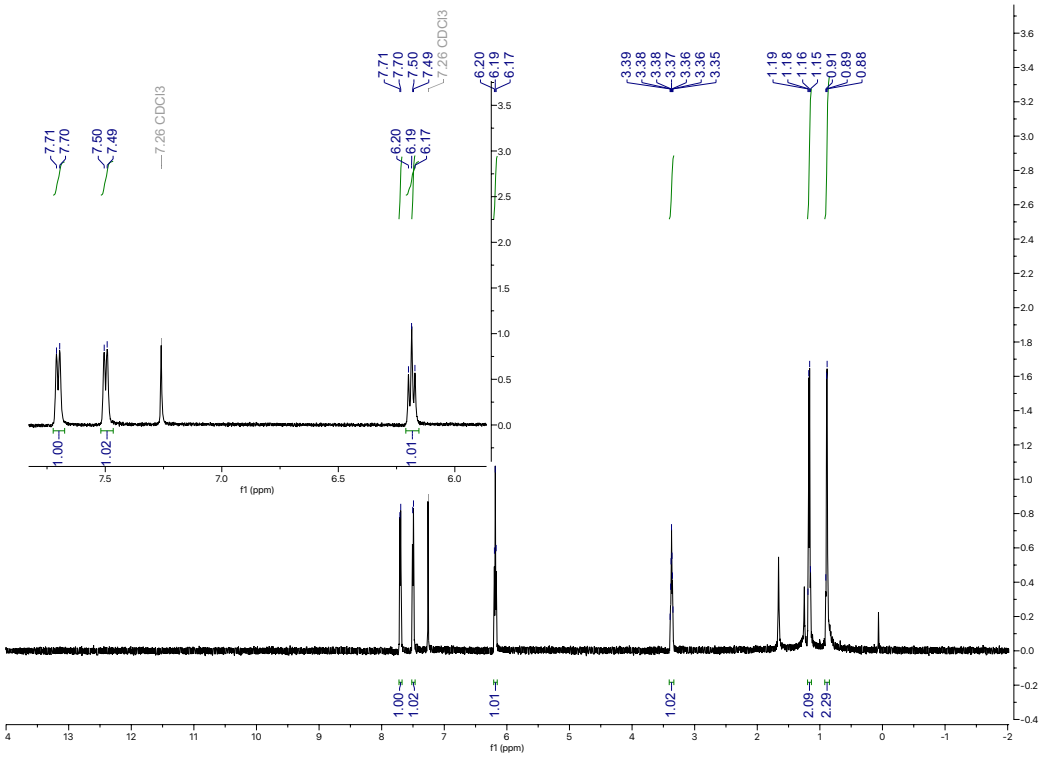


**Figure 2.5.43 500MHz $^{1}$HNMR of 2.6b**

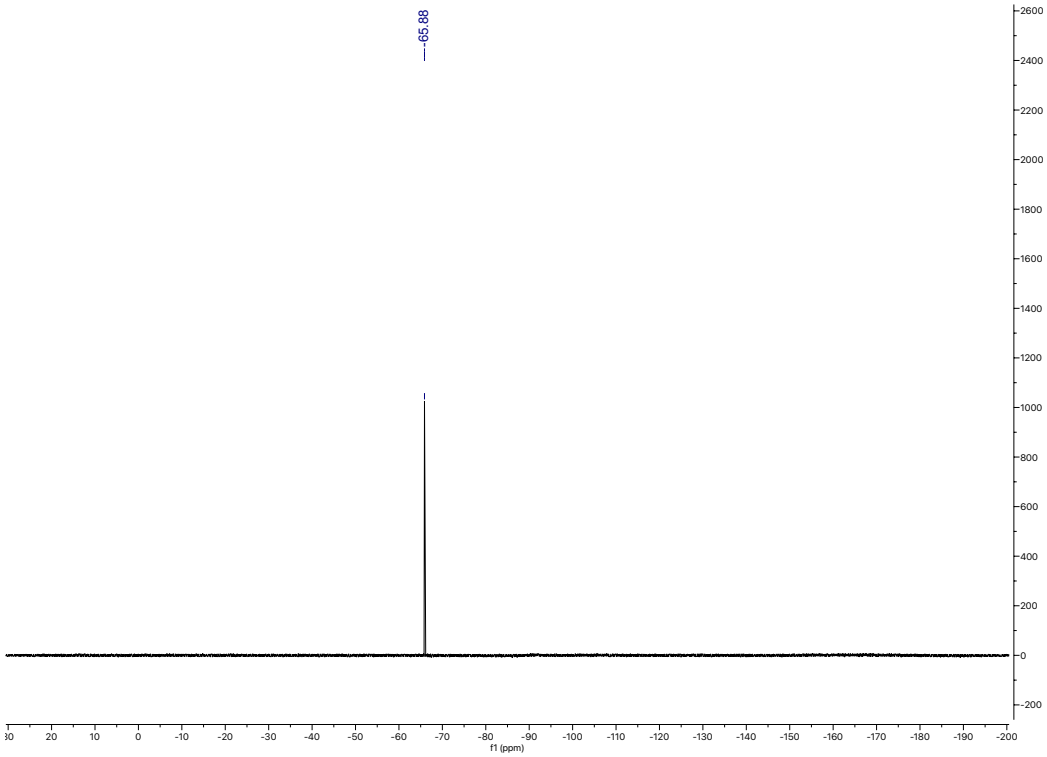


**Figure 2.5.44 376MHz $^{19}$FNMR of 2.6b**

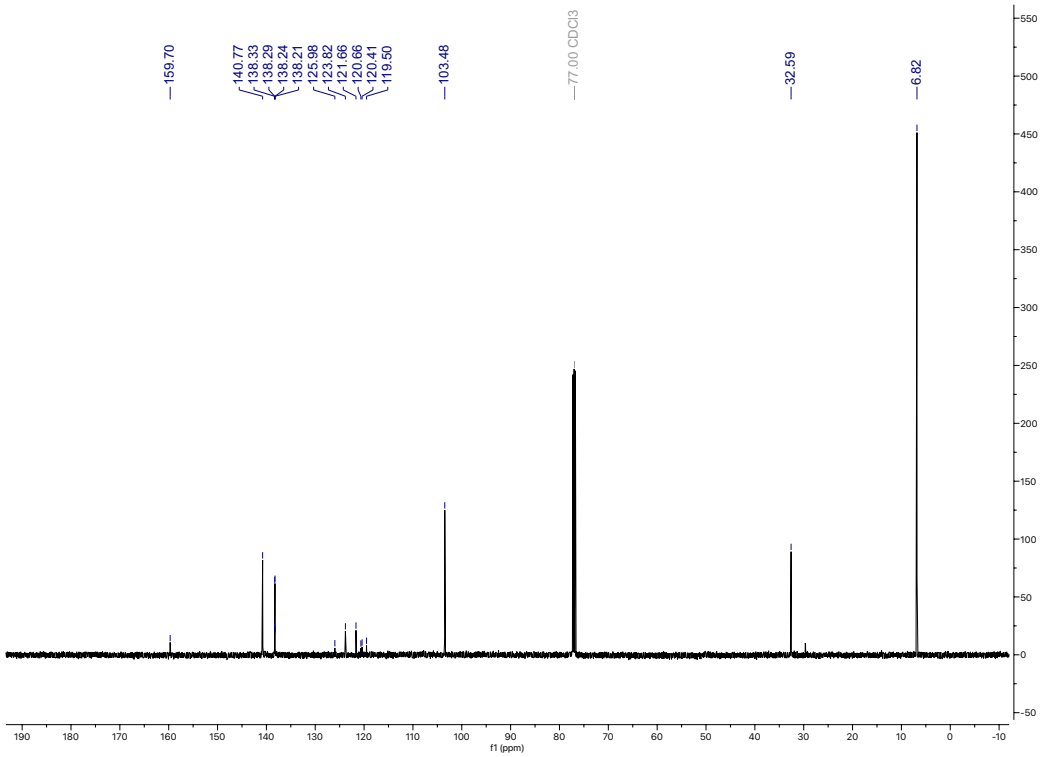


**Figure 2.5.45 126MHz $^{13}$CNMR of 2.6b**

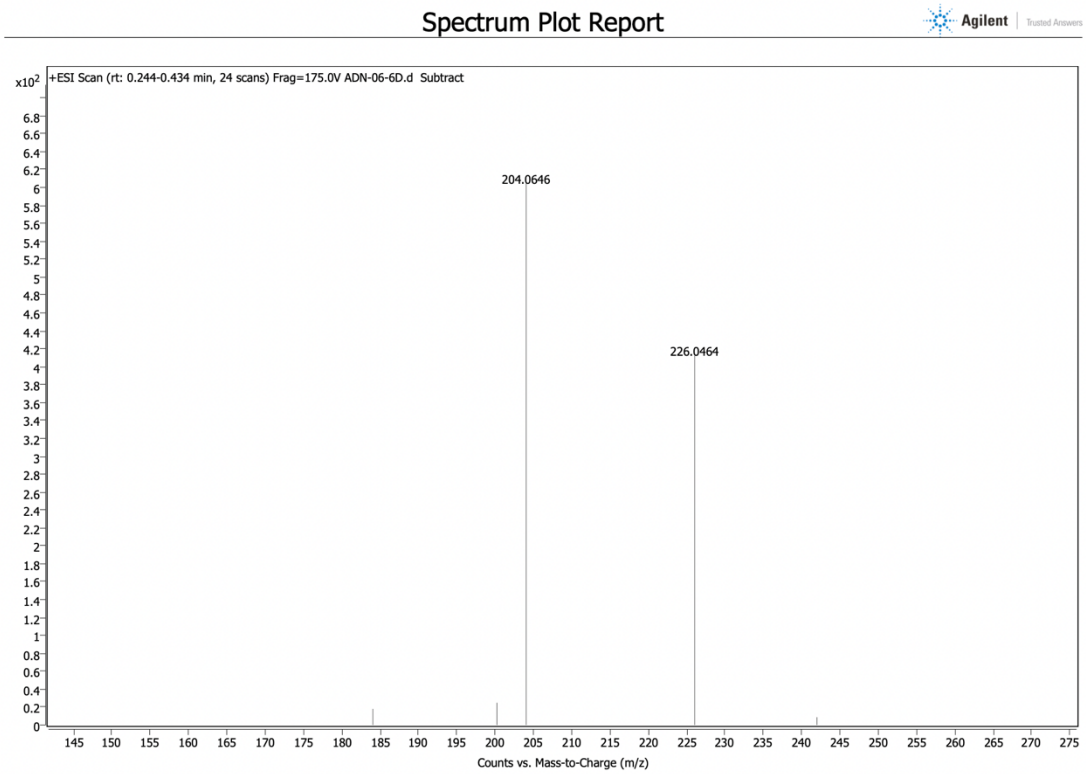


**Figure 2.5.46 HRMS (ESI) of 2.6b**

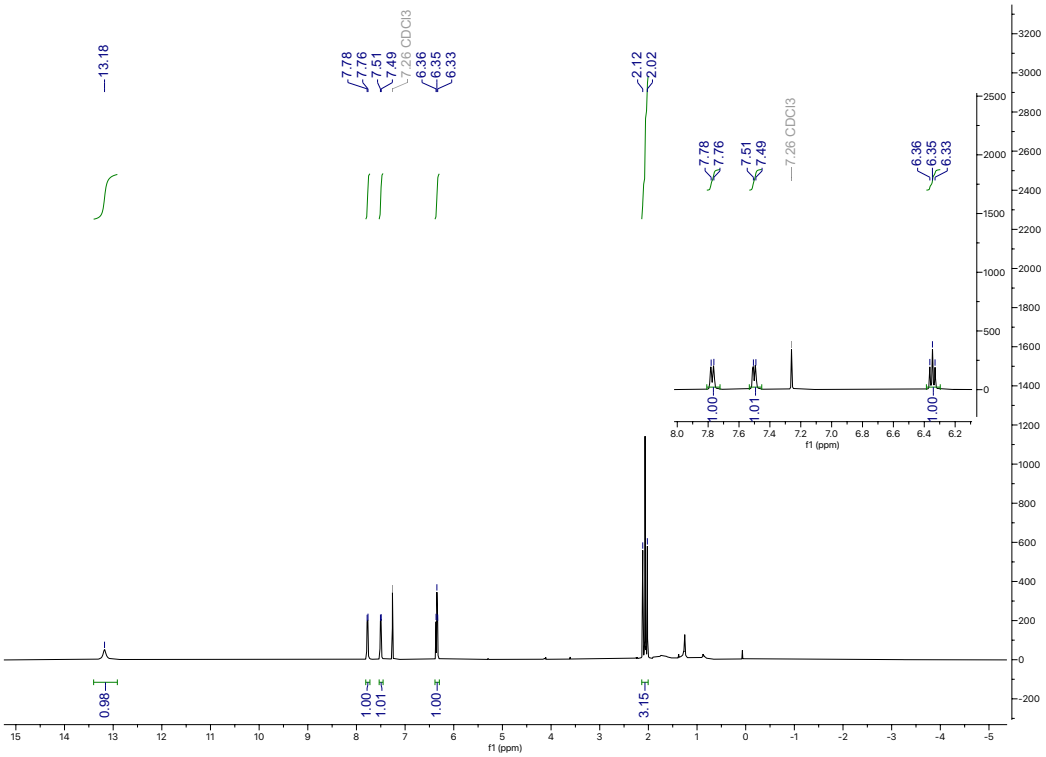


**Figure 2.5.47 400MHz $^{1}$HNMR of 2.7b**

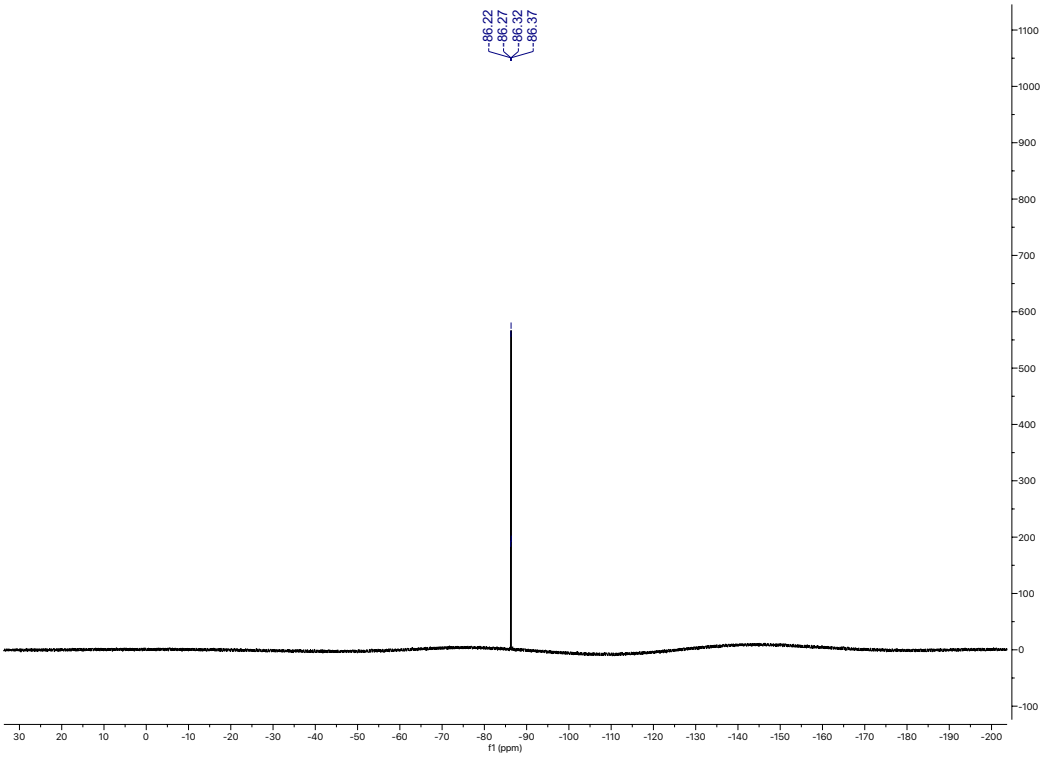


**Figure 2.5.48 376MHz $^{19}$FNMR of 2.7b**

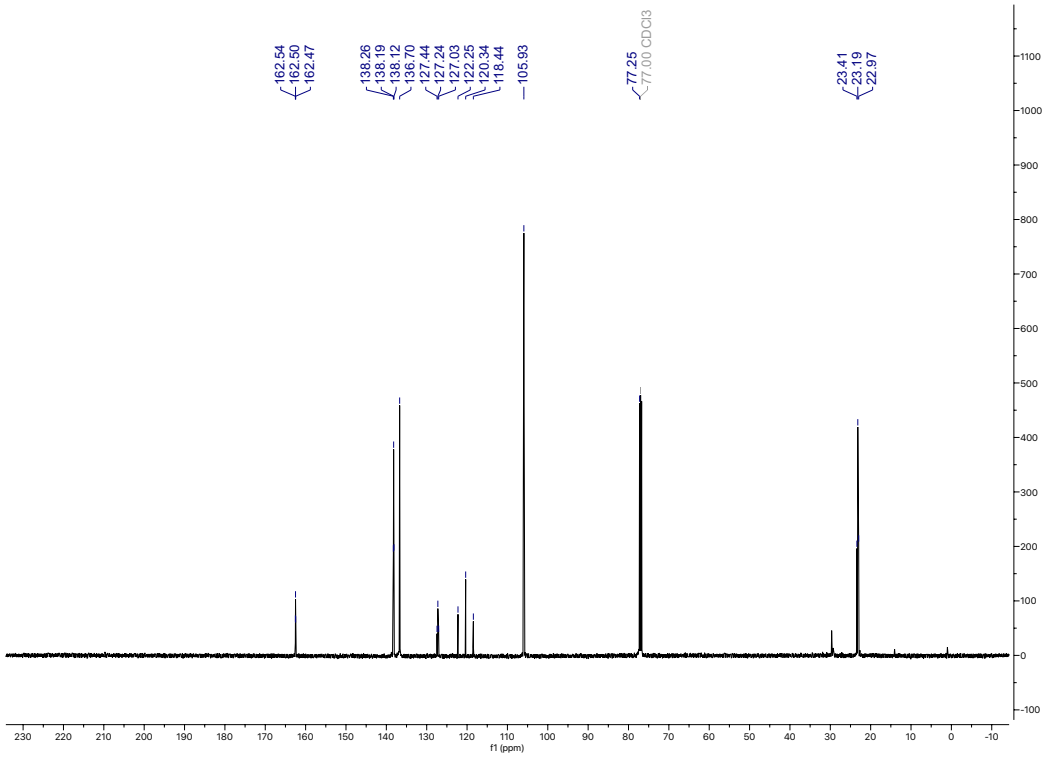


**Figure 2.5.49 126MHz $^{13}$CNMR of 2.7b**

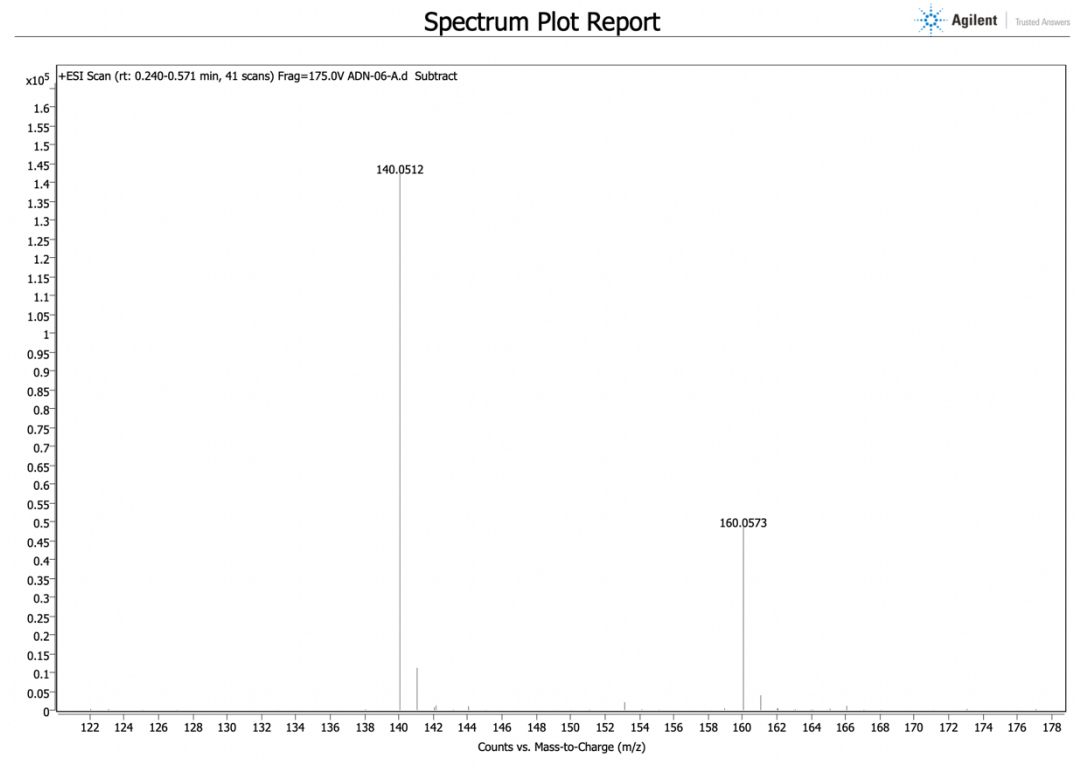


**Figure 2.5.50 HRMS (ESI) of 2.7b**

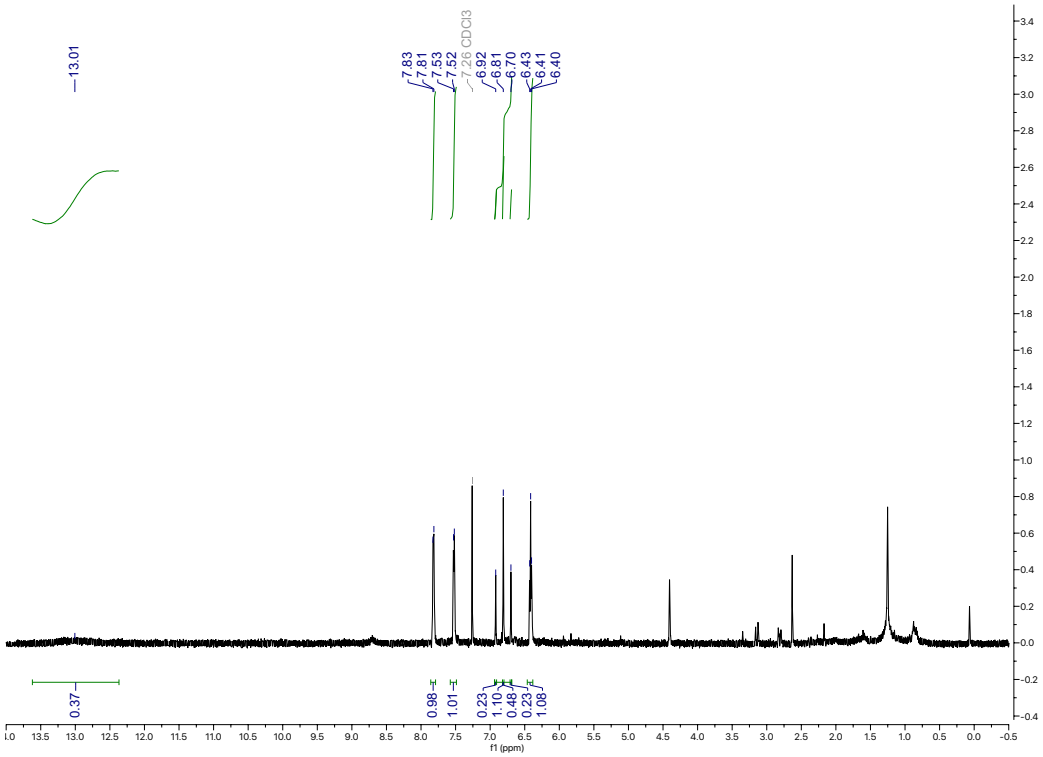


**Figure 2.5.51 500MHz $^{1}$HNMR of 2.8b**

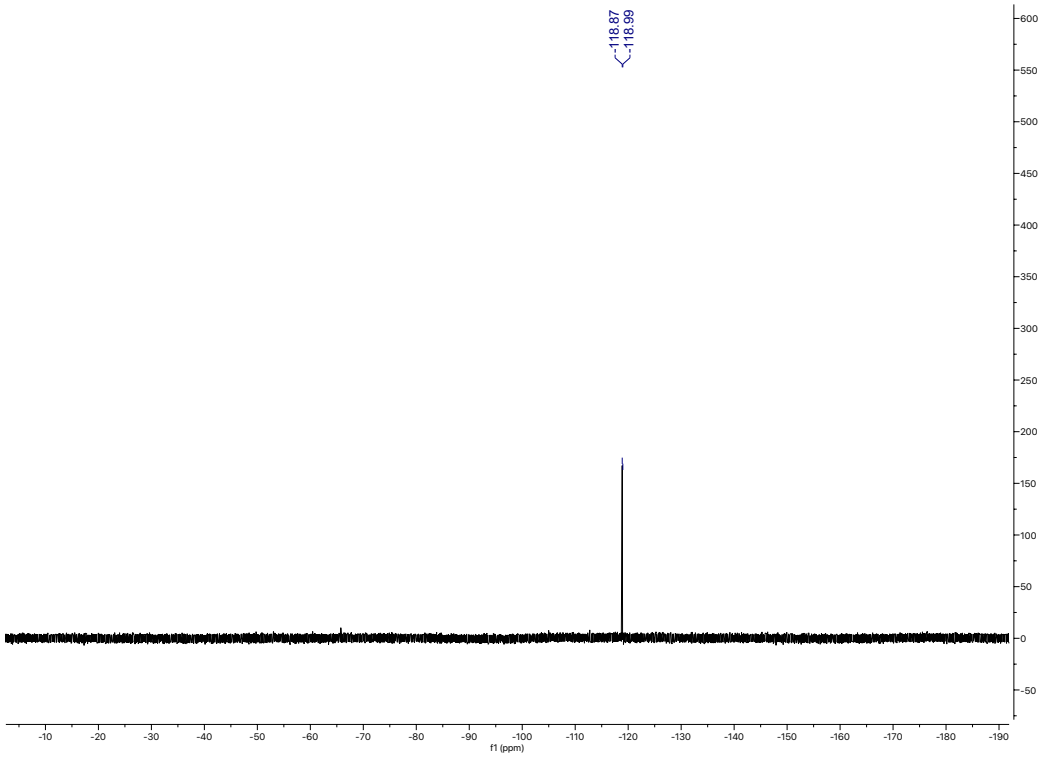


**Figure 2.5.52 376MHz $^{19}$FNMR of 2.8b**

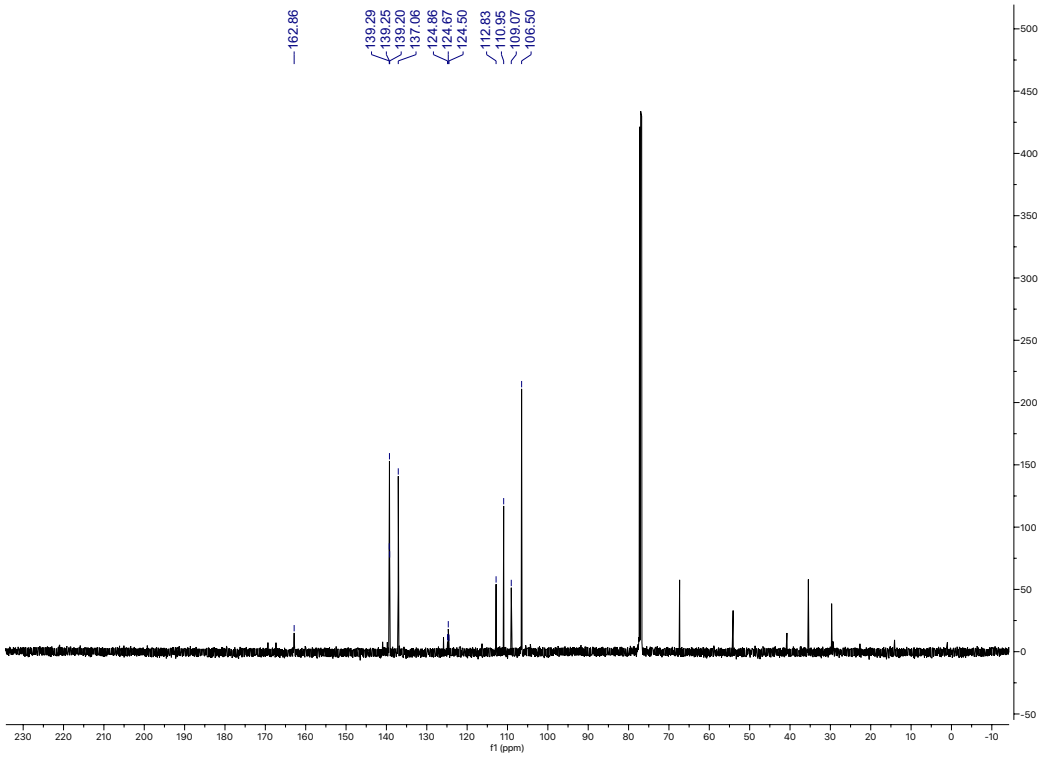


**Figure 2.5.53 126MHz $^{13}$CNMR of 2.8b**

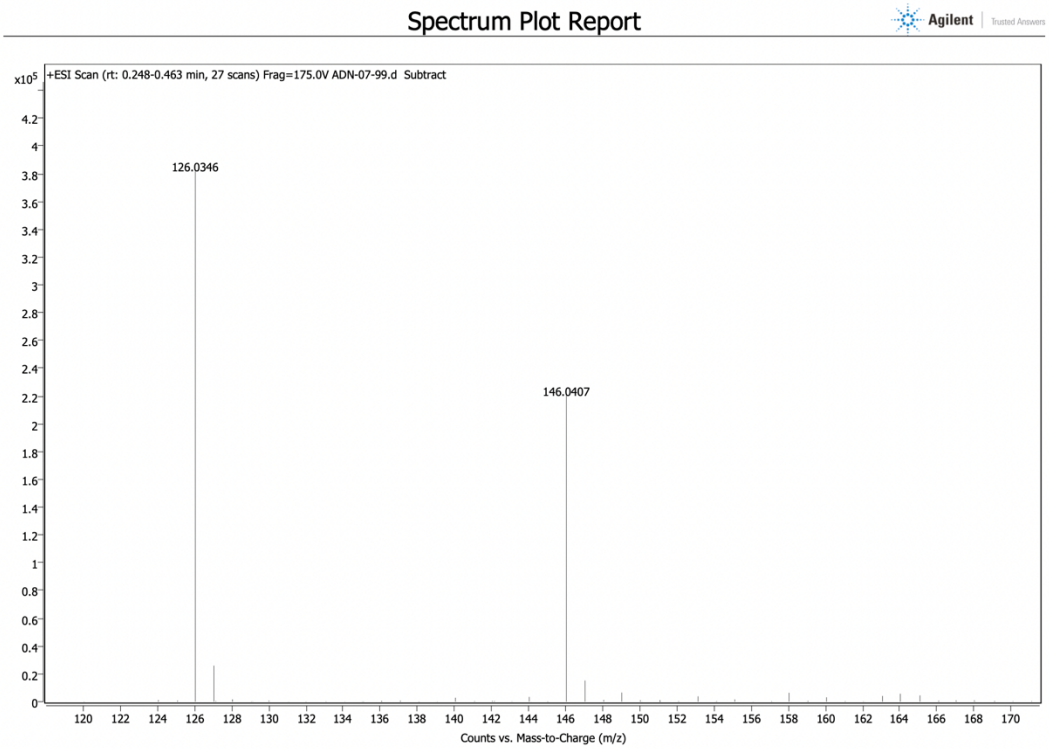


**Figure 2.5.54 HRMS (ESI) of 2.8b**

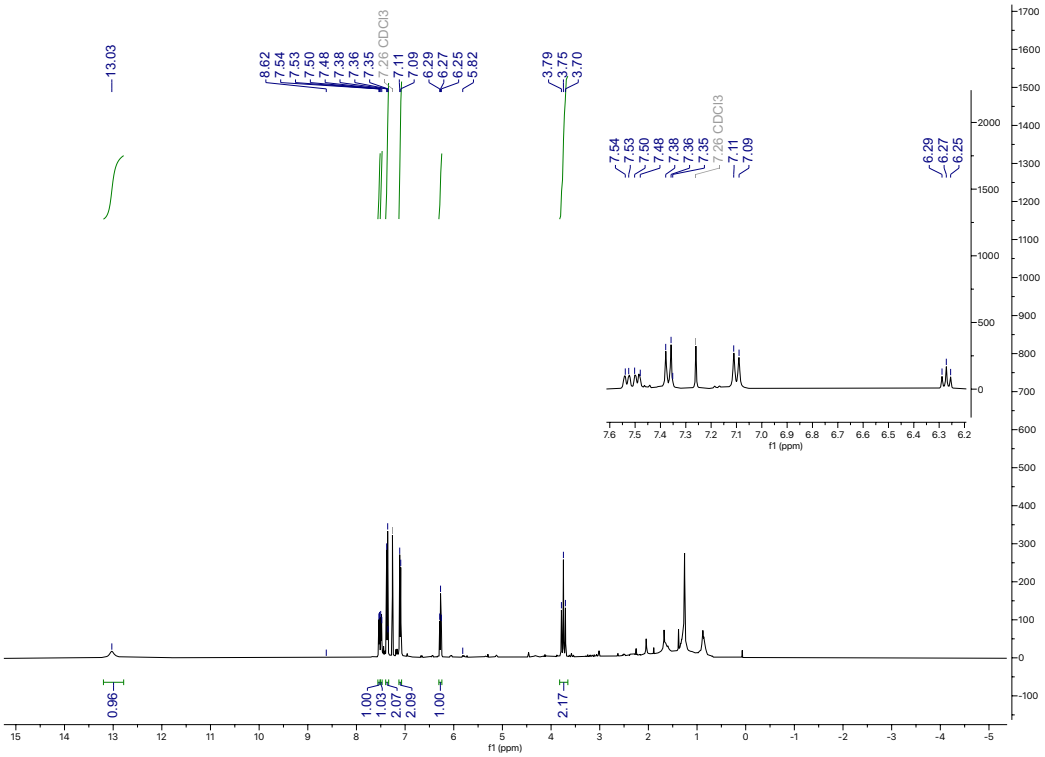


**Figure 2.5.55 400MHz $^{1}$HNMR of 2.9b**

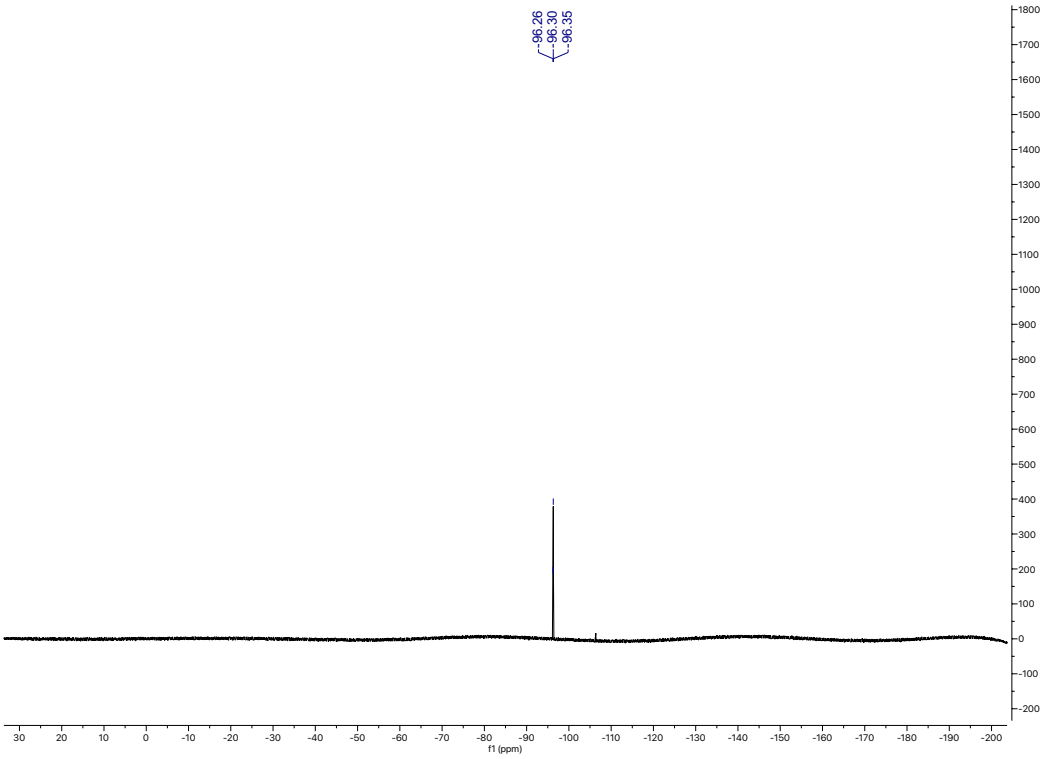


**Figure 2.5.56 376MHz $^{19}$FNMR of 2.9b**

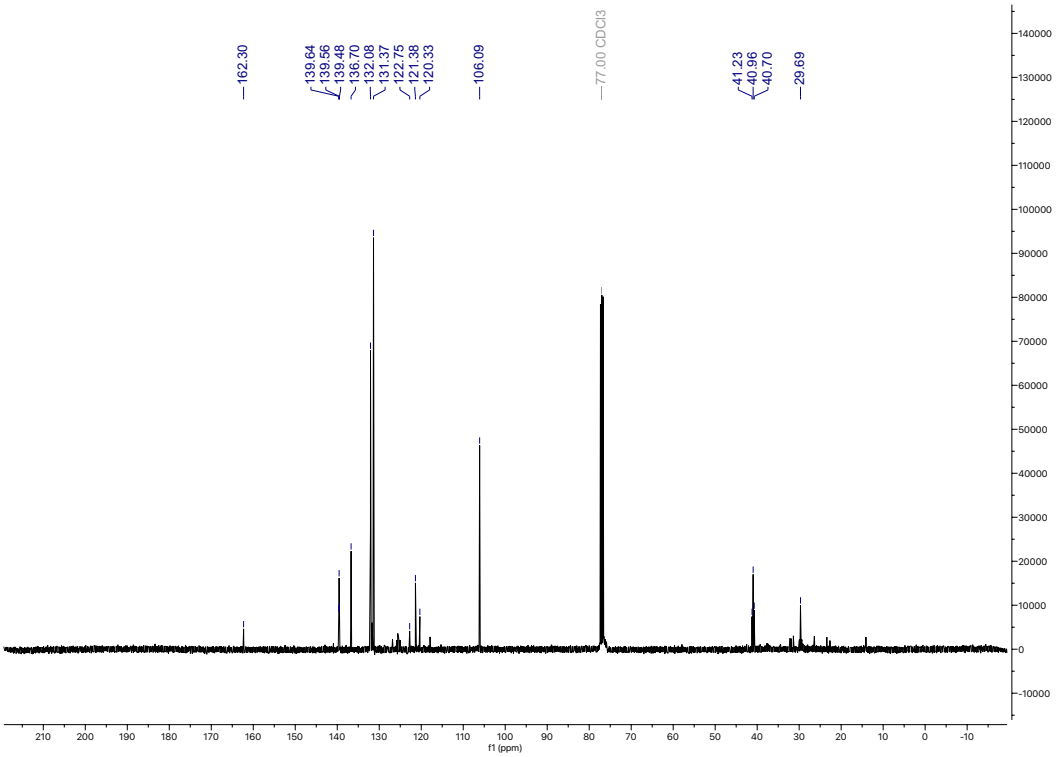


**Figure 2.5.57 126MHz $^{13}$CNMR of 2.9b**

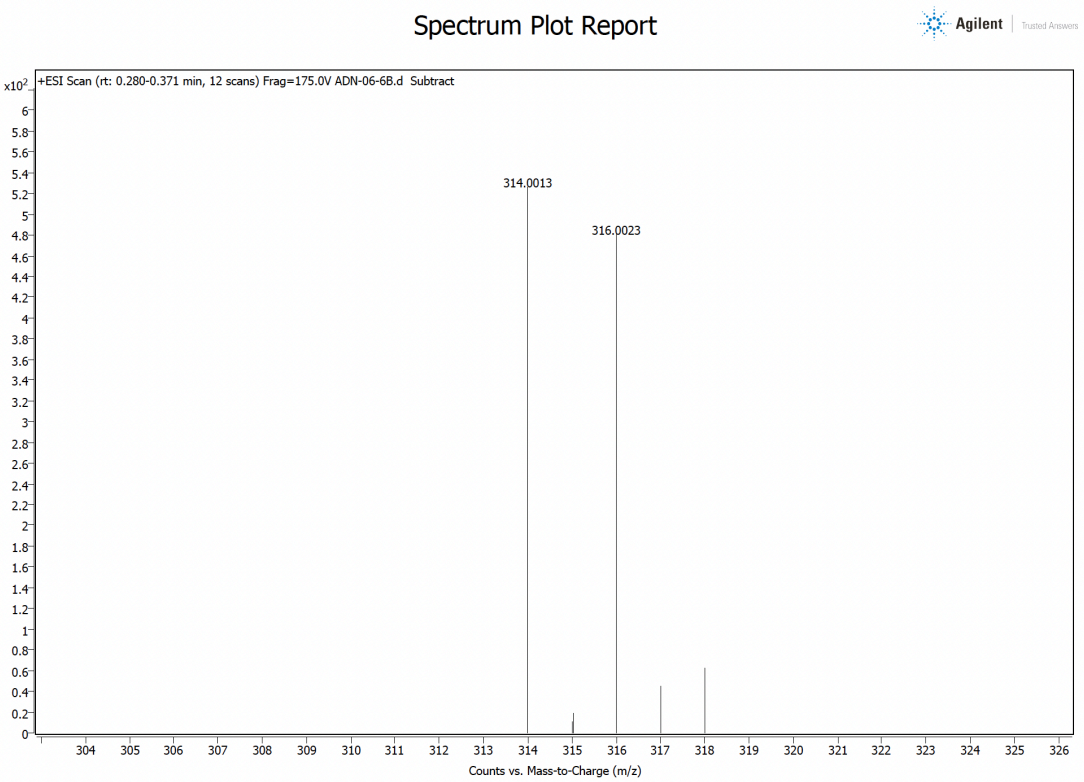


**Figure 2.5.58 HRMS (ESI) of 2.9b**

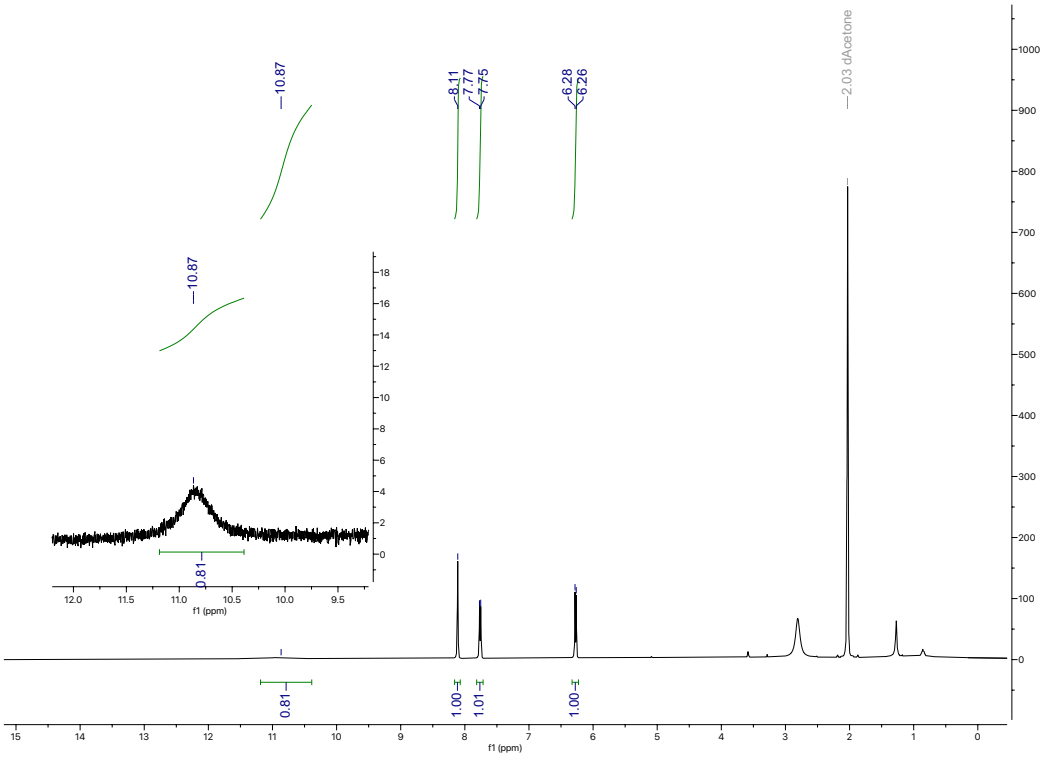


**Figure 2.5.59 500MHz $^{1}$HNMR of 2.10b**

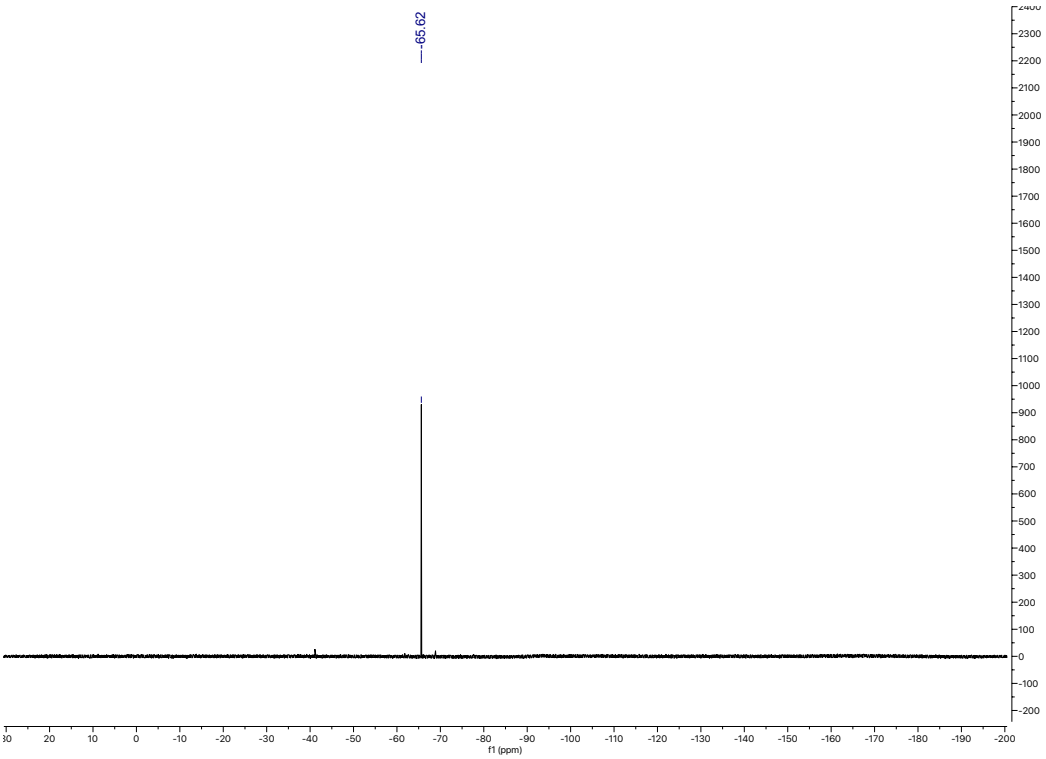


**Figure 2.5.60 376MHz $^{19}$FNMR of 2.10b**

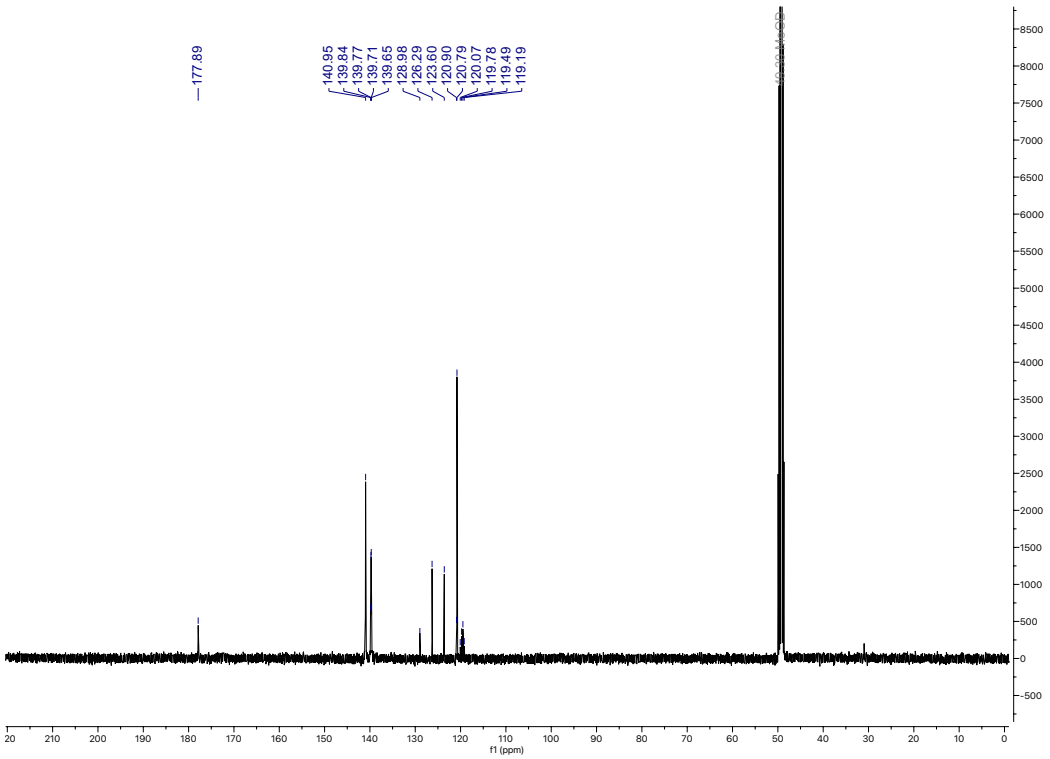


**Figure 2.5.61 126MHz $^{13}$CNMR of 2.10b**

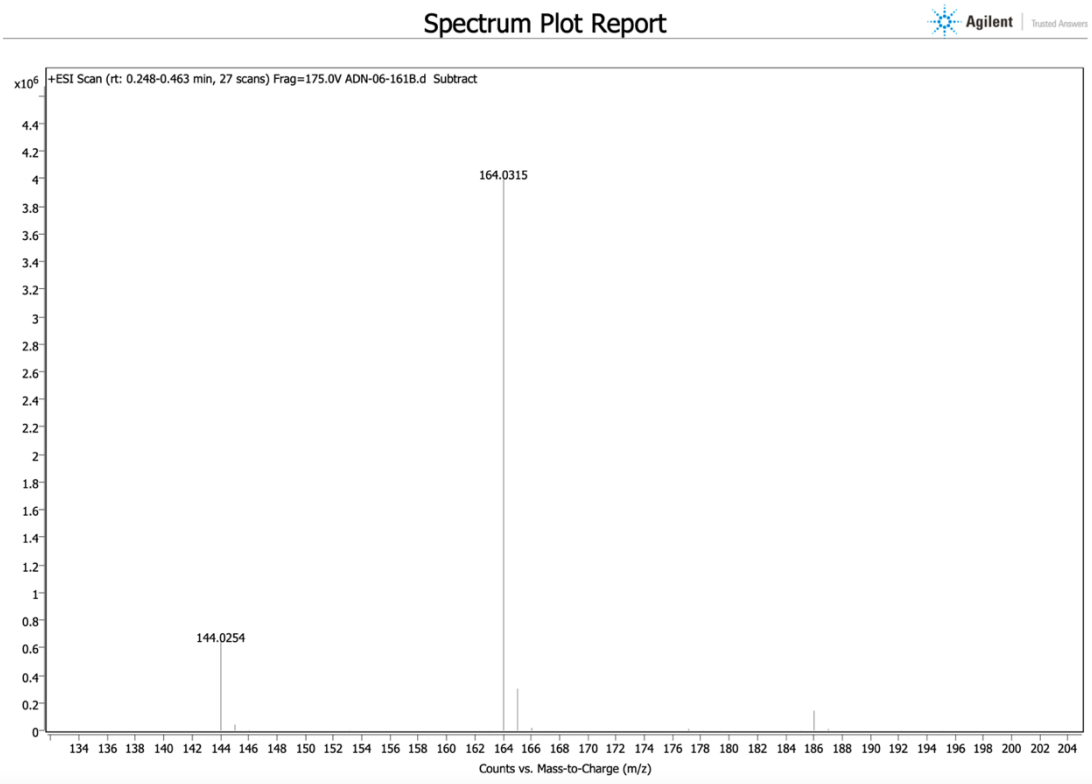


**Figure 2.5.62 HRMS (ESI) of 2.10b**

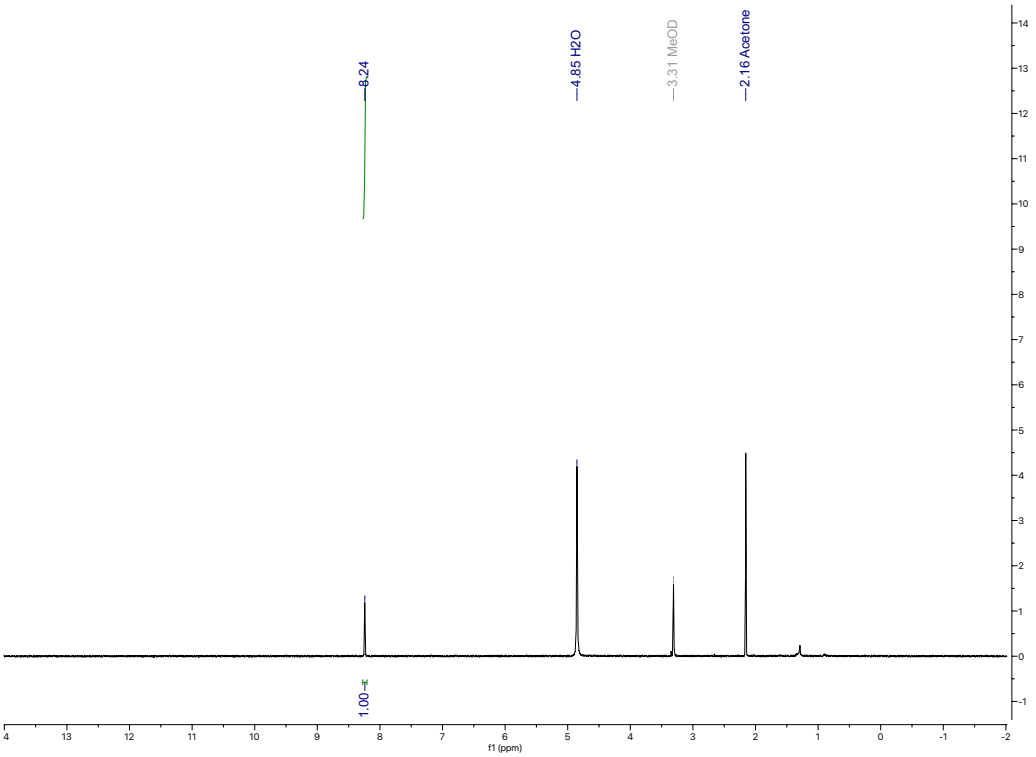


**Figure 2.5.63 400MHz $^{1}$HNMR of 2.11b**

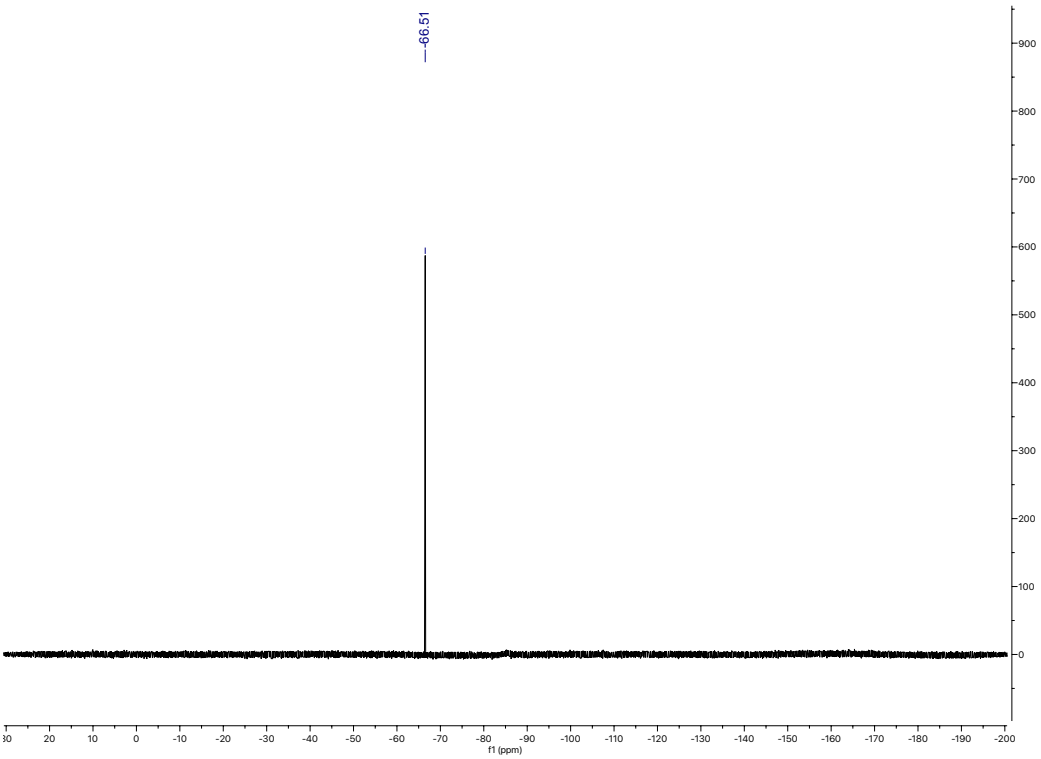


**Figure 2.5.64 376MHz $^{19}$FNMR of 2.11b**

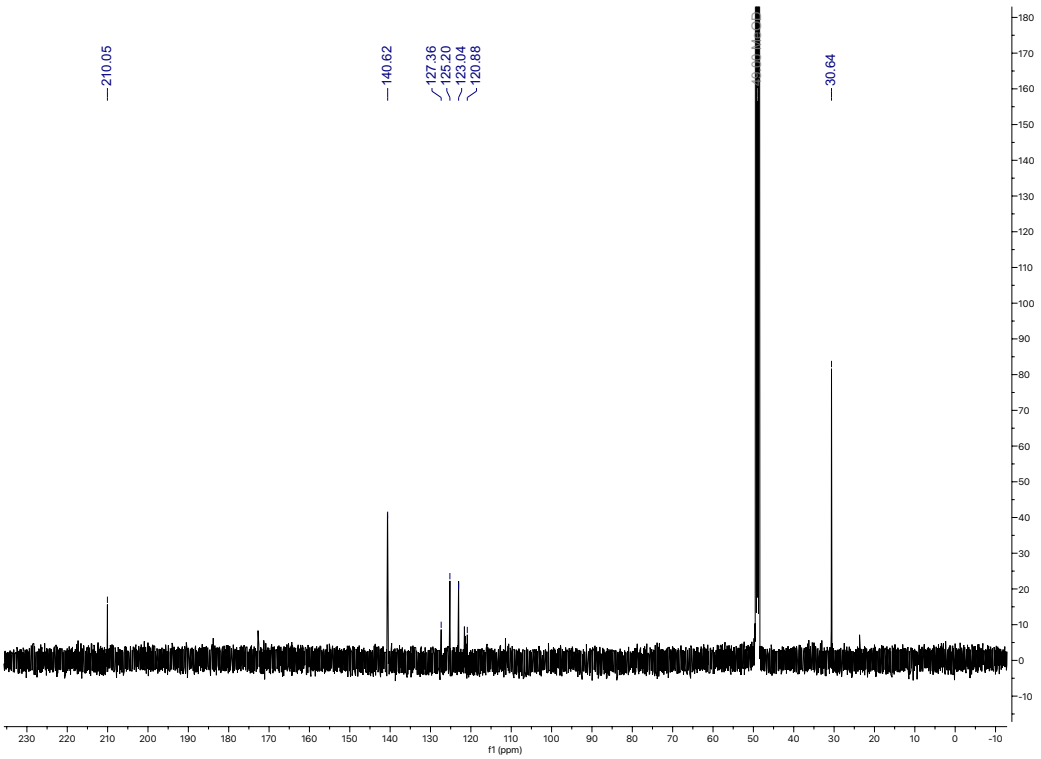


**Figure 2.5.65 126MHz $^{13}$CNMR of 2.11b**

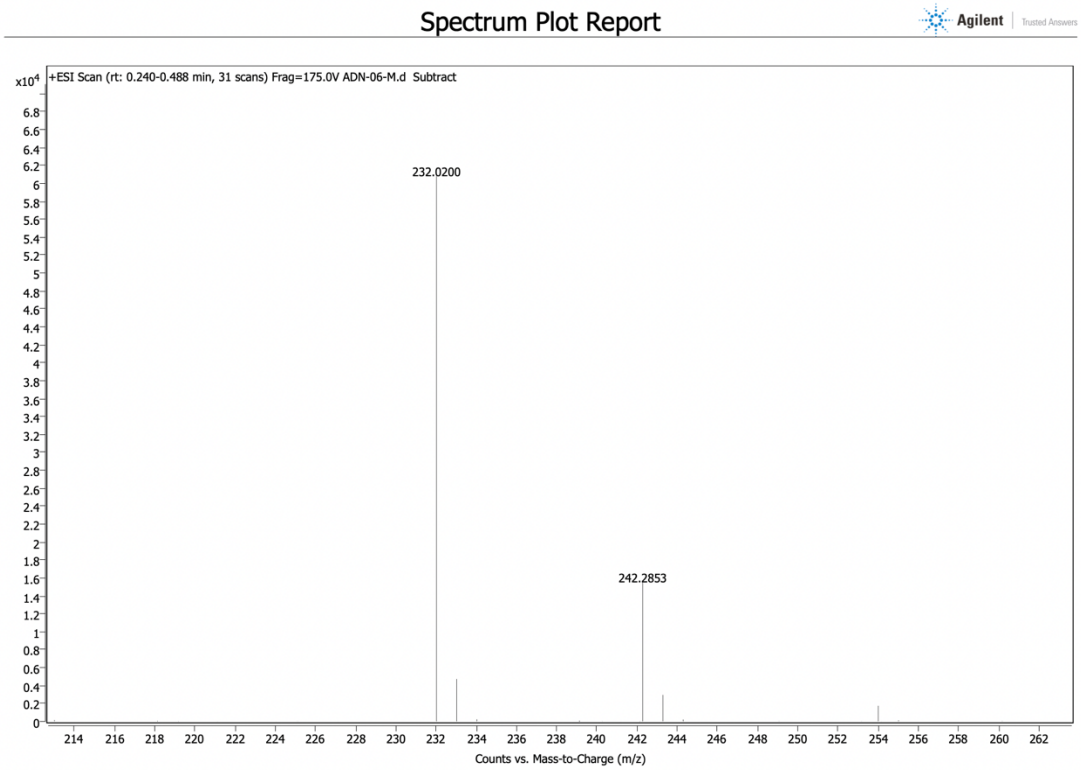


**Figure 2.5.66 HRMS (ESI) of 2.11b**

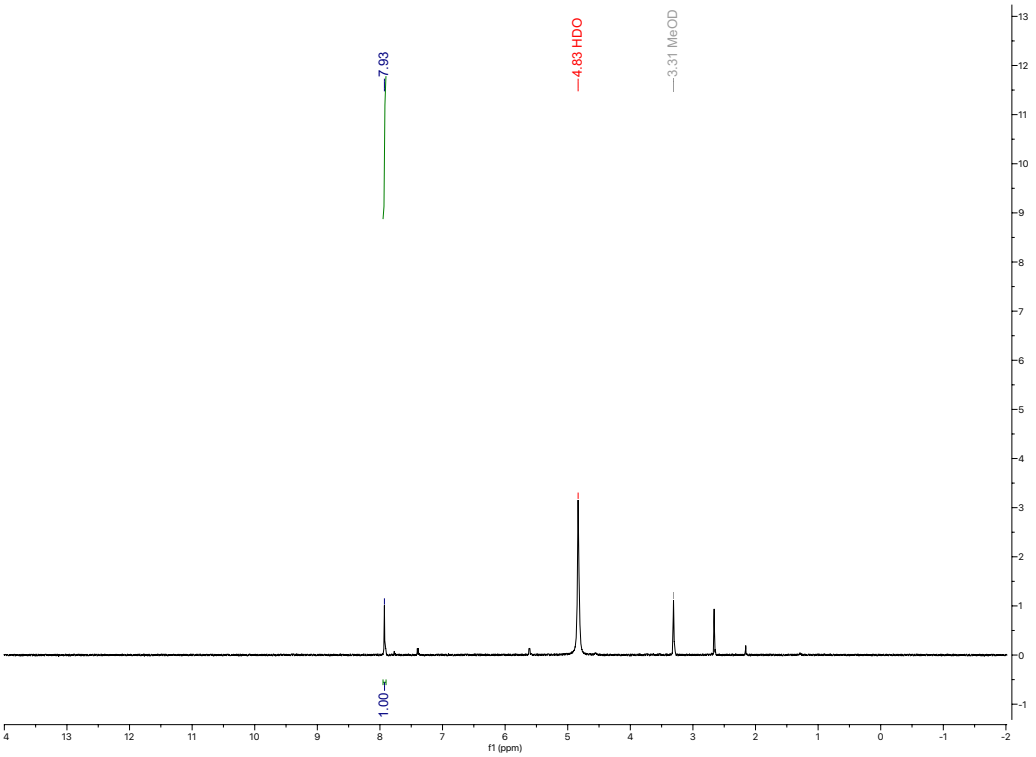


**Figure 2.5.67 400MHz $^{1}$HNMR of 2.12b**

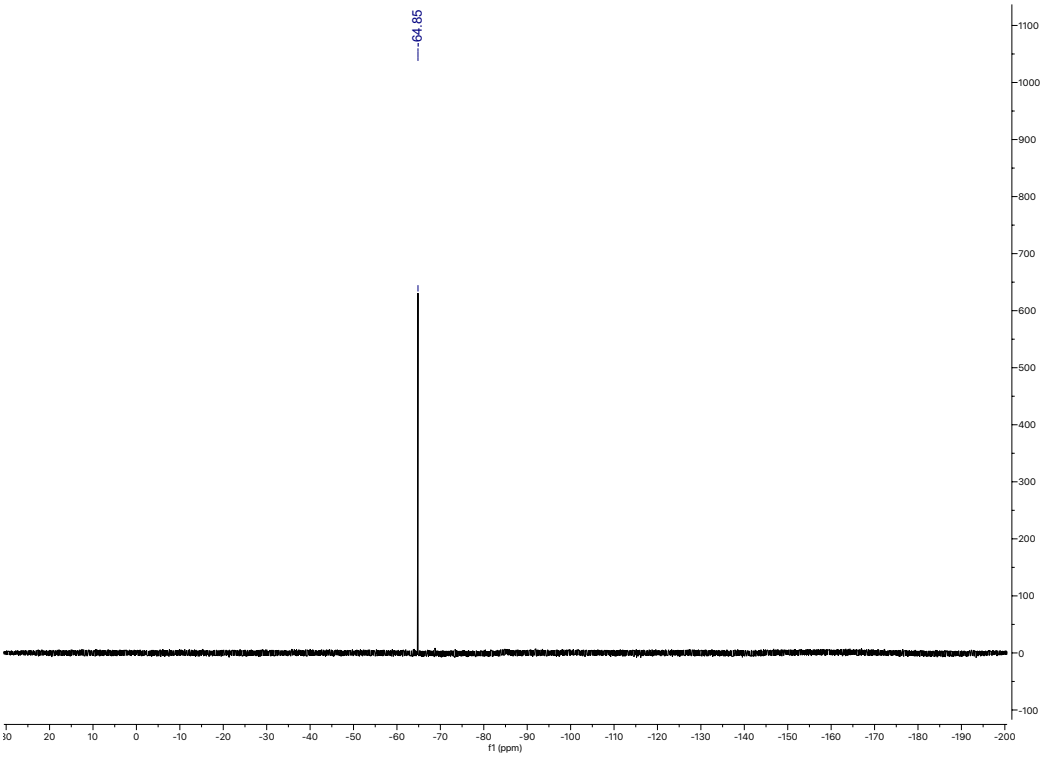


**Figure 2.5.68 376MHz $^{19}$FNMR of 2.12b**

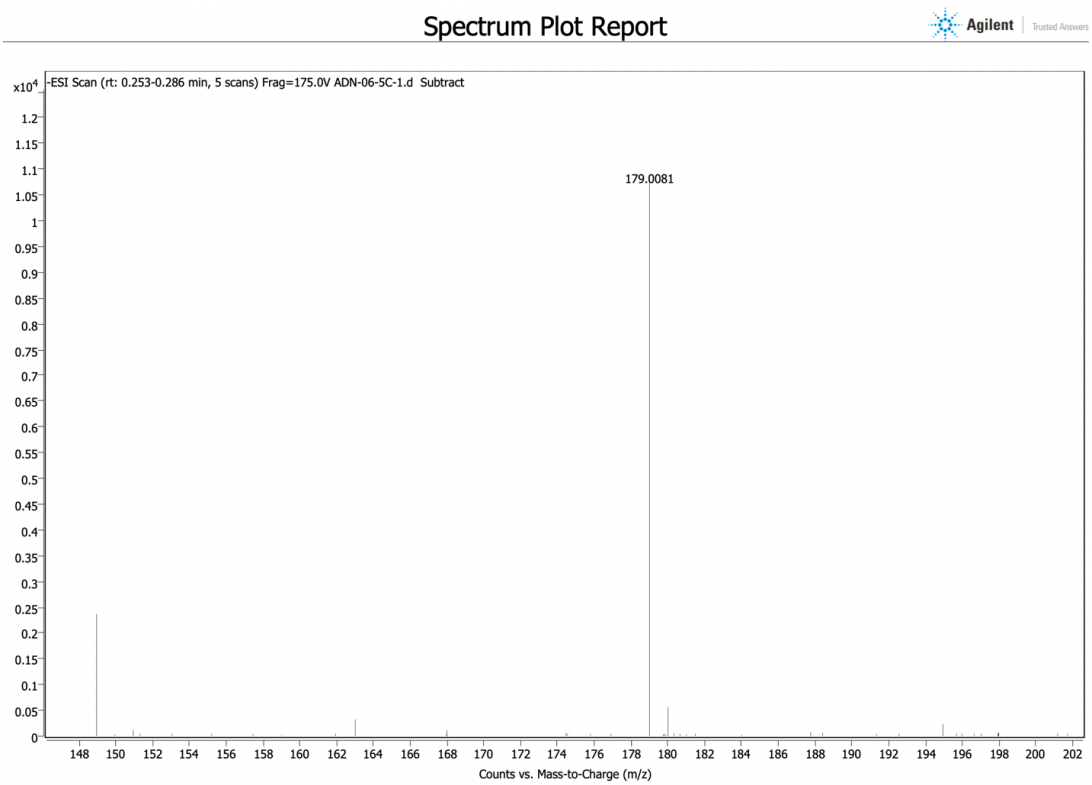


**Figure 2.5.69 HRMS (ESI) of 2.12b**

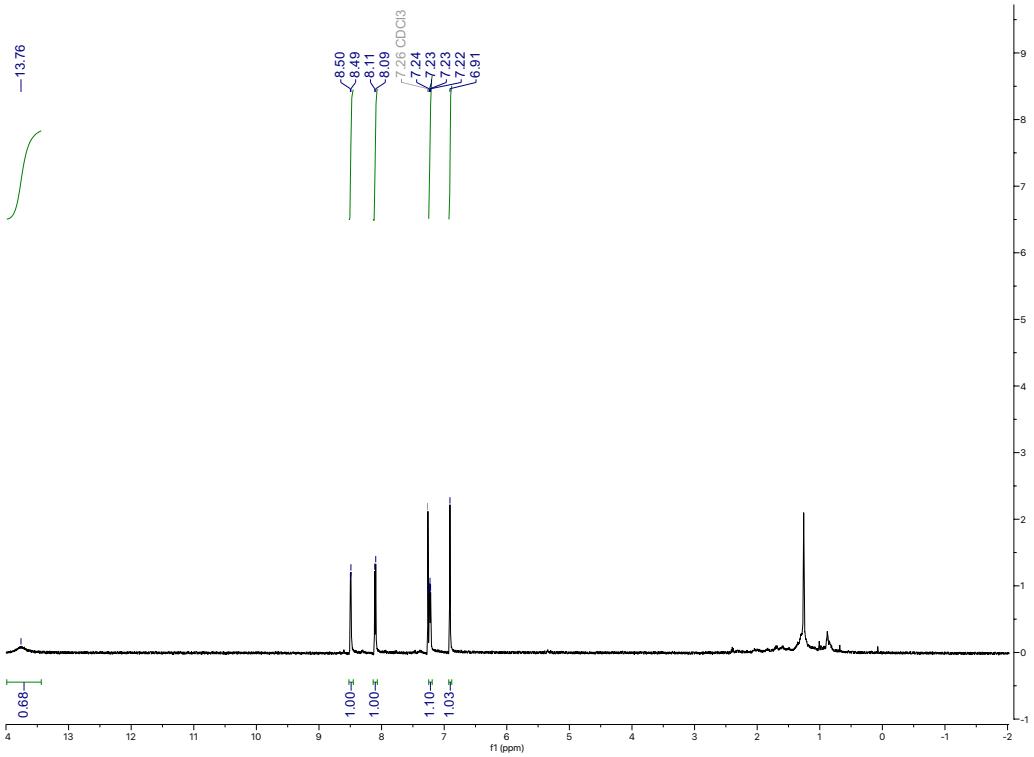


**Figure 2.5.70 400MHz $^{1}$HNMR of 2.13b**

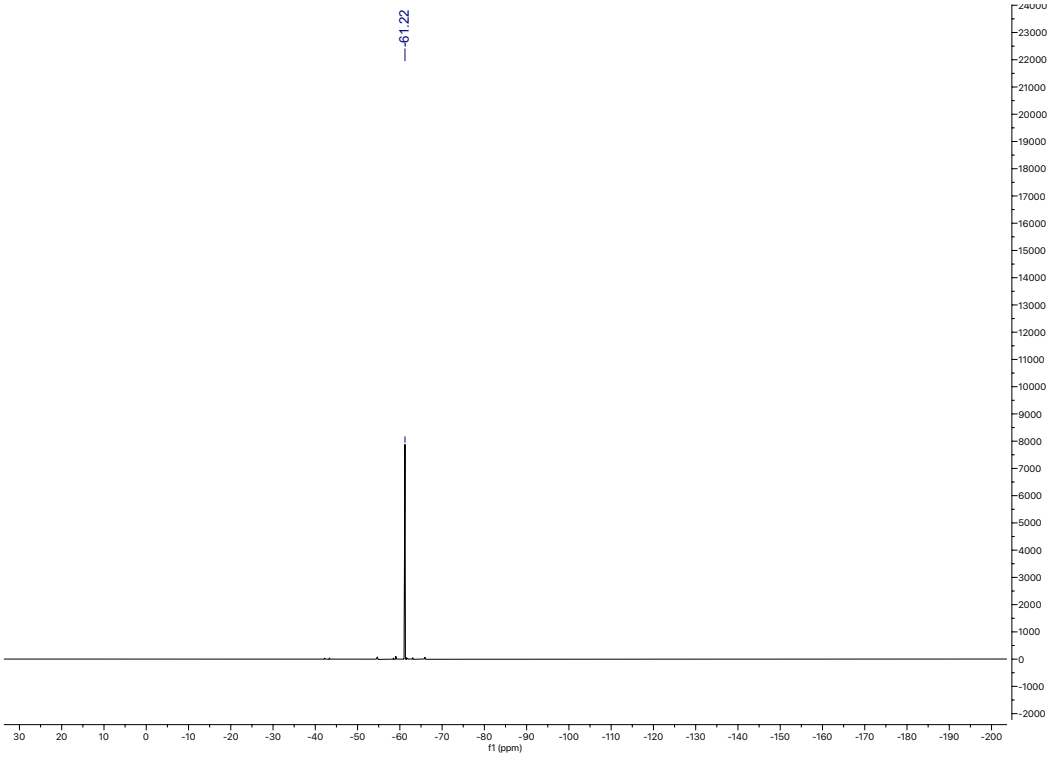


**Figure 2.5.71 400MHz $^{1}$HNMR of 2.13b**

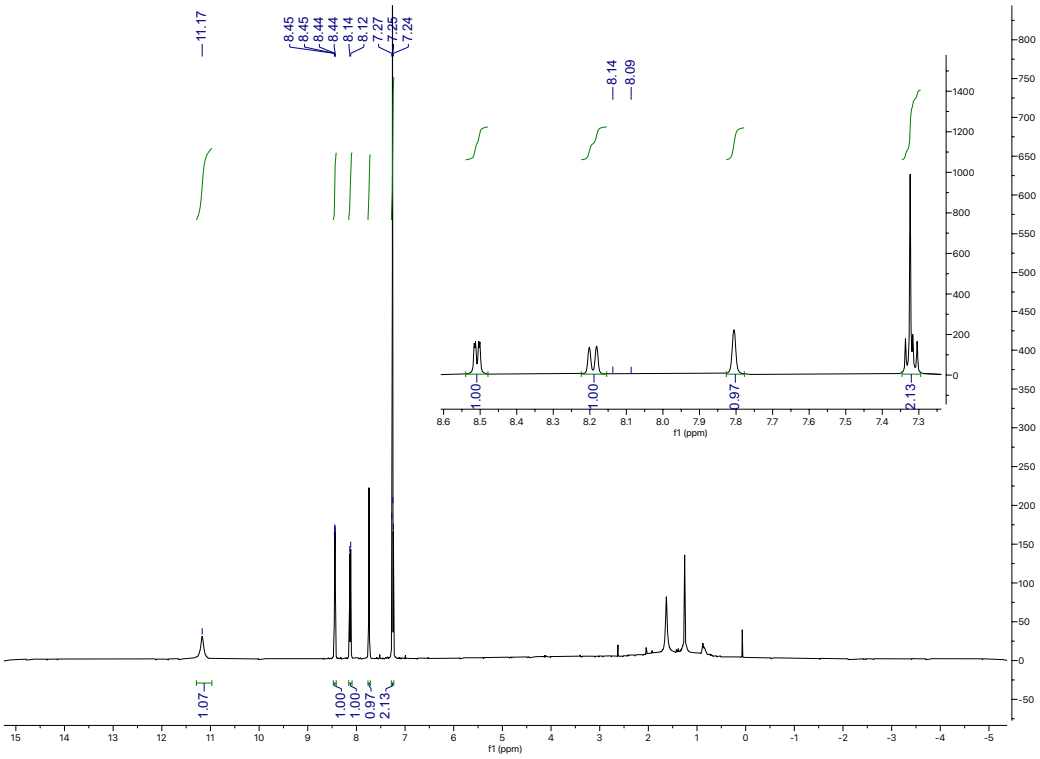


**Figure 2.5.72 400MHz $^{1}$HNMR of 2.14b**

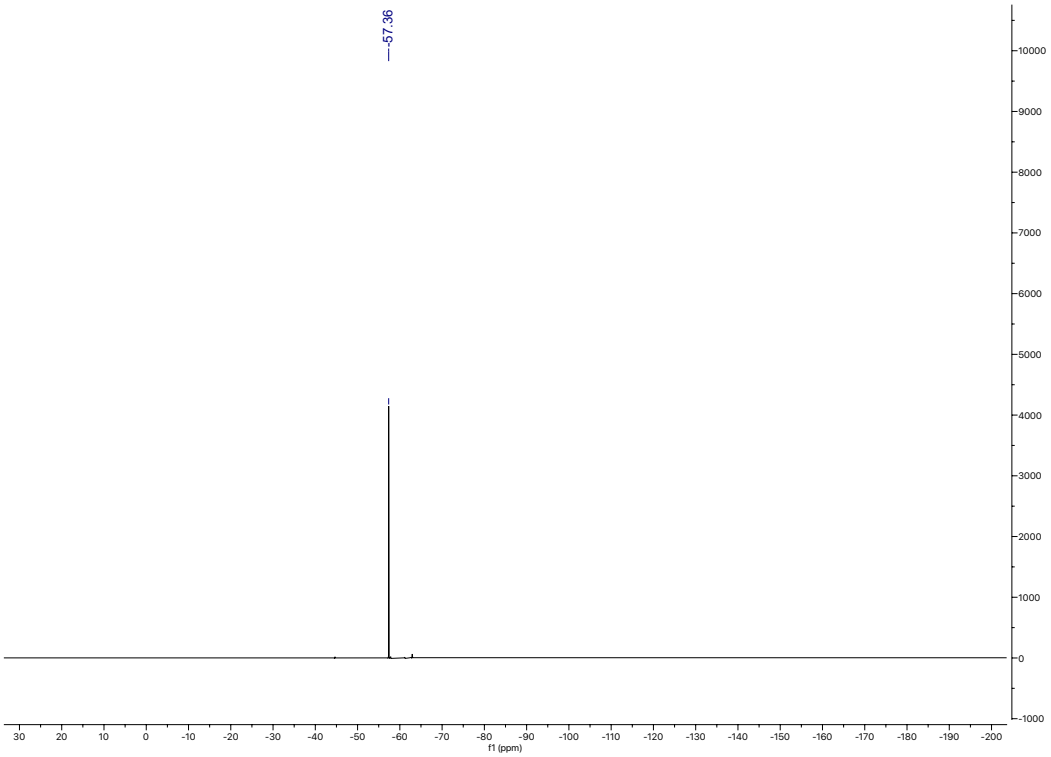


**Figure 2.5.73 376MHz $^{19}$FNMR of 2.14b**

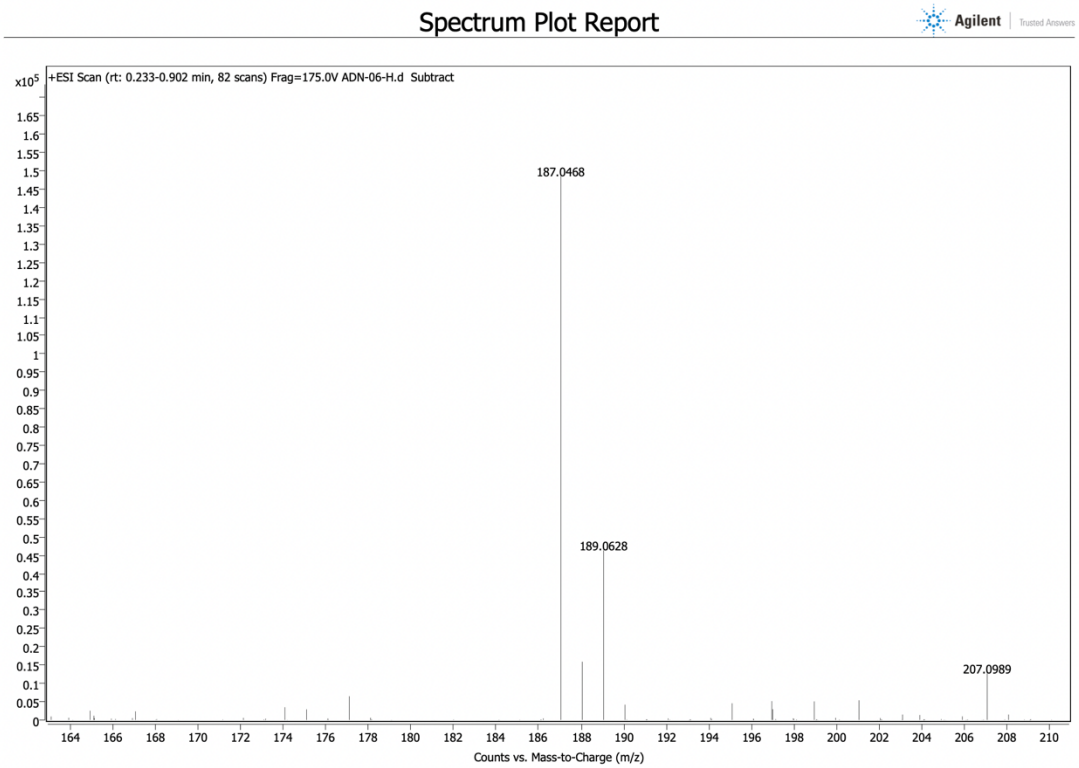


**Figure 2.5.74 HRMS (ESI) of 2.13b and 2.14b**

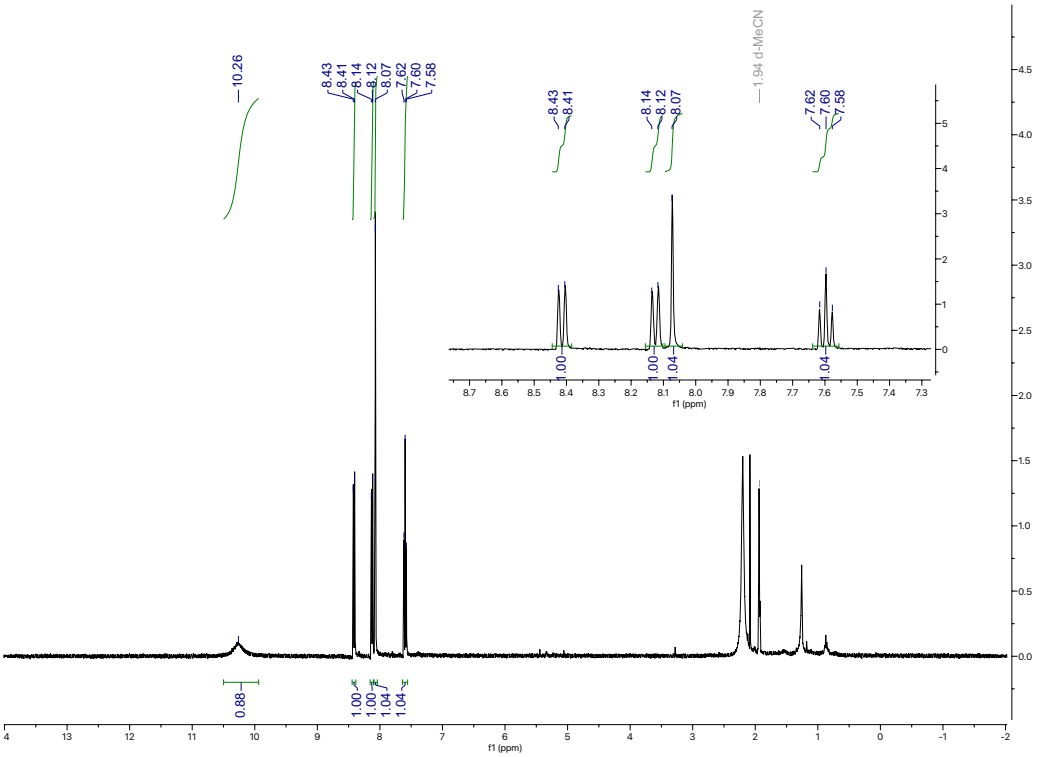


**Figure 2.5.75 400MHz $^{1}$HNMR of 2.15b**

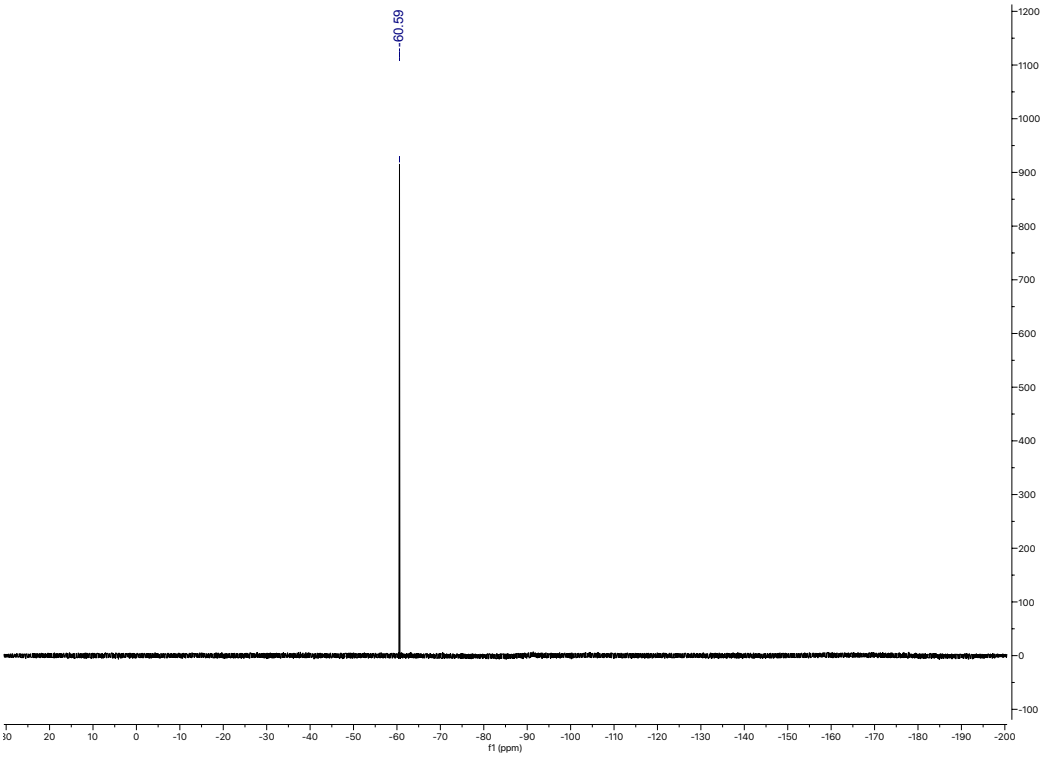


**Figure 2.5.76 376MHz $^{19}$FNMR of 2.15b**

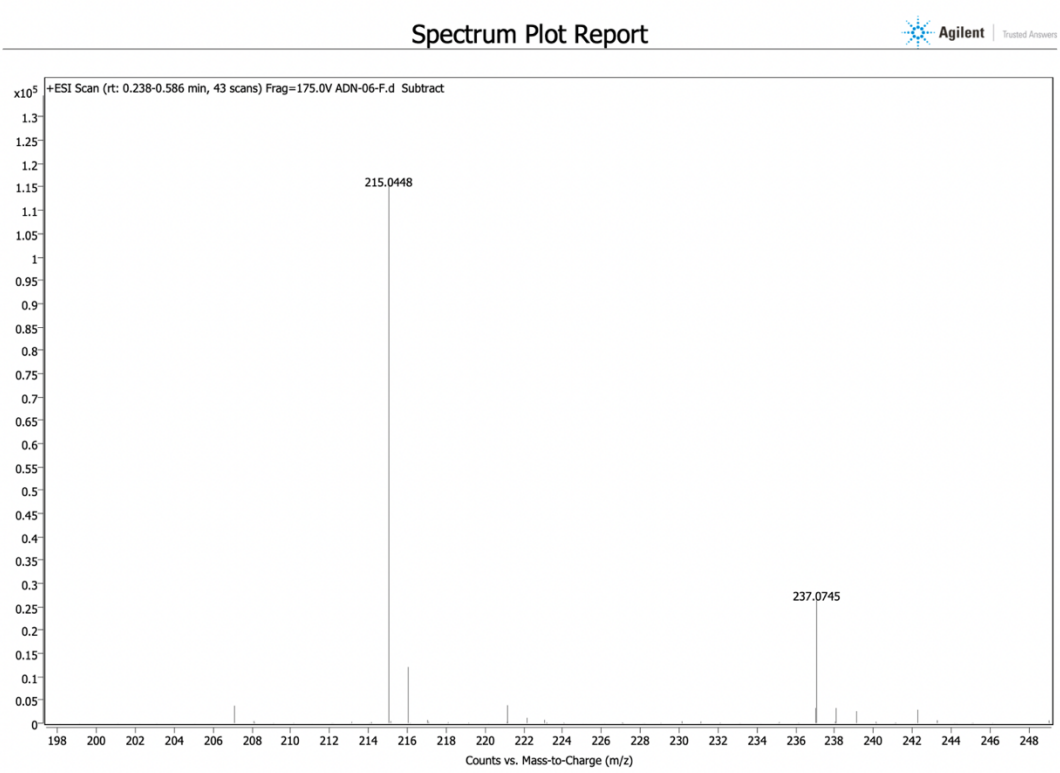


**Figure 2.5.77 HRMS (ESI) of 2.15b**

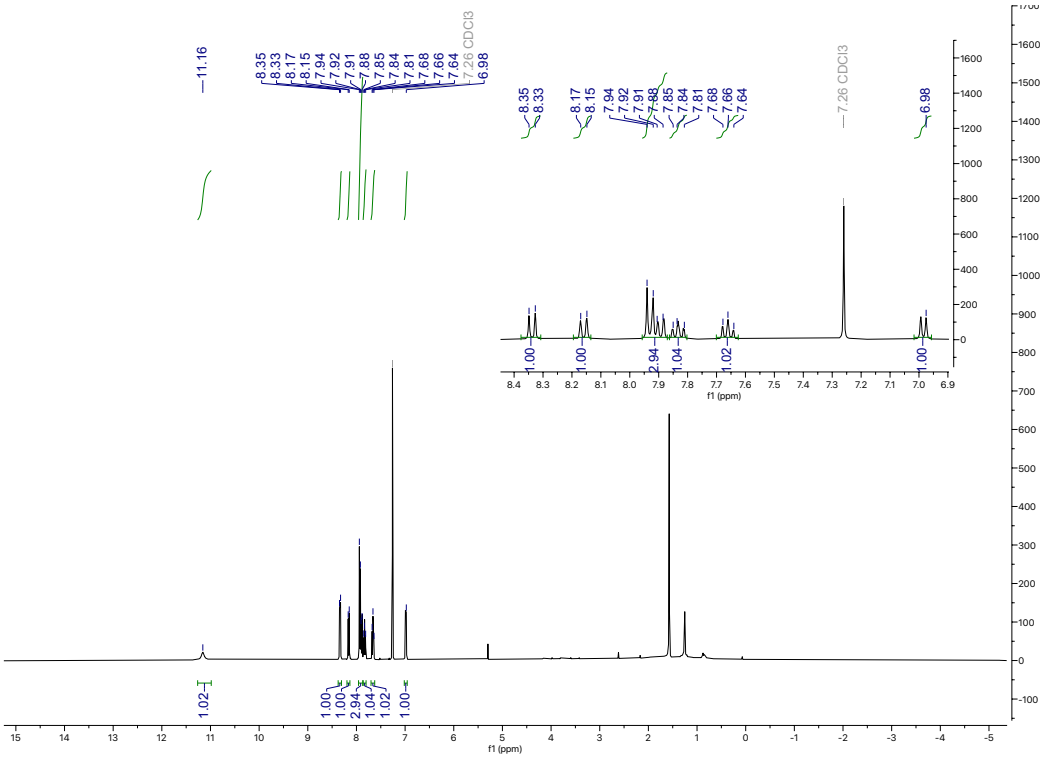


**Figure 2.5.78 400MHz $^{1}$HNMR of 2.16b**

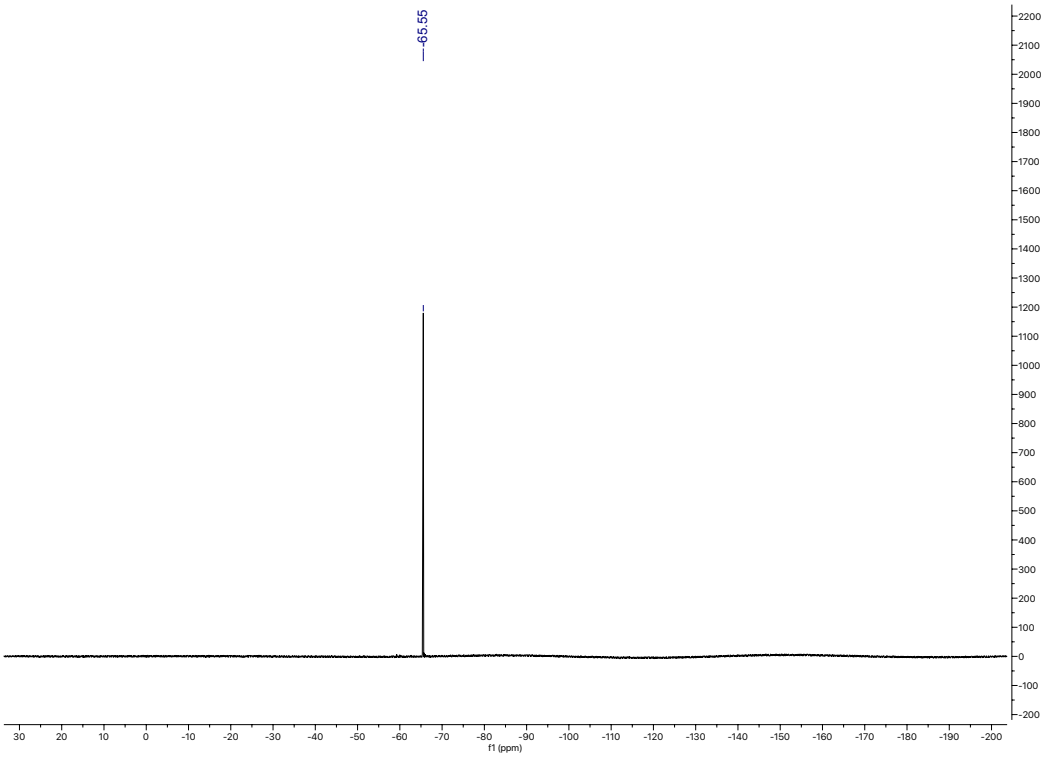


**Figure 2.5.79 376MHz $^{19}$FNMR of 2.16b**

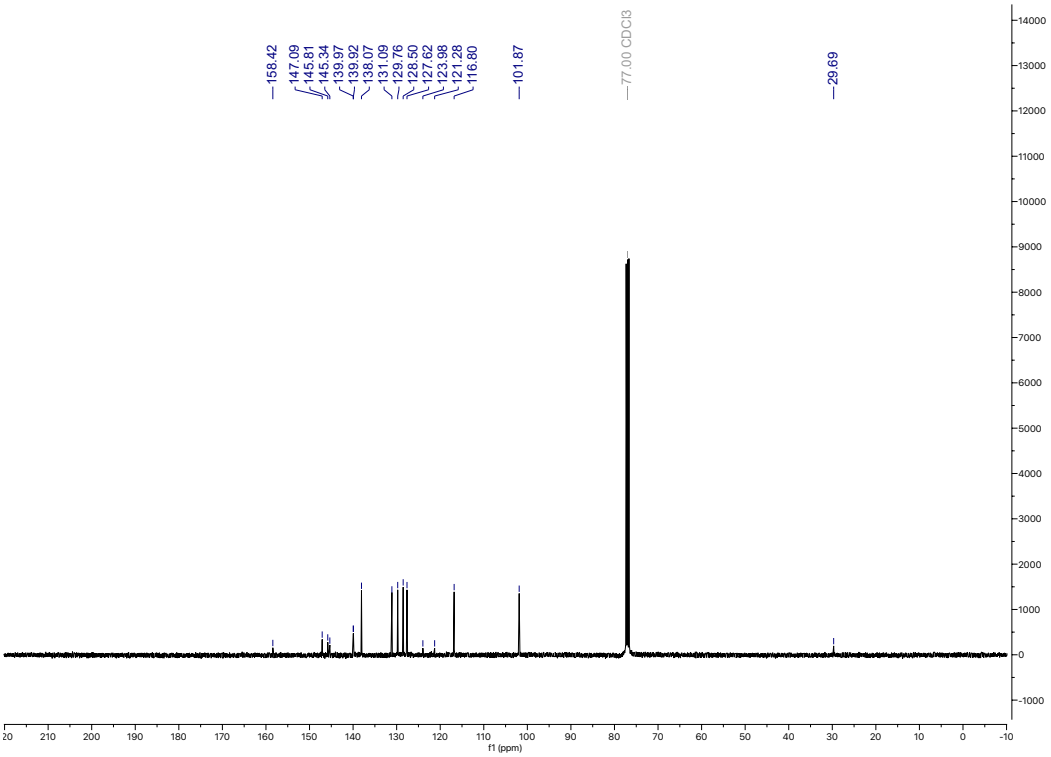


**Figure 2.5.80 126MHz $^{13}$CNMR of 2.16b**

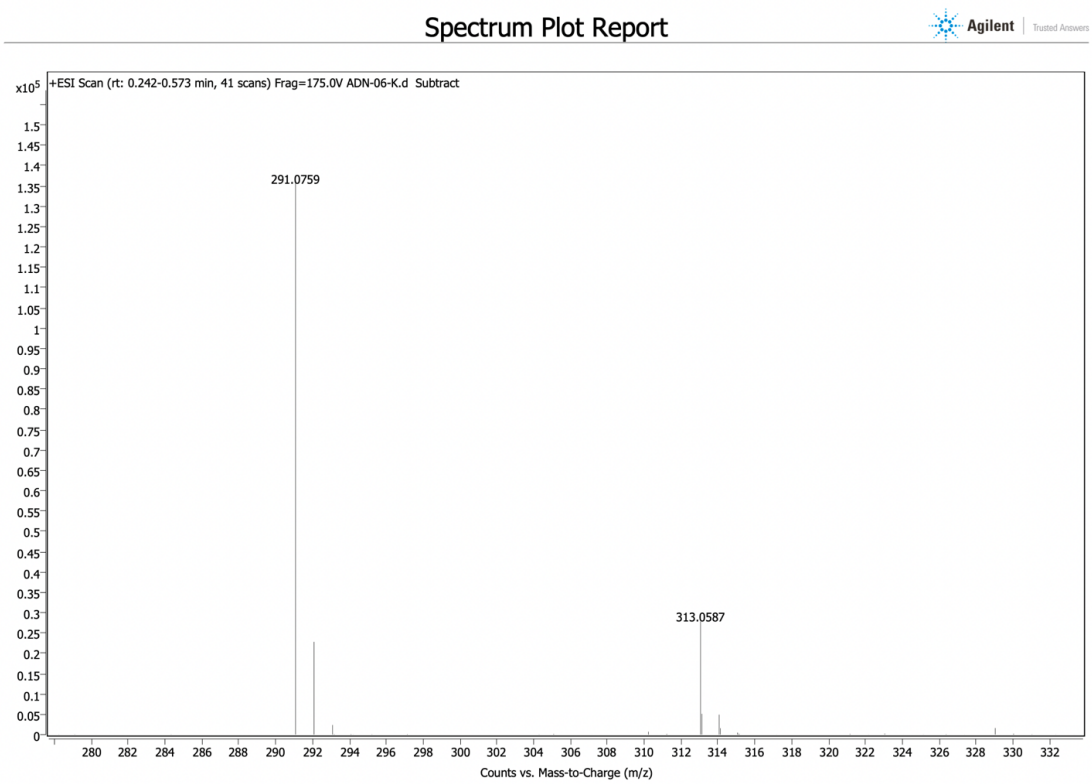


**Figure 2.5.81 HRMS (ESI) of 2.16b**

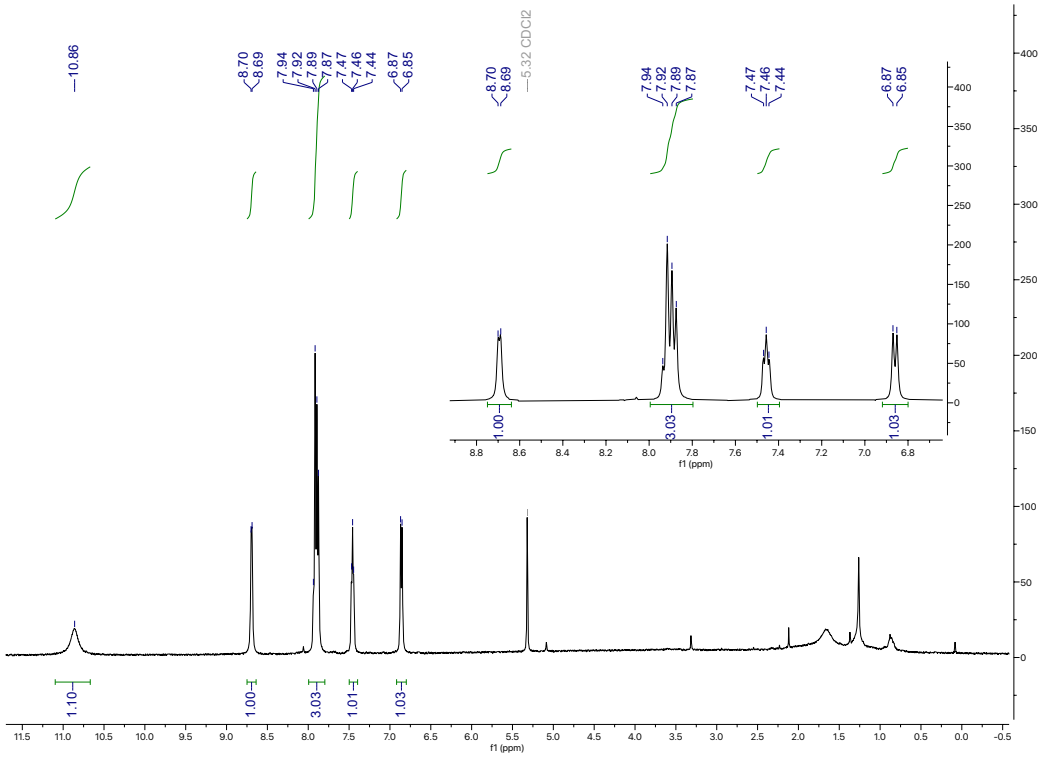


**Figure 2.5.82 400MHz $^{1}$HNMR of 2.17b**

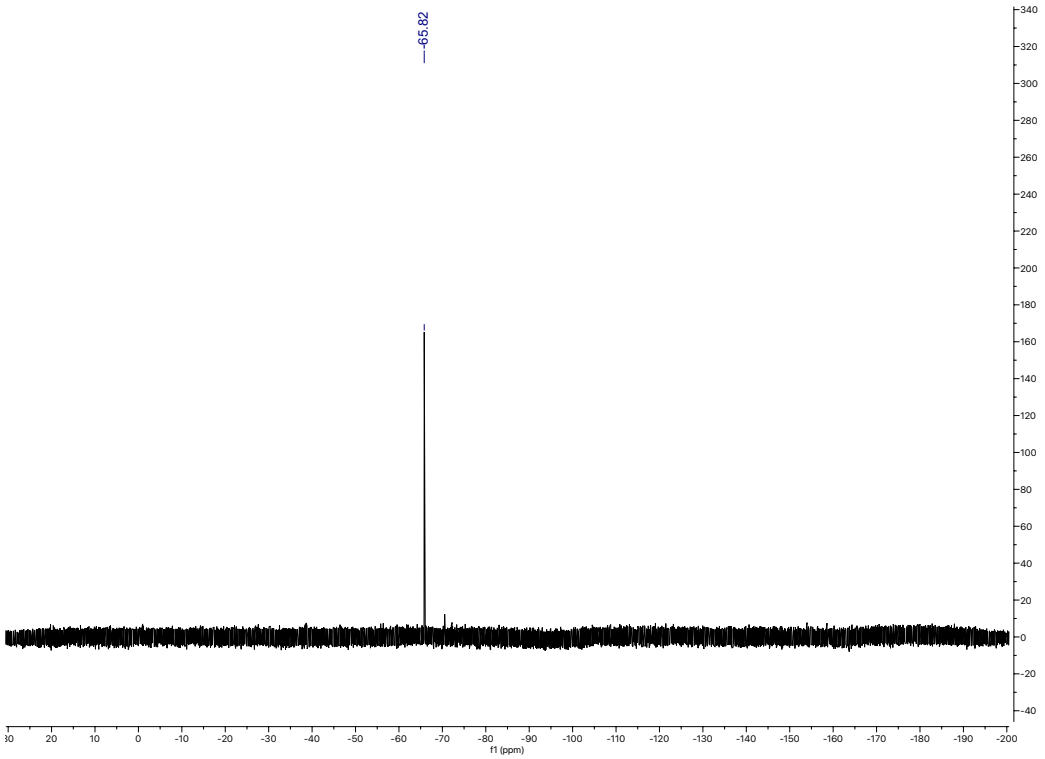


**Figure 2.5.83 376MHz $^{19}$FNMR of 2.17b**

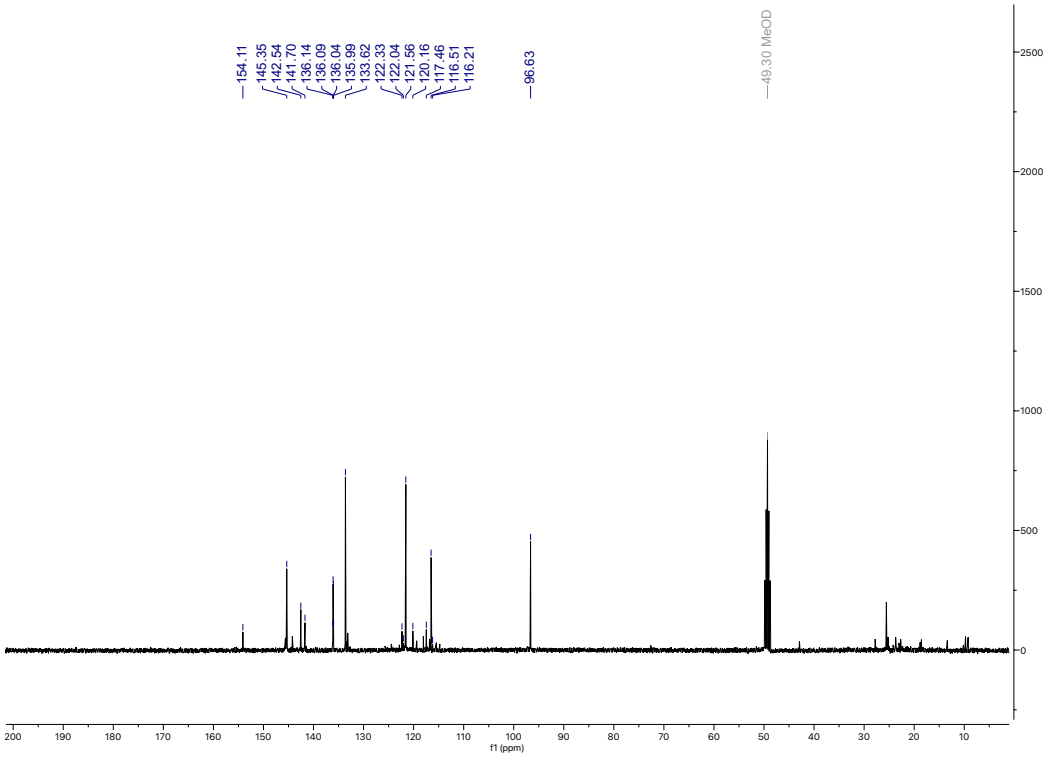


**Figure 2.5.84 126MHz $^{13}$CNMR of 2.17b**

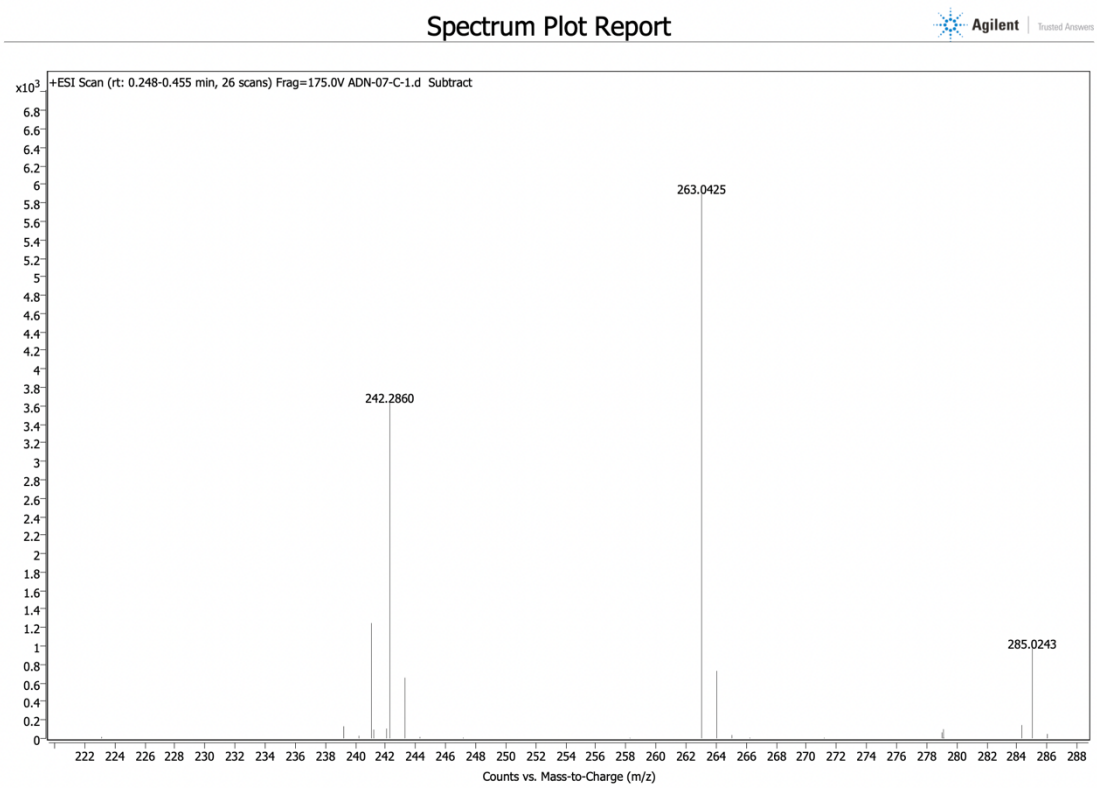


**Figure 2.5.85 HRMS (ESI) of 2.17b**

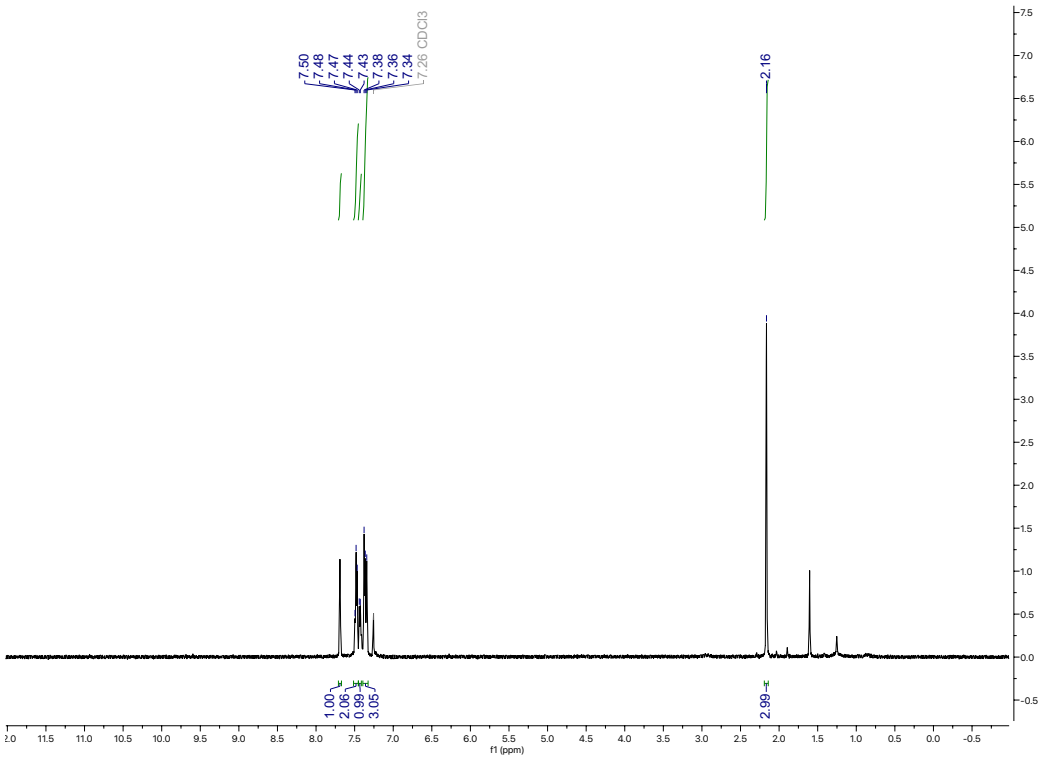


**Figure 2.5.86 400MHz $^{1}$HNMR of 2.18b**

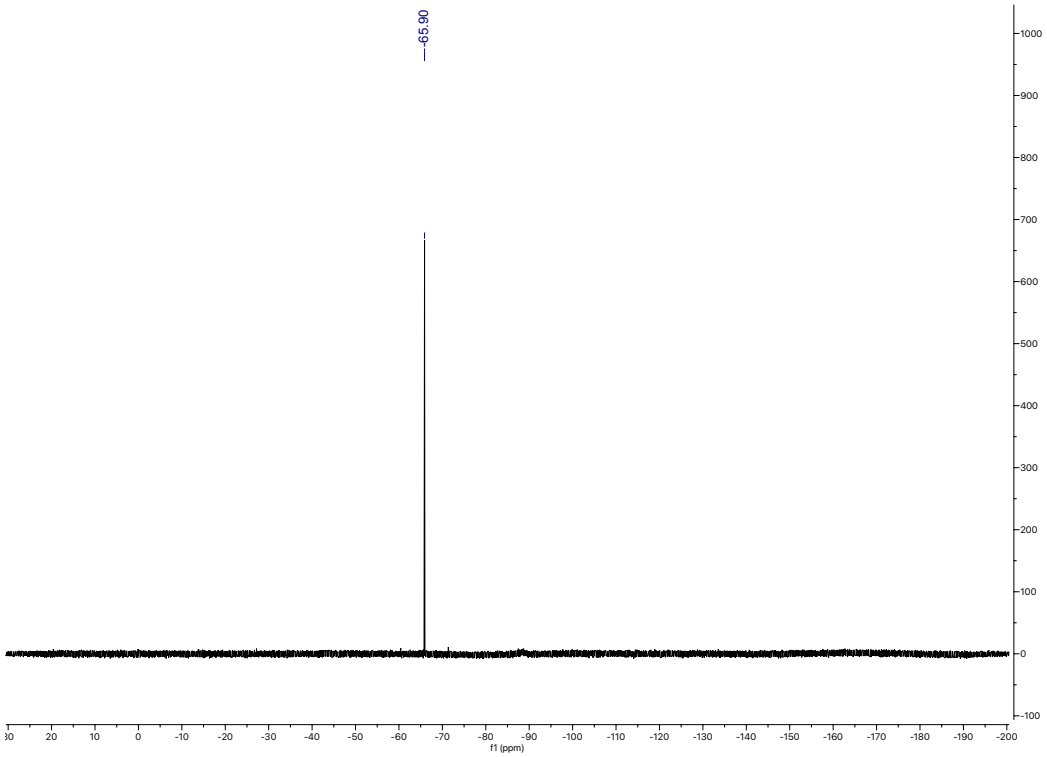


**Figure 2.5.87 376MHz $^{19}$FNMR of 2.18b**

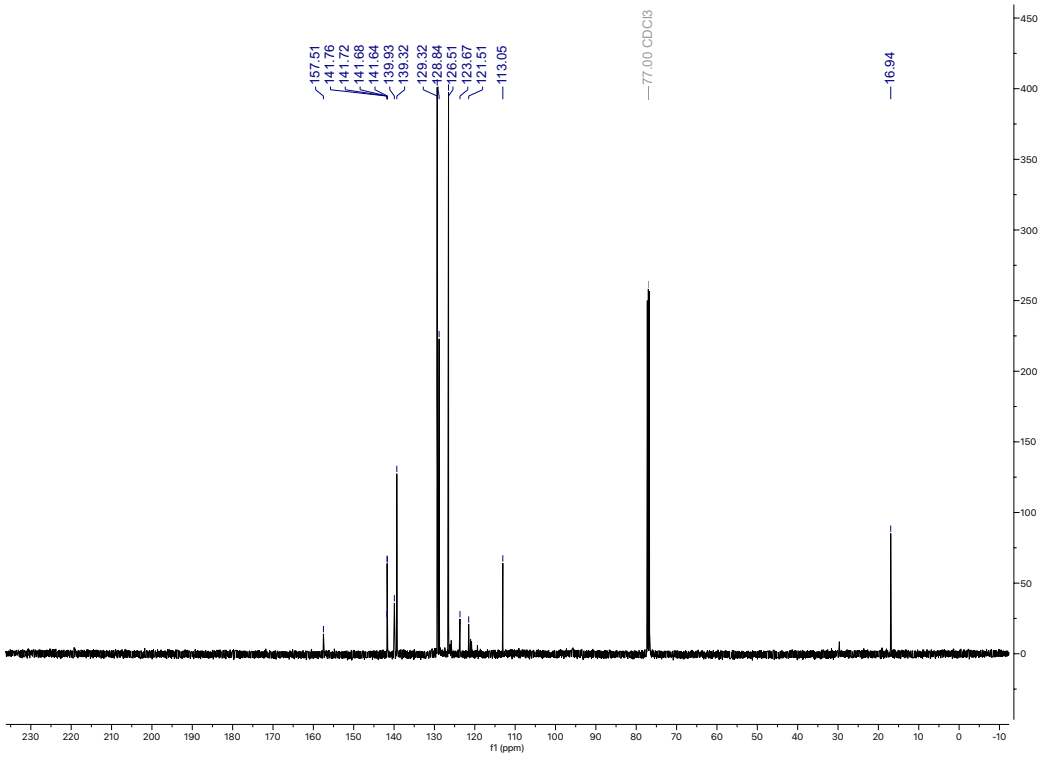


**Figure 2.5.88 126MHz $^{13}$CNMR of 2.18b**

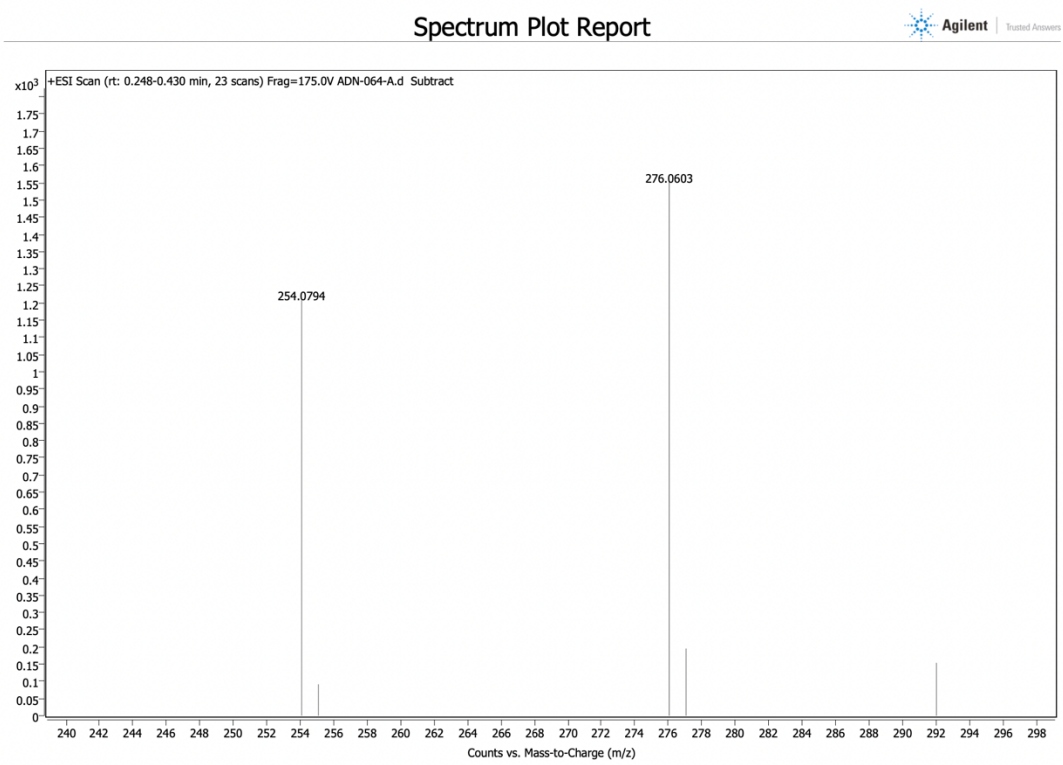


**Figure 2.5.89 HRMS (ESI) of 2.18b**

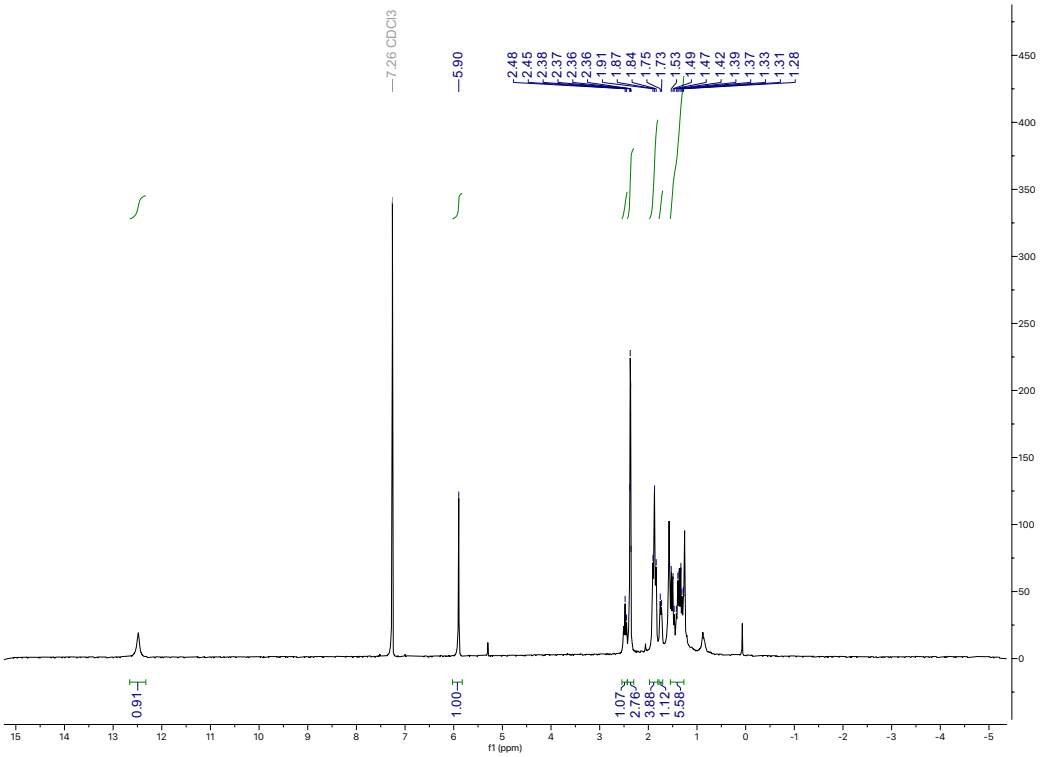


**Figure 2.5.90 400MHz $^{1}$HNMR of 2.19b**

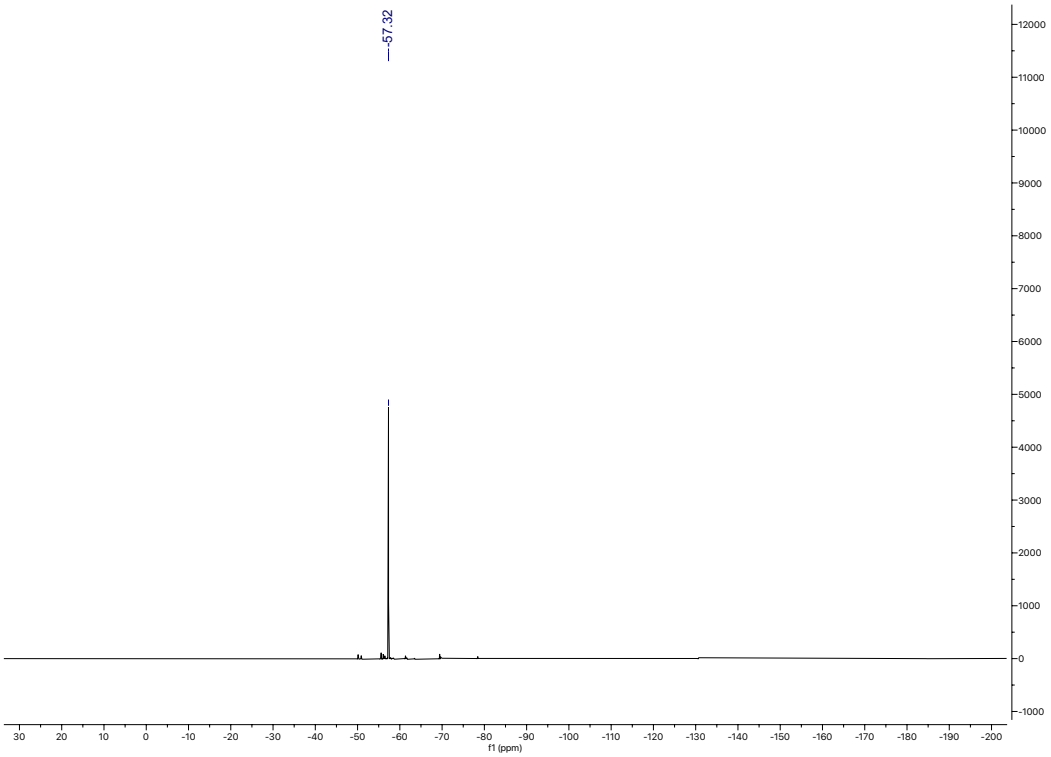


**Figure 2.5.91 376MHz $^{19}$FNMR of 2.19b**

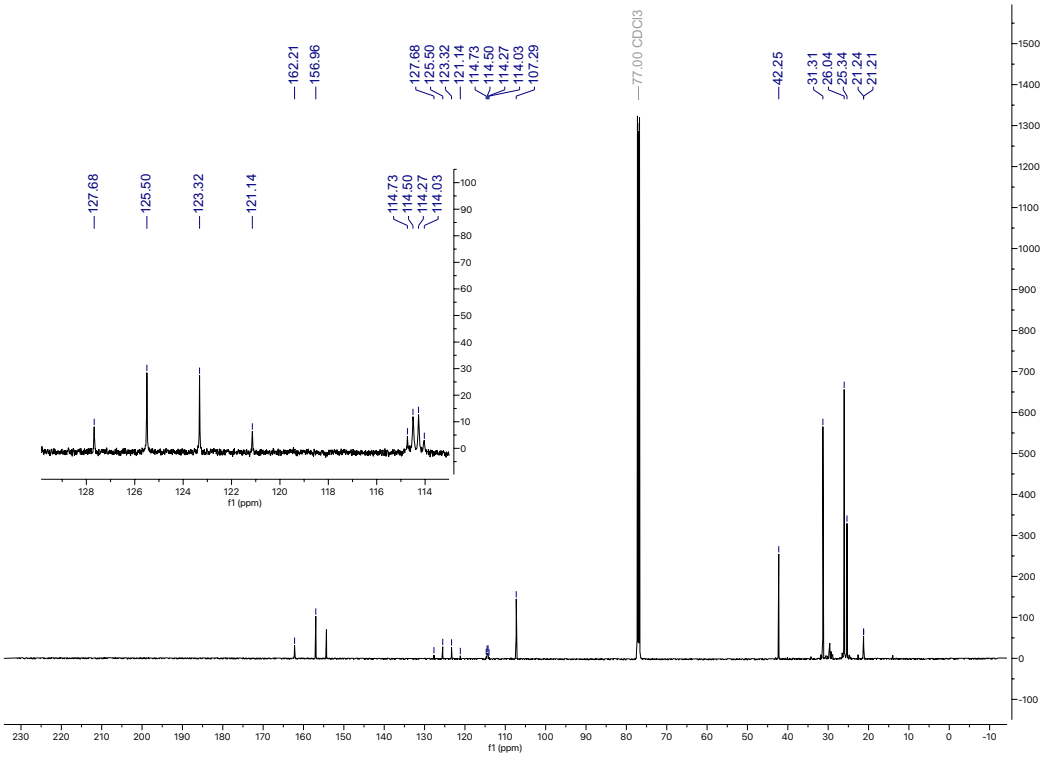


**Figure 2.5.92 126MHz $^{13}$CNMR of 2.19b**

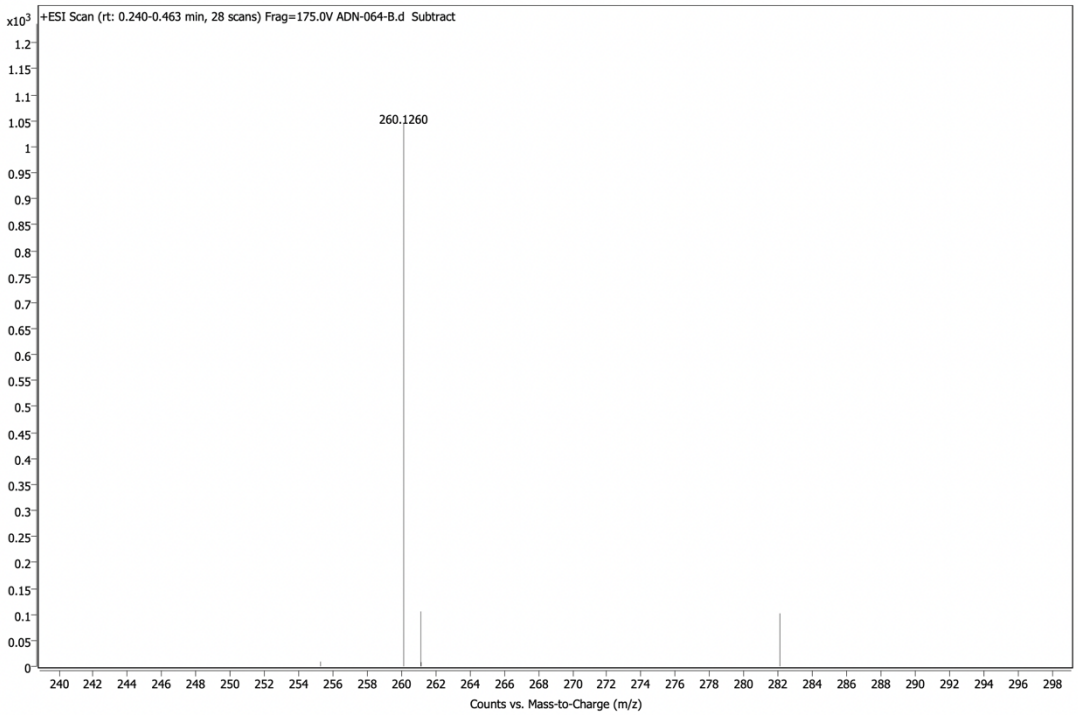


**Figure 2.5.93 HRMS (ESI) of 2.19b**

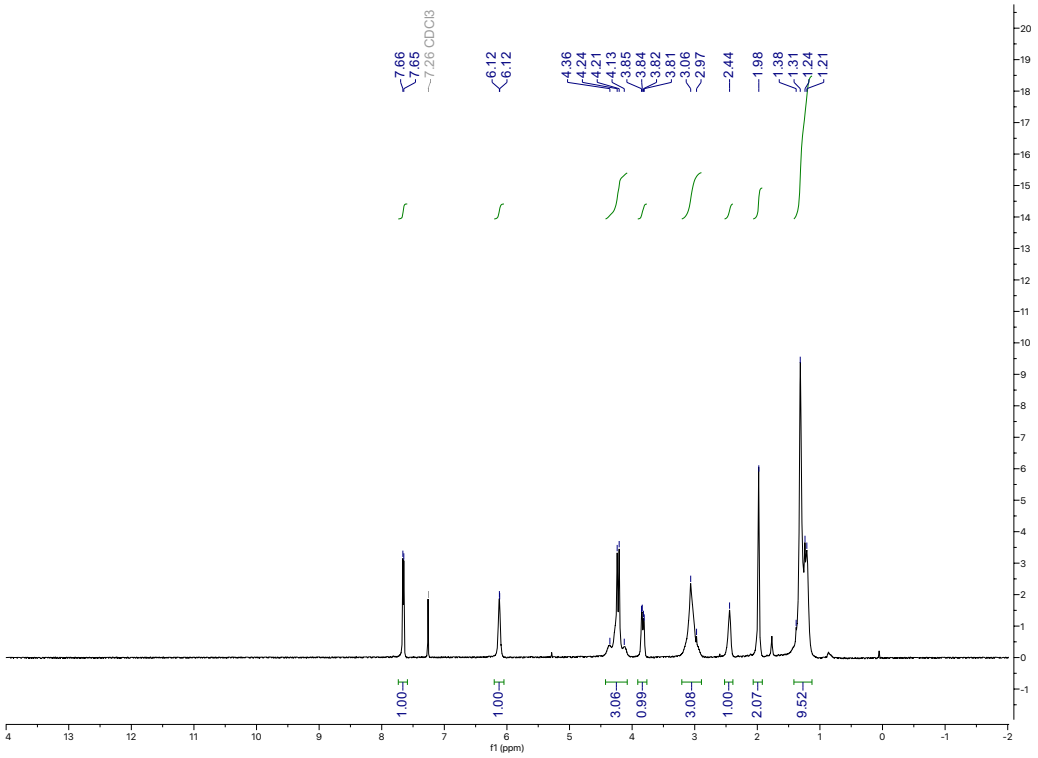


**Figure 2.5.94 400MHz $^{1}$HNMR of 2.20b**

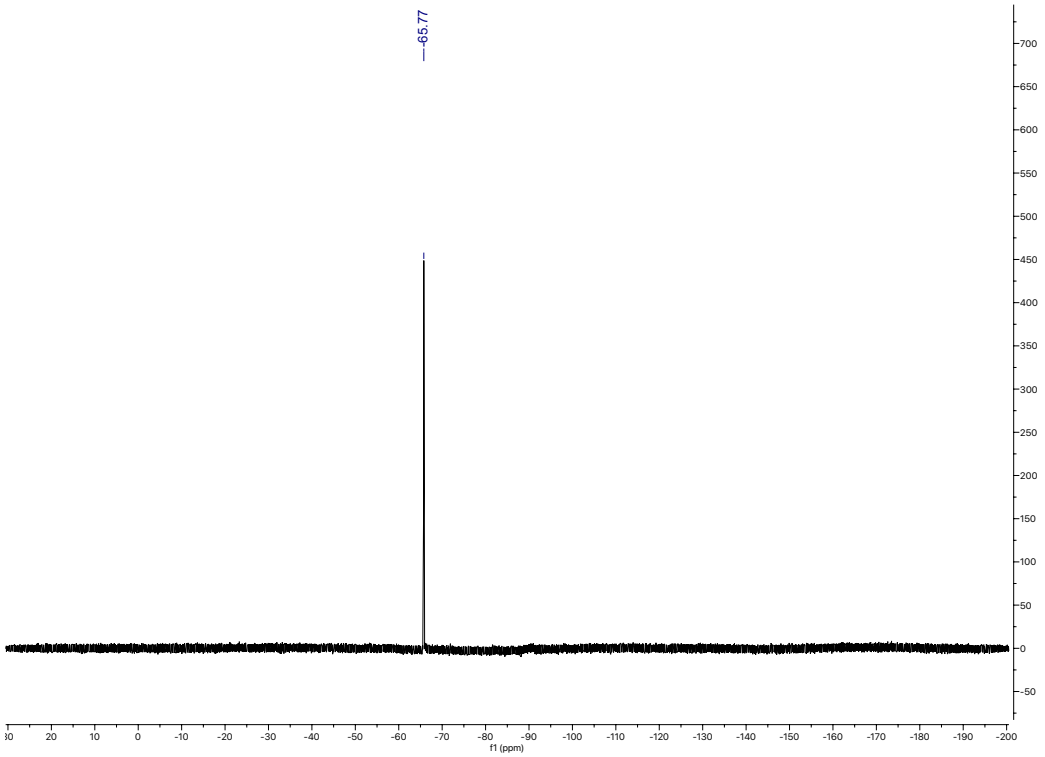


**Figure 2.5.95 376MHz $^{19}$FNMR of 2.20b**

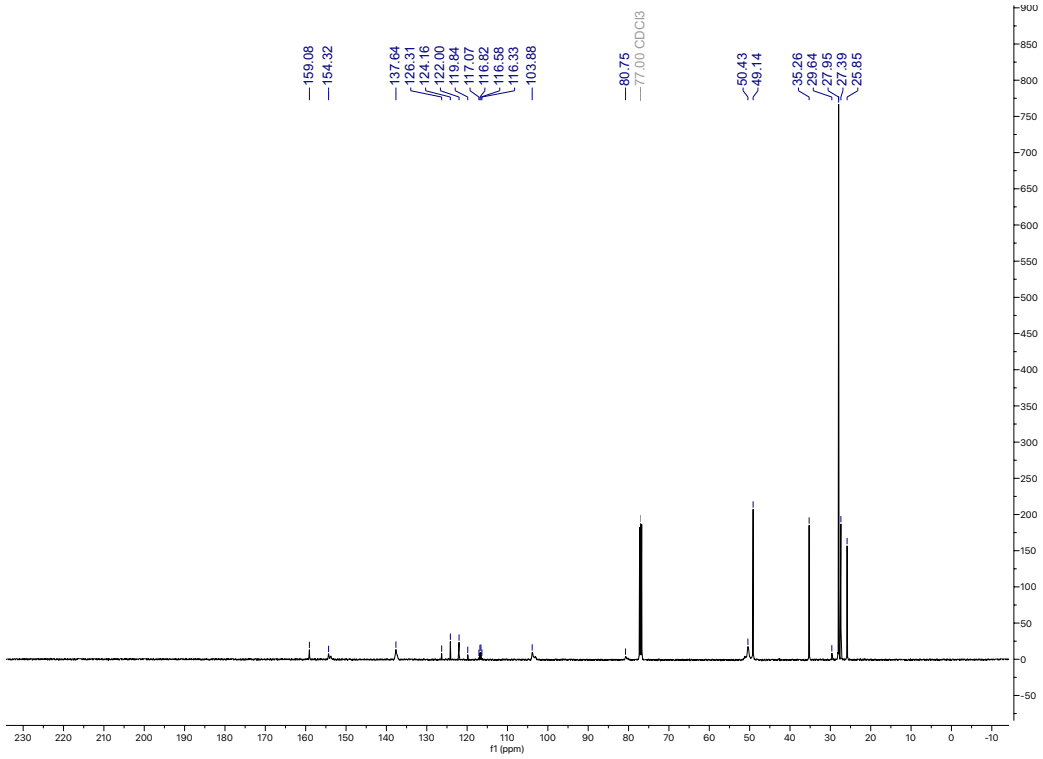


**Figure 2.5.96 126MHz $^{13}$CNMR of 2.20b**

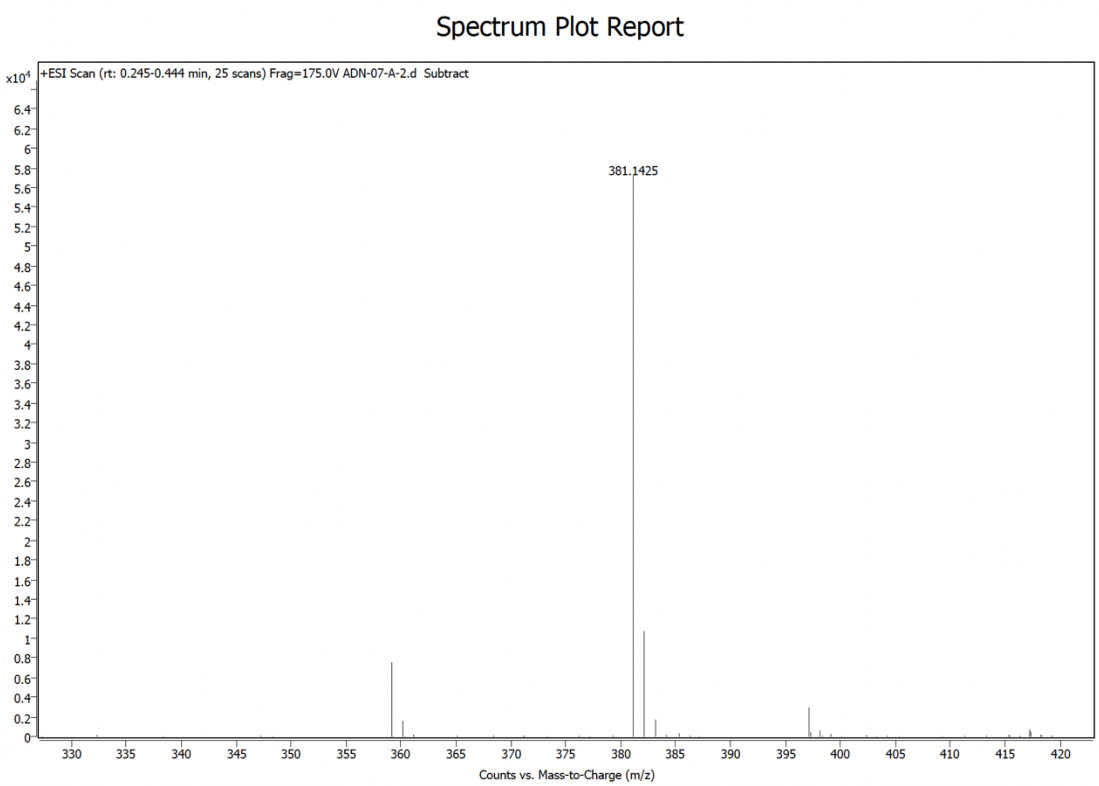


**Figure 2.5.97 HRMS (ESI) of 2.20b**

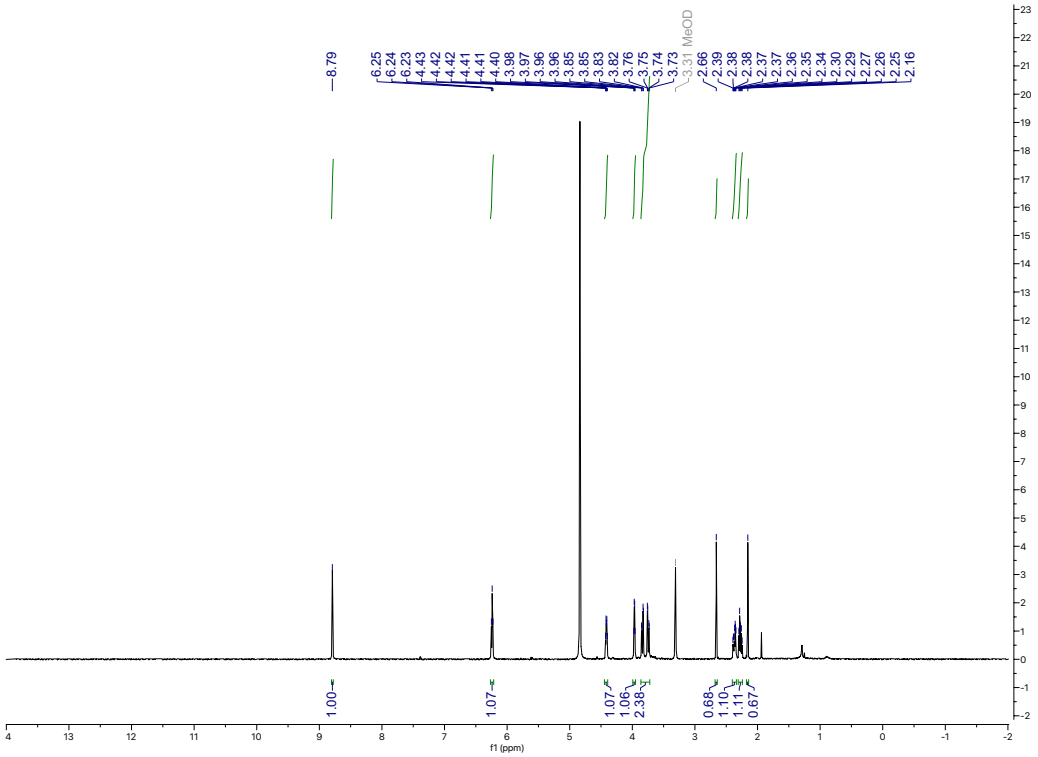


**Figure 2.5.98 400MHz $^{1}$HNMR of 2.21b**

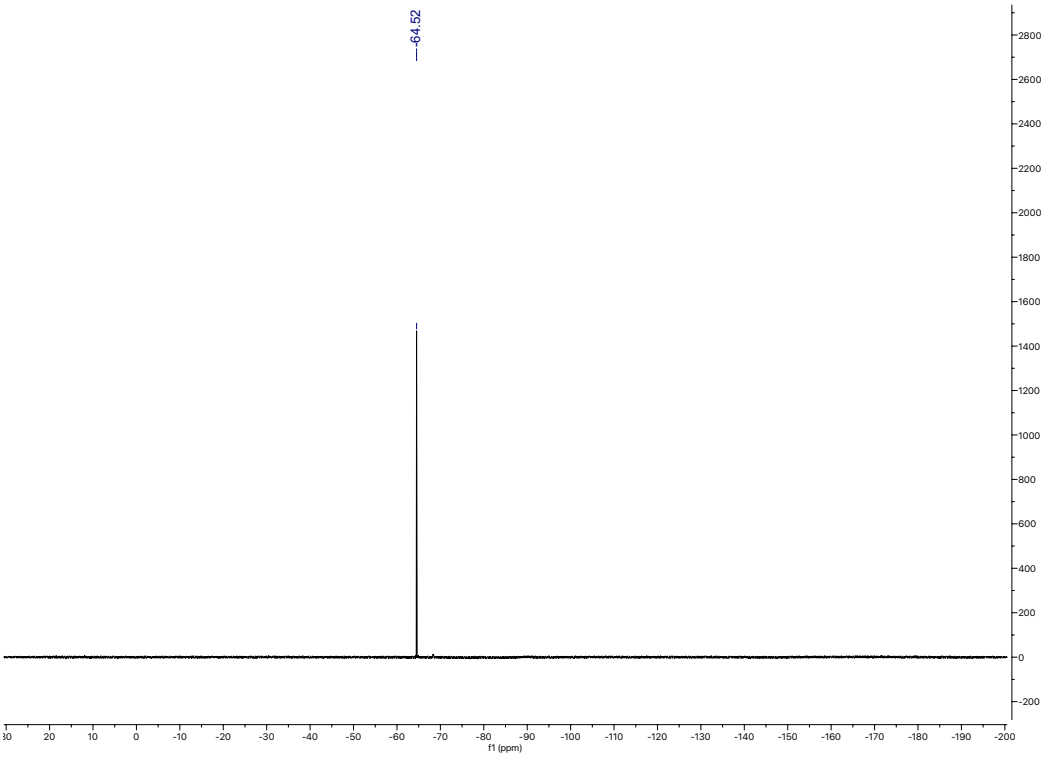


**Figure 2.5.99 376MHz $^{19}$FNMR of 2.21b**

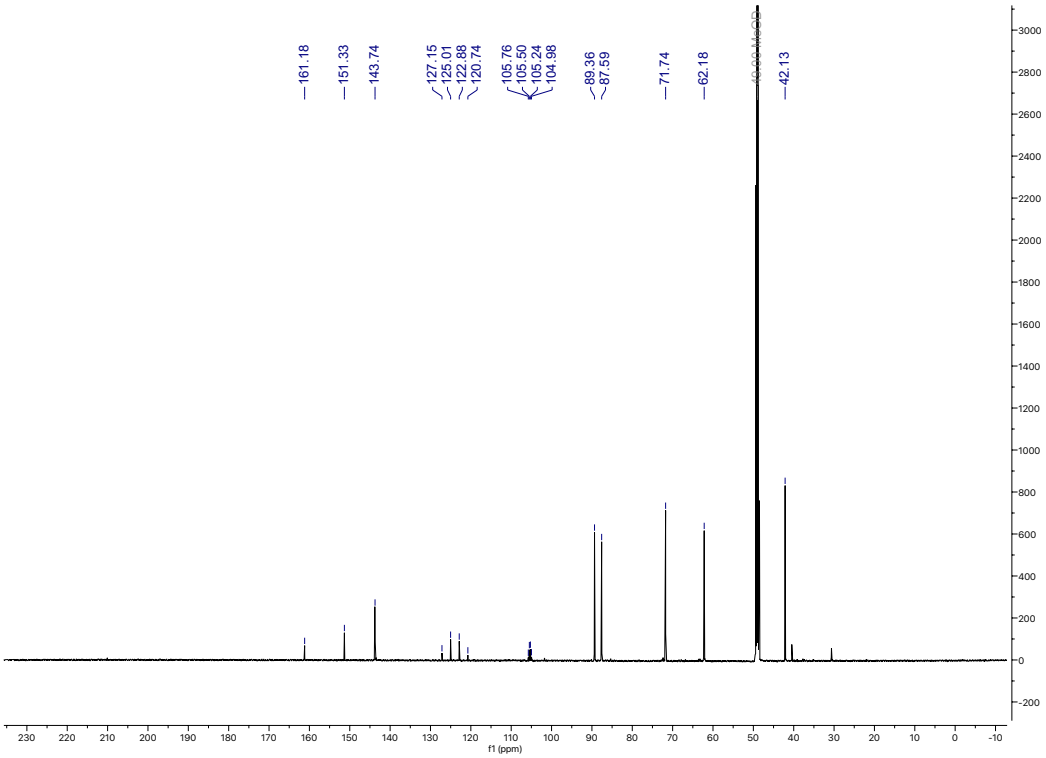


**Figure 2.5.100 126MHz $^{13}$CNMR of 2.21b**

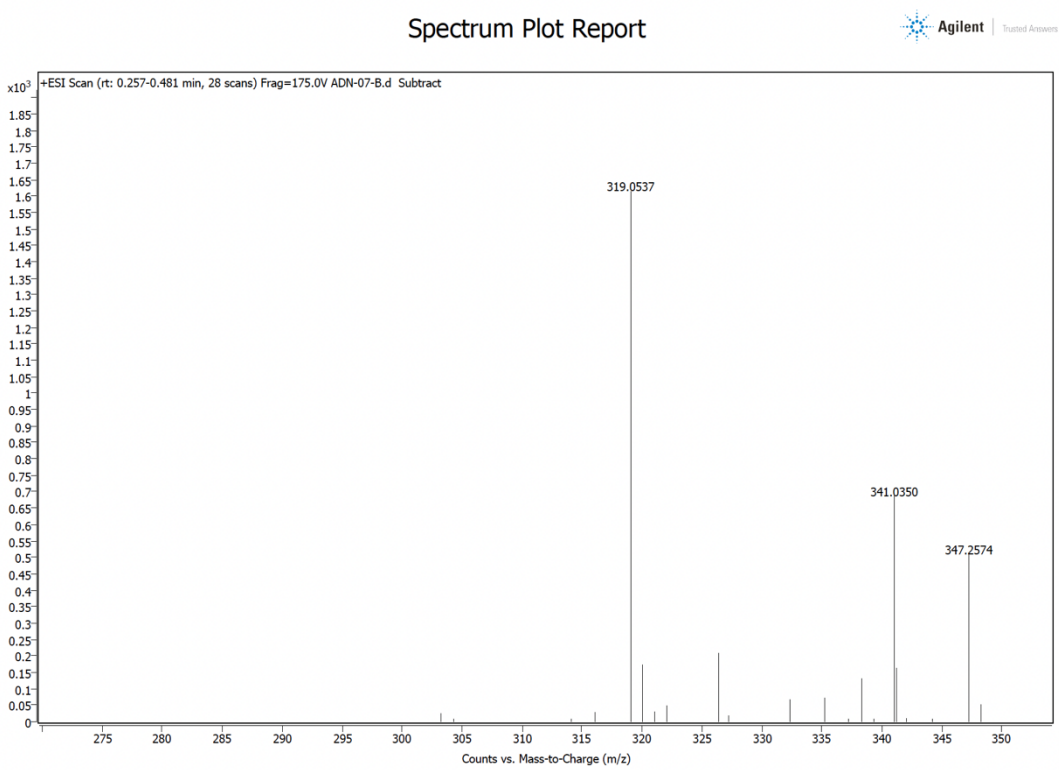


**Figure 2.5.101 HRMS (ESI) of 2.21b**

### 2.5.4 UV-Vis Studies

**General Information**: Measurements were carried out on an Agilent Cary 60 UV-Vis spectrophotometer using a Hellma semi-micro quartz cuvette with a 10mm path length. Analyses were exported as a .csv file and processed using Microsoft Excel. Zero/Background subtraction were corrected prior to running the experiment. Both the cuvette and vials storing solutions were oven-dried prior to use. Analyses were run in MeCN, H2O, and DMSO, however due to overlapping absorbances in DMSO, deionized H2O was preferred for analyses.

Preparation of Solutions: Stock Reagent Solutions: Several 0.01M solutions of individual reagents were made and stirred for 15 minutes prior to analyses. Aliquots (19.5μL) were added to 1400μL of deionized water for measurements.

0.01M of 2-pyridone (**1a**), 0.02mmol (1.90mg) in 2mL deionized $H_2O$

0.01M of Langlois' Reagent (**2a**), 0.02mmol (3.12mg) in 2mL deionized $H_2O$

0.01M of DMSO, 0.02mmol (1.42 μL) in 2mL deionized $H_2O$

Reaction Mixtures (RM) [**1a** : **2a** : DMSO, overall concentration 0.0625M, aliquot 3.12μL]:

1:1:0 – 0.125mmol of **1a** and **2a**

1:1:1 – 0.417mmol of **1a**, **2a**, and DMSO

2:1:2 – 0.025mmol of **1a**, 0.5 mmol of **2a** and DMSO

1:1:5 – 0.016mmol of **1a**, 0.03125 mmol of **2a**, 0.078125 mmol of DMSO

Standard reaction conditions – 0.125mmol of **1a** and 0.25mmol of **2a** were added to a vial containing 2mL of DMSO. This mixture was stirred for 15 minutes prior to analysis. An aliquot (1.04μL) was added to 1400μL of deionized water used for measurements.

**General Procedure:** A 10mm path length quartz cuvette (oven dried) was charged with an aliquot (19.5μL) of **1a**, **2a**, and DMSO separately in 1400μL of deionized water, respectively. All mixtures were shaken prior to analyses. For the irradiation-study, a vial was charged with all reagents using standard reaction conditions (see G2, RM) and stir bar. A 10mm path length quartz cuvette was charged with an aliquot (1.04μL) in 1400μL of deionized water. The reaction mixture was then irradiated at 390nm at a 4cm distance, for a set time interval where aliquots (1.04μL) were taken at specific time points and measured. For the titration study, a 10mm path length quartz cuvette (oven dried) was charged with an aliquot (19.5μL) of **1a**, and 1400μL of deionized water, respectively. Aliquots of 2.6μL of **2a** were added to solution, mixed thoroughly, and measured up to 2 equivalences (39μL total).

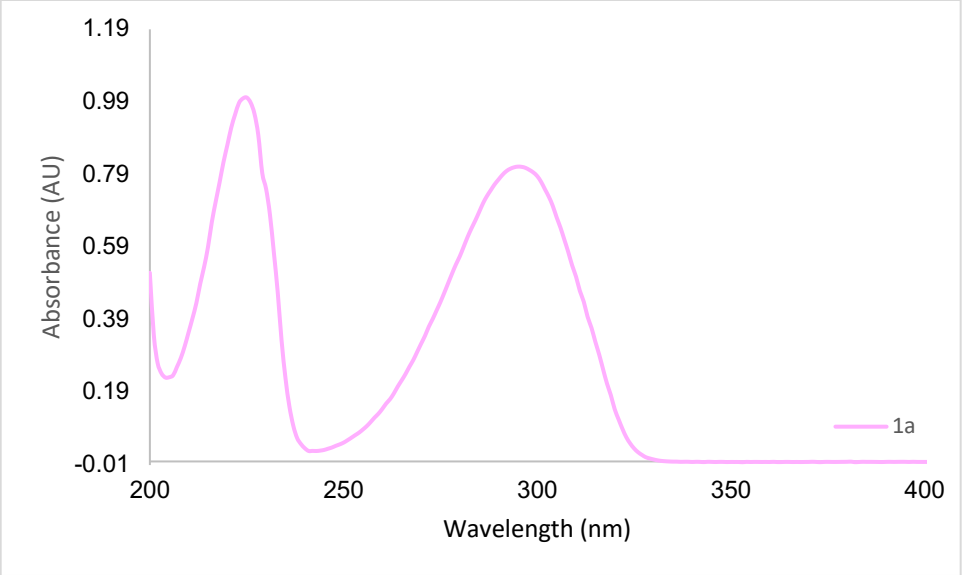


**Figure 2.5.102 UV-Vis Spectrum of 2.1b**

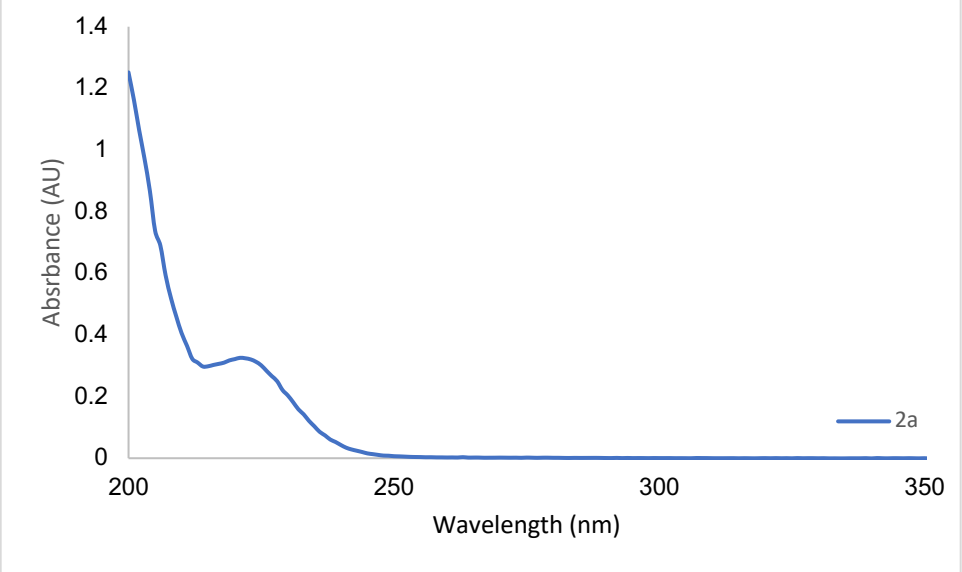


**Figure 2.5.103 UV-Vis Spectrum of DMSO**

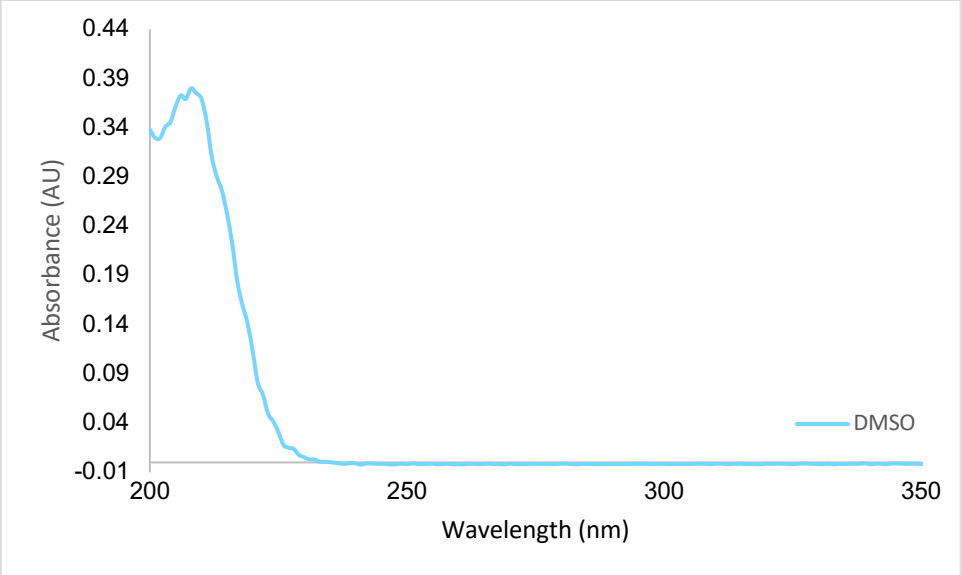


**Figure 2.5.104 UV-Vis Spectrum of Langlois' Reagent**

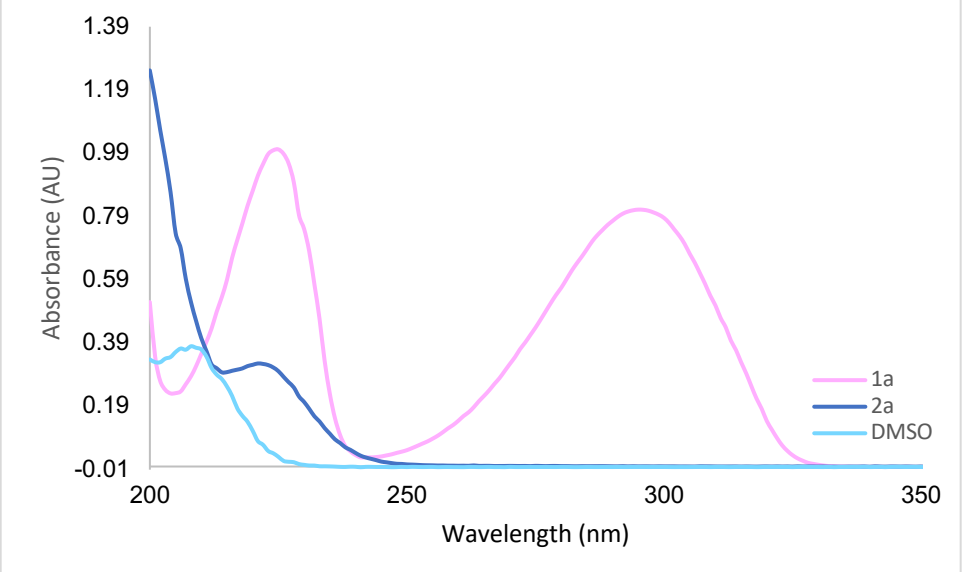


**Figure 2.5.105 UV-Vis Spectrum Overlay of All Reagents**

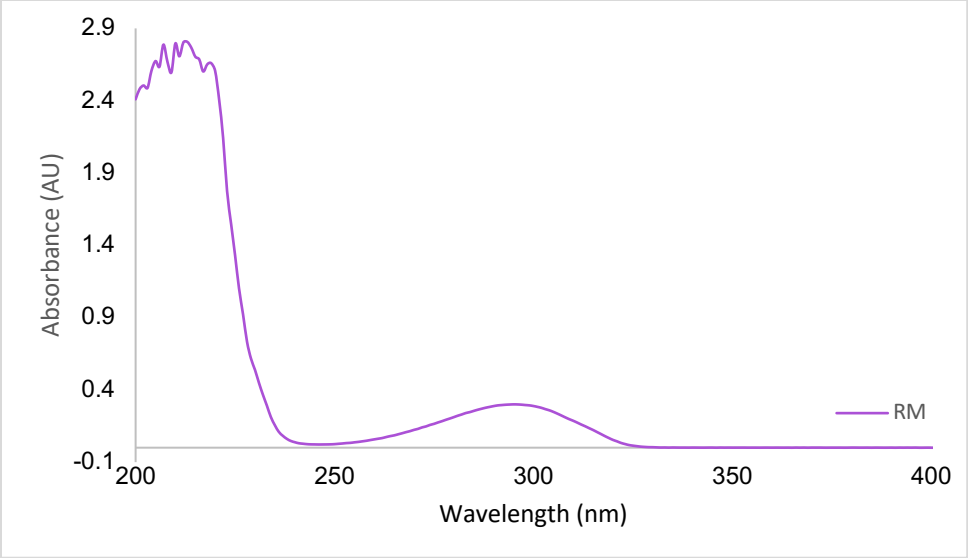


**Figure 2.5.106 UV-Vis Spectrum of Reaction Mixture**

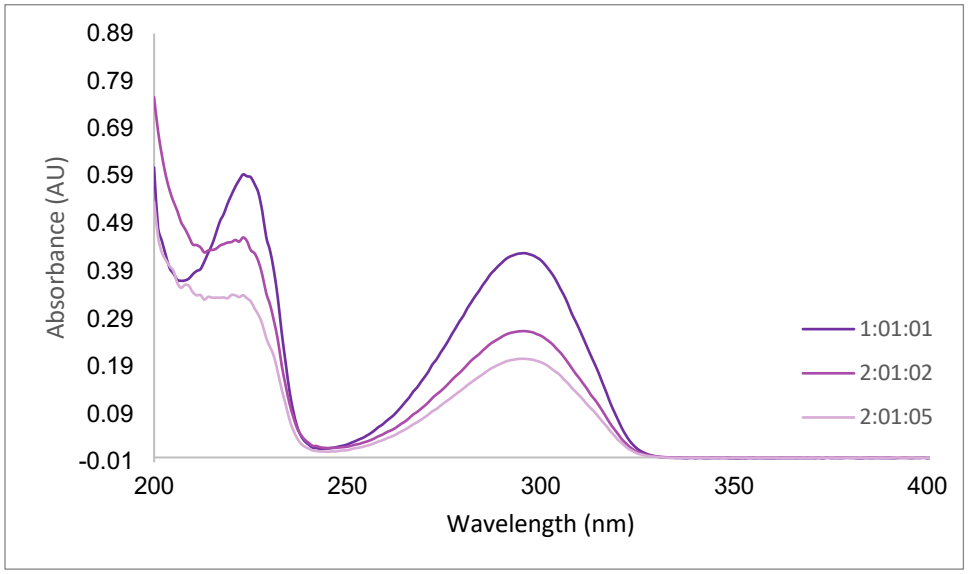


**Figure 2.5.107 UV-Vis Spectrum Overlay of All Reagents at Different Equivalences**

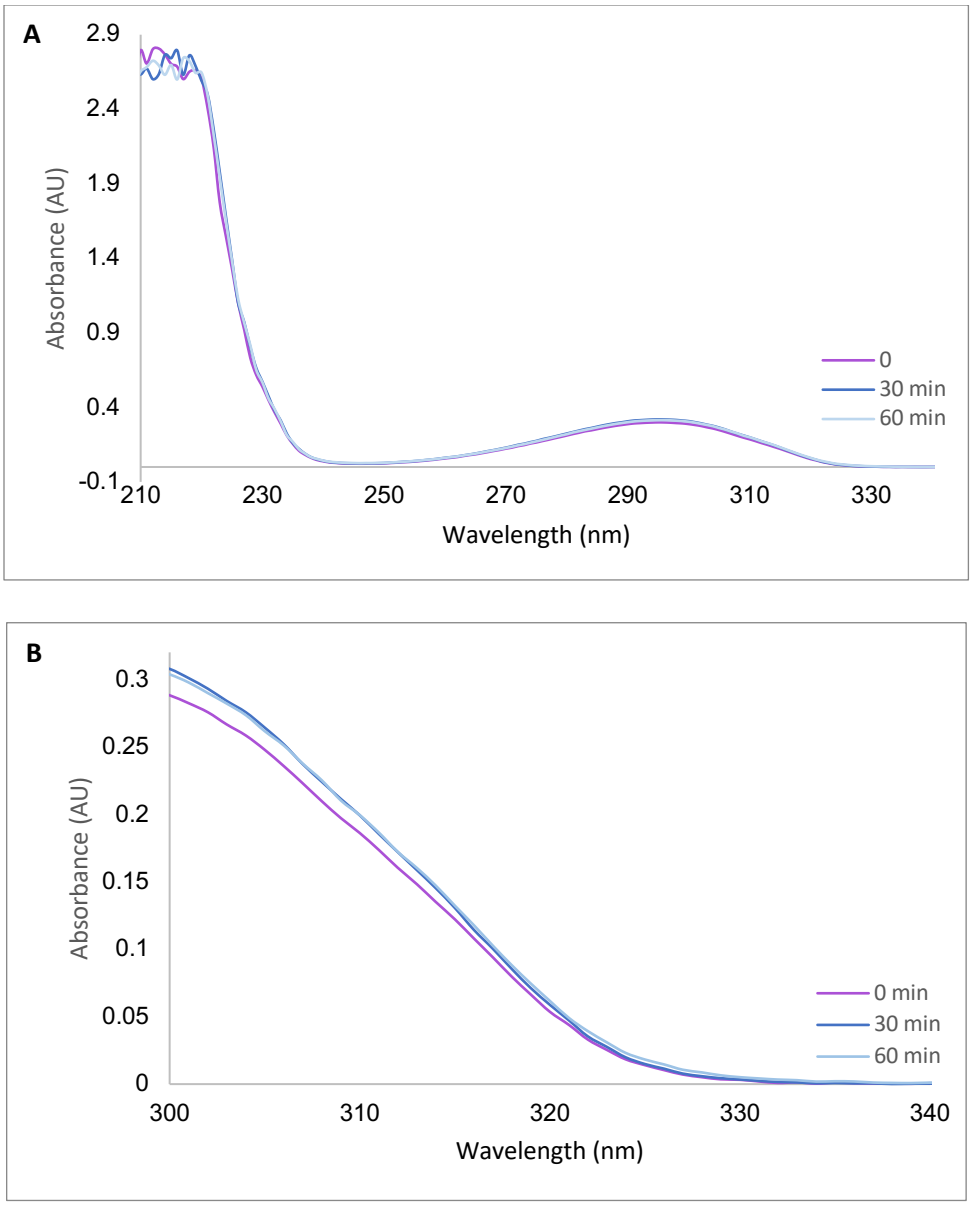


**Figure 2.5.108 UV-Vis Spectrum of Reaction Mixture Irradiated at 390nm**

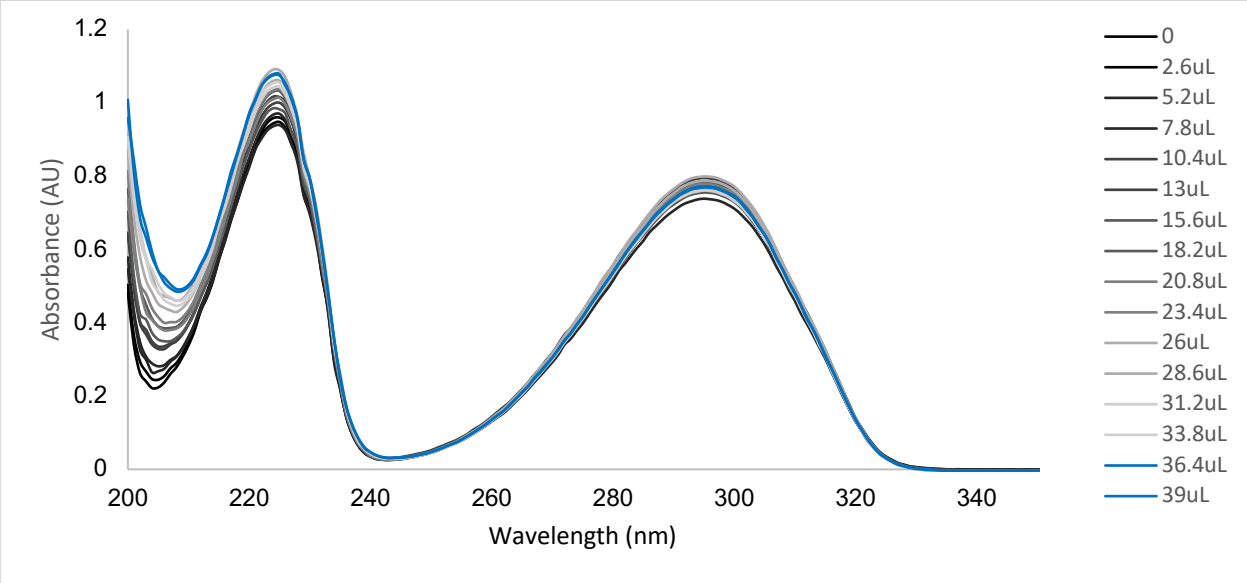


**Figure 2.5.109 UV-Vis Spectrum of 2.1 Titrated with Langlois' Reagent up to 2 equiv.**

### 2.5.5 Cyclic Voltammetry

**General Information**: Electrolyte solution was prepared using $NBu_4PF_6$ and HPLC grade reagent alcohol. The recrystallized salt was then dried in a Fisher Scientific Isotemp Vacuum Oven (model 280A) equipped with an Emerson Application Vacuum Pump (model S55NXMPF-6788).

The boron-doped diamond (BDD) working electrode was polished using Buehler MicroPolish (part no. 40-10075, batch B112-B-S1) and a small amount of deionized water on a Buehler MicroCloth Polishing Cloth (part no. 40-7212, batch 809-3).

All cyclic voltammograms were performed using a CH Instruments Electrochemical Workstation (model 660E) in a nitrogen-atmosphere Glove Box from Vigor Gas Purification Technologies (model SG1200/750TS) equipped with an Edwards Vacuum Two Stage Rotary Vane Pump (model RV12). Analyses were exported as a .csv file and processed using Microsoft Excel.

**Preparation of Electrolyte and Sample Solutions:** Approximately 200.0 mL of MeCN was refluxed over $CaH_2$. It was further dried by siphoning from the storage bottle into an oven-dried, nitrogen-flushed column packed with activated alumina.

To prepare the salt for the electrolyte solution, 14 grams of commercially available tetrabutylammonium hexafluorophosphate were added to a 250.0 mL Erlenmeyer flask. The salt was dissolved by adding 75 mL of 95% reagent alcohol–previously prepared using reagent alcohol and deionized water–and heating the flask in a water bath at 80ºC. Once the salt was dissolved, the flask was removed from the water bath and left on the benchtop to slowly cool to room temperature. The flask was then placed in an ice bath to cool further. The mixture was filtered using a fine fritted funnel, and the crystals were washed with ice cold 95% alcohol and then left to dry under vacuum. The dry crystals were poured into a clean Erlenmeyer flask and the recrystallization process was repeated two more times. After the third recrystallization, the salt was dried in a vacuum oven at 100ºC for 12 hours and then allowed to cool under vacuum. The salt dried in the vacuum oven at 100ºC for another 12 hours, then allowed to cool under vacuum before storage in the glovebox.

Electrolyte solution for analysis was prepared by dissolving 3.875g of the tetrabutylammonium hexafluorophosphate salt into 100.0 mL of dried acetonitrile using a 100.0 mL volumetric flask. Once dissolved, the solution was transferred to a glass amber bottle and a layer of 3Å activated molecular sieves was added to the bottom of the bottle. The solution was allowed to dry over the sieves for 48 hours and then was filtered into a clean and dry glass amber bottle using a PTFE syringe filter with 0.2 micrometer pore size.

**Sample Solution Calculation:**

**1a** stock solution: 100mM, 0.1mmol of **1a** in 2mL MeCN, aliquot 50µL

**2a** stock solution: 100mM, 0.1mmol of **2a** in 2mL MeCN, aliquot 50µL

50mM = 0.1mmol reagent in 2mL MeCN; aliquot 100µL

100mM = 0.2mmol reagent in 2mL MeCN; aliquot 25µL

200mM = 0.4mmol reagent in 2mL MeCN; aliquot 50µL

400mM = 0.8mmol reagent / 2mL MeCN; aliquot 12.5µL

**General voltammetry Procedure:** A silver wire, a platinum wire, and a teflon electrochemical cell cap were cleaned with deionized water and acetone prior to being moved into the glovebox. BDD electrode was polished with micropolish on a soft polishing pad before also being cleaned with deionized water and acetone. The glass electrochemical cell to be used for cyclic voltammetry was removed from a 105ºC oven and allowed to cool in a desiccator.

A clean and dry electrochemical cell was secured in place using a ring stand equipped with a clamp. The cell was filled with 5.0 mL of the prepared electrolyte solution, and a teflon cap was placed on top of the cell. A glass separate compartment was cleaned with a small amount of electrolyte solution, filled with the electrolyte solution, and then placed into the corresponding hold in the teflon cap. The silver wire reference electrode was inserted into the separate compartment and connected to the white lead. The boron-doped diamond working electrode and platinum wire counter electrode were then inserted into their corresponding holes in the teflon cap and connected to the green and red leads, respectively.

Conditioning of the electrode was performed by cycling through the potential window 2000 times at a scan rate of 10 V/s. Once the background current stabilized, background scans were collected at scan rates of 0.1, 0.2, 0.5, 1.0, 2.0, and 5.0 V/s. After background scans, an aliquot of sample stock solution was added to the cell for a final concentration of 1.0 mM. The sample

solution was also scanned at all the scan rates. Each of the sample scans were background subtracted.

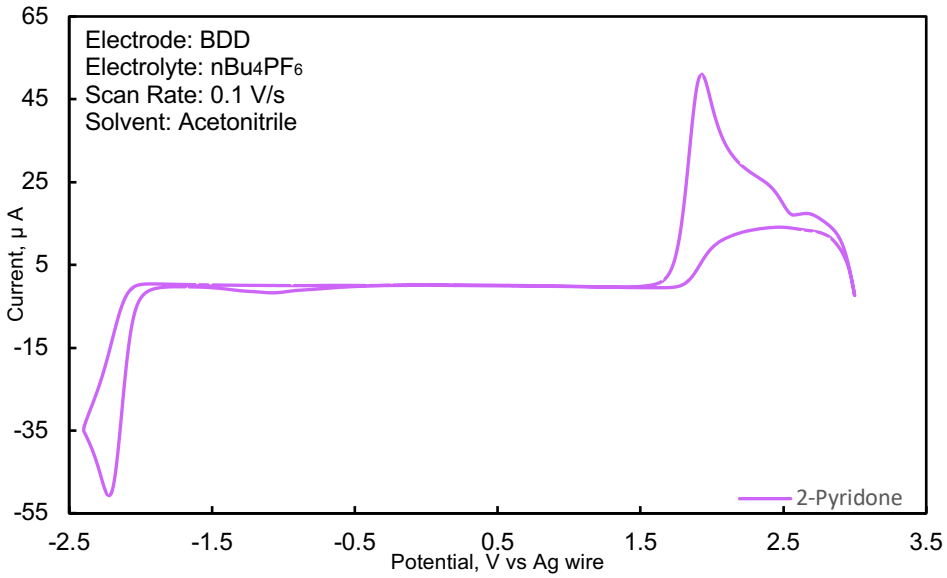


**Figure 2.5.110 CV Spectrum of 2.1a**

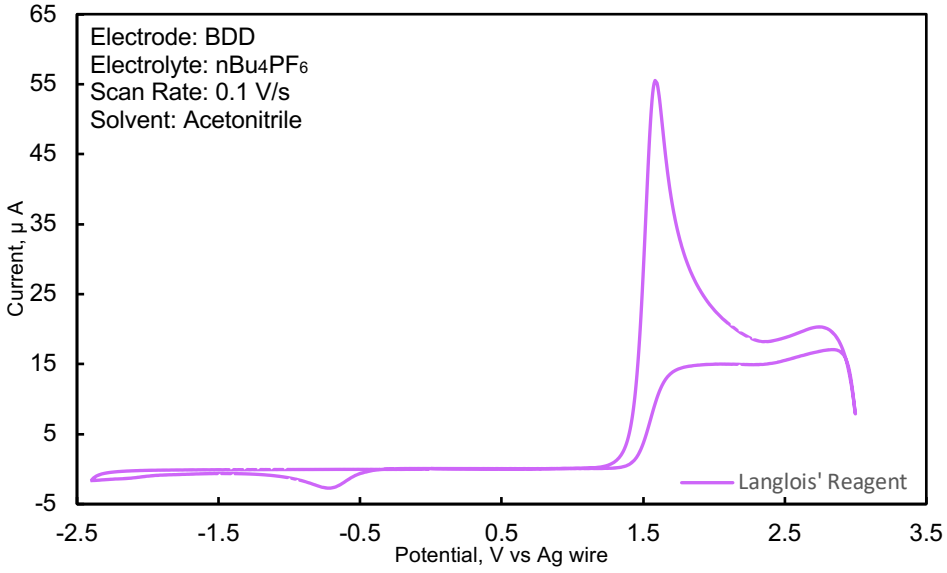


**Figure 2.5.111 CV Spectrum of Langlois' Reagent**

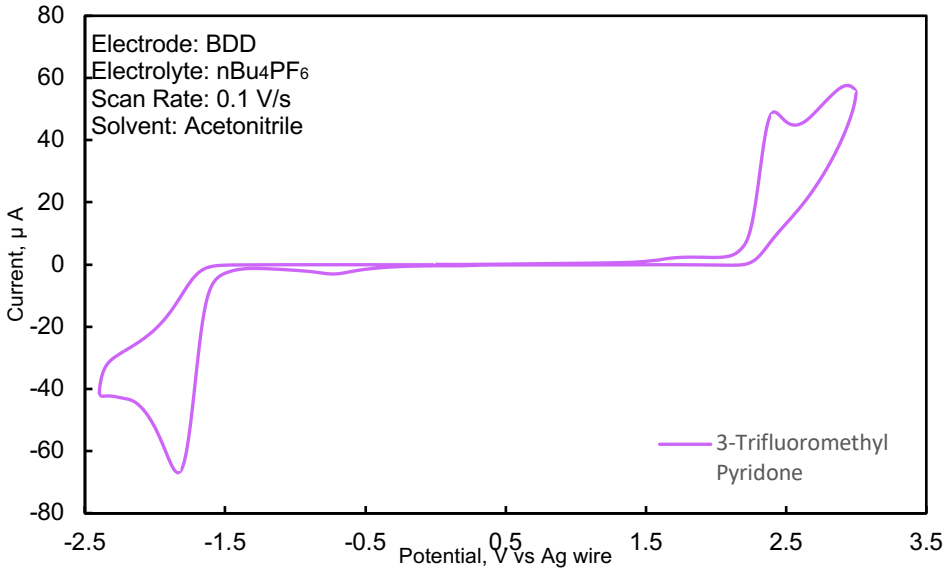


**Figure 2.5.112 CV Spectrum of 2.1b**

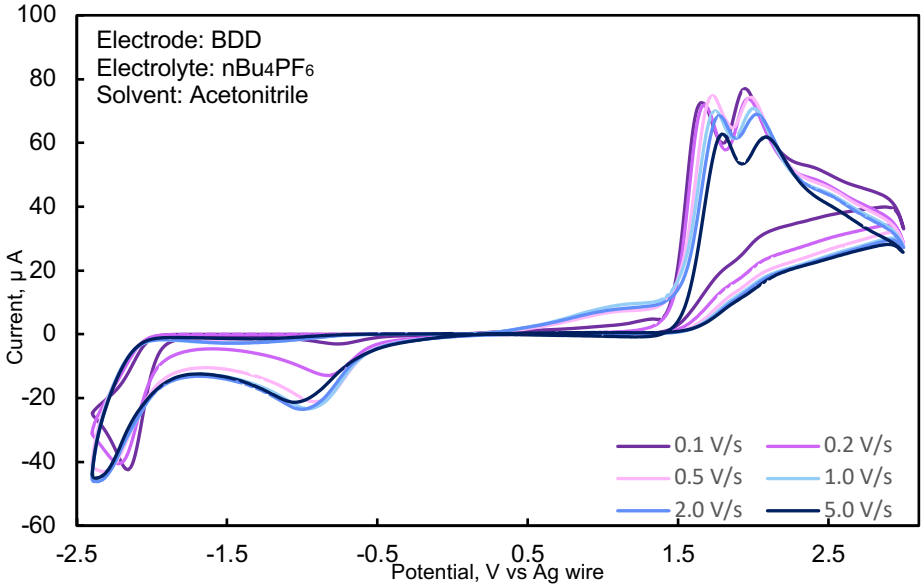


**Figure 2.5.113 CV Scan Rate Dependence Spectrum of 2.1a and Langlois' reagent**

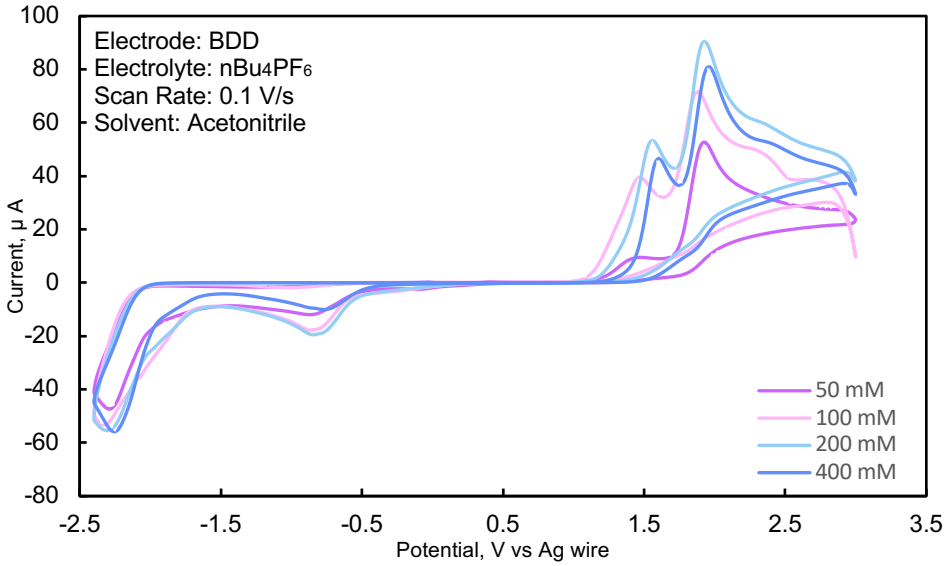


**Figure 2.5.114 CV Spectrum of Irradiation Interval Study of Reaction Mixture at 1h**

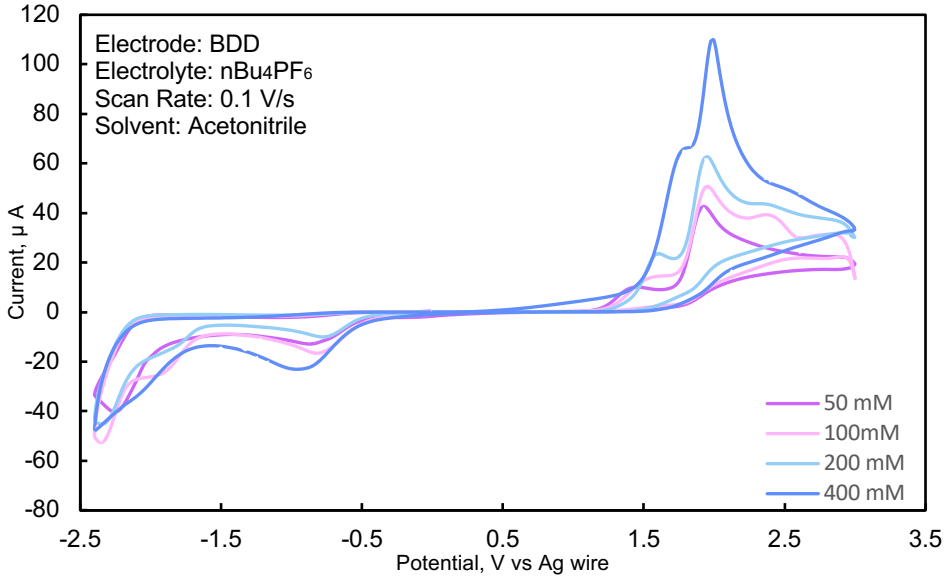


**Figure 2.5.115 CV Spectrum of Irradiation Interval Study of Reaction Mixture at 7h**

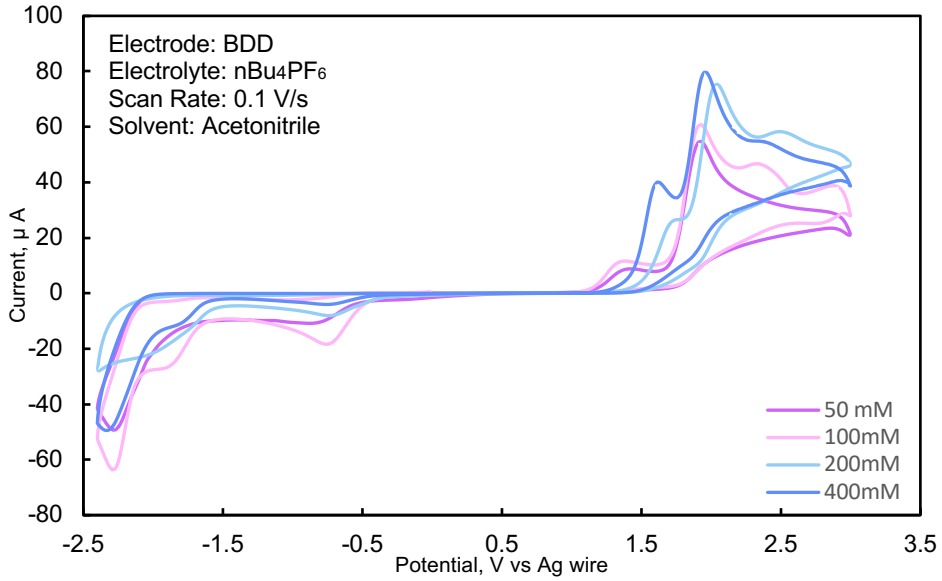


**Figure 2.5.116 CV Spectrum of Irradiation Interval Study of Reaction Mixture at 15h**

## 2.5.6 Photo-Chamber Set Up (2021-2023)

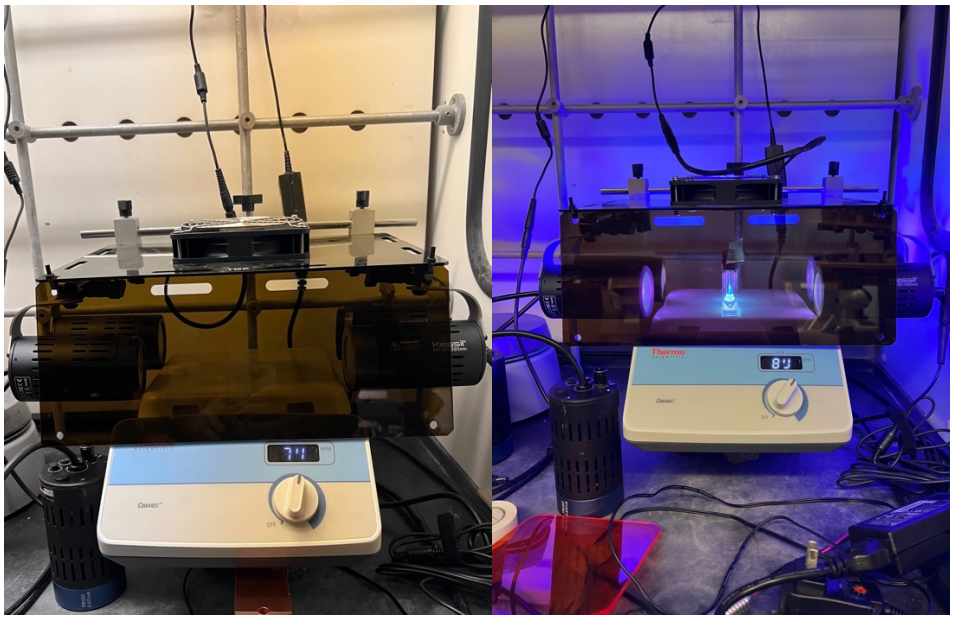

Three PR160L and one PR160s LED photoredox Kessil lamps (390nm) were used in the Kessil PR160 Fan Rig (Fan located on top of rig), stirring at >700 rpm. Average distance from lights to center is 6cm.

## 2.6 Acknowledgements

The contents in Chapter 2 are in part a reformatted reprint of the following manuscript with permission from *Organic Letters.* **2023**. 2023, *25,* 26, 4898-4902. https://doi.org/10.1021/acs.orglett.3c01710. I wrote the manuscript, provided work for the optimization, substrate scope evaluation, ran UV-Vis experiments and assisted in the CV experiments. Kristine Legaspi ran the CV experiments. Connor McCarty contributed to substrate scope evaluation. Dr. Diane Smith gave insightful discussions regarding the electrochemistry and mechanisms, while providing the facilities to run cyclic voltammetry before she passed away in October 2022. The dissertation author is the researcher for the data presented and this work was supported by the National Science Foundation (CHE – 1664565, 1955086) as well as the ARCS Foundation.

# CHAPTER 3: Development Towards a Regioselective Radical-based Trifluoromethylation

## 3.0 Wiley Copyright/Statement:



## 3.1 Electrophilic Aromatic Substitution ($S_EAr$); The Original C-H Functionalization of Arenes and *N*-Heteroarenes

$S_EAr$ is among the oldest classes of reactions used to functionalize aromatic C-H bonds.[117, 118] Canonical $S_EAr$, often exemplified by the Friedel-Crafts reaction, is a major topic covered in undergraduate organic chemistry and we often teach students that this reaction necessitates a strong Lewis acid catalyst that is needed to activate the electrophile of interest. This is one of the major disadvantages of this reaction as it decreases the tolerability of functional groups on the aryl substrate, many of which are known to interact with LAs.[119] Classical $S_EAr$ reactions are also typically performed under strongly acidic/basic conditions, elevated temperatures, have reduced reactivity towards electron-poor arenes, including some heteroarenes, and commonly produce mixtures of constitutional isomers due to multiple reactivity sites on aryl substrates (Figure 3.1.1).[120, 121]

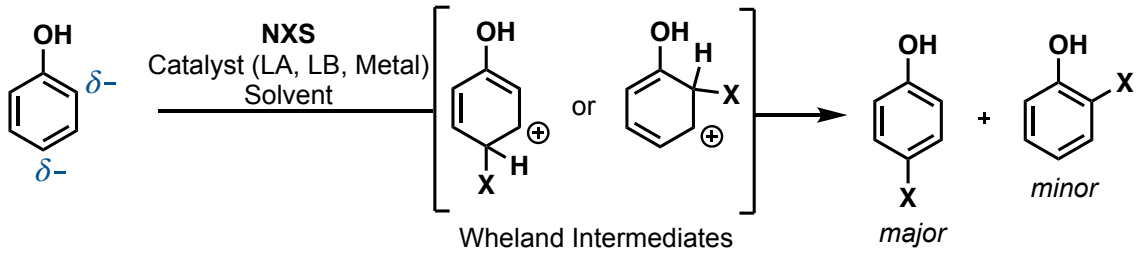


**Figure 3.1.1. Generic $S_EAr$ Halogenation of Phenol**

There have been numerous advances in recent years that have furnished milder conditions for the incorporation of diverse functionalities into both simple and complex aromatics, particularly towards halogenated arenes which are important building blocks in drug discovery. The myriad of functionalities that can be introduced via $S_EAr$ include, but are not limited to, halogens, perfluoroalkyl, sulfenyl, alkyl, acyl, and nitro substitutions.[51, 65, 122-124] It is also important to note that in classical $S_EAr$, the electrophilic halogen source was typically highly reactive such as bromine ($Br_2$) and chlorine ($Cl_2$), however there has been numerous developments towards milder reagents such as *N*-halosuccinimides (NXS, where X= Cl, Br, I) which paved the way in the development of mild $S_EAr$ amenable for more complex molecules and LSF.[70, 125, 126] While the additions that can be performed are diverse, the synthetic utility of $S_EAr$ is often limited by lack of efficiency to produce any product that is not innate. This is exemplified by the case of phenols, which typically yield an 'innate' ~4:1 mixture of *para*- to *ortho*- constitutional isomers.[122] This moderate innate selectivity, selectivity that is substrate controlled, leads to attenuated yields and often necessitates strenuous purifications, making it difficult to obtain large amounts of the minor constitutional isomer when needed. Intrigued by these challenges, several groups have developed strategies to both augment and override the innate selectivity of $S_EAr$ on both simple and complex aromatics using halogens,[123, 127, 128] however there is still a need to address regioselectivity issues using other electrophiles, such as trifluoromethyl groups, as well. Thus,

developing strategies to address issues regarding regioselectivity will be highly valued by the synthetic community.

## 3.2 Using Lewis Bases to Control the Selectivity of $S_EAr$ Halogenation

From an energetic perspective, development of a catalyst-controlled regioselective $S_EAr$ can be very difficult compared to a catalyst-controlled enantioselective reaction (Figure 3.2.1). In an enantioselective reaction, the energies of an uncatalyzed racemic reaction of both transition states for either enantiomer (S or R) are equal in energy, thus a catalyst must only overcome a specific set energy (~1.3 kcal/mol in a 90:10 e.r) to achieve good enantioselectivities. In comparison, in a regioselective reaction the reaction pathway possesses different transition states that are not equal in energy, thus a catalyst must first overcome the initial innate selectivity, plus an additional energetic difference belonging to the minor constitutional isomer to achieve good regioselectivities.[129]

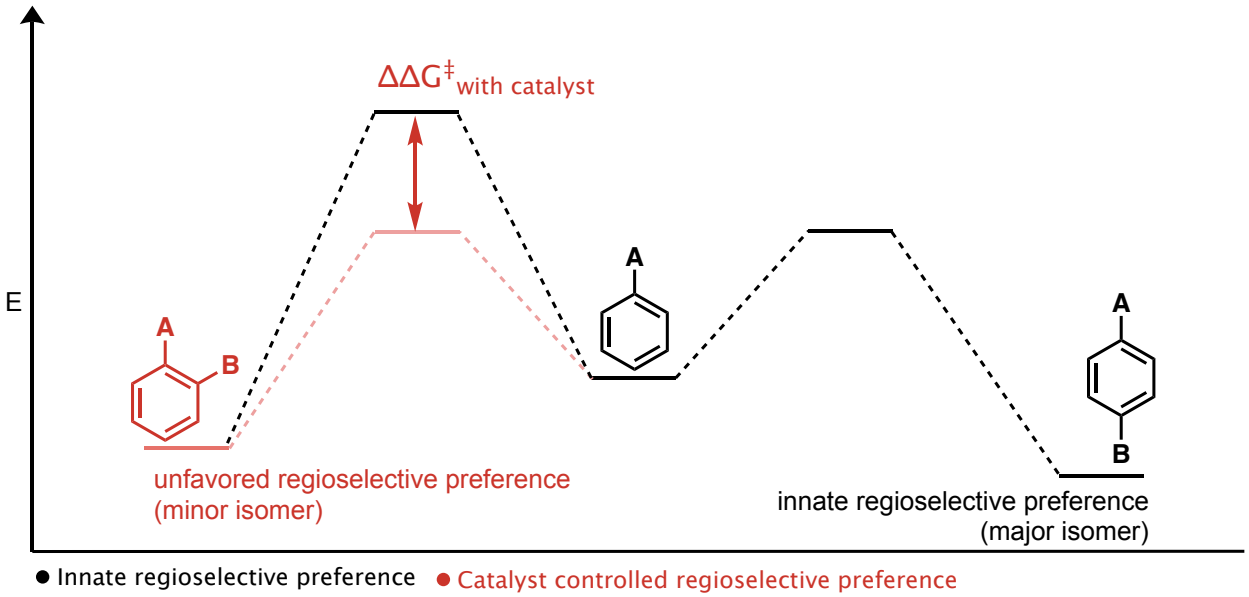


**Figure 3.2.1. Generic Energy Diagram of Regio- vs. Innate $S_EAr$**

Currently, there are few examples of catalyst-controlled regioselective $S_EAr$-type methodologies including seminal work on the selective bromination of complex molecules using

a peptide-based catalyst from Miller and coworkers,[130] and a site selective chlorination of tryptamines using engineered enzymes from Lewis and coworkers.[131] Additionally, previous reports from our group have demonstrated the use of Lewis base catalysts (LBCs) not only to activate electrophiles for both halogenation and sulfenylation of aromatics, but also their effectiveness as regioselective catalysts for the chlorination and bromination of phenols.[128] It was previously found that a bis-thiourea catalyst (Nagasawa's catalyst, G1 *o*-cat) generated *ortho*-halogenated phenols with regioselectivities up to 16:1 *o*:*p* and a phosphine sulfide derived from 2,2'Bis(diphenylphosphino)-1,1'-binapthyl (BINAP) (G1 *p*-cat) afforded *para*-halogenated phenols up to 1:20 *o*:*p* (Scheme 3.2.1).[123] This strategy represents a concise, regiodivergent halogenation of phenols that contextualizes the use of LBCs to control the regio-outcome of the reaction. The authors postulated that phenol non-covalently interacts via H-bonding to one of the thioureas on Nagasawa's catalyst, while the other thiourea, specifically the sulfur atom, forms a Lewis-base adduct with the halogen. The orientation at which phenol coordinates to the catalyst allows for increased halogenation at phenol's *ortho*- position via a proximity effect. Conversely, both triphenylphosphine sulfide (G1 *p*-cat)[122] and G2 *p*-cat (shown below) are bulky LBCs hindering the ability to form the constitutional isomer or allowing for a quick, facile transformation of the innate constitutional isomer, which in the context of electron-donating activators, is typically *para*.[70]

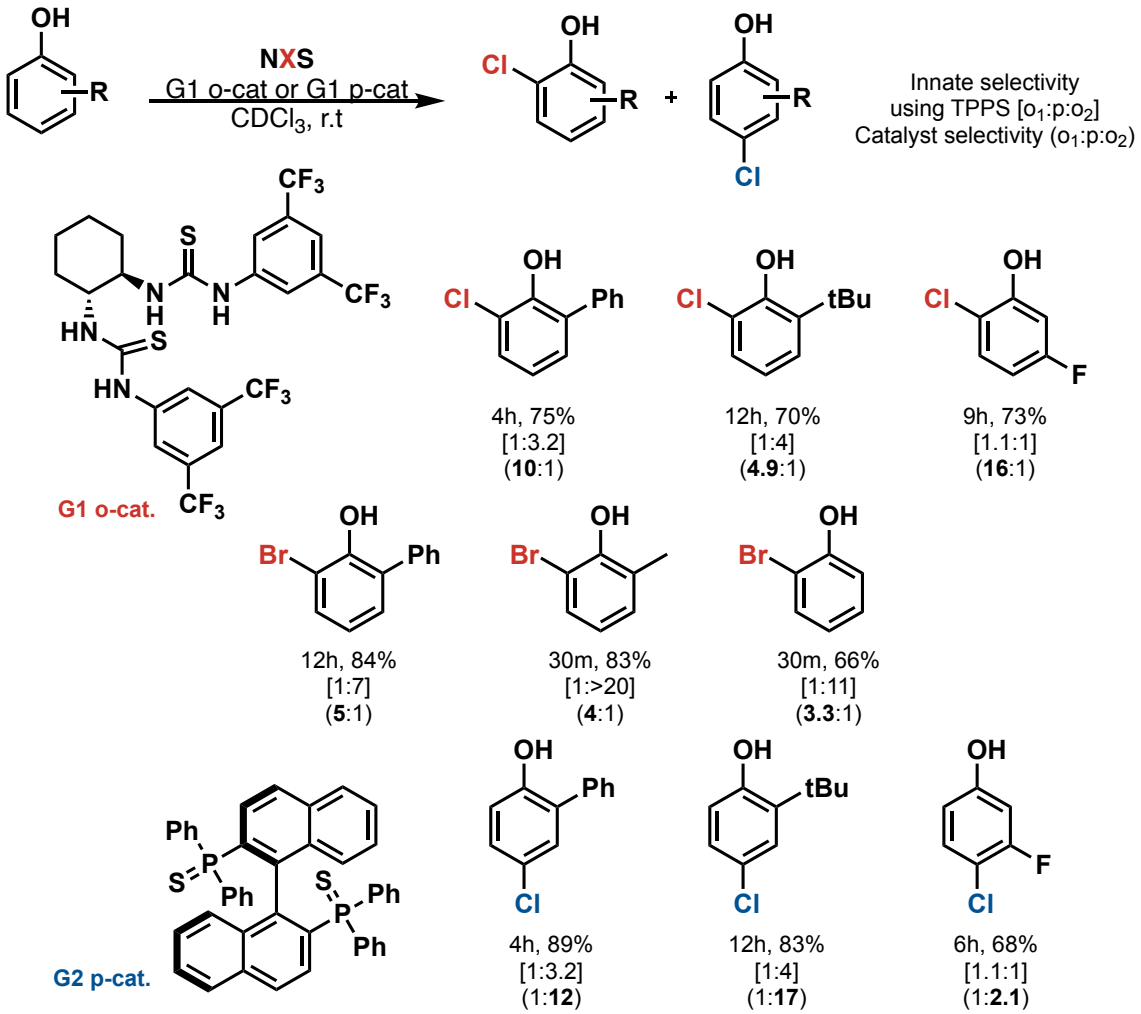


**Scheme 3.2.1 Gustafson's Regiodivergent Halogenation of Phenols**

While Nagasawa's catalyst has been shown to produce the *ortho*-halogenated product, the authors noted a potential degradation pathway where one of the thioureas, specifically one of the nitrogen atoms, 'attacks' the other thiourea, specifically the $sp^2$ electrophilic carbon, forming a guanidinium adduct that is not catalytically active towards regioselectivity. This finding led to further development of another *ortho*-selective catalyst that does not degrade.

In 2021, the Gustafson group published another *ortho*-selective chlorination of phenols with even greater selectivities, achieving up to >20:1 *o*:*p* using a Lewis basic selenoether catalyst (Scheme 3.2.2, G2 *o*-cat)[128] This catalyst contains a Lewis basic selenoether as well as a thiourea

on an indane-based scaffold that is unbiased in the chlorination reaction compared to phenol which is more electron rich. The authors hypothesize that this catalyst coordinates in a similar fashion as Nagasawa's catalyst, where one of the thioureas interacts via H-bonding to phenol, while the selenoether forms a Lewis-base halenium adduct in proximity to the *ortho*-position of phenol as depicted below. It is important to note that thiourea moieties have multiple possible H-bonding coordination possibilities, one of which is depicted below which is known as a cis binding mode (*Z*,*Z* orientation) where the nitrogen and hydrogen atoms are cis with respect to each other. The other binding mode is considered a trans binding mode (*E*,*Z* orientation), where the nitrogen and hydrogen atoms on the thiourea are orthogonal.[132]In this case, it is possible that either modes are plausible for the H-bonding step.

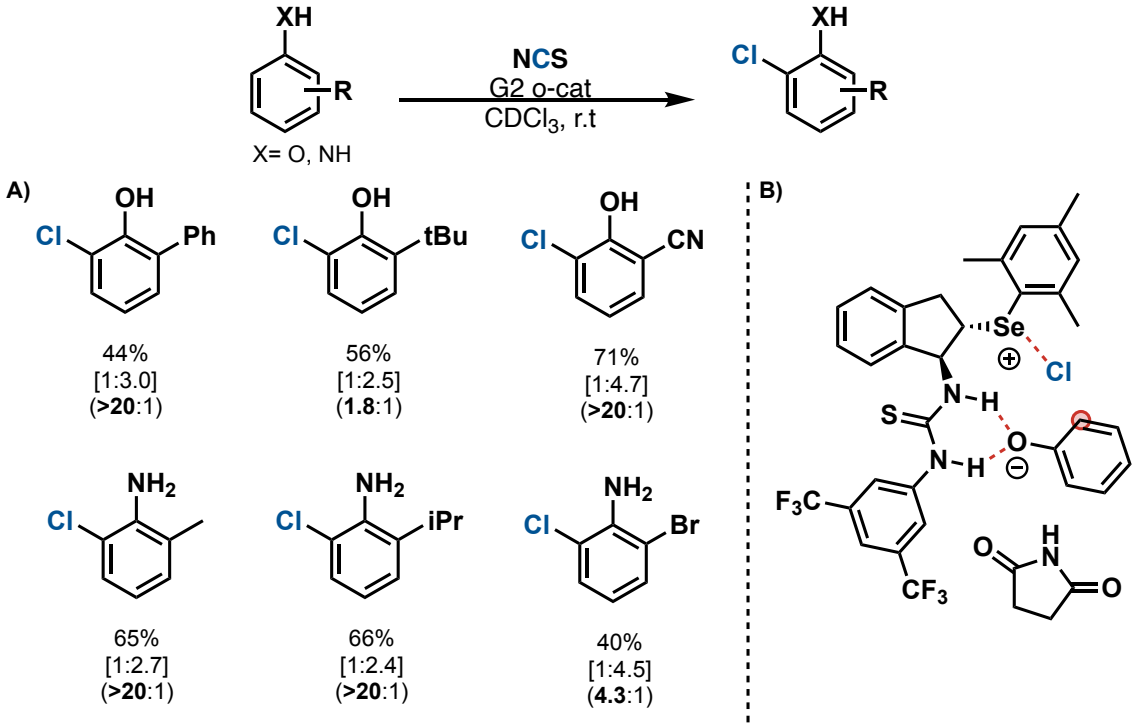


**Scheme 3.2.2 Gustafson's Improved *ortho*-Chlorination of Phenol and Anilines**

Intrigued by the potential binding orientations of the G2 *o*-cat, and the ability to diversify the core scaffold, I hypothesized that this catalyst scaffold can be tuned for electrophiles beyond

halogens such as chlorine and bromine, specifically towards larger electrophiles such as electrophilic perfluoroalkyl groups. Traditional $S_EAr$ is not considered a radical reaction, however with recent developments in photochemistry there are emerging examples that demonstrate a potentially new classification as radical-based $S_EAr$, through the generation of electrophilic radicals.[51, 96]

## 3.3 Radical Philicity: Electrophilicity of Perfluoroalkyl Radicals

While there have been multiple reports classifying molecules or compounds on an empirical scale of electrophilicity and nucleophilicity,[133-135] there are very few regarding the classification of radicals according to this scale or similar.[136]Regardless of a formal classification, it can be stated that the electronic nature of a radical can affect its behavior in a reaction and what moieties it can react with. For example, a radical with electrophilic character will react on sites that are electron-rich, whereas a more nucleophilic radical will prefer electron-poor sites.[137] In the context of perfluoroalkylation, there are several examples where perfluoroalkyl radicals exhibit divergent behavior based on the activation of either nucleophilic reagents, such as the Ruppert-Prakash regant,[138] or electrophilic perfluoroalkylation reagents, such as Togni's[139] or Umememoto's reagent,[92] however this chapter will focus on electrophilic radical perfluoroalkylations. Upon homolysis of the electrophilic perfluoroalkylation reagent, the subsequent radical formation can be described as such: difluoromethyl- radicals are less electrophilic than difluorochloro- or trifluoromethyl- radicals (Figure 3.3.1. Notably, this trend is remains true and is observed in the methodology as described in chapter 2 regarding the perfluoroalkylation of pyridones.[51, 140, 141]

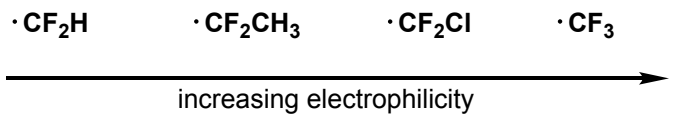


**Figure 3.3.1. Generic Scale of Perfluoroalkyl Radical Electrophilicity**

## 3.4 Electrophillic Aromatic (Radical) Trifluoromethylation: Let's EAT

The potential for electrophilic aromatic trifluoromethylation was first studied by Yagupolskii through the introduction of trifluoromethyl chalcogenium salts in 1984,[142, 143] which were further explored in the early 1990s by Umemoto and coworkers.[92] Simultaneously, Langlois also demonstrated the use of sodium trifluoromethanesulfinate as a source for generating an electrophilic trifluoromethyl radical that could trifluoromethylate a variety of electron rich arenes. Despite this early work, electrophilic trifluoromethylation was sparsely studied until the early 2010s. Since then, there have been several breakthroughs for the electrophilic trifluoromethylation of arenes and heteroarenes, exemplified by Togni's hypervalent iodine trifluoromethylating reagents and others (Figure 3.4.1). As of now, electrophilic trifluoromethylation, often via an electrophilic radical, yields predominately the innate regioisomer due to the electronic properties of the aryl substrate.[109]

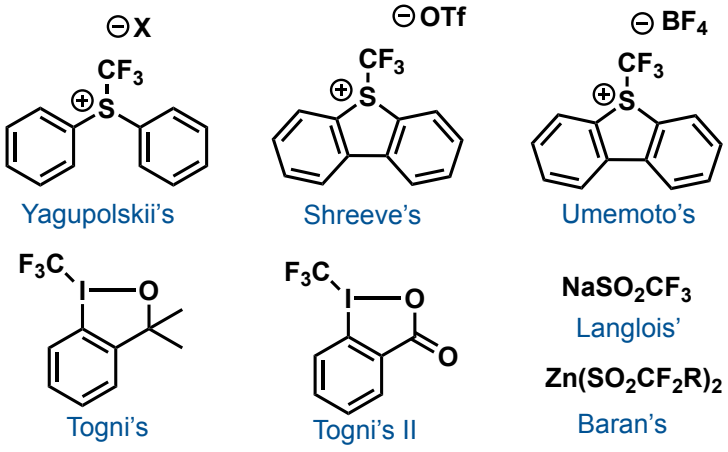


**Figure 3.4.1 Examples of Electrophilic Perfluoroalkylation Reagents**

The development of these reagents led to further development of complementing chemistries that utilize them to perfluoroalkylate a variety of arenes and heteroarenes. There are more examples of trifluoromethylation than other perfluoroalkylations, due to its biological relevance as mentioned in the previous chapter. Additionally for this chapter, we will focus on strategies that note issues with regioselectivities as well as contain examples of LSF, which is the ultimate goal of the works contained in this thesis.

There are several works that highlight the arene diversity via substrate scope for the electrophilic trifluoromethylations. Recent work by Baran, uses the Langlois reagent in conjunction with excess *tert*-butyl hydrogen peroxide for the trifluoromethylation of heteroarenes with yields from 47-96% (Scheme 3.4.1A). Baran and coworkers were able to extend these conditions to include LSF on varenicline (Chantix) observing a 4:1 C5:C2 selectivity with 50% yield.[144] Stephenson and coworkers developed a method for radical trifluoromethylation uses photochemistry and pyridine N-oxide to induce the formation of a $CF_3$ radical from trifluoroacetic acid (TFAA), which previously required highly oxidizing conditions, to functionalize electron rich arenes and N-heterocycles in moderate yields up to 65%.[96] The MacMillan approach for radical trifluoromethylation is a simple and efficient method for both arenes and heterocycles using commercially available triflyl chloride under photocatalytic conditions. (Scheme 3.4.1B). LSF was also achieved on a number of biologically active molecules, including Lipitor, a polyaromatic drug that was trifluoromethylated in a 1:1:1 ratio across the more electron rich rings with 74% yield.[51] However, the lack of regio-control is a major limitation preventing its widespread use in synthetic chemistry as the innate selectivity of the substrate dictates the regiochemical outcome. Interestingly, the mechanisms for these trifluoromethylations propose the generation of an electrophilic $CF_3$ radical which then undergoes a radical coupling to the arene, forming a radical

intermediate. A second oxidation event generates a Wheland intermediate that is analogous to $S_EAr$.(Scheme 3.4.1C). Based on the proposed mechanism of these reactions, *we hypothesize that we can utilize LBCs to direct the addition of the $CF_3$ radical to prefer a single constitutional isomer.*

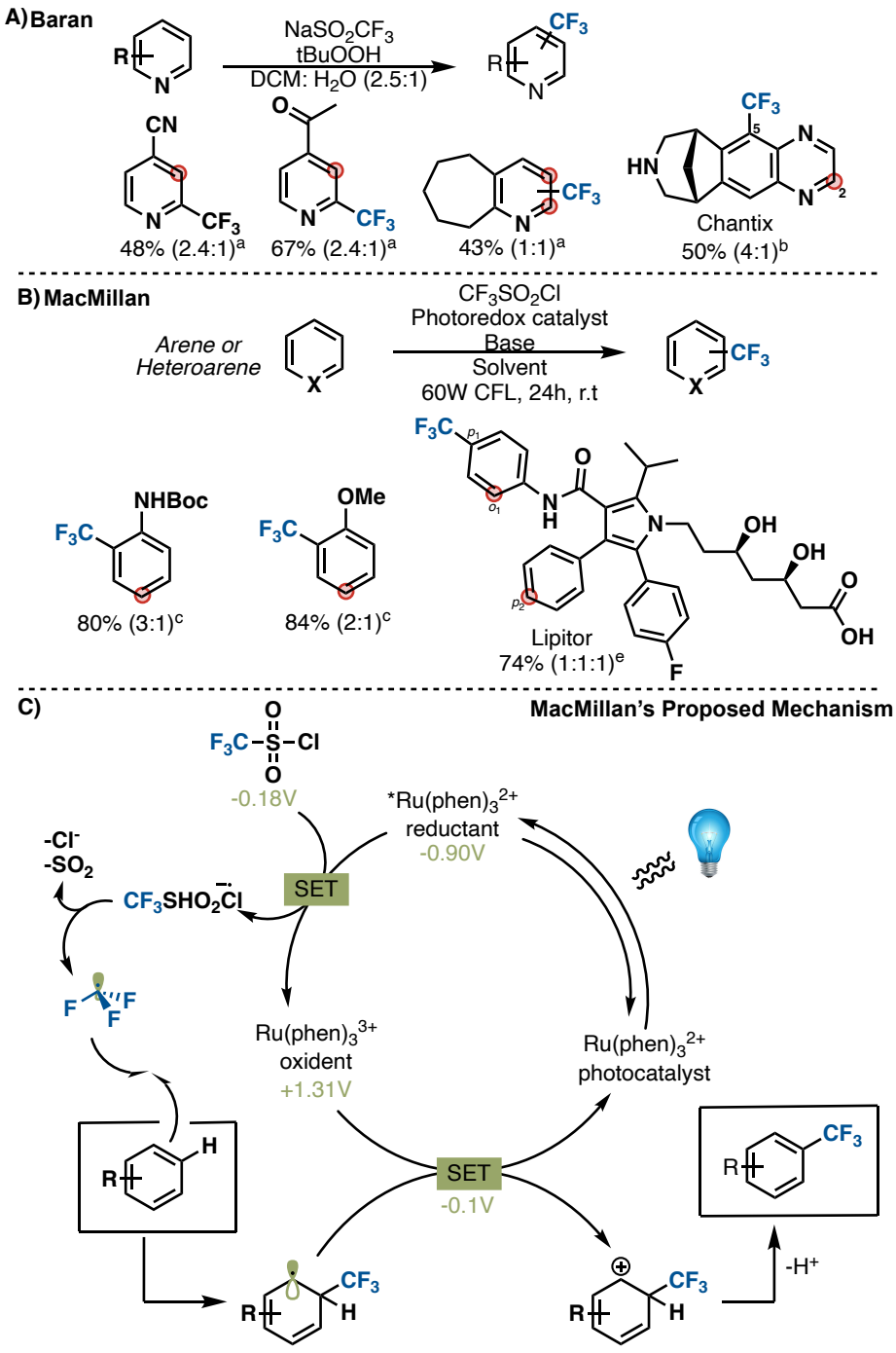


A) Regioselctivity issues of Baran's trifluoromethylation of heteroarenes. [a](Ratios shown as C2:C3). [b](Ratio shown as C5:C2). B) Regioselectivity issues of MacMillan's trifluoromethylation on arenes and heterocycles. [c](Ratios shown in *o:p).* [d](Ratio shown as C2:C3). [e](Ratio shown as $p_1$:$o_1$:$p_2$). C) $S_EAr$-type mechanism for MacMillan's trifluoromethylation.

**Scheme 3.4.1 Examples of Electrophilic Aromatic Trifluoromethylation**

It is also important to mention a very recent example from Zhao and coworkers published in 2022, where they report the use of Langlois' reagent for the innate trifluoromethylation of anilides, achieving exclusive *para*-selectivity (Scheme 3.4.2).[145] This reaction proceeds innately, and due to the exclusivity of the reaction it would be interesting to see an *ortho*-perfluoroalkylation. Both this strategy and the MacMillan trifluoromethylation reaction will be discussed in further detail in the next section as these works are the ideal electrophilic radical trifluoromethylations that will be used to develop a regioselective trifluoromethylation due to the simplicity of reagents and methodology.

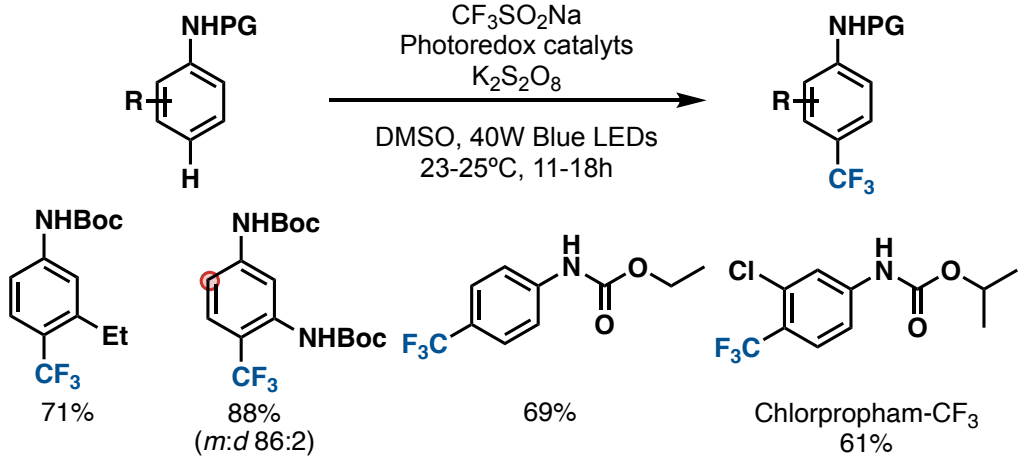


**Scheme 3.4.2 Zhao's Innate Trifluoromethylation of Anilides**

## 3.5 Preliminary Development of a Regioselective Trifluoromethylation

The aformentioned chemistries from the MacMillan and Zhao groups are somewhat analogous to $S_EAr$ and the working hypothesis that our LBC catalyst-controlled approach can be extended to control the regio-outcome of these trifluoromethylations. *My hypothesis is that the Lewis basic moiety on the LBC can intercept electrophilic $CF_3$ radicals by forming a covalent adduct, while the H-bonding handle on the catalyst can interact with the substrate bringing both species in close enough proximity to effect the regio-outcome.* As this approach relies on non-

covalent interactions between the LBC and substrate, the first step was to confirm that this chemistry could be done using less polar solvents in order to maximize the impact of these interactions using *N*-Boc Aniline (Table 3.5.1). It is important to note that MacMillan's method uses MeCN, which increases the efficacy of the photocatalyst allowing near completion is 24 hours (Table 3.5.1, entry 1). When evaluating less polar solvents, such as chloroform, I observed diminished yields by nearly 40% (Table 3.5.1, entry 2). When changing the base of the reaction to something more soluble in chloroform, the overall conversion increased, however at this point in the optimization supply chain issues of the photocatalyst Ir(p-F-ppy)$_3$ was unavailable, which is when an alternative catalyst Ir(dFppy)$_3$ was implemented, and the reaction was re-evaluated using this photocatalyst (Table 3.5.1, entry 4). Due to the moderate conversion, futher base evaluation was performed and sodium carbonate anhydrous gave a slight improvement on conversion (Table 3.5.1, entry 5). Due to issues pertaining to the stability of the trifluoromethylation source, triflyl chloride, I found that allowing the reaction to proceed over two days with excess amount of triflyl chloride added after 24 hours improves the yields relative to the reported work (Table 3.5.1, entry 6). Dichloroethane was found to be comparable to chloroform (Table 3.5.1, entry 7) as well as a mixture of acetonitrile and water (Table 3.5.1, entry 8). Carbon tetrachloride was determined not a suitable solvent for this reaction (Table 3.5.1, entry 9). It should also be noted that the choice of solvent affected the innate selectivities of the substrates, for example, in acetonitrile N-Boc Aniline yields a 2:1 (*o*:*p*) ratio of trifluoromethylated product compared to 1:1.8 (*o*:*p*) in chloroform (Table 3.5.1).

**Table 3.5.1 Condensed Optimization for Trifluoromethylation on *N*-Boc Aniline**

| entry | photocatalyst | base | time (h) | solvent | conversion (%)[a] | *ortho*: *para* |
|---|---|---|---|---|---|---|
| 1 | $Ir(p\text{-}F\text{-}ppy)_3$ | $K_2HPO_4$ | 24 | MeCN | 75 | 2:1 |
| 2 | $Ir(p\text{-}F\text{-}ppy)_3$ | $K_2HPO_4$ | 24 | $CHCl_3$ | 37 | 1:1.1 |
| 3 | $Ir(p\text{-}F\text{-}ppy)_3$ | $(NH_4)_2HPO_4$ | 24 | $CHCl_3$ | 60 | 1:1.3 |
| 4 | $Ir(dFppy)_3$ | $(NH_4)_2HPO_4$ | 24 | $CHCl_3$ | 53 | 1:1.3 |
| 5 | $Ir(dFppy)_3$ | $Na_2CO_3$ | 24 | $CHCl_3$ | 60 | 1:1.6 |
| **6** | **$Ir(dFppy)_3$** | **$Na_2CO_3$** | **48** | **$CHCl_3$** | **77** | **1:1.8** |
| 7 | $Ir(dFppy)_3$ | $Na_2CO_3$ | 48 | DCE | 68 | 1:1.2 |
| 8 | $Ir(dFppy)_3$ | $Na_2CO_3$ | 48 | Hex:MeCN* | 65 | 1: 2.9 |
| 9 | $Ir(dFppy)_3$ | $Na_2CO_3$ | 48 | $CCl_4$ | 0 | - |

Solvent optimization for the trifluoromethylation of *N*-Boc Aniline. [a] % based on the sum of *ortho*-, *para*-, and *di*- trifluoromethylated product. *10:1 ratio of Hex:MeCN

To obtain a proof-of-concept, the optimized conditions were sufficient to begin exploring whether selectivity can be induced via LBCs. I have synthesized several LBCs that can be used to determine the regiochemical outcome of trifluoromethylation in chloroform. Using N-Boc Aniline as a control substrate, I observed two different catalysts able to prefer either the *ortho*- or *para*-addition. A Lewis basic selenoether catalyst was observed to prefer the *ortho*- constitutional isomer generating up to 3:1 (*o*:*p*) ratios yielding ~70% product of trifluoromethylated *N*-Boc aniline. It is important to note that when switching the photocatalyst from $Ir(pFppy)_3$ to $Ir(dFppy)_3$, there was a decrease in the formation of difunctionalized product. This result suggests a possible "secondary kinetic resolution" affecting initial results, where the minor monofunctionalized product undergoes a second trifluoromethylation event, causing a possible inflation of regioselectivity and an increase in difunctionalized product.[146] A bulky phosphine based catalyst, similar to known Buchwald ligands, was observed to prefer the *para*- constitutional isomer generating up to 1:3.7 (*o*:*p*) yielding ~72% of trifluoromethylated product.

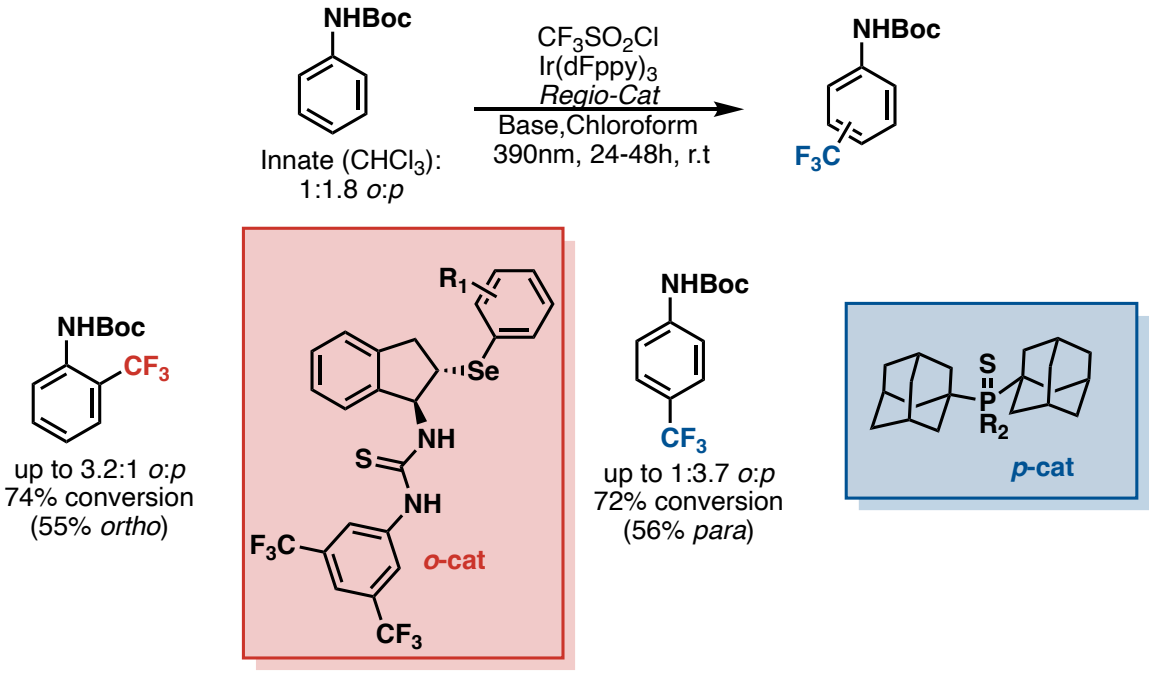


**Scheme 3.5.1 Proof-of-Concept for a Selective Trifluoromethylation of *N*-Boc Aniline**

My preliminary data supports my hypothesis that Lewis base catalysts can affect the regio-outcome for this reaction, however I recently discovered that this approach may be more general than originally anticipated. The Zhao trifluoromethylation, using sodium trifluoromethylsulfinate, of protected anilines are ran in DMSO. Initially I didn't expect that the LBC could affect any regio-control in this solvent as DMSO can participate in non-covalent interactions, however my preliminary results using DMSO has shown that LBC are still effective in these conditions as well in similar conversions and regioselectivities (Table 3.5.3).

**Table 3.5.3 Initial Selectivity Exploration on Zhao's Trifluoromethylation**

| entry | photocatalyst | oxidant | solvent | Regio-Cat | conversion (%)[a] | ortho: para |
|---|---|---|---|---|---|---|
| 1 | Eosin Y | $Na_2S_2O_8$ | DCE | - | 19 | 1:3.5 |
| 2 | Eosin Y | $Na_2S_2O_8$ | DCE | 2%RC | 14 | 1:4.2 |
| 3 | Eosin Y | $Na_2S_2O_8$ | EtOAc | - | 22 | 1:3.5 |
| 4 | Eosin Y | $Na_2S_2O_8$ | EtOAc | 2%RC | 24 | 1:3.3 |
| 5 | Eosin Y | $Na_2S_2O_8$ | tBuOAc | - | 14 | 1:5 |
| 6 | Eosin Y | $Na_2S_2O_8$ | tBuOAc | 2%RC | 15 | 1:2.7 |
| 7 | Eosin Y | $Na_2S_2O_8$ | MeCN | - | 35 | 1:5 |
| 8 | Eosin Y | $Na_2S_2O_8$ | MeCN | 2%RC | 28 | 1:3.2 |
| **9** | **Eosin Y** | **$Na_2S_2O_8$** | **DMSO** | **-** | **27** | **1:5.6** |
| **10** | **Eosin Y** | **$Na_2S_2O_8$** | **DMSO** | **2%RC** | **30** | **3.8:1** |

Based on precedent mechanisms in the literature,[51] I am propsing that the 'selective-step' is followed by the photoactivation of the electrophilic trifluoromethylation reagent (Figure 3.5.1). Selenium is known to participate in radical reactions, thus it is plausible to form a Se-$CF_3$ bond where the radical is now delocalized on Selenium before homolysis via a nucleophilic arene.[147] Subsequent SET of the Wheland-type intermediate followed by rearomatization may give the desired product. In order to find evidence of this transformation, cyclic voltammetry should be utilized to find the redox potentials of all reagents, especially the LBC, as well as implementing Stern-Vollmer quenching studies to determine the liklihood of reactivity.

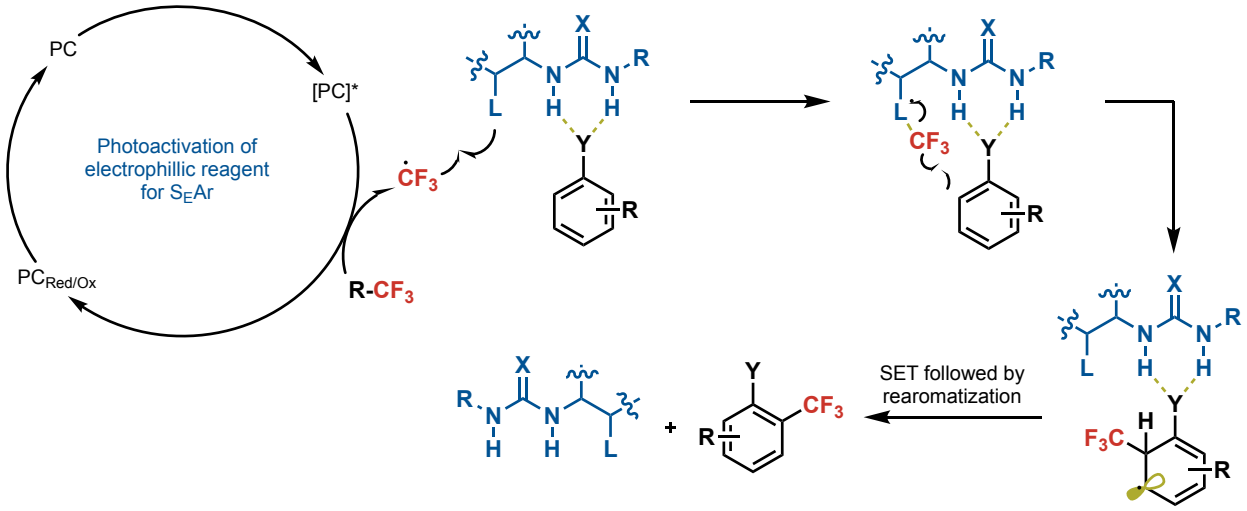


**Figure 3.5.1 Proposed Mechanism for *ortho*-Selective Trifluoromethylation**

Now that proof-of-concept was established, there are a considerable amount of factors to be realized before a generalized *ortho*-selective trifluoromethylation procedure can be synthetically useful. Firstly, the work mentioned was obtained on *N*-Boc Aniline and it would be an improvement to explore how other protecting groups will be affected using this approach (i.e, sterics). It is important to note that the substrate scope for the MacMillan trifluoromethylation is very diverse, thus it would be interesting to see the limits at which the LBCs can control the selectivity across substrates other than anilides, anilines, and phenols, all of which have proven to have induced selectivities in the context of chlorination.[128] The LBCs used have diversifiable moieties as both the Lewis base and the H-bonding handle can be tuned to the substrate and the radical. For example, trifluoromethyl groups are larger than chlorine atoms, however the rotation about the Se-Aryl bond allows for physical compensation as the aryl ring can freely rotate. This can be explored experimentally but computational chemistry would be most helpful. Also, it is important to note that these studies were focused on catalyst scaffolds previously reported from the Gustafson group to affect regioselectivity, however there are many 'organocatalysts', developed in the context of enantioselectivity, that exist and can be evaluated for additional

selectivity control. The LBCs should be evaulated through electrochemistry as it should not interact with the photocatalyst in order to maximize its affect on selectivity. Development of this reaction would aid LSF efforts and could be synthetically useful in drug discovery endeavors.

## 3.6 Experimental Section

### 3.6.1 General Information

All $^{1}H$ and $^{13}C$ NMR Spectra were recorded on Varian VNMRS 400 MHz, Bruker Avance $AV_1$ 400MHz, Varian Inova 500 MHz, and Bruker Avance III HD 600MHz at room temperature. All chemical shifts were reported in parts per million (δ) and internally referenced to residual solvent proton signals unless otherwise noted. All spectral data were reported as follows: (multiplicity [singlet (s), doublet (d), doublet of doublets (dd), doublet of doublet of doublets (ddd), doublet of triplets (dt), triplet (t), triplet of triplets (tt), quartet (q), quintet (qn), and multiplet (m), heptet (h)], coupling constants [Hz], integration). Carbon spectra were recorded with complete decoupling. Conventional mass spectra were obtained using Advion Expression$^{s}$ CMS APCI/ASAP. All chemicals and catalysts were purchased from Acros Organics, Cambridge Isotope Laboratories, Fisher Scientific, Frontier Scientific, Oakwood Chemicals, Sigma Aldrich, or TCI America. All normal phase flash column chromatography (FCC) was performed using Grade 60 Silica Gel (230-400 mesh) purchased from Fisher Scientific. Preparative Thin Layer Chromatography (TLC) plates contained grade 60 silica gel coated with fluorescent indicator $F_{254}$ and were purchased from Fisher Scientific. Reflux conditions were done using an Anton Paar Monowave 400, G10, and G30 vials.

### 3.6.2 General Procedure: Synthesis of Indane-Based Catalysts and Related Fragments

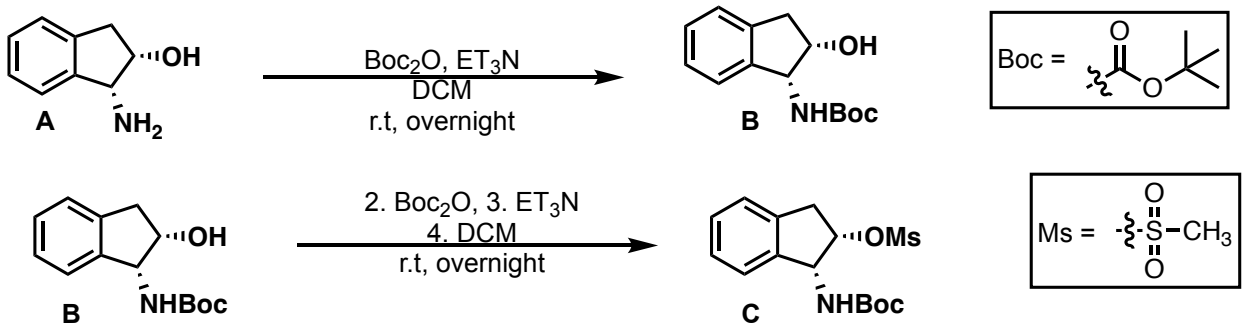


**Scheme 3.6.1 General Procedure for Protection of Indane Catalyst Scaffold**

The following procedure is based on a general procedure from published literature.[128] To a two-neck round bottom flask and stir bar (oven-dried), **(1S, 2R)-1-amino-2,3-dihydro-1H-inden-2-ol** (33.5mmol, 1.0 equiv.), **A**, and anhydrous DCM (0.2M) were added. Triethylamine (50.25mmol, 1.5 equiv.) was then added and the reaction was stirred for 15 minutes until the addition of $Boc_2O$ (36.8mmol, 1.1 equiv.). The reaction was stirred until completion by TLC before rotary evaporation of solvent and base to give **(1S,2R)-2-hydroxy-2,3-dihydro-1H-inden-1-yl)** carbamate, **B** , as a off-white solid, albeit clear oil if residual solvent or base is present. This product was then used, as is, in the next reaction adapted from the same published literature.

After drying, **B**, was added to a single neck round bottom flask where anhydrous triethylamine (1.5 equiv.) and anhydrous DCM. The reaction was cooled to 0ºC and MsCl (1.2 equiv.) was then added dropwise. The reaction was allowed to stir overnight at room temperature. The reaction was quenched with 1M $NaHCO_3$ solution and extracted twice with two equal portions of DCM, dried with Na2SO4, filtered, and concentrated under reduced pressure to give **(1S, 2R)-1-((tert-butoxycarbonyl)amino)-2,3-dihydro-1H-inden-2-ylmethanesulfonate**, C, as an off-white solid. No further purification was needed and the NMR spectra matched literature precedence.

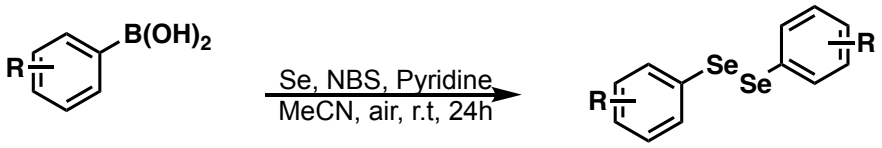


**Scheme 3.6.2 General Synthesis of Diaryl Diselenides**

The following procedure is based on a general procedure from published literature.[128] To a round bottom flask, selenium powder (1.2 equiv.) and *N*-bromosuccinimide (1.2 equiv.) were added along with 0.2M of MeCN. This solution was stirred for 20 minutes before aryl boronic acid (1.0 equiv.) was added followed by pyridine (2.5 equiv.). The resulting solution was stirred in open air overnight at 60ºC . The reaction was then concentrated under reduced pressure and purified by FCC in 100% hexanes or a 10:1 Hexanes:EtOAc to afford the desired product.

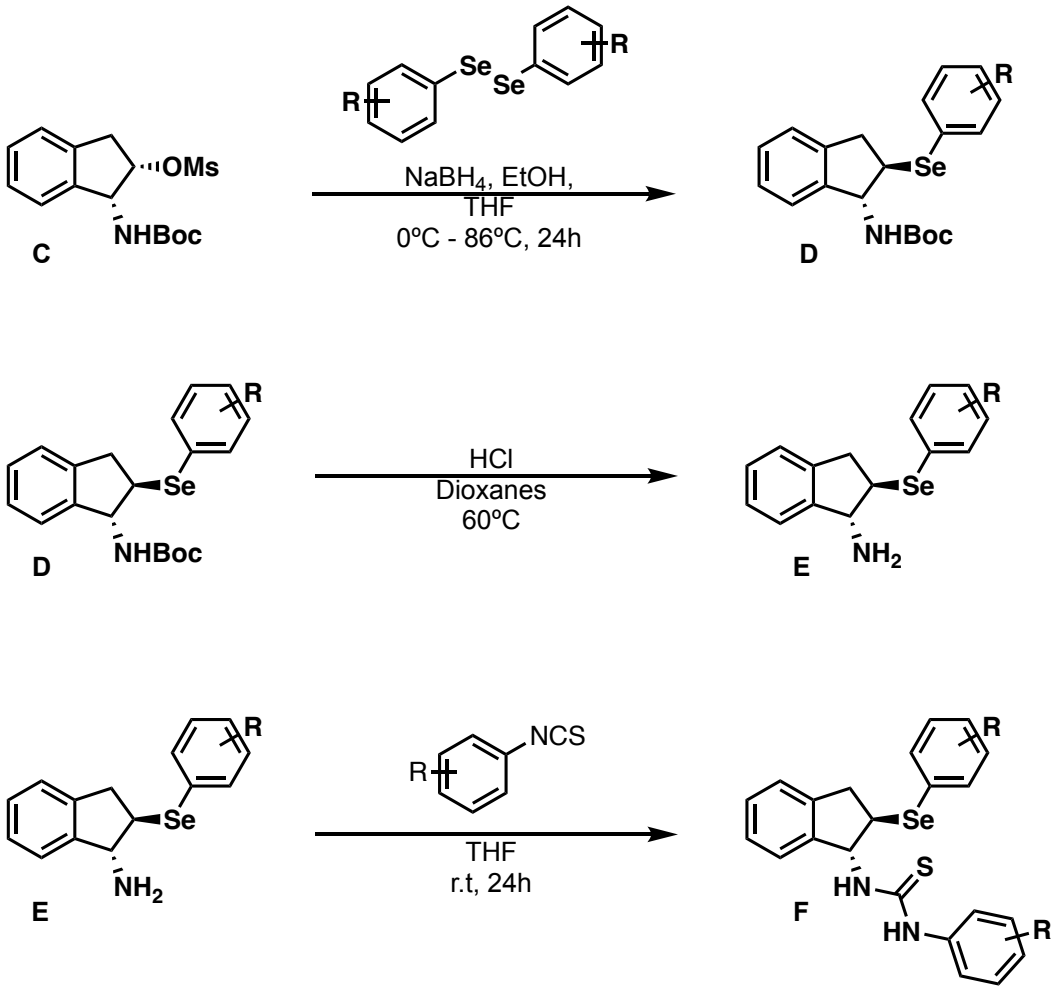


**Scheme 3.6.3 General Synthesis of Lewis Base Substitution and H-Bonding Handle**

The following procedure is based on a general procedure from published literature.[128] To an oven-dried two-neck round bottom flask with a stir bar, $NaBH_4$ (2.0 equiv) was added to anhydrous ethanol (0.15M) at 0ºC for 15 minutes. A solution of diselenide in anhydrous THF (0.15M) was then injected drop wise at 0ºC, and the resulting solution was stirred at r.t for 15 minutes.* (This step is typically colorless and is used as an indicator of anhydrous technique. If color remains upon reduction, it was found that water was present and the reduction did not occur.) The reaction was then cooled to 0ºC again, and a solution of **C** in anhydrous THF (0.15M) was added dropwise. Upon complete addition, the reaction was heavily purged with Argon gas and connected to a reflux condenser and was refluxed overnight at 85ºC. The reaction was quenched

with aqueous $NH_4Cl$ and extracted twice with equal portions of DCM. The combined organic layers were dried over $Na_2SO_4$,and concentrated under reduced pressure in a tared round bottom. No further purification is necessary as the crude material, **D**, was used entirely in the next step.

When dried, the weight of the crude was measured before addition of a stir bar was added to **D**. The product was then deprotected using a solution of 6M HCl (10 equiv.) in dioxanes (0.1M) and stirred at 60ºC under Argon for 12 hours. The reaction was quenched with 1M NaOH solution until pH 14. The resulting solution was extracted three times with EtOAc and the combined organic layers were dried with $Na_2SO_4$ before concentration under reduced pressure. The crude material, **E**, was dried in a tared was used directly in the next step without further purification.

The last step is to subject **E** to an isothiocyanate (1.5 equiv.) or isocyante (1.5 equiv.) in THF (0.2M). The reaction is stirred overnight before rotary evaporation. Crude material is purified by FCC in 75:25 Hexanes:EtOAc.

### 3.6.2 General Procedure for Trifluoromethylation of Anilides and DFCS Photocatalyst

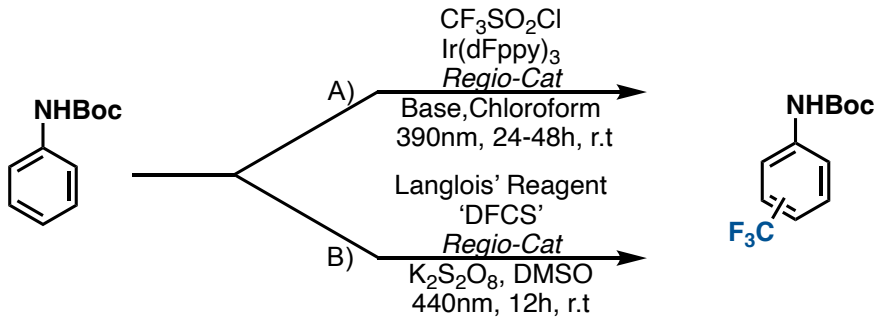


**Scheme 3.6.4 General Trifluoromethylation Procedures**

A) The following procedure was adapted from precendent literature procedure.[51] To an 8mL boroscilicate vial and stir bar was added *N*-BocAniline (0.125mmol, 1.0 equiv.), $Ir(dFppy)_3$ (0.02 equiv.), $Na_2CO_3$ (3.0 equiv.), $CF_3SO_2Cl$ (4 equiv.), and regiocatalyst (1-5 mol%) were added. The reaction was sealed with a septa-containing cap and oxygen was removed with a Schlenck line and backfilled with $N_2$ gas. Anhydrous chloroform (0.0625M) was added and the resulting

mixture was subjected to freeze-pump-thaw three times before irradiation for 24 hours. The reaction was then quenched with brine and extracted three times with DCM before drying with $Na_2SO_4$.

B) The following procedure was adapted from precendent literature procedure.[145] To an 8mL boroscilicate vial and stir bar was added *N*-BocAniline (0.125mmol, 1.0 equiv.), DFCS (0.02 equiv.), $K_2S_2O_8$ (2.0 equiv.), Langlois' reagent (2.0 equiv.), and regiocatalyst (0.02 equiv.) were added. 0.0625M of DMSO was added and the reaction was quickly flushed with $N_2$ before irradiation overnight. The reaction was then quenched with 10% LiCl solution and extracted three times with DCM before drying with $Na_2SO_4$ and concentration under reduced pressure.

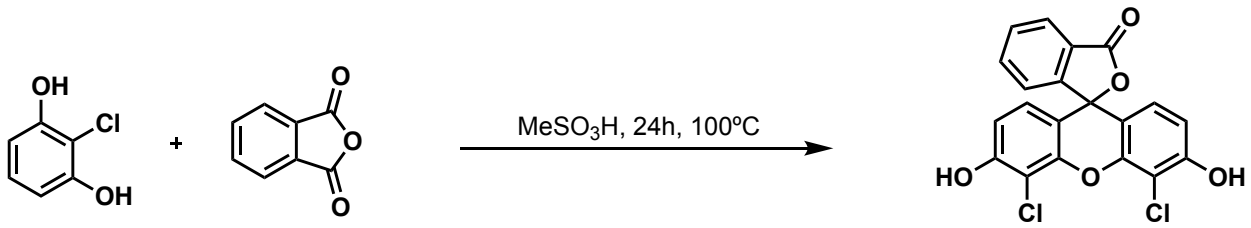


**Scheme 3.6.5 'DFCS' Synthesis**

The following procedure was adapted from precendent literature procedure.[145] To a round bottom flask and stirbar was added phthalic anhydride (741mg, 5 mmol, 1.0 equiv.) and 2-chlororesorcinol (1.6g, 11 mmol, 2.2 equiv.) in 7.5mL $Me_3SOH$. The reaction was heated under Argon for 24 hours at 100ºC. The solution was cooled to room temperature and the reaction was poured into 30mL of ice water to precipitate a solid. The solid was filtered and does not need to be dried completely. The solid was then transferred to an Erlenmeyer flask where it was dissolved in 30mL of 4M NaOH and stirred for 30 minutes. The solution was then adjusted to pH <5 with concentrated HCl and a large amount of precipitate was formed. The precipitate was then filtered off, rinsed with water, and purified by FCC in 1:1 DCM:EtOAc to afford the desired product as an orange solid.

### 3.6.3 Characterization of Catalysts and Trifluoromethylated *N*-Boc Aniline

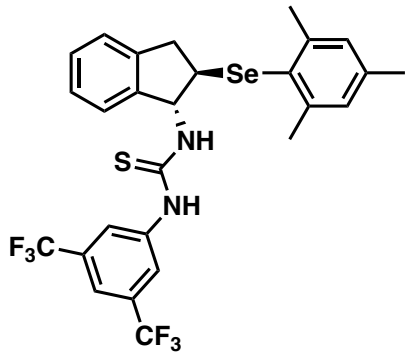


**Figure 3.6.1 Compound 3.6.1a**

The following was synthesized using the general synthesis procedure for the Lewis base substitution and H-Bonding handle and literature precedence.[128] **Yields** (3 mmol scale): 800mg, 44% overall yield, pale white solid. **$^{1}$H NMR (400MHz, dDMSO):** $\delta$ = 9.99 (s, 1H), 8.59 (d, 1H, J = 5.3 Hz), 8.25 (s, 2H), 7.78 (s, 1H), 7.38 (m, 1H), 7.25 (m, 3H), 6.97 (s, 2H), 5.94 (brs, 1H), 3.91 (q, 1H, J = 6.8 Hz), 3.36 (s, 1H), 3.24 (dd, 1H, J= 16.3, 6.8 Hz), 2.79 (dd, 1H, J = 16.3, 6.6 Hz), 2.5 (s, 6H), 2.2 (s, 3H). **$^{13}$CNMR (126 MHz, dDMSO):** $\delta$ = 180.7, 142.9, 141.8, 141.7, 130.1 (q, J = 32 Hz), 128.3, 128.1, 126.8, 126.4, 124.5, 124.3, 124.2, 122.2, 122.1, 119.9, 116.2, 64.9, 45.2, 37.5, 24.3, 20.4. **$^{19}$F NMR (dDMSO, 376 MHz):** $\delta$ = -61.57. **HRMS (ESI) m/z: $[M+H]^+$** Calcd for $C_{27}H_{25}F_6N_2SSe$ $[M+H]^+$, 603.080784; Found 603.0835. This is in spectral agreement with precedent literature.[128]

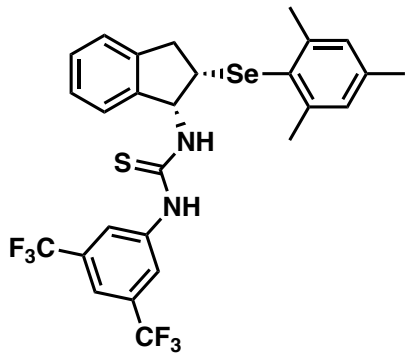


**Figure 3.6.2 Compound 3.6.2a**

The following was synthesized using the general synthesis procedure for the Lewis base substitution and H-Bonding handle and literature precedence.[128] **Yields** (3 mmol scale): 740mg, 41% overall yield, pale white solid. **$^{1}$H NMR (500MHz, dDMSO):** $\delta$ = 10.22 (s, 1H), 8.66 (d, 1H, J = 7.4 Hz), 8.36 (s, 2H), 7.79 (s, 1H), 7.29 (m, 4H), 6.93 (s, 2H), 6.00 (t, 1H, J = 6.9 Hz), 4.61 (t, 1H, J = 5.5 Hz), 3.33 (s, 3H), 3.21 (dd, 1H, J = 17.1, 5.9 Hz), 2.66 (d, 1H, J = 16.6 Hz), 2.36 (s, 6H), 2.18 (s, 3H). **$^{13}$CNMR (126 MHz, dDMSO)** $\delta$ = 181.1, 143.2, 141.9, 141.2, 137.8, 130.3 (q, J= 36 Hz), 128.4, 128.2, 126.7, 126.3, 125.1, 124.6, 123.5, 121.6, 116.4, 61.8, 48.3, 37.0, 24.0, 20.5. **$^{19}$F NMR (dDMSO, 376 MHz):** -63.87. **HRMS (ESI) m/z: [M+H]$^{+}$** Calcd for $C_{27}H_{25}F_6N_2SSe$ $[M+H]^{+}$, 603.080784; Found 603.0829

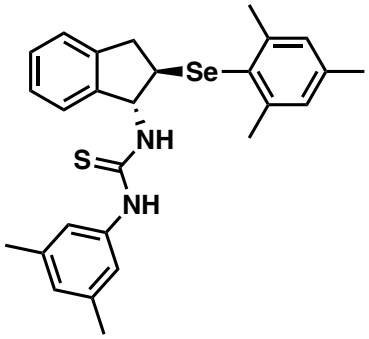


**Figure 3.6.3 Compound 3.6.3a**

The following was synthesized using the general synthesis procedure for the Lewis base substitution and H-Bonding handle and literature precedence.[128] **Yields** (3 mmol scale): 340mg, 23% overall yield, beige solid. **$^{1}$H NMR (500MHz, dDMSO):** $\delta$ = 9.45 (s, 1H), 7.98 (d, 1H, J = 7.9 Hz), 7.28 (m, 1H), 7.18 (m, 3H), 6.97 (s, 2H), 6.91 (s, 2H), 6.74 (s, 1H), 6.00 (t, 1H, J = 7.3 Hz), 3.88 (q, 1H, J = 7.5 Hz), 3.14 (dd, 1H, J = 15.9, 7.5 Hz), 2.78 (dd, 1H, J = 16.6, 7.8 Hz), 2.50 (s, 6H), 2.20 (s, 9H). **$^{13}$CNMR (126 MHz, dDMSO)** $\delta$ = 180.5, 143.0, 142.7, 141.4, 138.5, 137.8,

137.7, 128.4, 127.8, 126.8, 126.7, 125.9, 124.3, 124.1, 121.0, 65.1, 45.6, 37.8, 24.5, 20.9, 20.6. **HRMS (ESI) m/z: $[M+H]^+$** Calcd for $C_{27}H_{31}N_2SSe$ $[M+H]^+$, 495.1373 ; Found 495.1402

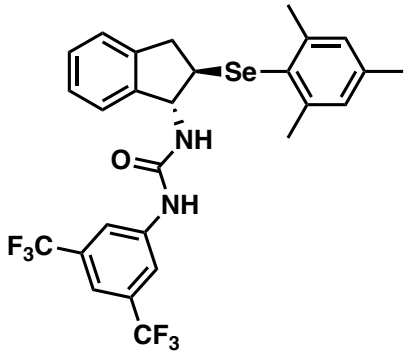


**Figure 3.6.4 Compound 3.6.4a**

The following was synthesized using the general synthesis procedure for the Lewis base substitution and H-Bonding handle and literature precedence.[128] **Yields** (3 mmol scale): 641mg, 36% overall yield, white solid. **$^1$H NMR (500MHz, dDMSO):** $\delta$ = 9.12 (s, 1H), 8.11 (s, 2H), 7.58 (s, 1H), 7.22 (m, 4H), 6.91 (s, 2H), 5.19 (t, 1H, J = 7.9 Hz), 3.76 (q, 1H, J = 7.9 Hz), 3.19 (dd, 1H, J = 16.3, 7.7 Hz), 2.79 (dd, 1H, J= 16.3, 8.1 Hz), 2.47 (s, 6H), 2.11 (s, 3H). **$^{13}$CNMR (126 MHz, dDMSO):** $\delta$ = 154.5, 143.1, 142.9, 142.5, 141.1, 137.8, 130.8, 130.5, 128.4, 127.8, 126.9, 126.5, 124.4, 123.7, 117.6 (q, J= 4 Hz), 113.6, 61.0, 46.0, 37.6, 24.2, 20.4. **$^{19}$F NMR (dDMSO, 376 MHz):** -61.71. **HRMS (ESI) m/z: $[M+H]^+$** Calcd for $C_{27}H_{25}F_6N_2OSe$ $[M+H]^+$, 587.1036; Found 587.1047

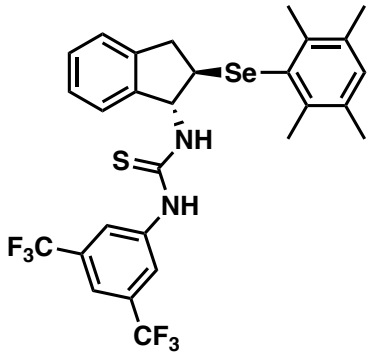


**Figure 3.6.5 Compound 3.6.5a**

The following was synthesized using the general synthesis procedure for the Lewis base substitution and H-Bonding handle and literature precedence.[128] **Yields** (3 mmol scale): 210mg, 11% overall yield, yellow-white solid. **$^{1}$H NMR (500MHz, dDMSO):** $\delta$ = 9.92 (s, 1H), 8.5 (d, 1H, J = 6.4 Hz), 8.23 (s, 2H), 7.76 (s, 1H), 7.34 (m, 1H), 7.22 (m, 3H), 6.90 (s, 1H), 5.90 (brs, 1H), 3.84 (q, 1H, J = 6.9 Hz), 3.22 (dd, 1H, J = 16.8, 7.0 Hz), 2.79 (dd, 1H, J = 16.8, 7.0 Hz), 2.5 (s, 6H), 2.17 (s, 6H). **$^{13}$CNMR (126 MHz, CDCl3)** $\delta$ = 180.6, 141.9, 141.7, 141.5, 138.7, 133.4, 131.9, 130.9, 130.1 (q, J = 33 Hz), 128.0, 126.7, 124.4, 124.3, 122.1, 116.2, 64.8, 45.6, 37.5, 21.3, 20.7. **$^{19}$F NMR ($CDCl_3$, 376 MHz):** -61.58. **HRMS (ESI) m/z: $[M+H]^+$** Calcd for $C_{28}H_{27}F_6N_2SSe$ $[M+H]^+$, 617.0964; Found 617.0979. This is in spectral agreement with precedent literature.[128]

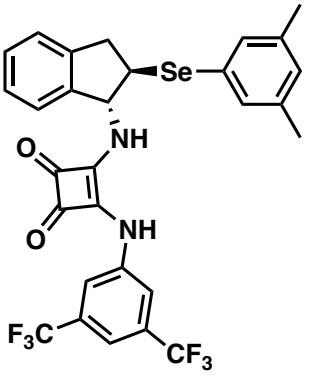


**Figure 3.6.6 Compound 3.6.6a**

The following was synthesized using the general synthesis procedure for the Lewis base substitution and H-Bonding handle and literature precedence.[128] **Yields** (3 mmol scale): 760mg, 40% overall yield, light brown solid. **$^{1}$H NMR (500MHz, dDMSO):** $\delta$ = 9.90 (s, 1H), 7.95 (s, 2H), 7.69 (s, 1H), 7.30 (m, 4H), 7.18 (s, 2H), 6.68 (s, 1H), 5.71 (t, 1H, J = 7.1 Hz), 4.01 (q, 1H, J = 8.4 Hz), 3.43 (dd, 1H, J = 17.3, 7.6 Hz), 2.95 (dd, 1H, J = 16.6, 9.0 Hz), 2.12 (s, 6H). **$^{13}$CNMR (126 MHz, dDMSO):** $\delta$ = 180.9, 169.4, 162.3, 141.4, 141.0, 140.8, 138.4, 131.6, 128.9, 128.7, 127.3, 127.1, 124.6, 124.3, 123.7, 117.9 (q, J = 11 Hz), 114.7, 66.0, 47.1, 36.8, 20.6. **$^{19}$F NMR (dDMSO, 376 MHz):** -61.73. **HRMS (ESI) m/z: [M+H]$^{+}$** Calcd for $C_{29}H_{23}F_6N_2O_2Se$ $[M+H]^{+}$, 625.0829; Found 625.0846

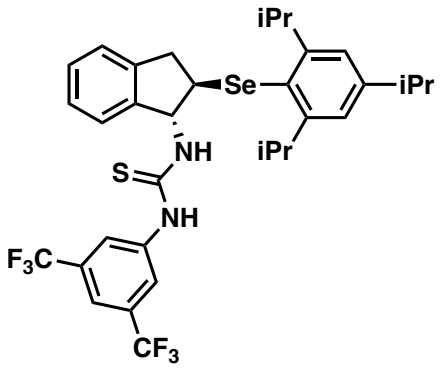


**Figure 3.6.7 Compound 3.6.7a**

The following was synthesized using the general synthesis procedure for the Lewis base substitution and H-Bonding handle and literature precedence.[128] **Yields** (3 mmol scale): 368mg, 17% overall yield, pale white solid.**$^1$H NMR (500MHz, $CDCl_3$):** $\delta$ = 9.99 (s, 1H), 8.68 (m, 1H), 8.25 (s, 2H), 7.75 (s, 1H), 7.41 (m, 1H), 7.25 (m, 3H), 7.07 (s, 2H), 5.93 (brs, 1H), 3.82 (h, 3H, J = 6.5 Hz), 3.27 (dd, 1H, J = 16.5, 7.3 Hz), 2.87 (p, 1H, J = 6.7 Hz), 2.78 (dd, 1H, J = 16.5, 5.5 Hz), 1.17 (m, 18H). **HRMS (ESI) m/z: $[M+H]^+$** Calcd for $C_{33}H_{37}F_6N_2SSe$ $[M+H]^+$, 687.1747 Found 687.1770. This is in spectral agreement with precedent literature.[128]

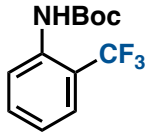


**Figure 3.6.8 Compound 3.6.8a**

The following was synthesized using the general procedure for ttrifluoromethylation of anilides and literature precedence.[51] **Yields** (0.125 mmol scale): 10.3mg, 30% overall innate yield,[51] white solid.**$^1$H NMR (400MHz, $CDCl_3$):** $\delta$ = 8.14 (d, 1H, J= 9.1 Hz), 7.57 (d, 1H, J = 8.0 Hz), 7.54 (t, 1H, J = 6.8 Hz), 7.15 (t, 1H, J = 6.8 Hz), 6.80 (brs, 1H), 1.53 (s, 9H). **$^{19}$F NMR (400MHz, $CDCl_3$):** -60.88. This is in spectral agreement with precedent literature.[51]

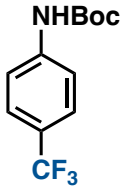


**Figure 3.6.9 Compound 3.6.9a**

The following was synthesized using the general procedure for trifluoromethylation of anilides and literature precedence.[51] **Yields** (0.125 mmol scale): 21.3mg, 68% innate yield,[145] white solid.**$^1$H NMR (400MHz, $CDCl_3$):** $\delta$ = 7.49 (d, 2H, J = 6.7 Hz), 7.35 (d, 2H, J = 8.7 Hz), 6.7 (brs,

1H), 1.63 (s, 9H). **$^{19}$F NMR (400MHz, $CDCl_3$):** -61.96. This is in spectral agreement with precedent literature.[51]

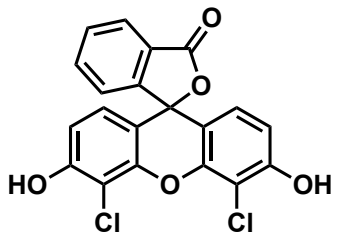


**Figure 3.6.10 Compound 3.6.10a**

This compound was synthesized using the general procedure for the 'DFCS' catalyst.[145] Yield (5 mmol): 1.68g, 84% yield, bright orange solid. **$^1$H NMR (500MHz, dDMSO):** $\delta$ = 10.93 (s, 1H), 8.01 (s, 1H), 7.76 (dd, 2H, J = 23, 7 Hz), 7.72 (s, 1H), 6.8 (m, 2H), 6.57 (m, 2H), 3.35 (s, 1H). This is in spectral agreement with precedent literature.[145]

## 3.6.4 Spectral Data for Characterized Molecules ($^{1}H$, $^{13}C$, $^{19}F$ NMR)

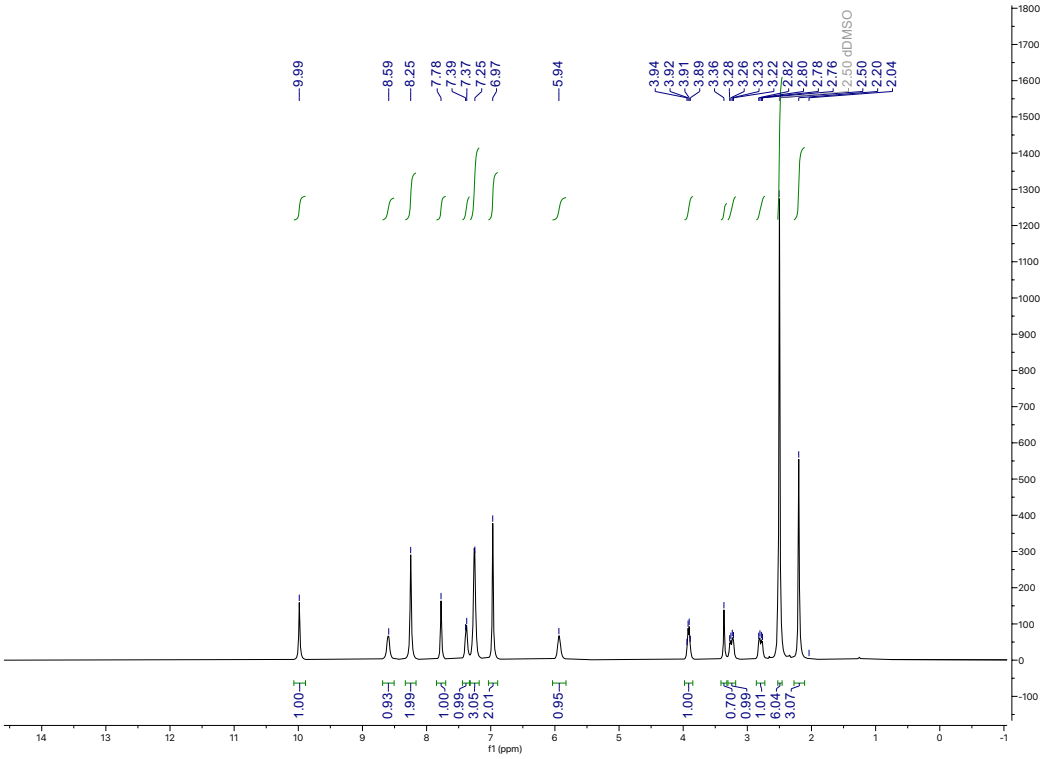


**Figure 3.6.11 $^{1}$HNMR Spectra of 3.6.1a**

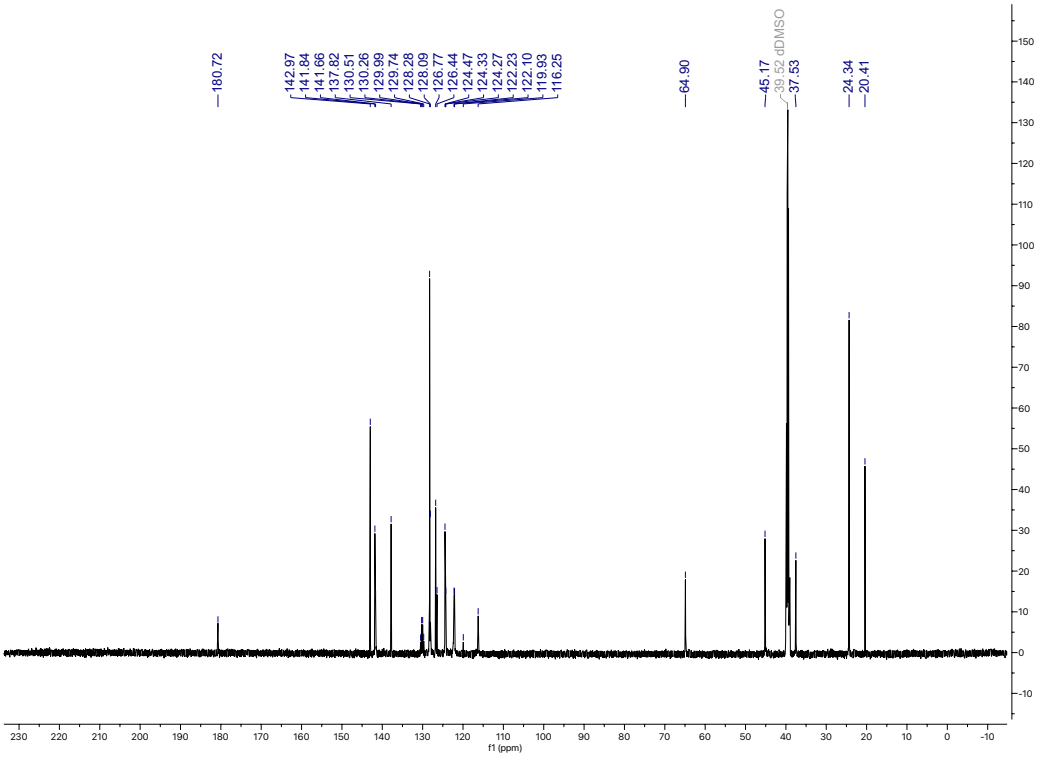


**Figure 3.6.12 $^{13}$CNMR Spectra of 3.6.1a**

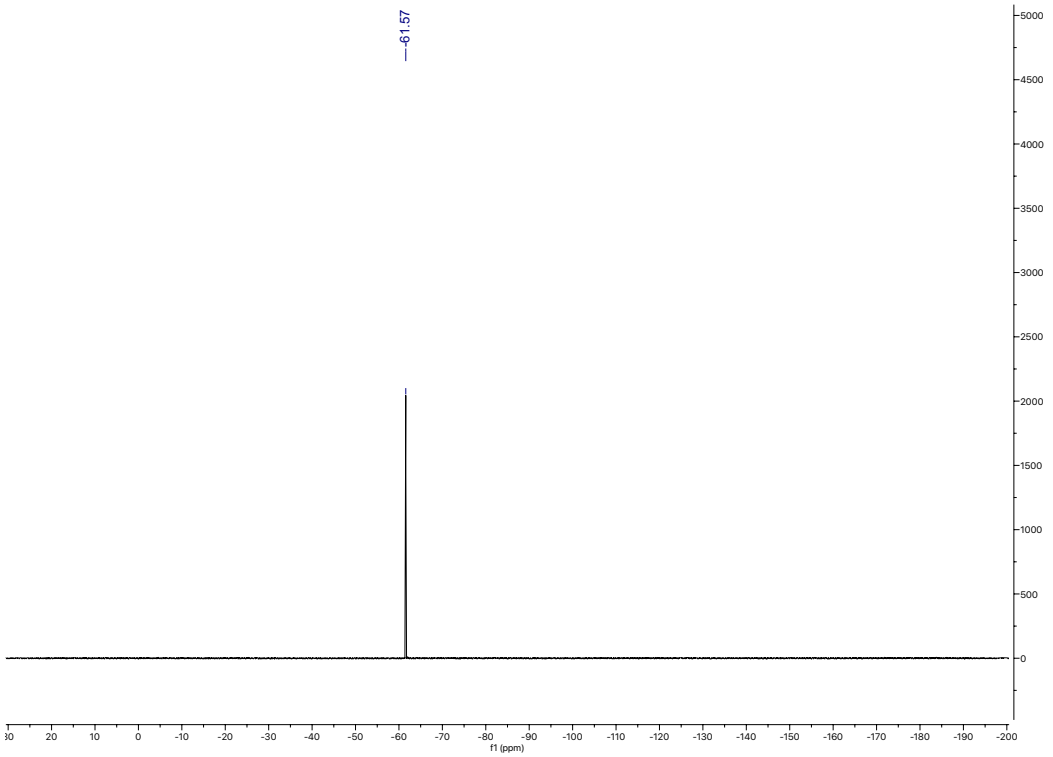


**Figure 3.6.13 $^{19}$FNMR Spectra of 3.6.1a**

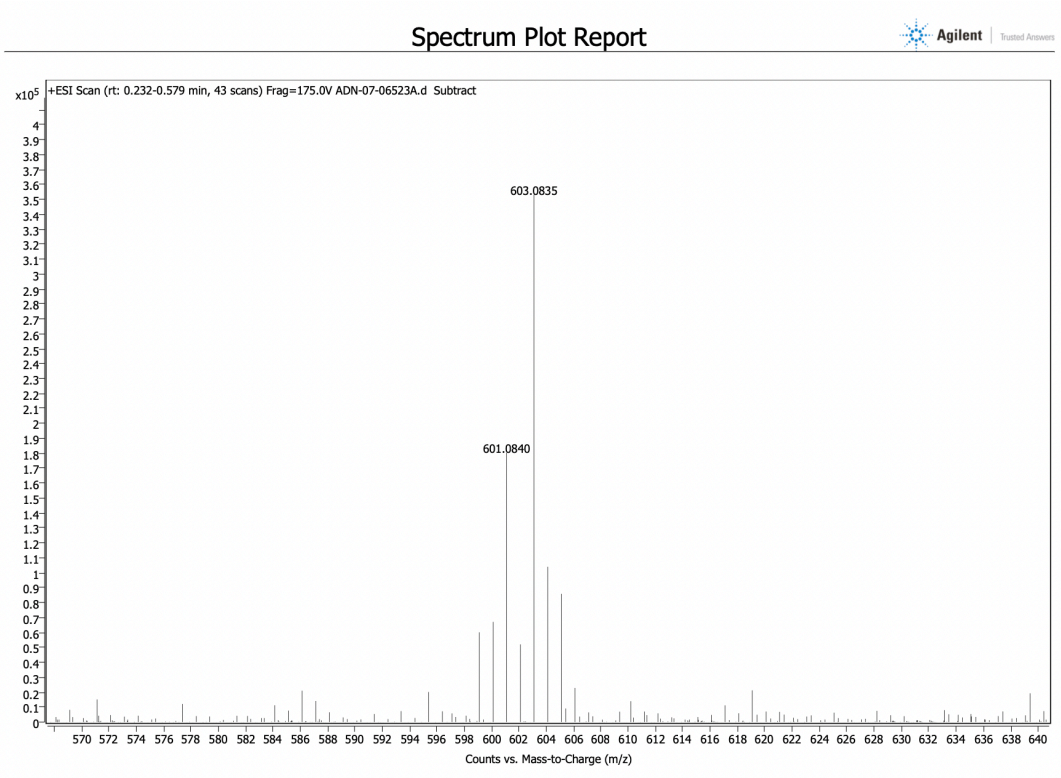


**Figure 3.6.14 HRMS (ESI) Spectra of 3.6.1a**

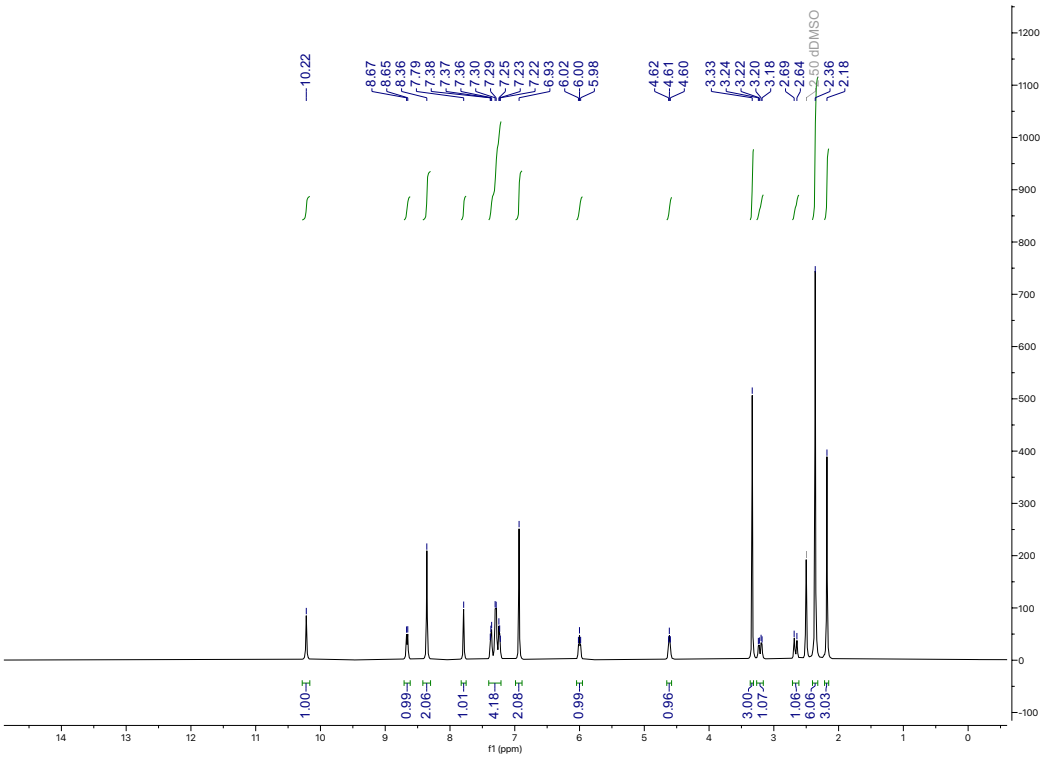


**Figure 3.6.15 $^{1}$HNMR Spectra of 3.6.2a**

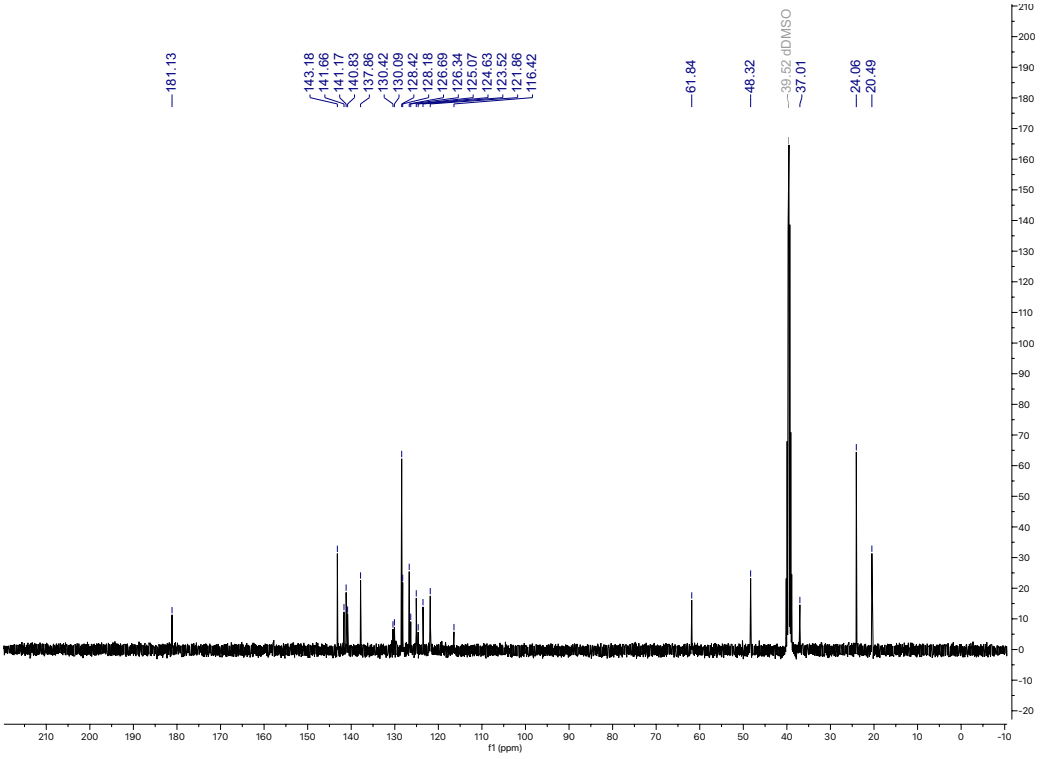


**Figure 3.6.16 $^{13}$CNMR Spectra of 3.6.2a**

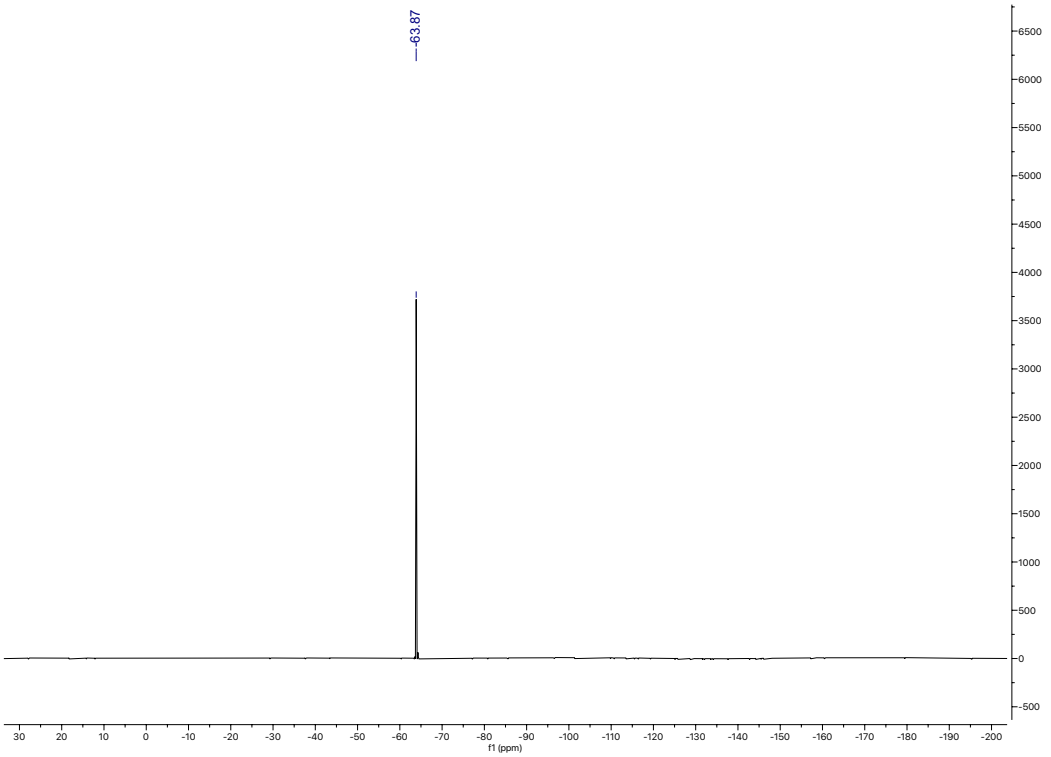


**Figure 3.6.17 $^{19}$FNMR Spectra of 3.6.2a**

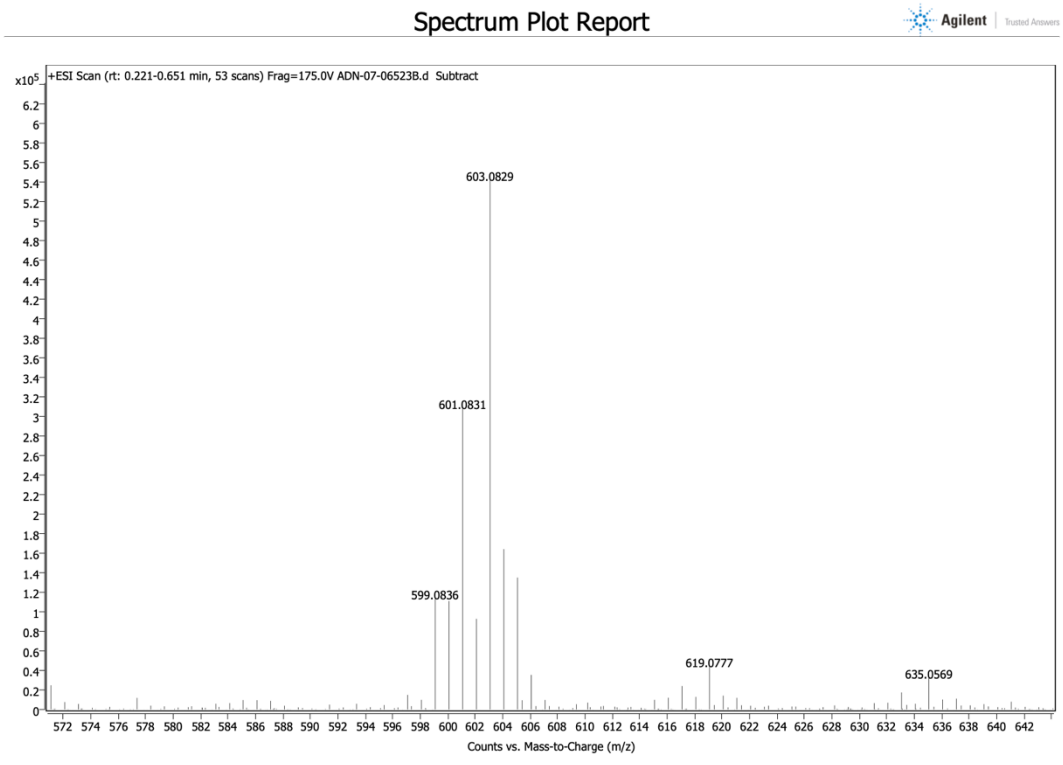


**Figure 3.6.18 HRMS (ESI) Spectra of 3.6.2a**

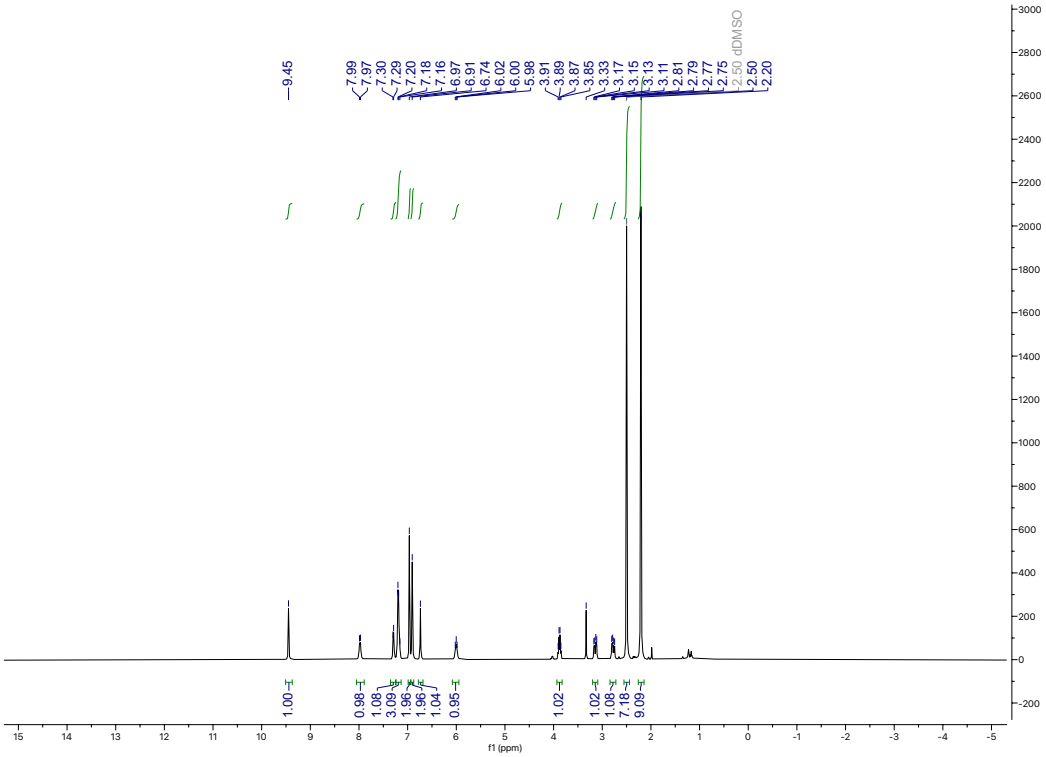


**Figure 3.6.19 $^{1}$HNMR Spectra of 3.6.3a**

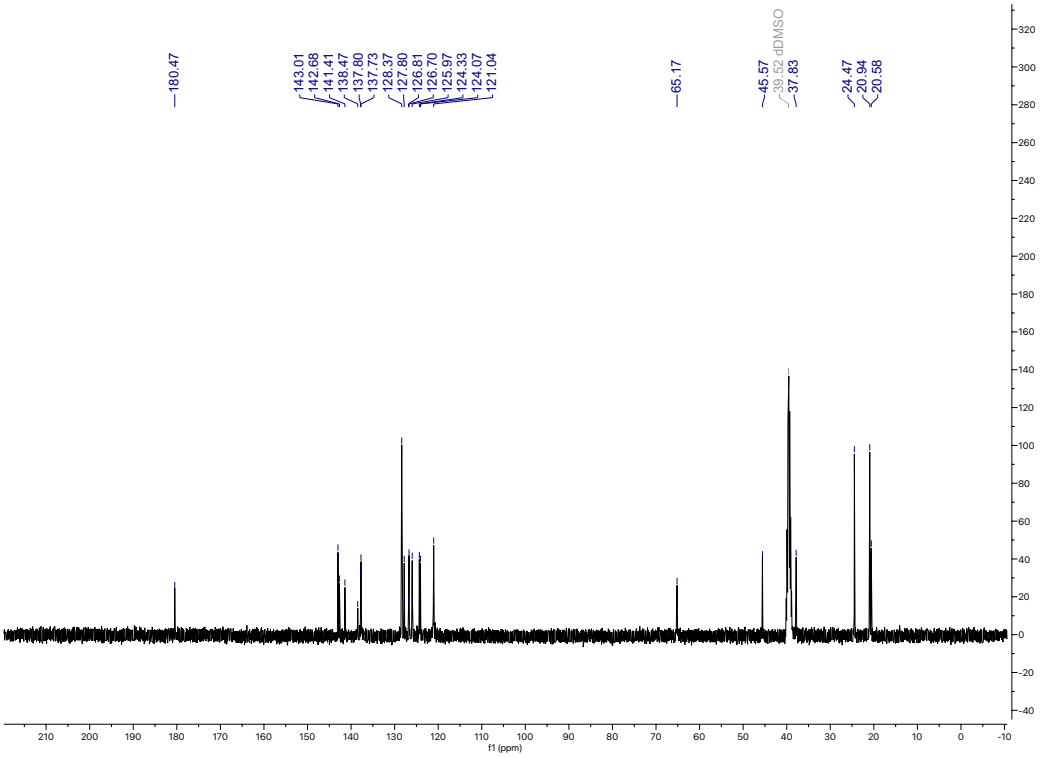


**Figure 3.6.20 $^{13}$CNMR Spectra of 3.6.3a**

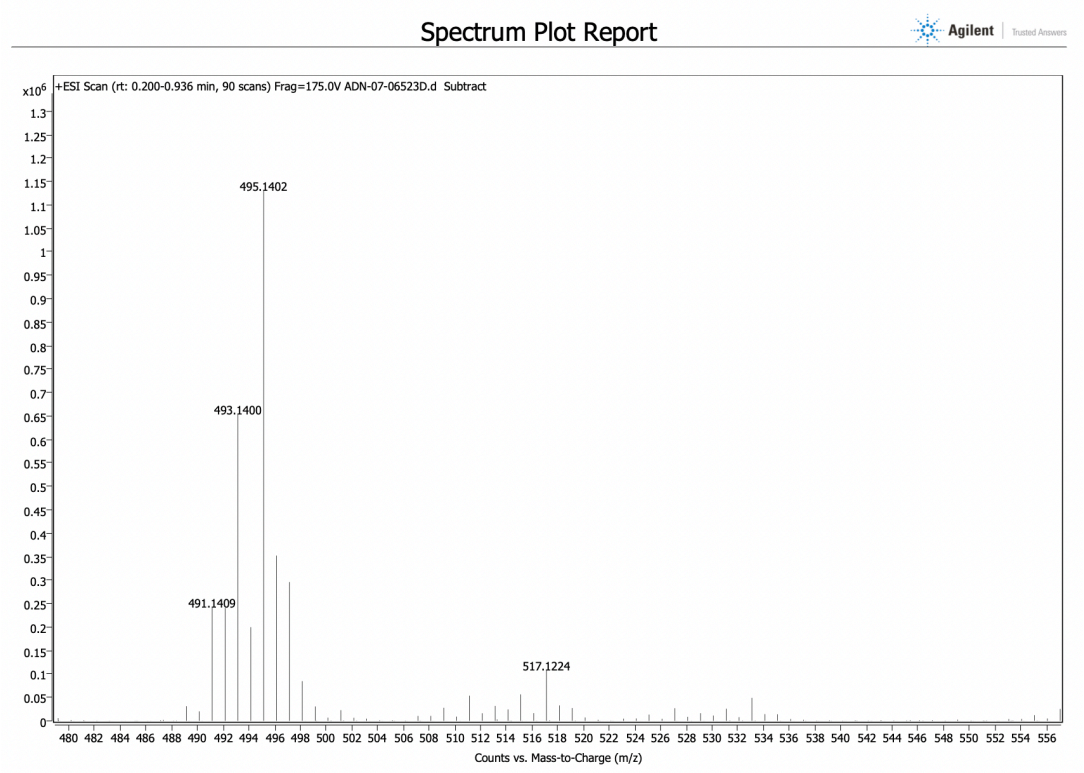


**Figure 3.6.21 HRMS (ESI) Spectra of 3.6.3a**

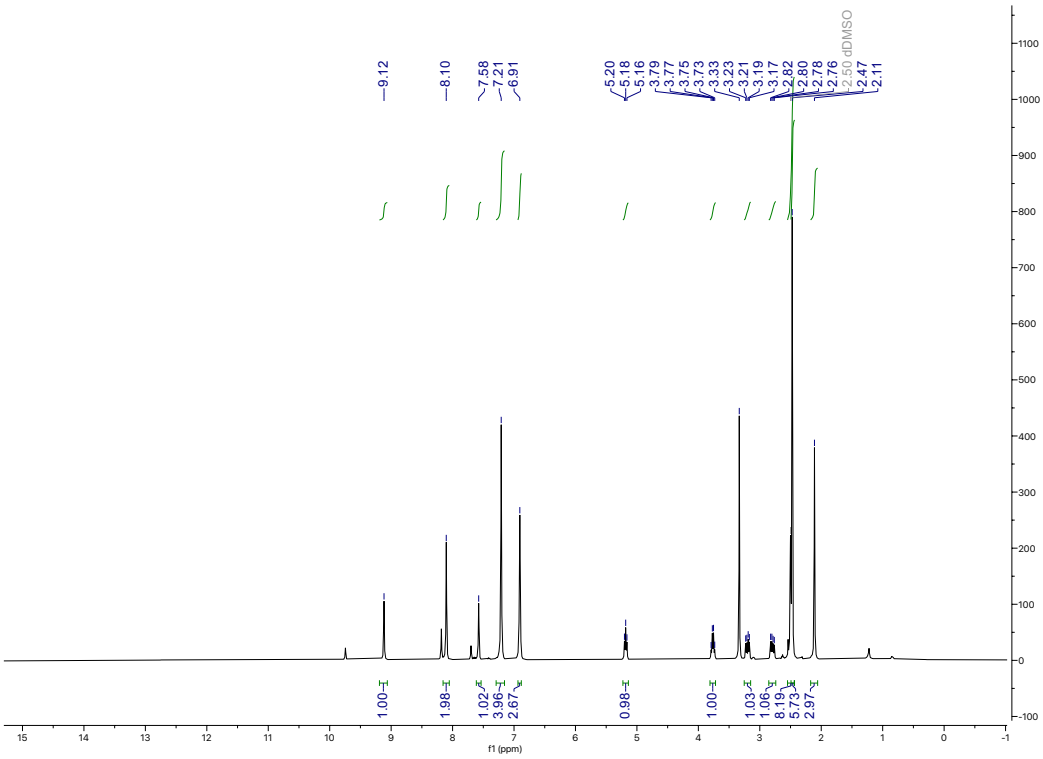


**Figure 3.6.22 1HNMR Spectra of 3.6.4a**

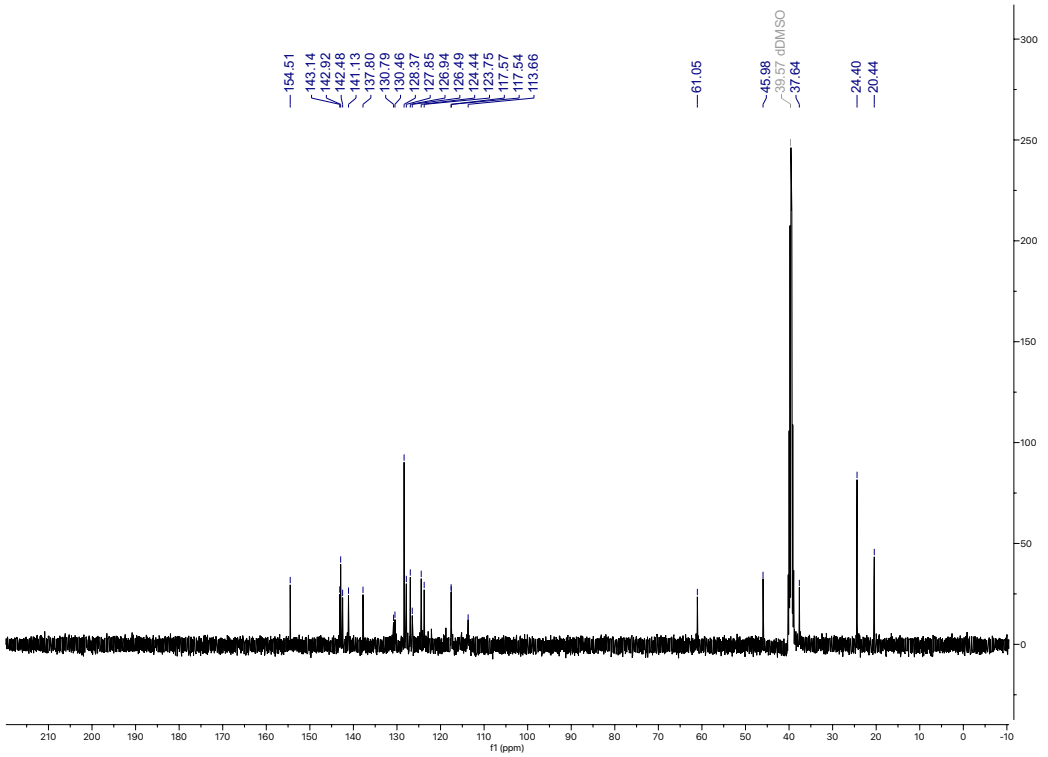


**Figure 3.6.23 $^{13}$CNMR Spectra of 3.6.4a**

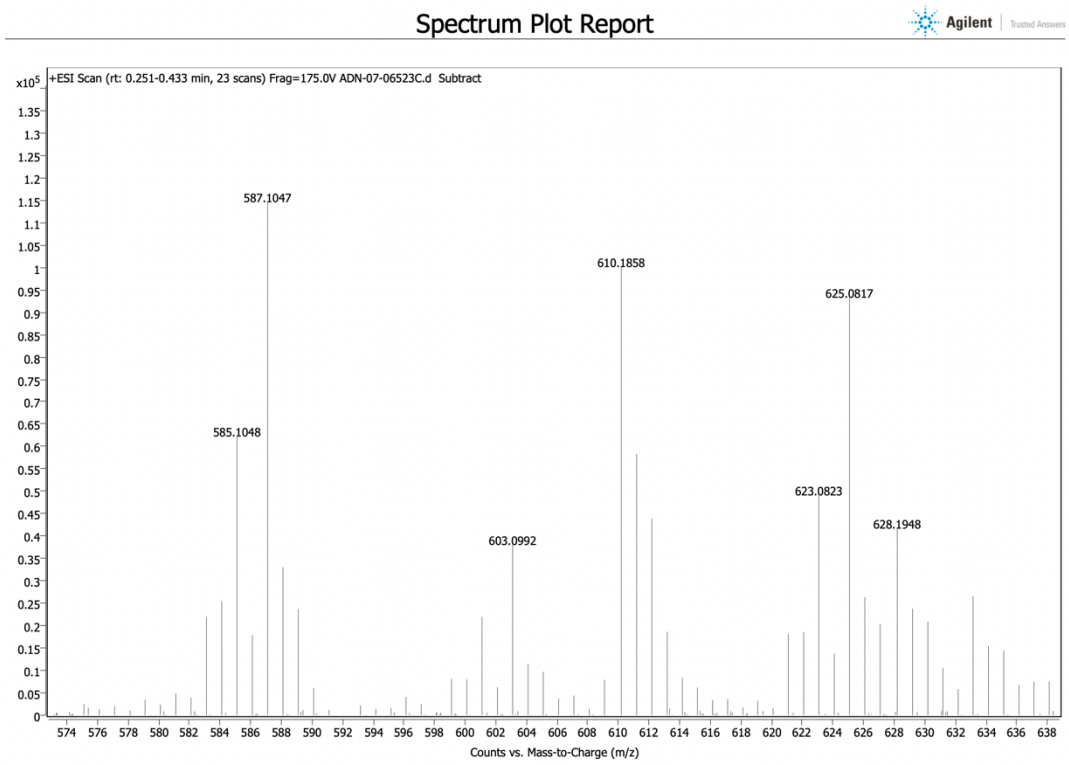


**Figure 3.6.24 HRMS (ESI) Spectra of 3.6.4a**

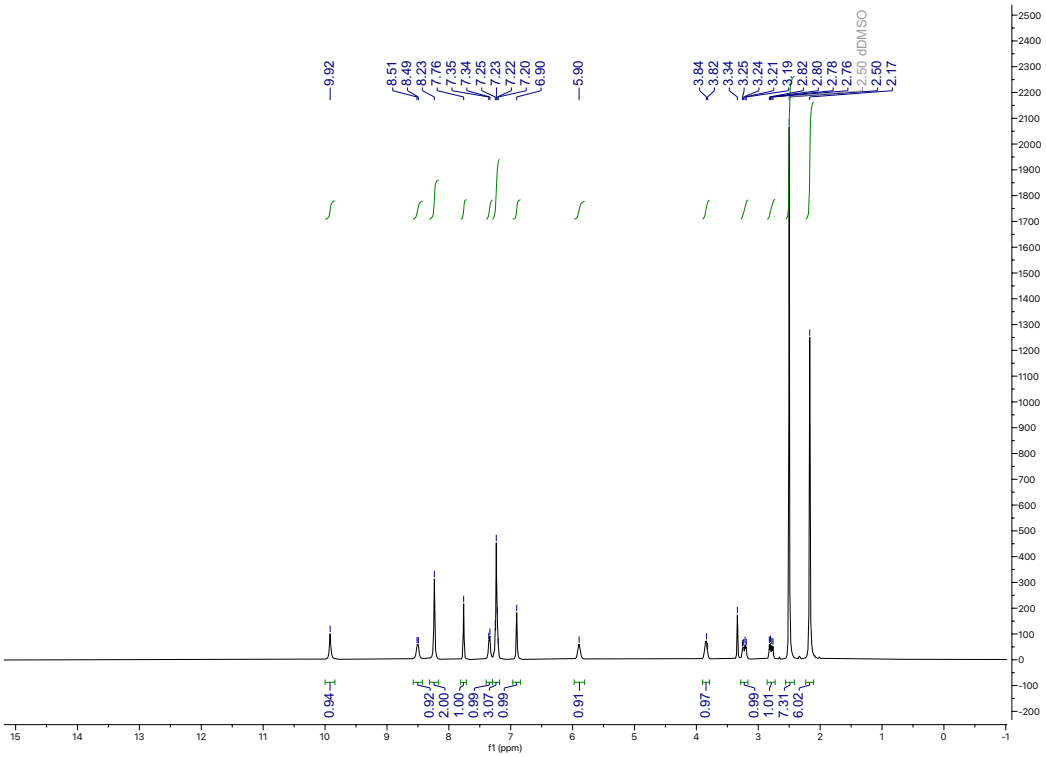


**Figure 3.6.25 $^{1}$HNMR Spectra of 3.6.5a**

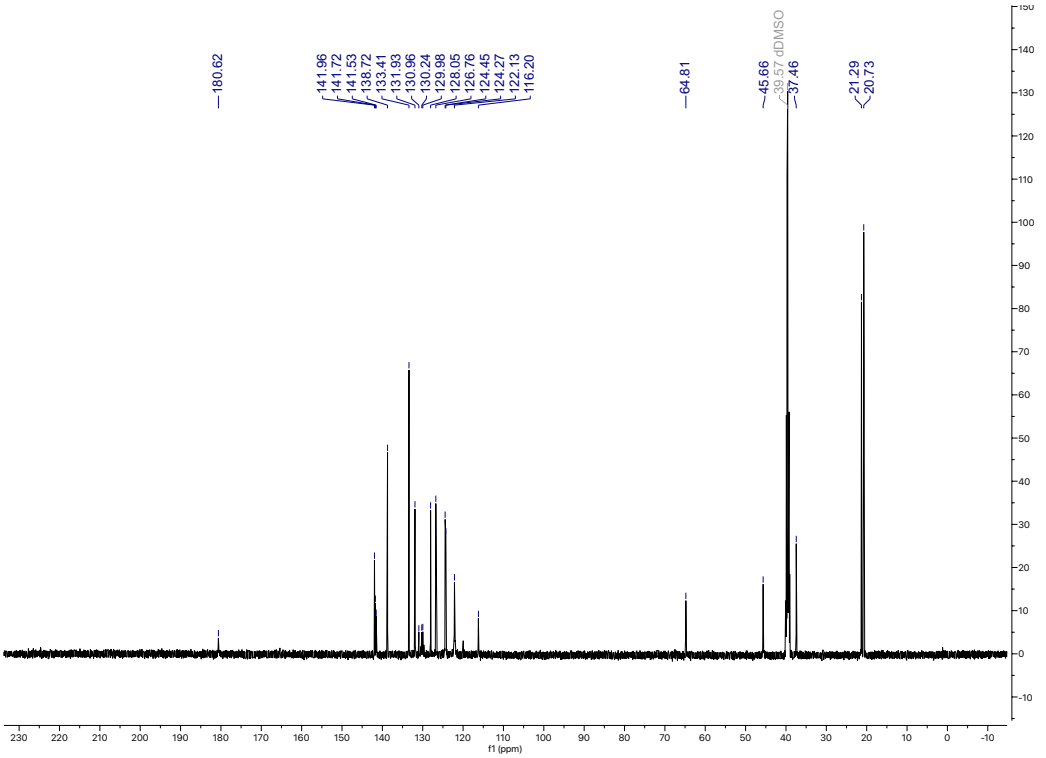


**Figure 3.6.26 $^{13}$CNMR Spectra of 3.6.5a**

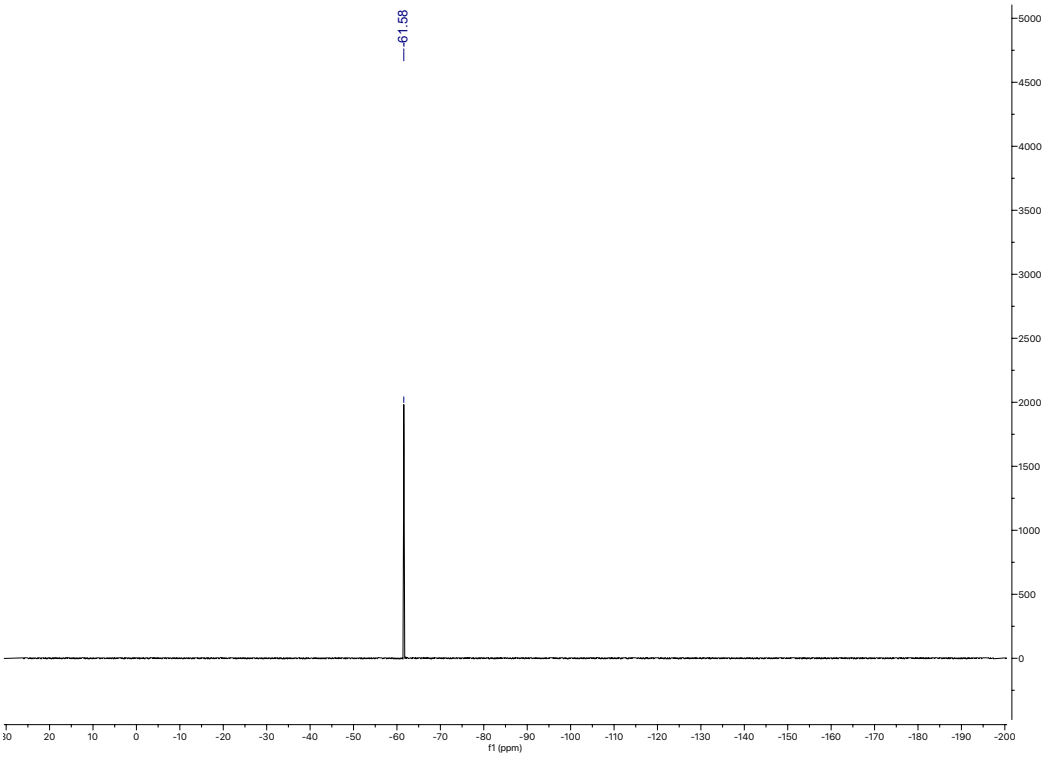


**Figure 3.6.27 $^{19}$FNMR Spectra of 3.6.5a**

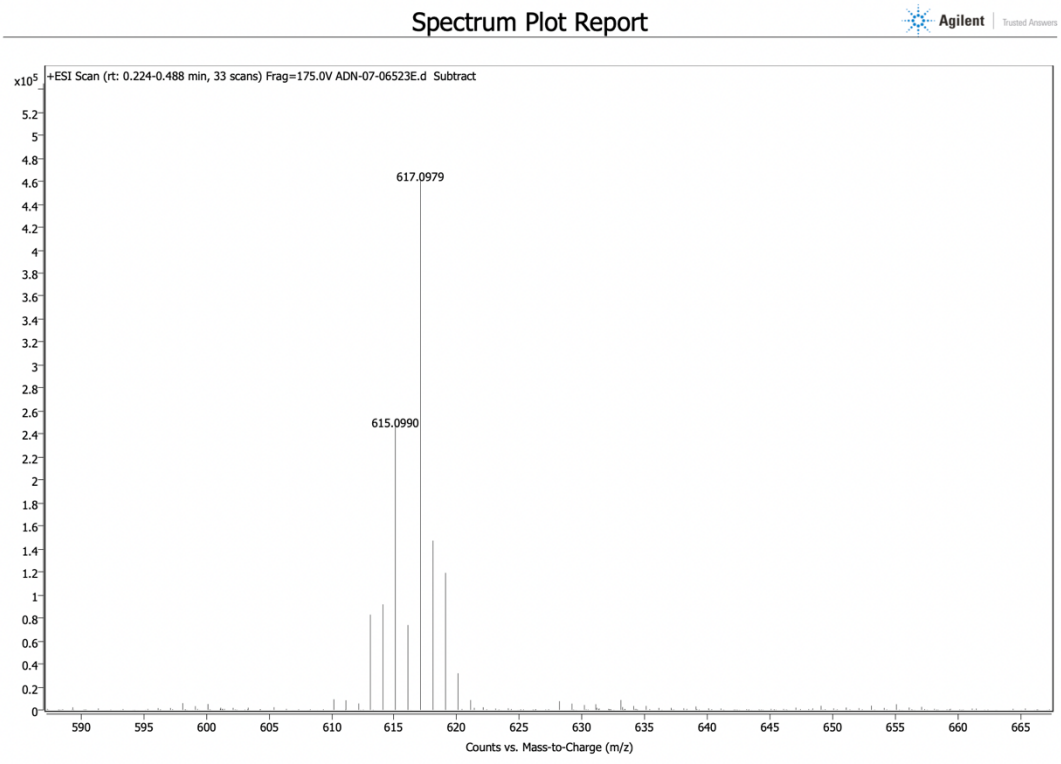


**Figure 3.6.28 HRMS (ESI) Spectra of 3.6.5a**

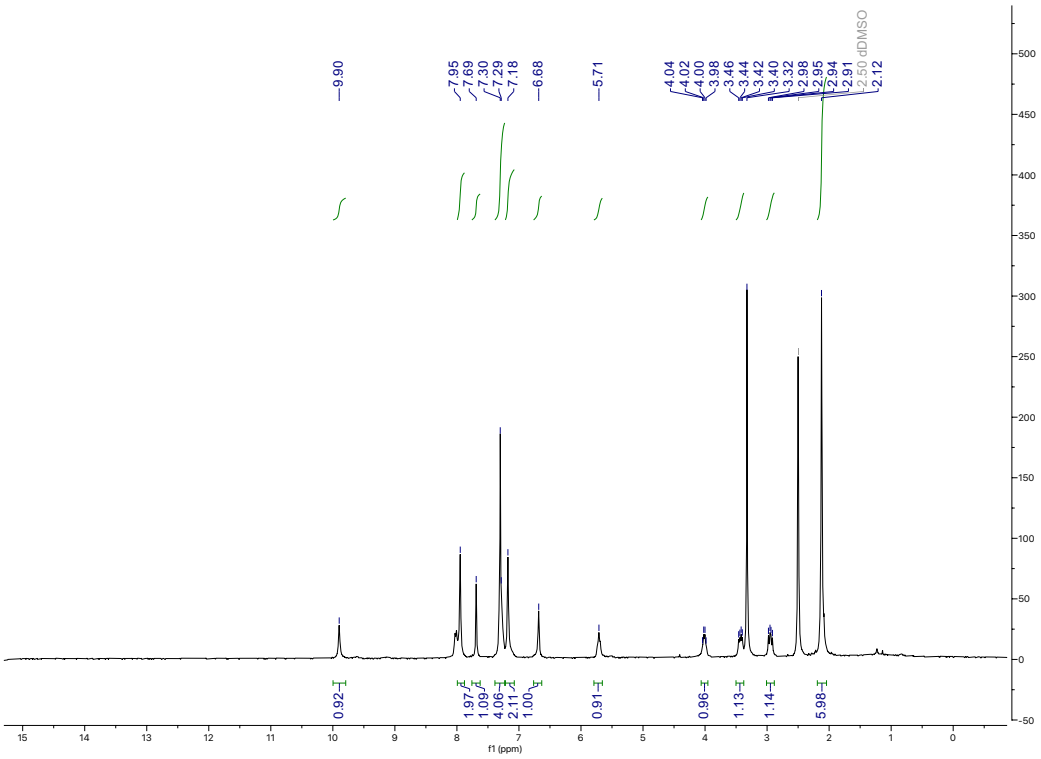


**Figure 3.6.29 $^{1}$HNMR Spectra of 3.6.6a**

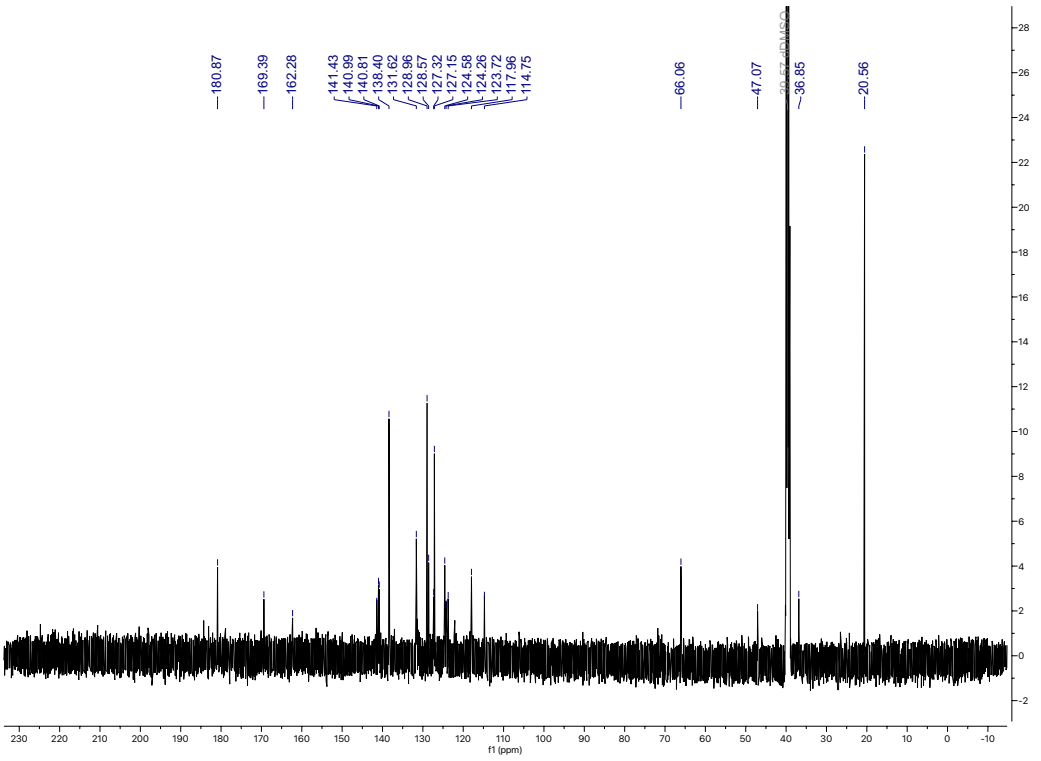


**Figure 3.6.30 $^{13}$CNMR Spectra of 3.6.6a**

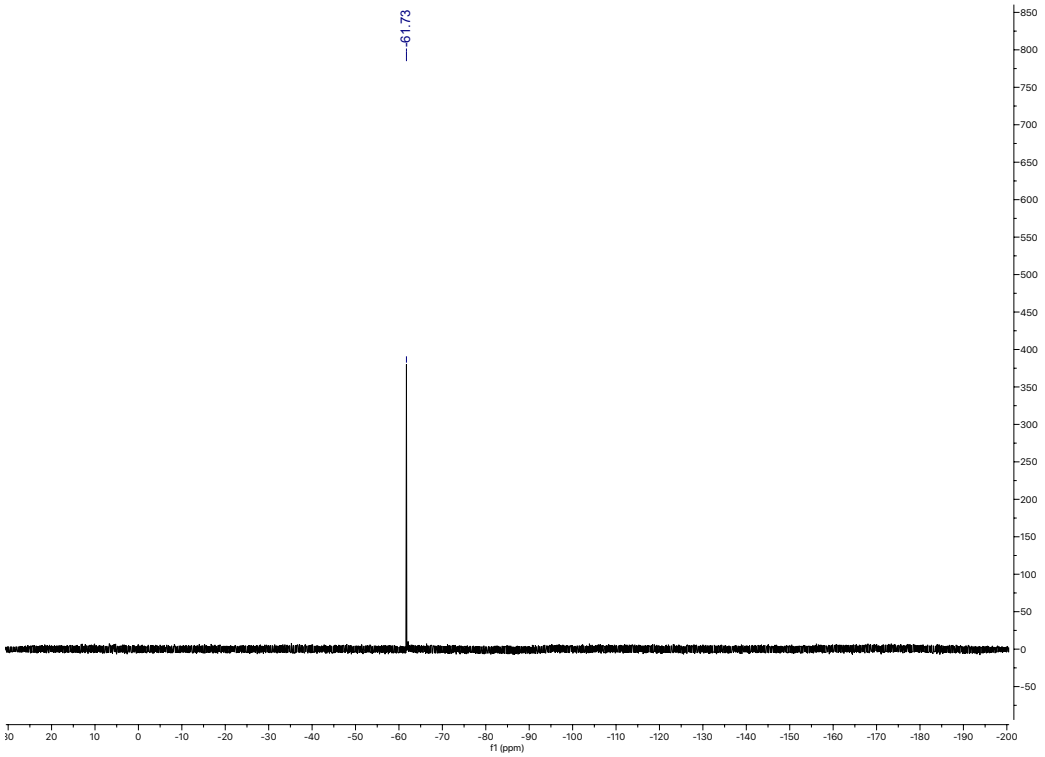


**Figure 3.6.31 $^{19}$FNMR Spectra of 3.6.6a**

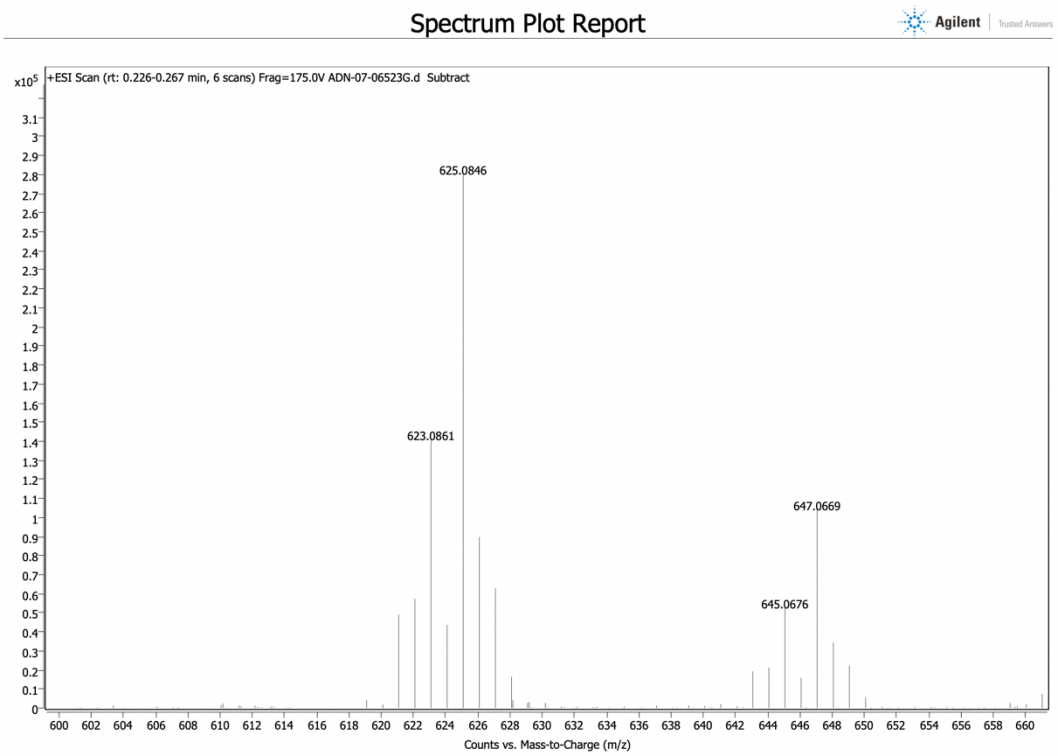


**Figure 3.6.31 HRMS (ESI) of 3.6.6a**

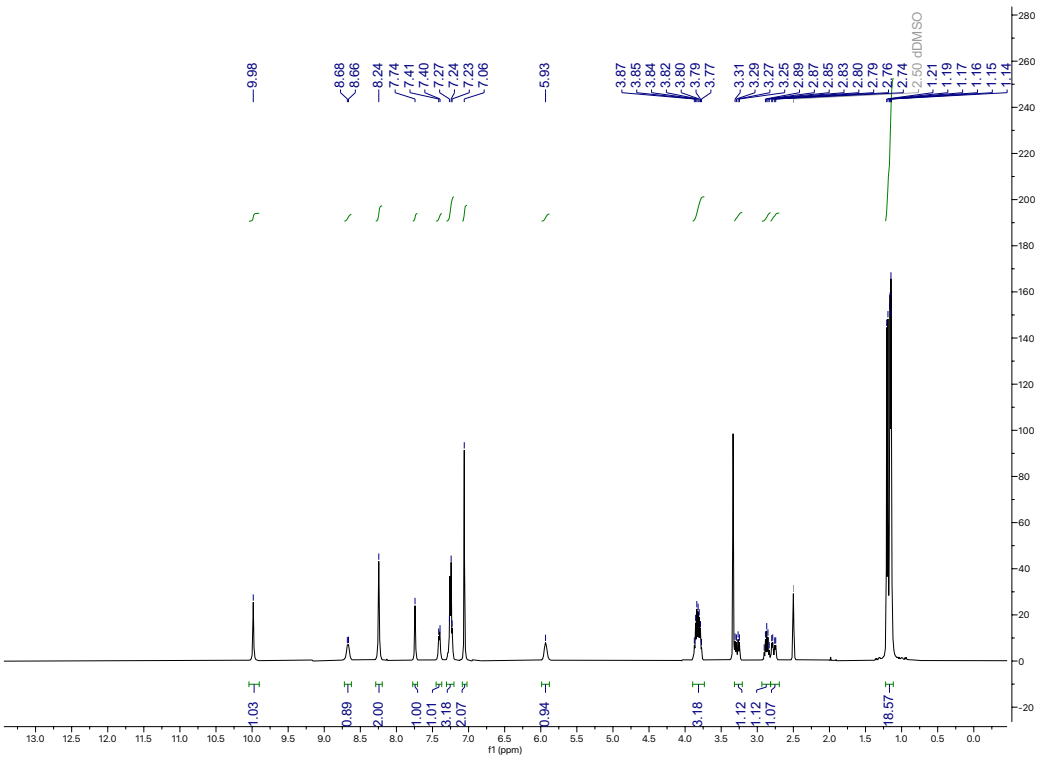


**Figure 3.6.32 $^{1}$HNMR Spectra of 3.6.7a**

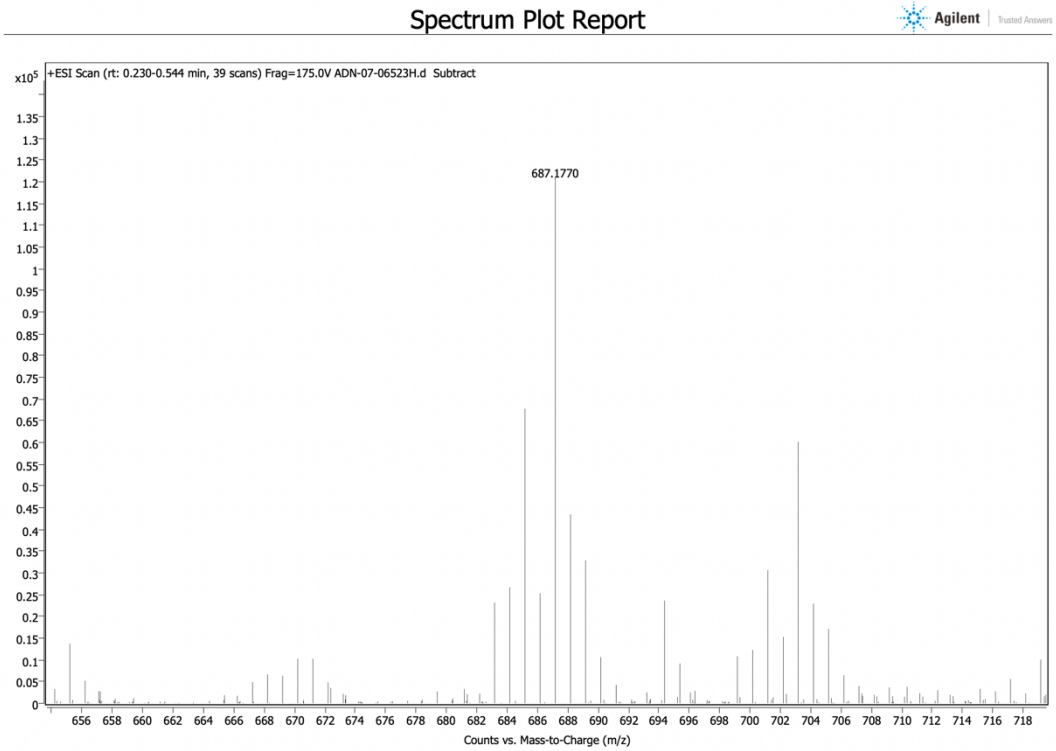


**Figure 3.6.33 HRMS (ESI) Spectra of 3.6.7a**

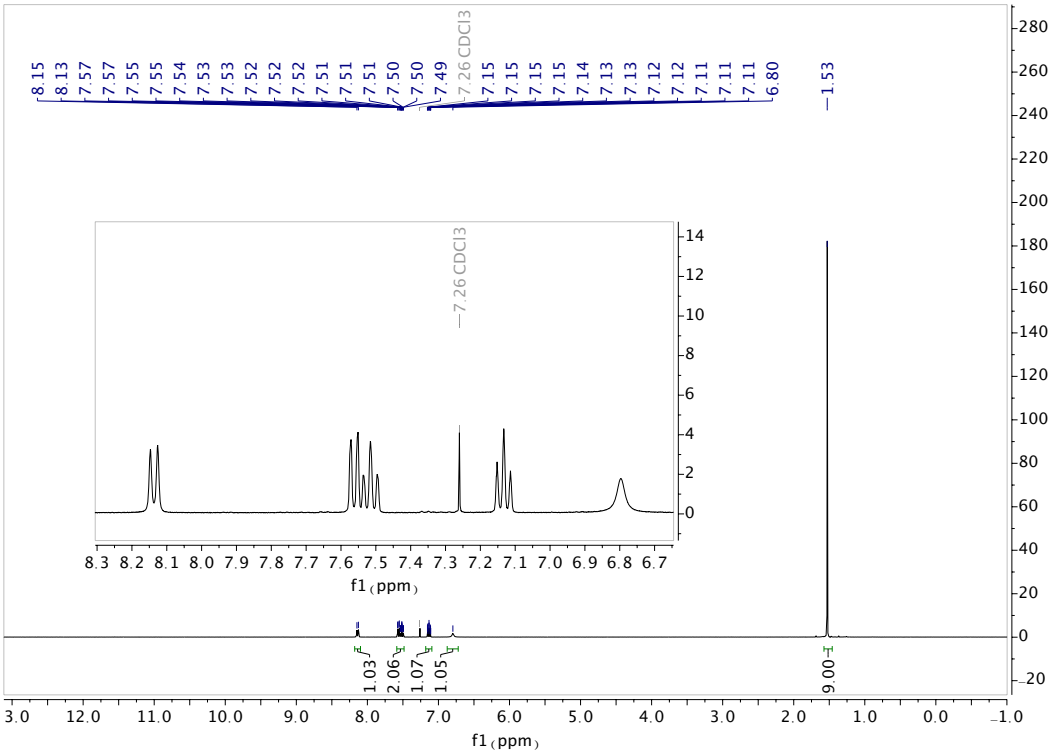


**Figure 3.6.34 $^{1}$HNMR Spectra of 3.6.8a**

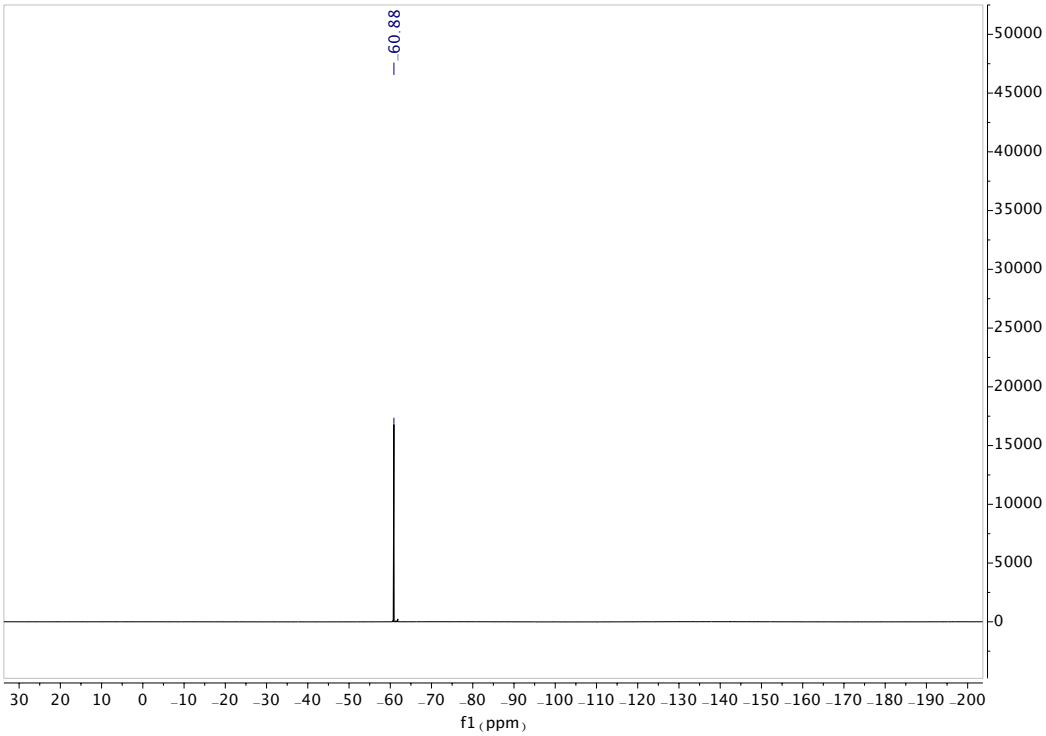


**Figure 3.6.34 $^{19}$FNMR Spectra of 3.6.8a**

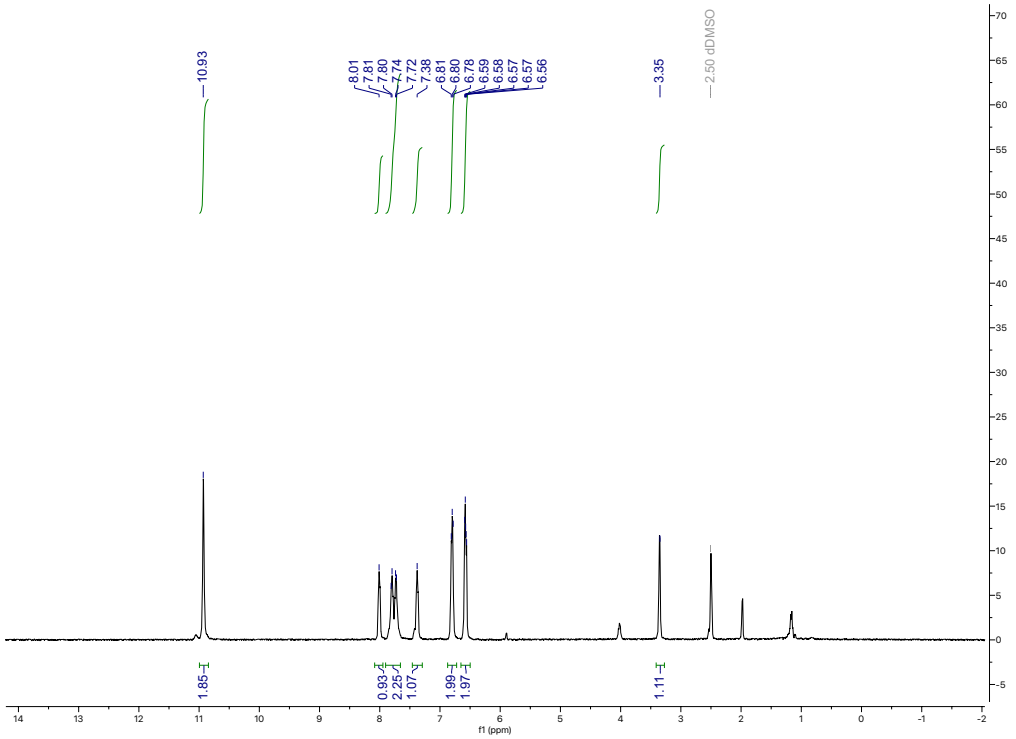


**Figure 3.6.35 $^{1}$HNMR Spectra of 3.6.10a**

## 3.7 Acknowledgments

The contents of Chapter 3 are in part a reformatted reprint of the following manuscript with permission from Wiley. Nguyen, A. D.; Zanolini, R. J.; Gustafson, J. L. 'Selective Functionalizations of Arenes and Heteroarenes via $S_EAr$ and Related Transformation'. *Wiley*. Handbook of C-H Functionalization. **2022.** ISBN: 9783527834242. I was the primary author who wrote the manuscript and made the figures. Ryan Zanolini contributed by providing supplemental figures for bromination schemes. The data in this chapter is unpublished and the dissertation author is the primary investigator for the work. Undergraduate researchers who worked with the dissertation author and contributed to the library of Gustafson regiocatalysts include: Ernesto Milan (2019-2020), Connor McCarty (2021-2023), Nicholas Tabares (2022-2023), Chase Totherow (2023) and are acknowledged for their synthetic work.

## References


(1) Altus, K. M.; Love, J. A. The Continuum of Carbon-Hydrogen (C-H) Activation Mechanisms and Terminology. *Chem. Comm.* **2021**, *4* (1), 173. DOI: 10.1038/s42004-021-00611-1.

(2) He, J.; Wasa, M.; Chan, K. S. L.; Shao, Q.; Yu, J. Q. Palladium-Catalyzed Transformations of Alkyl C-H Bonds. *Chem. Rev.* **2017**, *117* (13), 8754-8786. DOI: 10.1021/acs.chemrev.6b00622.

(3) Qin, Y.; Zhu, L.; Luo, S. Organocatalysis in Inert C-H Bond Functionalization. *Chem. Rev.* **2017**, *117* (13), 9433-9520. DOI: 10.1021/acs.chemrev.6b00657.

(4) Gutekunst, W. R.; Baran, P. S. C-H Functionalization Logic in Total Synthesis. *Chem. Soc. Rev.* **2011**, (40), 1976-1991.

(5) Godula, K.; Sames, D. C-H Bond Functionalization in Complex Organic Synthesis. *Science.* **2006**, *312*, 67-72.

(6) Engle, K. M.; Mei, T. S.; Wasa, M.; Yu, J. Q. Weak Coordination as a Powerful Means Developing Broadly Useful C-H Functionalization Reactions. *Acc. Chem. Res.* **2012**, *45* (6), 788-802.

(7) Mancuso, A.; Sacco, O.; Sannino, D.; Venditto, V.; Vaiano, V. One-Step Catalytic or Photocatalytic Oxidation of Benzene to Phenol: Possible Alternative Routes for Phenol Synthesis. *Catalysts.* **2020**, *10* (12). DOI: 10.3390/catal10121424.

(8) Bruckl, T.; Baxter, R. D.; Ishihara, Y.; Baran, P. S. Innate and Guided C-H Functionalization Logic. *Acc. Chem. Res.* **2011**, *45* (6), 826-839.

(9) Wang, P.; Verma, P.; Xia, G.; Shi, J.; Qiao, J. X.; Tao, S.; Cheng, P. T. W.; Poss, M. A.; Farmer, M. E.; Yeung, K. S.; et al. Ligand-Accelerated Non-Directed C-H Functionalization of Arenes. *Nature.* **2017**, *551* (7681), 489-493. DOI: 10.1038/nature24632.

(10) Jeong, S.; Joo, J. M. Transition-Metal-Catalyzed Divergent C-H Functionalization of Five-Membered Heteroarenes. *Acc. Chem. Res.* **2021**, *54* (24), 4518-4529. DOI: 10.1021/acs.accounts.1c00547.

(11) Docherty, J. H.; Lister, T. M.; McArthur, G.; Findlay, M. T.; Domingo-Legarda, P.; Kenyon, J.; Choudhary, S.; Larrosa, I. Transition-Metal-Catalyzed C-H Bond Activation for the Formation of C-C Bonds in Complex Molecules. *Chem. Rev.* **2023**. DOI: 10.1021/acs.chemrev.2c00888.

(12) Sarkar, T.; Shah, T. A.; Maharana, P. K.; Talukdar, K.; Das, B. K.; Punniyamurthy, T. Transition-Metal-Catalyzed Directing Group Assisted (Hetero)aryl C-H Functionalization:

Construction of C-C/C-Heteroatom Bonds. *Chem. Rev.* **2021**, *21* (12), 3758-3778. DOI: 10.1002/tcr.202100143.

(13) Matsui, J. K.; Molander, G. A. Organocatalyzed, Photoredox Heteroarylation of 2-Trifluoroboratochromanones via C-H Functionalization. *Org. Lett.* **2017**, *19* (4), 950-953. DOI: 10.1021/acs.orglett.7b00196.

(14) Lopat'eva, E. R.; Krylov, I. B.; Lapshin, D. A.; Terent'ev, A. O. Redox-Active Molecules as Organocatalysts for Selective Oxidative Transformations - An Unperceived Organocatalysis Field. *Beilstein. J. Org. Chem.* **2022**, *18*, 1672-1695. DOI: 10.3762/bjoc.18.179.

(15) Shaw, M. H.; Twilton, J.; MacMillan, D. W. Photoredox Catalysis in Organic Chemistry. *J. Org. Chem.* **2016**, *81* (16), 6898-6926. DOI: 10.1021/acs.joc.6b01449.

(16) Reischauer, S.; Pieber, B. Emerging Concepts in Photocatalytic Organic Synthesis. *iScience.* **2021**, *24* (3), 102209. DOI: 10.1016/j.isci.2021.102209.

(17) Singh, A.; Teegardin, K.; Kelly, M.; Prasad, K. S.; Krishnan, S.; Weaver, J. D. Facile Synthesis and Complete Characterization of Homoleptic and Heteroleptic Cyclometalated Iridium(III) Complexes for Photocatalysis. *J. Org. Met. Chem.* **2015**, *776*, 51-59. DOI: 10.1016/j.jorganchem.2014.10.037.

(18) Düsel, S. J. S.; König, B. Oxidative Photochlorination of Electron-Rich Arenes via in situ Bromination. *Eur. J. Org. Chem.* **2019**, *2020* (10), 1491-1495. DOI: 10.1002/ejoc.201900411.

(19) Margrey, K. A.; Czaplyski, W. L.; Nicewicz, D. A.; Alexanian, E. J. A General Strategy for Aliphatic C-H Functionalization Enabled by Organic Photoredox Catalysis. *J. Am. Chem. Soc.* **2018**, *140* (12), 4213-4217. DOI: 10.1021/jacs.8b00592.

(20) Glaser, G. Base Sustainable Development Goals on Science. *Nature.* **2012**, *491*, 35.

(21) Schneider, F.; Kläy, A.; Zimmermann, A. B.; Buser, T.; Ingalls, M.; Messerli, P. How can science support the 2030 Agenda for Sustainable Development? Four tasks to tackle the normative dimension of sustainability. *Sust. Sci.* **2019**, *14* (6), 1593-1604. DOI: 10.1007/s11625-019-00675-y.

(22) DeVierno Kreuder, A.; House-Knight, T.; Whitford, J.; Ponnusamy, E.; Miller, P.; Jesse, N.; Rodenborn, R.; Sayag, S.; Gebel, M.; Aped, I.; et al. A Method for Assessing Greener Alternatives between Chemical Products Following the 12 Principles of Green Chemistry. *ACS. Sust. Chem. Eng.* **2017**, *5* (4), 2927-2935. DOI: 10.1021/acssuschemeng.6b02399.

(23) Dalton, T.; Faber, T.; Glorius, F. C-H Activation: Toward Sustainability and Applications. *ACS. Cent. Sci.* **2021**, *7* (2), 245-261. DOI: 10.1021/acscentsci.0c01413.

(24) Crisenza, G. E. M.; Melchiorre, P. Chemistry Glows Green with Photoredox Catalysis. *Nat. Comm.* **2020**, *11* (1), 803. DOI: 10.1038/s41467-019-13887-8.

(25) Oelgemöller, M.; Jung, C.; Mattay, J. Green Photochemistry: Production of Fine Chemicals with sunlight. *Pure. App. Chem.* **2007**, *79* (11), 1939-1947. DOI: 10.1351/pac200779111939.

(26) Joshi-Pangu, A.; Levesque, F.; Roth, H. G.; Oliver, S. F.; Campeau, L. C.; Nicewicz, D.; DiRocco, D. A. Acridinium-Based Photocatalysts: A Sustainable Option in Photoredox Catalysis. *J. Org. Chem.* **2016**, *81* (16), 7244-7249. DOI: 10.1021/acs.joc.6b01240.

(27) Nesvadba, P. Radical Polymerization in Industry. In *Encyclopedia of Radicals in Chemistry, Biology and Materials*, 2012.

(28) Destarac, M. Controlled Radical Polymerization: Industrial Stakes, Obstacles and Achievements. *Mac. Reac. Eng.* **2010**, *4* (3-4), 165-179. DOI: 10.1002/mren.200900087.

(29) Carraher, C. E.; Seymour, R. *Polymer Chemistry*; Marcel Dekker Inc., 2003.

(30) Ziegler, K. V.; Spath, A.; Schaaf, E.; Schumann, W.; Winkelmann, E. Die Halogenierung ungesattigter Substanzen in der Allylstellung. *Chem. Eur. J.* **1942**, *551* (1), 80-119.

(31) Day, J. C.; Lindstrom, M. J.; Skell, P. S. Succinimidyl Radical as a Chain Carrier. Mechanism of Allylic Bromination. *J. Am. Chem. Soc.* **1974**, *96* (17), 5616-5617.

(32) Incremona, J. H.; Martin, J. C. N-Bromosuccinimide. Mechanisms of Allylic Bromination and Related Reactions. *J. Am. Chem. Soc.* **1969**, *92* (3), 627-634.

(33) Zard, S. Z. Radicals in Action: A Festival of Radical Transformations. *Org. Lett.* **2017**, *19* (6), 1257-1269. DOI: 10.1021/acs.orglett.7b00531.

(34) Banares, L. Unexpected Intersystem Crossing. *Nat. Chem.* **2019**, *11* (2), 103-104. DOI: 10.1038/s41557-018-0207-4.

(35) Giese, B. Formation of C-C Bonds by Addition of Free Radicals to Alkenes. *Angew. Chem. Int. Ed.* **1983**, *22* (10), 753-764. DOI: 10.1002/anie.198307531.

(36) Yan, M.; Lo, J. C.; Edwards, J. T.; Baran, P. S. Radicals: Reactive Intermediates with Translational Potential. *J. Am. Chem. Soc.* **2016**, *138* (39), 12692-12714. DOI: 10.1021/jacs.6b08856.

(37) Barton, D. H. R.; McCombie, S. W. A New Method for the Deoxygenation of Secondary Alcohols. *J. Chem. Soc. Perkin. Trans. 1*. **1975**, (16), 1574-1585.

(38) Meyer, T. Optical and Thermal Electron Transfer in Metal Complexes. *Acc. Chem. Res.* **1977**, *11* (3), 94-100.

(39) Takeda, H.; Ishitani, O. Development of Efficient Photocatalytic Systems for $CO_2$ Reduction Using Mononuclear and Multinuclear Metal Complexes Based on Mechanistic Studies. *Coord. Chem. Rev.* **2010**, *254* (3-4), 346-354. DOI: 10.1016/j.ccr.2009.09.030.

(40) Kalyanasundaram, K.; Gratzel, M. Applications of Functionalized Transition Metal Complexes in Photonic and Optoelectronic Devices. *Coord. Chem. Rev,* **1998**, *77*, 347-414.

(41) Li, P.; Terrett, J. A.; Zbieg, J. R. Visible-Light Photocatalysis as an Enabling Technology for Drug Discovery: A Paradigm Shift for Chemical Reactivity. *ACS Med Chem Lett* **2020**, *11* (11), 2120-2130. DOI: 10.1021/acsmedchemlett.0c00436

(42) Cannalire, R.; Pelliccia, S.; Sancineto, L.; Novellino, E.; Tron, G. C.; Giustiniano, M. Visible Light Photocatalysis in the Late-Stage Functionalization of Pharmaceutically Relevant Compounds. *Chem. Soc. Rev.* **2021**, *50* (2), 766-897. DOI: 10.1039/d0cs00493f.

(43) Dauben, W.; Salem, L.; Turro, N. J. A Classification of Photochemical Reactions. *Acc. Chem. Res.* **1974**, *8* (2), 41-54.

(44) Gentry, E. C.; Knowles, R. R. Synthetic Applications of Proton-Coupled Electron Transfer. *Acc. Chem. Res.* **2016**, *49* (8), 1546-1556. DOI: 10.1021/acs.accounts.6b00272.
(45) Capaldo, L.; Ravelli, D. Hydrogen Atom Transfer (HAT): A Versatile Strategy for Substrate Activation in Photocatalyzed Organic Synthesis. *Eur. J. Org. Chem.* **2017**, *2017* (15), 2056-2071. DOI: 10.1002/ejoc.201601485.

(46) Allen, A. R.; Noten, E. A.; Stephenson, C. R. J. Aryl Transfer Strategies Mediated by Photoinduced Electron Transfer. *Chem. Rev.* **2022**, *122* (2), 2695-2751. DOI: 10.1021/acs.chemrev.1c00388.

(47) Thoi, V. S.; Kornienko, N.; Margarit, C. G.; Yang, P.; Chang, C. J. Visible-Light Photoredox Catalysis: Selective Reduction of Carbon Dioxide to Carbon Monoxide by a Nickel N-Heterocyclic Carbene-Isoquinoline Complex. *J. Am. Chem. Soc.* **2013**, *135* (38), 14413-14424. DOI: 10.1021/ja4074003.

(48) Das, A.; Thomas, K. R. J. Tuning Selectivity in the Visible-Light-Promoted Coupling of Thiols with Alkenes by EDA vs TOCO Complex Formation. *ACS. Omega.* **2023**, *8* (20), 18275-18289. DOI: 10.1021/acsomega.3c02070.

(49) Wang, J.; Reynolds, M.; Ibanez, I.; Sasaki, Y.; Tanaka, Y.; Kikuchi, F.; Ohashi, T.; Sato, S.; Miyabayashi, M.; Fujii, T.; et al. Photoredox-Based Late-Stage Functionalization in SAR study for in Vivo Potent Glucosylceramide Synthase Inhibitor. *Bioorg, Med. Chem. Lett.* **2022**, *77*, 129039. DOI: 10.1016/j.bmcl.2022.129039.

(50) Hughes, J. P.; Rees, S.; Kalindjian, S. B.; Philpott, K. L. Principles of Early Drug Discovery. *Br. J. Pharmacol.* **2011**, *162* (6), 1239-1249. DOI: 10.1111/j.1476-5381.2010.01127.

(51) Nagib, D. A.; MacMillan, D. W. Trifluoromethylation of Arenes and Heteroarenes by Means of Photoredox Catalysis. *Nature.* **2011**, *480* (7376), 224-228. DOI: 10.1038/nature10647.

(52) Yu, W.; Xu, X. H.; Qing, F. L. Photoredox Catalysis Mediated Application of Methyl Fluorosulfonyldifluoroacetate as the $CF_2CO_2R$ Radical Source. *Org. Lett.* **2016**, *18* (19), 5130-5133. DOI: 10.1021/acs.orglett.6b02580.

(53) Jampilek, J. Heterocycles in Medicinal Chemistry. *Molecules.* **2019**, *24* (21). DOI: 10.3390/molecules24213839.

(54) Laxmikeshav, K.; Kumari, P.; Shankaraiah, N. Expedition of Sulfur-Containing Heterocyclic Derivatives as Cytotoxic Agents in Medicinal Chemistry: A Decade Update. *Med. Res. Rev.* **2022**, *42* (1), 513-575. DOI: 10.1002/med.21852.

(55) Kaiser, D.; Klose, I.; Oost, R.; Neuhaus, J.; Maulide, N. Bond-Forming and -Breaking Reactions at Sulfur(IV): Sulfoxides, Sulfonium Salts, Sulfur Ylides, and Sulfinate Salts. *Chem. Rev.* **2019**, *119* (14), 8701-8780. DOI: 10.1021/acs.chemrev.9b00111.

(56) Kano, N.; Itoh, Y.; Watanabe, Y.; Kusaka, S.; Kawashima, T. Structure and Properties of a Sulfur(IV)-Sulfur(II)-Bond Compound: Reversible Conversion of a Sulfur-Substituted Organosulfurane into a Thiol. *Angew. Chem. Int. Ed.* **2008**, *47* (49), 9430-9433. DOI: 10.1002/anie.200803945.

(57) Lohmayer, R.; Kappler, A.; Losekann-Behrens, T.; Planer-Friedrich, B. Sulfur Species as Redox Partners and Electron Shuttles for Ferrihydrite Reduction by Sulfurospirillum Deleyianum. *Appl. Environ. Microbiol.* **2014**, *80* (10), 3141-3149. DOI: 10.1128/AEM.04220-13.

(58) Wiedemann, C.; Kumar, A.; Lang, A.; Ohlenschlager, O. Cysteines and Disulfide Bonds as Structure-Forming Units: Insights From Different Domains of Life and the Potential for Characterization by NMR. *Front. Chem.* **2020**, *8*, 280. DOI: 10.3389/fchem.2020.00280.

(59) Zhao, C.; Rakesh, K. P.; Ravidar, L.; Fang, W. Y.; Qin, H. L. Pharmaceutical and Medicinal Significance of Sulfur (S(VI))-Containing Motifs for Drug Discovery: A Critical Review. *Eur. J. Med. Chem.* **2019**, *162*, 679-734. DOI: 10.1016/j.ejmech.2018.11.017.

(60) Scott, K. A.; Njardarson, J. T. Analysis of US FDA-Approved Drugs Containing Sulfur Atoms. *Top. Curr. Chem.* **2018**, *376* (1), 5. DOI: 10.1007/s41061-018-0184-5.

(61) Vasquez-Cespedes, S.; Ferry, A.; Candish, L.; Glorius, F. Heterogeneously Catalyzed Direct C-H Thiolation of Heteroarenes. *Angew. Chem. Int. Ed.* **2015**, *54* (19), 5772-5776. DOI: 10.1002/anie.201411997.

(62) Beletskaya, I. P.; Ananikov, V. P. Transition-metal-catalyzed C-S, C-Se, and C-Te bond formation via cross-coupling and atom-economic addition reactions. *Chem. Rev.* **2011**, *111* (3), 1596-1636. DOI: 10.1021/cr100347k.

(63) Lee, C. F.; Liu, Y. C.; Badsara, S. S. Transition-Metal-Catalyzed C-S Bond Coupling Reaction. *Chem. Asian. J.* **2014**, *9* (3), 706-722. DOI: 10.1002/asia.201301500.

(64) Nalbandian, C. J.; Miller, E. M.; Toenjes, S. T.; Gustafson, J. L. A Conjugate Lewis Base-Bronsted Acid Catalyst for the Sulfenylation of Nitrogen Containing Heterocycles Under Mild Conditions. *Chem. Comm.* **2017**, *53* (9), 1494-1497. DOI: 10.1039/c6cc09998j.

(65) Nalbandian, C. J.; Brown, Z. E.; Alvarez, E.; Gustafson, J. L. Lewis Base/Bronsted Acid Dual-Catalytic C-H Sulfenylation of Aromatics. *Org. Lett.* **2018**, *20* (11), 3211-3214. DOI: 10.1021/acs.orglett.8b01066.

(66) Yadav, J. S.; Reddy, B. V. S.; Reddy, Y. J. A Rapid Synthesis of 3-Sulfenyl Indoles Using Selectfluor™. *Tet. Lett.* **2007**, *48* (39), 7034-7037. DOI: 10.1016/j.tetlet.2007.07.130.

(67) Schlosser, K. M.; Krasutsky, A. P.; Hamilton, H. W.; Reed, J. E.; Sexton, K. A Highly Efficient Procedure for 3-Sulfenylation of Indole-2-Carboxylates. *Org. Lett.* **2004**, *6* (5), 819-821.

(68) Yang, K.; Chen, J.; Kim, S.; Xiong, P.; Chen, W.; Cho, M.; Lee, Y. Achieving Fast and Reversible Sulfur Redox by Proper Interaction of Electrolyte in Potassium Batteries. *ACS. Energy. Lett.* **2023**, *8* (5), 2169-2176. DOI: 10.1021/acsenergylett.3c00529.

(69) Wu, H.; Fang, R.; Tao, J.; Wang, D.; Qiao, X.; Yang, X.; Hartl, F.; Li, H. Diacenaphthylene-Fused Benzo[1,2-b:4,5-b']dithiophenes: Polycyclic Heteroacenes Containing Full-Carbon Five-Membered Aromatic Rings. *Chem. Comm.* **2017**, *53* (4), 751-754. DOI: 10.1039/c6cc09184a.

(70) Berger, F.; Plutschack, M. B.; Riegger, J.; Yu, W.; Speicher, S.; Ho, M.; Frank, N.; Ritter, T. Site-Selective and Versatile Aromatic C-H Functionalization by Thianthrenation. *Nature.* **2019**, *567* (7747), 223-228. DOI: 10.1038/s41586-019-0982-0.

(71) Wimmer, A.; Konig, B. Photocatalytic Formation of Carbon-Sulfur Bonds. *Beilstein. J. Org. Chem.* **2018**, *14*, 54-83. DOI: 10.3762/bjoc.14.4.

(72) Johnson, T. C.; Elbert, B. L.; Farley, A. J. M.; Gorman, T. W.; Genicot, C.; Lallemand, B.; Pasau, P.; Flasz, J.; Castro, J. L.; MacCoss, M.; et al. Direct Sulfonylation of Anilines Mdiated by Visible Light. *Chem. Sci.* **2018**, *9* (3), 629-633. DOI: 10.1039/c7sc03891g.

(73) Liu, B.; Lim, C. H.; Miyake, G. M. Visible-Light-Promoted C-S Cross-Coupling via Intermolecular Charge Transfer. *J. Am. Chem. Soc.* **2017**, *139* (39), 13616-13619. DOI: 10.1021/jacs.7b07390.

(74) Zhang, G.; Liu, C.; Yi, H.; Meng, Q.; Bian, C.; Chen, H.; Jian, J. X.; Wu, L. Z.; Lei, A. External Oxidant-Free Oxidative Cross-Coupling: A Photoredox Cobalt-Catalyzed Aromatic C-H Thiolation for Constructing C-S Bonds. *J. Am. Chem. Soc.* **2015**, *137* (29), 9273-9280. DOI: 10.1021/jacs.5b05665.

(75) Qian, X.-Y.; Li, S.-Q.; Song, J.; Xu, H.-C. TEMPO-Catalyzed Electrochemical C–H Thiolation: Synthesis of Benzothiazoles and Thiazolopyridines from Thioamides. *ACS. Catal.* **2017**, *7* (4), 2730-2734. DOI: 10.1021/acscatal.7b00426.

(76) Guo, W.; Tan, W.; Zhao, M.; Tao, K.; Zheng, L.-Y.; Wu, Y.; Chen, D.; Fan, X.-L. Photocatalytic Direct C–S Bond Formation: Facile Access to 3-Sulfenylindoles via Metal-Free C-3 Sulfenylation of Indoles with Thiophenols. *RSC. Adv,* **2017**, *7* (60), 37739-37742. DOI: 10.1039/c7ra08086g.

(77) Rahaman, R.; Das, S.; Barman, P. Visible-Light-Induced Regioselective Sulfenylation of Imidazopyridines with Thiols Under Transition Metal-Free Conditions. *Green. Chem.* **2018**, *20* (1), 141-147. DOI: 10.1039/c7gc02906c.

(78) Das, A.; Maity, M.; Malcherek, S.; Konig, B.; Rehbein, J. Synthesis of Aryl Sulfides via Radical-Radical Cross Coupling of Rlectron-Rich Arenes using Visible Light Photoredox Catalysis. *Beilstein. J. Org. Chem.* **2018**, *14*, 2520-2528. DOI: 10.3762/bjoc.14.228.

(79) Dinh, A. N.; Nguyen, A. D.; Aceves, E. M.; Albright, S. T.; Cedano, M. R.; Smith, D. K.; Gustafson, J. L. Photocatalytic Oxidative C–H Thiolation: Synthesis of Benzothiazoles and Sulfenylated Indoles. *Synlett.* **2019**, *30* (14), 1648-1655. DOI: 10.1055/s-0039-1690107.

(80) Zhang, L.; Hu, X. Room Temperature C($sp^2$)-H Oxidative Chlorination via Photoredox Catalysis. *Chem. Sci.* **2017**, *8* (10), 7009-7013. DOI: 10.1039/c7sc03010j.

(81) Hua, A. M.; Bidwell, S. L.; Baker, S. I.; Hratchian, H. P.; Baxter, R. D. Experimental and Theoretical Evidence for Nitrogen–Fluorine Halogen Bonding in Silver-Initiated Radical Fluorinations. *ACS. Catal.* **2019**, *9* (4), 3322-3326. DOI: 10.1021/acscatal.9b00623.

(82) Elgrishi, N.; Rountree, K. J.; McCarthy, B. D.; Rountree, E. S.; Eisenhart, T. T.; Dempsey, J. L. A Practical Beginner's Guide to Cyclic Voltammetry. *J. Chem. Ed.* **2017**, *95* (2), 197-206. DOI: 10.1021/acs.jchemed.7b00361.

(83) Cruz, C. L.; Nicewicz, D. A. Mechanistic Investigations into the Cation Radical Newman–Kwart Rearrangement. *ACS. Catal.* **2019**, *9* (5), 3926-3935. DOI: 10.1021/acscatal.9b00465.

(84) Morse, P. D.; Nicewicz, D. A. Divergent Regioselectivity in Photoredox-Catalyzed Hydrofunctionalization Reactions of Unsaturated Amides and Thioamides. *Chem. Sci.* **2015**, *6* (1), 270-274. DOI: 10.1039/C4SC02331E.

(85) Denes, F.; Pichowicz, M.; Povie, G.; Renaud, P. Thiyl Radicals in Organic Synthesis. *Chem. Rev.* **2014**, *114* (5), 2587-2693. DOI: 10.1021/cr400441m.

(86) Tsukamoto, M.; Nakamura, T.; Kimura, H.; Nakayama, H. Synthesis and Application of Trifluoromethylpyridines as a Key Structural Motif in Active Agrochemical and Pharmaceutical Ingredients. *J. Pest. Sci.* **2021**, *46* (2), 125-142. DOI: 10.1584/jpestics.D21-012.

(87) Gillis, E. P.; Eastman, K. J.; Hill, M. D.; Donnelly, D. J.; Meanwell, N. A. Applications of Fluorine in Medicinal Chemistry. *J. Med. Chem.* **2015**, *58* (21), 8315-8359. DOI: 10.1021/acs.jmedchem.5b00258.

(88) Grand, D. L.; Gosling, M.; Baettig, U.; Bahra, P.; Bala, K.; Brocklehurst, C.; Budd, E.; Butler, R.; Cheung, A. K.; Choudhury, H.; et al. Discovery of Icenticaftor (QBW251), a Cystic Fibrosis Transmembrane Conductance Regulator Potentiator with Clinical Efficacy in Cystic Fibrosis and Chronic Obstructive Pulmonary Disease. *J. Med. Chem.* **2021**, *64* (11), 7241-7260. DOI: 10.1021/acs.jmedchem.1c00343.

(89) Prakash, S. G. K.; Krishnamurti, R.; Olah, G. A. Fluoride-Induced Trifluoromethylation of Carbonyl Compounds with Trifluoromethyltrimethylsilane (TMS-$CF_3$). A Trifluoromethide Equivalent. *J. Am. Chem. Soc.* **1989**, *111*, 393-395.

(90) Langlois, B. R.; Laurent, E.; Roidoit, N. Trifluoromethylation of Aromatic Compounds with Sodium Trifluoromethanesulfinate under Oxidative Conditions. *Tet. Lett.* **1991**, *32* (51), 7525-7528.

(91) Wiehn, M. S.; Vinogradova, E. V.; Togni, A. Electrophilic Trifluoromethylation of Arenes and N-Heteroarenes using Hypervalent Iodine Reagents. *J. Fluor. Chem.* **2010**, *131* (9), 951-957. DOI: 10.1016/j.jfluchem.2010.06.020.

(92) Umemoto, T.; Zhang, B.; Zhu, T.; Zhou, X.; Zhang, P.; Hu, S.; Li, Y. Powerful, Thermally Stable, One-Pot-Preparable, and Recyclable Electrophilic Trifluoromethylating Agents: 2,8-Difluoro- and 2,3,7,8-Tetrafluoro-S-(trifluoromethyl)dibenzothiophenium Salts. *J. Org. Chem.* **2017**, *82* (15), 7708-7719. DOI: 10.1021/acs.joc.7b00669.

(93) Fujiwara, Y.; Dixon, J. A.; Rodriguez, R. A.; Baxter, R. D.; Dixon, D. D.; Collins, M. R.; Blackmond, D. G.; Baran, P. S. A New Reagent for Direct Difluoromethylation. *J. Am. Chem. Soc.* **2012**, *134* (3), 1494-1497. DOI: 10.1021/ja211422g.

(94) Jia, H.; Haring, A. P.; Berger, F.; Zhang, L.; Ritter, T. Trifluoromethyl Thianthrenium Triflate: A Readily Available Trifluoromethylating Reagent with Formal $CF_3$(+), $CF_3$(*), and $CF_3$(-) Reactivity. *J. Am. Chem. Soc.* **2021**, *143* (20), 7623-7628. DOI: 10.1021/jacs.1c02606.

(95) Kino, T.; Nagase, Y.; Ohtsuka, Y.; Yamamoto, K.; Uraguchi, D.; Tokuhisa, K.; Yamakawa, T. Trifluoromethylation of Various Aromatic Compounds by $CF_3I$ in the Presence of Fe(II)

Compound, $H_2O_2$ and Dimethylsulfoxide. *J. Fluor. Chem.* **2010**, *131* (1), 98-105. DOI: 10.1016/j.jfluchem.2009.09.007.

(96) Beatty, J. W.; Douglas, J. J.; Cole, K. P.; Stephenson, C. R. A Scalable and Operationally Simple Radical Trifluoromethylation. *Nat. Comm.* **2015**, *6*, 7919. DOI: 10.1038/ncomms8919.

(97) Yin, D.; Su, D.; Jin, J. Photoredox Catalytic Trifluoromethylation and Perfluoroalkylation of Arenes Using Trifluoroacetic and Related Carboxylic Acids. *Cell. Rep. Phys. Sci.* **2020**, *1* (8). DOI: 10.1016/j.xcrp.2020.100141.

(98) Parsaee, F.; Senarathna, M. C.; Kannangara, P. B.; Alexander, S. N.; Arche, P. D. E.; Welin, E. R. Radical Philicity and its Role in Selective Organic Transformations. *Nat. Rev. Chem.* **2021**, *5* (7), 486-499. DOI: 10.1038/s41570-021-00284-3.

(99) Xiao, H.; Zhang, Z.; Fang, Y.; Zhu, L.; Li, C. Radical Trifluoromethylation. *Chem. Soc. Rev.* **2021**, *50* (11), 6308-6319. DOI: 10.1039/d1cs00200g.

(100) Zhang, Y.; Pike, A. Pyridones in Drug Discovery: Recent Advances. *Bioorg. Med. Chem. Lett.* **2021**, *38*, 127849. DOI: 10.1016/j.bmcl.2021.127849

(101) Good, J. A. D.; Kulen, M.; Silver, J.; Krishnan, K. S.; Bahnan, W.; Nunez-Otero, C.; Nilsson, I.; Wede, E.; de Groot, E.; Gylfe, A.; et al. Thiazolino 2-Pyridone Amide Isosteres As Inhibitors of Chlamydia trachomatis Infectivity. *J. Med. Chem.* **2017**, *60* (22), 9393-9399. DOI: 10.1021/acs.jmedchem.7b00716.

(102) Lin, S.; Liu, C.; Zhao, X.; Han, X.; Li, X.; Ye, Y.; Li, Z. Recent Advances of Pyridinone in Medicinal Chemistry. *Front. Chem.* **2022**, *10*, 869860. DOI: 10.3389/fchem.2022.869860.

(103) Burriss, A.; Edmunds, A. J.; Emery, D.; Hall, R. G.; Jacob, O.; Schaetzer, J. The Importance of Trifluoromethyl Pyridines in Crop Protection. *Pest. Manag. Sci.* **2018**, *74* (6), 1228-1238. DOI: 10.1002/ps.4806.

(104) Jelich, H.; Lindel, H. Preparation of 3-Trichloromethyl-Pyridine. Germany 1992.

(105) Fujioka, G. S. Preparation of (Trifluoromethyl)Pyridines. USA 1983.

(106) Campeau, L.-C.; Chen, Q.; Gauvreau, D.; Girardin, M.; Belyk, K.; Maligres, P.; Zhou, G.; Gu, C.; Zhang, W.; Tan, L.; et al. A Robust Kilo-Scale Synthesis of Doravirine. *Org. Proc. Res. Dev.* **2016**, *20* (8), 1476-1481. DOI: 10.1021/acs.oprd.6b00163.

(107) Trofymchuk, S.; Bugera, M. Y.; Klipkov, A. A.; Razhyk, B.; Semenov, S.; Tarasenko, K.; Starova, V. S.; Zaporozhets, O. A.; Tananaiko, O. Y.; Alekseenko, A. N.; et al. Deoxofluorination of (Hetero)aromatic Acids. *J. Org. Chem.* **2020**, *85* (5), 3110-3124. DOI: 10.1021/acs.joc.9b03011.

(108) Hirano, K.; Miura, M. A Lesson for Site-Selective C-H Functionalization on 2-Pyridones: Radical, Organometallic, Directing Group and Steric Controls. *Chem. Sci.* **2018**, *9* (1), 22-32. DOI: 10.1039/c7sc04509c.

(109) O'Hara, F.; Blackmond, D. G.; Baran, P. S. Radical-Based Regioselective C-H Functionalization of Electron-Deficient Heteroarenes: Scope, Tunability, and Predictability. *J. Am. Chem. Soc.* **2013**, *135* (32), 12122-12134. DOI: 10.1021/ja406223k

(110) Meng, D.; Li, L.; Brown, A.; Desrosiers, J.-N.; Duan, S.; Hayward, C. M.; He, Z.; Hu, J.; Makowski, T.; Maloney, M.; et al. A Radical Chlorodifluoromethylation Protocol for Late-Stage Difluoromethylation and its Application to an Oncology Candidate. *Cell. Rep, Phys, Sci,* **2021**, *2* (4). DOI: 10.1016/j.xcrp.2021.100394.

(111) Qian, S.; Li, Z. Q.; Li, M.; Wisniewski, S. R.; Qiao, J. X.; Richter, J. M.; Ewing, W. R.; Eastgate, M. D.; Chen, J. S.; Yu, J. Q. Ligand-Enabled Pd(II)-Catalyzed C($sp^3$)-H Lactonization Using Molecular Oxygen as Oxidant. *Org. Lett.* **2020**, *22* (10), 3960-3963. DOI: 10.1021/acs.orglett.0c01243.

(112) Li, Y. H.; Ouyang, Y.; Chekshin, N.; Yu, J. Q. Pd(II)-Catalyzed Site-selective beta- and gamma-C($sp^3$)-H Arylation of Primary Aldehydes Controlled by Transient Directing Groups. *J. Am. Chem. Soc.* **2022**, *144* (11), 4727-4733. DOI: 10.1021/jacs.1c13586

(113) Chan, H. S. S.; Yang, J. M.; Yu, J. Q. Catalyst-Controlled Site Selective Methylene C-H Lactonization of Dicarboxylic Acids. *Science.* **2022**, *376*, 1481-1487.

(114) Jacquet, J.; Blanchard, S.; Derat, E.; Desage-El Murr, M.; Fensterbank, L. Redox-Ligand Sustains Controlled Generation of $CF_3$ Radicals by Well-Defined Copper Complex. *Chem. Sci.* **2016**, *7* (3), 2030-2036. DOI: 10.1039/c5sc03636d.

(115) Cismesia, M. A.; Yoon, T. P. Characterizing Chain Processes in Visible Light Photoredox Catalysis. *Chem. Sci.* **2015**, *6* (10), 5426-5434. DOI: 10.1039/C5SC02185E.

(116) Li, L.; Mu, X.; Liu, W.; Wang, Y.; Mi, Z.; Li, C. J. Simple and Clean Photoinduced Aromatic Trifluoromethylation Reaction. *J. Am. Chem. Soc.* **2016**, *138* (18), 5809-5812. DOI: 10.1021/jacs.6b02782

(117) Armstrong, H. E. The Structure of Cycloid Hydrocarbons. *Proc. Chem. Soc. London.* **1890**, *85*, 101-105.

(118) Wheland, G. W. The Quantum Mechanics of Unsaturated and Aromatic Molecules: A Comparison of Two Methods of Treatment. *J. Chem. Phys.* **1934**, *2* (8), 474-481. DOI: 10.1063/1.1749513.

(119) Galabov, B.; Nalbantova, D.; Schleyer, P.; Schaefer, H. F., 3rd. Electrophilic Aromatic Substitution: New Insights into an Old Class of Reactions. *Acc. Chem. Res.* **2016**, *49* (6), 1191-1199. DOI: 10.1021/acs.accounts.6b00120.

(120) Watson, W. D. Regioselective para-Chlorination of Activated Aromatic Compounds. *J. Org. Chem.* **1985**, *50* (12), 2145-2148.

(121) P., K.; Brace, N. O. Chlorination of Aromatic Compounds with Metal Chlorides. *J. Am. Chem. Soc.* **1954**, *76* (21), 5491-5494.

(122) Maddox, S. M.; Nalbandian, C. J.; Smith, D. E.; Gustafson, J. L. A Practical Lewis Base Catalyzed Electrophilic Chlorination of Arenes and Heterocycles. *Org. Lett.* **2015**, *17* (4), 1042-1045. DOI: 10.1021/acs.orglett.5b00186.

(123) Maddox, S. M.; Dinh, A. N.; Armenta, F.; Um, J.; Gustafson, J. L. The Catalyst-Controlled Regiodivergent Chlorination of Phenols. *Org. Lett.* **2016**, *18* (21), 5476-5479. DOI: 10.1021/acs.orglett.6b02650.

(124) Lu, L.; Liu, H.; Hua, R. $HNO_3$/HFIP: A Nitrating System for Arenes with Direct Observation of pi-Complex Intermediates. *Org. Lett.* **2018**, *20* (11), 3197-3201. DOI: 10.1021/acs.orglett.8b01028.

(125) Rodriguez, R. A.; Pan, C. M.; Yabe, Y.; Kawamata, Y.; Eastgate, M. D.; Baran, P. S. Palau'chlor: A Practical and Reactive Chlorinating Reagent. *J. Am. Chem. Soc.* **2014**, *136* (19), 6908-6911. DOI: 10.1021/ja5031744.

(126) Song, S.; Li, X.; Wei, J.; Wang, W.; Zhang, Y.; Ai, L.; Zhu, Y.; Shi, X.; Zhang, X.; Jiao, N. DMSO-Catalysed Late-Stage Chlorination of (hetero)Arenes. *Nat. Catal.* **2019**, *3* (2), 107-115. DOI: 10.1038/s41929-019-0398-0.

(127) Xiong, X.; Yeung, Y.-Y. Highly ortho-Selective Chlorination of Anilines Using a Secondary Ammonium Salt Organocatalyst. *Angew. Chem. Int. Ed.* **2016**, *55* (52), 16101-16105. DOI: 10.1002/anie.201607388.

(128) Dinh, A., N.; Maddox, S. M.; Vaidya, S. D.; Saputra, M. A.; Nalbandian, C. J.; Gustafson, J. L. Catalyst-Controlled Regioselective Chlorination of Phenols and Anilines through a Lewis Basic Selenoether Catalyst. *J. Org. Chem.* **2020**, *85* (21), 13895-13905. DOI: 10.1021/acs.joc.0c01917.

(129) Cardenas, M. M.; Nguyen, A. D.; Brown, Z. E.; Heydari, B. S.; Heydari, B. S.; Vaidya, S. D.; Gustafson, J. L. Atropisomerism as Inspiration for New Chemistry. *Arkivoc.* **2021**, *2021* (1), 20-47. DOI: 10.24820/ark.5550190.p011.382.

(130) Pathak, T. P.; Miller, S. J. Site-Selective Bromination of Vancomycin. *J. Am. Chem. Soc.* **2012**, *134* (14), 6120-6123. DOI: 10.1021/ja301566t.

(131) Payne, J. T.; Poor, C. B.; Lewis, J. C. Directed Evolution of RebH for Site-Selective Halogenation of Large Biologically Active Molecules. *Angew. Chem. Int. Ed.* **2015**, *54* (14), 4226-4230. DOI: 10.1002/anie.201411901.

(132) Schreiner, P.; Wittkopp, A. H-Bonding Additives Act Like Lewis Acid Catalysts *Org. Lett.* **2002**, *4* (2), 217-220.

(133) Breugst, M.; Corral Bautista, F.; Mayr, H. Nucleophilic Reactivities of the Anions of Nucleobases and Their Subunits. *Eur. J. Org. Chem.* **2012**, *18* (1), 127-137. DOI: 10.1002/chem.201102411.

(134) Edwards, J. O. Correlation of Relative Rates and Equilibria with a Double Basicity Scale. *J. Am. Chem. Soc.* **1954**, *76*, 1540-1547.

(135) Mayr, H.; Kempf, B.; Ofial, A. R. π-Nucleophilicity in Carbon−Carbon Bond-Forming Reactions. *Acc. Chem. Res.* **2002**, *36* (1), 66-77. DOI: 10.1021/ar020094c.

(136) Heberger, K.; Lopata, A.; Jaszberenyi, J. C. Separation of Polar and Enthalpy Effects in Radical Addition Reactions using Polar and Radical Sigma Scales. *J. Phys. Org. Chem.* **2000**, *13* (3), 151-156. DOI: 10.1002/1099-1395(200003)

(137) Vleeschouwer, F. D.; Speybroeck, V. V.; Waroquier, M.; Geerlings, P.; Proft, F. D. Electrophilicity and Nucleophilicity Index for Radicals. *Org. Lett.* **2007**, *9* (14), 2721-2724.

(138) Cai, Y.; Zhu, W.; Zhao, S.; Dong, C.; Xu, Z.; Zhao, Y. Difluorocarbene-Mediated Cascade Cyclization: The Multifunctional Role of Ruppert-Prakash Reagent. *Org. Lett.* **2021**, *23* (9), 3546-3551. DOI: 10.1021/acs.orglett.1c00962.

(139) Charpentier, J.; Früh, N.; Togni, A. Electrophilic Trifluoromethylation by Use of Hypervalent Iodine Reagents. *Chem. Rev.* **2014**, *115* (2), 650-682. DOI: 10.1021/cr500223h.

(140) Chen, X.; Geng, Y.; Liu, B.; Zhu, Y.; Zou, D.; Wu, Y.; Wu, Y. Photochemical Difluoromethylation of Alkynes: Synthesis of $CF_2H$-Substituted Seven-Membered Dioxodibenzothiazepines and Dibenzazepines. *Org. Chem. Front.* **2023**, *10* (8), 1968-1974. DOI: 10.1039/d3qo00020f.

(141) Liu, J.; Zhang, J.; Wu, C.; Liu, H.; Liu, H.; Sun, F.; Li, Y.; Liu, Y.; Dong, Y.; Li, X. 1,1-Difluoroethyl Chloride ($CH_3CF_2Cl$), a Novel Difluoroalkylating Reagent for 1,1-Difluoroethylation of Arylboronic Acids. *RSC. Adv.* **2019**, *9* (49), 28409-28413. DOI: 10.1039/c9ra06406k.

(142) Yagupolskii, L. M.; Matsnev, A. V.; Orlova, R. K.; Deryabkin, B. G.; Yagupolskii, Y. L. A New Method for the Synthesis of Trifluoromethylating Agents—Diaryltrifluoromethylsulfonium Salts. *J. Fluor. Chem.* **2008**, *129* (2), 131-136. DOI: 10.1016/j.jfluchem.2007.10.001.

(143) Yagupolskii, L. M. Aromatic Compounds With New Fluorine-Containing Substituents. *J. Fluor. Chem.* **1987**, *36*, 1-28.

(144) Ji, Y.; Brueckl, T.; Baxter, R. D.; Fujiwara, Y.; Seiple, I. B.; Su, S.; Blackmond, D. G.; Baran, P. S. Innate C-H Trifluoromethylation of Heterocycles. *Proc Natl Acad Sci U S A* **2011**, *108* (35), 14411-14415. DOI: 10.1073/pnas.1109059108

(145) Jiang, Y.; Li, B.; Ma, N.; Shu, S.; Chen, Y.; Yang, S.; Huang, Z.; Shi, D.; Zhao, Y. Photoredox Catalyst Enabled para-Selective Trifluoromethylation of tert-Butyl Arylcarbamates. *Angew. Chem. Int. Ed.* **2021**, *60* (35), 19030-19034. DOI: 10.1002/anie.202105631.

(146) Schreiber, S. L.; Schreiber, T. S.; Smith, D. B. Reactions that Proceed with a Combination of Enantiotopic Group and Diastereotopic Face Selectivity can Deliver Products with Very High Enantiomeric Excess: Experimental Support of a Mathematical Model. *J. Am. Chem. Soc.* **1987**, *109*, 1525-1529.

(147) Ayonon, A.; Nalbandian, C. J.; Guillemard, L.; Gustafson, J. L. Benzylic Bromination Catalyzed by Triphenylphosphine Selenide via Lewis Basic Activation. *Tet. Lett.* **2017**, *58* (30), 2940-2943. DOI: 10.1016/j.tetlet.2017.06.042.